Synthesis of polymer-bound small-molecule kinase inhibitors as anti-tumour agents

by

Lebusetsa Taleli

Thesis presented in partial fulfilment of the requirements for the degree, Doctor of Philosophy in Chemistry

Supervisor: Prof Bert Klumperman

Co-supervisor: Prof Willem van Otterlo

Department of Chemistry and Polymer Science, Stellenbosch University

December 2017

Declaration

I, the undersigned, hereby declare that the work contained in this thesis is my own original work and that I have not previously in its entirety or in part submitted it for the academic examination towards any qualification.

……..

Lebusetsa Taleli (December 2017)

Abstract

Inhibition of kinase activities using small molecules for the treatment of various diseases, including lung cancer, is one of the most pursued therapeutic targets. Molecularly targeted therapy aimed at the inhibition of specific protein kinase signalling activities, *e.g.* epidermal growth factor receptor (EGFR), has changed the treatment landscape of clinical oncology into personalised medicine. Today, lung cancer patients are stratified according to tumour genetic mutations and are further profiled into kinase inhibitor treatment options. The 4-anilinoquinazoline class of small molecules are EGFR kinase inhibitors, used for the treatment of adenocarcinoma NSCLC. Therapeutic challenges affecting the efficacy of these molecules include low bioavailability, off-target reactive toxicities, and acquired drug resistance.

The core objective of this study was to investigate the formulation of 4-anilinoquinazoline small molecules into polymer-drug conjugates. These conjugates were intended for use in a micellar drug delivery mechanism using poly(*N*-vinylpyrrolidone) (PVP) and pH-responsive linker groups. The 4-anilinoquinazoline anti-tumour agents carrying Michael acceptor electrophiles (acrylamide and acrylates) were synthesised by assembling various quinazolin-4(3*H*)-one derivatives. The preparation of a PVP delivery carrier was achieved by means of triazole-based RAFT/MADIX polymerisation. The ω-end group transformation of PVP into a thiol functionality was realised by aminolysis and the polymer-drug conjugates were then developed by 1,4-conjugated Michael addition reaction. The conjugates were allowed to self-organise into characteristic micelles in aqueous solutions. Assessments of the drug release profiles under variable pH conditions showed that release is favoured in the acidic tumour microenvironment. Furthermore, the *in vitro* anti-tumour efficacy of the amide-linked conjugate was demonstrated to match the Gefitinib ATP-competitive EGFR kinase inhibitor against EGFR wild-type and EGFR L858R/T790M mutant. The overall anti-tumour efficacy suggests that the mode of EGFR kinase inhibition is a critical determinant of anti-tumour efficacy. Further developments related to the present formulation are however necessary to enhance bioactivities of the conjugates.

Opsomming

Verskeie siektes, insluitend longkanker, word behandel deur die kinase-aktiwiteite te inhibeer met behulp van klein molekules en is daarom een van die mees gefokusde terapeutiese teikens. Molekulêr-geteikende terapie wat gefokus is op die inhibering van spesifieke proteïenkinase seinaktiwiteite, bv EGFR, het die manier waarop hierdie siektes behandel word verbeter. Pasiënte met longkanker word huidiglikglik geklassifiseer op grond van die genetiese mutasie van hul tumor en word verder gegroepeer in die behandeling wat beskikbaar is om die spesifieke kinase te inhibeer. 4-anilinoquinazoline is ‘n klas van klein molekules wat EGFR kinase inhibeer en word gebruik om adenokarsinoom nie-klein selkanker te behandel. Lae bio-beskikbaarheid, nie-geteikende reaktiewe toksisiteite en die verworwe geneesmiddelweerstand is nog terpeutiese uitdagings wat die effektiwiteit van hierdie molekules beïnvloed. Die doel van hierdie studie was om die formulering van 4-anilinoquinazolin klein molekules in polimeer-dwelmkonjugate te ondersoek. Hierdie was bedoel vir 'n misellige geneesmiddelleweringsmeganisme wat PVP-polimeer en pH-sensitiewe verbindende groepe gebruik. Die 4-anilinoquinazoline anti-tumor middels wat die Michael-akseptor elektrofiele (akrielamied en akrelaat) vervoer, was gesintetiseer deur verskillende quinazolin-4 (3*H*)-oon derivate te verbind. Triasool-gebaseerde RAFT/MADIX-polimerisasie is gebruik om die PVP-vervoer draer te berei. Aminolise is verder gebruik om die ω-eindgroepe van PVP om te skakel na die terminale tiol groepe waarna die polimeer-dwelmkonjugate ontwikkel was deur middel van ‘n 1,4- gekonjugeerde Michael-addisie reaksie. Hierdie konjugate vorm kenmerkende miselle in waterige oplossings. Evaluering van die geneesmiddel-vrystelling-profiel onder verskillende pH-kondisies demonstreer dat die tumor mikro-omgewing verkies ‘n suur omgewing. Verder het ons gedemonstreer dat die *in vitro* anti-tumor effektiwiteit van die amied-verbindende konjugate ooreenstem met die Gefitinib ATP kompeterende EGFR kinase inhibeerder teen EGFR wilde-tipe en EGFR L858R/T790M mutant. Die algehele anti-tumor effektiwiteit diu daarop dat die metode van EGFR kinase inhibisie ‘n bepalende faktor is in die anti-tumor effektiwiteit. Verdere ontwikkelings op die huidige formulering is egter nodig om die bioaktiwiteite van die konjugate te verbeter.

Acknowledgements

As Steven R. Covey is famously quoted, “interdependence is a higher value than independence,” this work is a synergistic product of many minds that I stoop and bestow my gratitude.

If I have seen any farther, it is not because of the modicum of intelligence but it is by standing on the shoulders of the giants. I thank these supervisors, Prof Bert Klumperman and Prof Willem van Otterlo. Their kindness and tireless guidance throughout this study have been lively by many-folds.

Secondly, I extend my gratitude to the Groups of Organic&Medicinal Chemistry and Polymer Free Radical for being welcoming and always open to assist. In particular, I acknowledge a friend and a colleague Ms Mabank for saving up my breath once, and Prof Ivan Robert Green for furthering our academic experiences in the lab 2020. I also thank Dr Paul Reader, Dr Rueben Pfukwa and Nusrat Begum, whom I have always consulted during my introduction to polymer synthesis. Ms Elrika Harmzen for all the STEM imaging initiatives that were always during the sunrise.

The Polymer Science Laboratories is also acknowledged; Anna Kargaard, Siyasanga Mbizana, Ingrid Heyns, and Dr Helen Pfukwa have all been a wonderful experience. I permissively adopt Upenyu Lucky Muza into ‘team Helen’ for DLS measurements, which were often out of demanding time of his thesis preparation. The CAF team at Stellenbosch: Dr Jaco Brand and Elsa Malherbe were the NMR tag team that allowed for access to the unit even under inconvenient arrangements; Dr Marietjie Stander and Mr Malcolm Taylor for all the effort of LC-MS analysis; Ms Dumisile Lumkwana and Mrs Lize Engelbrecht for the fluorescence microscopy imaging; and Mrs Madelaine Frazenburg for STEM imaging.

I extend my gratitude to the group of Prof Daniel Rauh (and Jonas) for the biological assays reported in this work. The sponsors for this research who made this studies possible, SARChi, NRF SA and the DAAD, are thanked dearly.

Lastly, I am grateful for colleagues and friends that were made, and my family that always joined in my scuffles to provide assurances. Khotso! Pula! Nala!

Table of Contents

List of abbreviations

The following index describes various abbreviations and nonstandard acronyms used throughout the thesis, listed according to the order of appearance.

Abbreviation	Description
EGFR	epidermal growth factor receptor
ATP	adenosine triphosphate
EGFR TK	epidermal growth factor receptor tyrosine kinase
TKI(s)	tyrosine kinase inhibitor(s)
SMKI(s)	small-molecule kinanase inhibitor(s)
NSCLC	non-small-cell lung cancer
SCLC	small cell lung cancer
ICH	immunohistochemistry
HER/ ErbB	human epidermal growth factor receptors
RTKs	receptor tyrosine kinases
VEGFR	vascular endothelial growth factor receptor
FDA	Food and Drug Administration
PVP	poly(*N*-vinyl pyrrolidone)
NVP	*N*-vinyl pyrrolidone
PEG-PLA	polyethylene glycol-polylactic acid
PEG	polyethylene glycol
RDRP	reversible deactivation radical polymerisation
RAFT	reversible addition-fragmentation chain transfer
MADIX	macromolecular design via the interchange of xanthates
EPR	enhanced permeability and retention
NMR	nuclear magnetic resonance
DCM	dichloromethane
TLC	thin layer chromatography
DMAP	4-dimethylaminopyridine
HSQC	heteronuclear single quantum coherence
HMBC	heteronuclear multiple bond correlation
UPLC-MS	ultra-performance liquid chromatography-tanderm mass spectroscopy
UV	ultraviolet
ADRs	adverse drug reactions
NMP	nitrogen-mediated polymerisation
ATRP	atom radical transformation
DP_n	degree of polymerisation
M_n	number average molecular weight
SEC	size-exclusion chromatography
MS	mass spectrometry
MALDI-TOF MS	matrix assisted laser desorption ionization-time of flight mass spectrometry
PDI (*Đ*)	polydispersity indices
DRI	differential refractive index

PMMA	poly(methyl methacrylate
TCEP	tris(2-carboxyethyl)phosphine
DMAc	*N,N*-dimethylacetamide
UV-Vis	ultraviolet-visible
DLS	dynamic light scattering
STEM	Scanning transmission electron microscopy
CM	confocal microscopy
STEM	scanning transmission electron microscopy
AIBN	α,α′-azobisisobutyronitrile
ESI	electrospray ionisation
LC-MS	liquid chromatography-mass spectroscopy

Chapter 1: Introduction and research objectives

Chapter 1: Introduction and research objectives

Abstract

This chapter introduces cancer of epithelial origin and the role played by epidermal growth factor receptor (EGFR) kinase signalling activity in promoting tumour growth through sustained phosphorylation. The 4-anilinoquinazoline class of small molecules is used in clinical oncology to inhibit the kinase signalling activity by occupying the adenosine triphosphate (ATP) pocket. There are challenges in the clinical application of these molecules. Some illustrative shortcomings are discussed, along with possible solutions thereof. One possible solutions is the development of polymer-drug conjugates to form a micellar drug delivery system. The research objectives are then formulated, as outlined in the final section of this chapter.

1.1 Introduction

Cancer is a deadly disease that accounts for over 11% of global death cases annually. The prevalence of cancer is highest among Eastern Asians (55%), while the African continent represents 7% of this incoming pandemic blight.[1] There are different types of cancer, but carcinomas of the lung are ranked the most lethal subtype.[1b] Morbidity and prevalence of cancer is statistically projected to escalate in the economically developing world, such as in South Africa, as per GLOBOCAN's collective data.[1]

1.2 Phosphorylation in tumour cells and the EGFR kinase activity

The description of cancer is based upon the intricacies of genetic mutations and epigenetic changes within biological cells. Accumulation of these alterations in normal cells can stimulate the development of autonomous qualities that are permissive to sustained cell proliferation.[2] The manifestation of malignant properties in biosynthetic activities of cells was examined in the early 1920s by Otto Warburg.[3] 'The Warburg effect' is consistent with the increased metabolism in proliferative tumour cells, particularly enhanced aerobic glycolysis for generating ATP. To meet the energetic demands of cell proliferation, tumours ingest nutrients from their environment using growth factors.[4] The acquired mutations in growth factor receptors are then utilised to activate metabolic pathways to support tumour survival.[4-5] In this way, the reprogrammed metabolic activities in tumours can be considered as consisting of a diversely arrayed crosstalk

between signalling pathways and protein phosphorylation processes, which are mediated by kinases.[5b]

Thus, it can be cautiously emphasised that the biosynthetic pathways underlying the proliferative state of tumours are profoundly influenced by growth factors and phosphorylation. Protein phosphorylation is a widespread process,[6] while a salient feature of the EGFR is that of fostering cell proliferation and chronically enhancing intracellular phosphorylation.[7] The EGFR is a type of tyrosine kinase receptor that is frequently used as a therapeutic prognostic marker in numerous solid tumours, such as lung cancer.[8] Its overexpression in most cells is known to indicate the manifestation of a malignant phenotype.[9] A landmark discovery by the Nobel Laureates Fischer and Krebs, established protein phosphorylation as a key regulatory mechanism in biochemical signalling pathways.[10] The catalytic role played by the kinases in transferring a γ-phosphate group from ATP to the hydroxyl group of serine, threonine, or tyrosine amino acids is thus well known (see a shematic sketch in **Fig. 1.2**). Given the fact that metabolic activities and cellular growth are intertwined through signalling pathways, it is no surprise that mutant EGFR stimulates phosphorylation to regulate the biochemical activities.[7a, 11] The cascaded biological reactions ensuing from phosphorylation (also known as downstream signalling) have been demonstrated in many human tumour cell lines and xenograft models.[12]

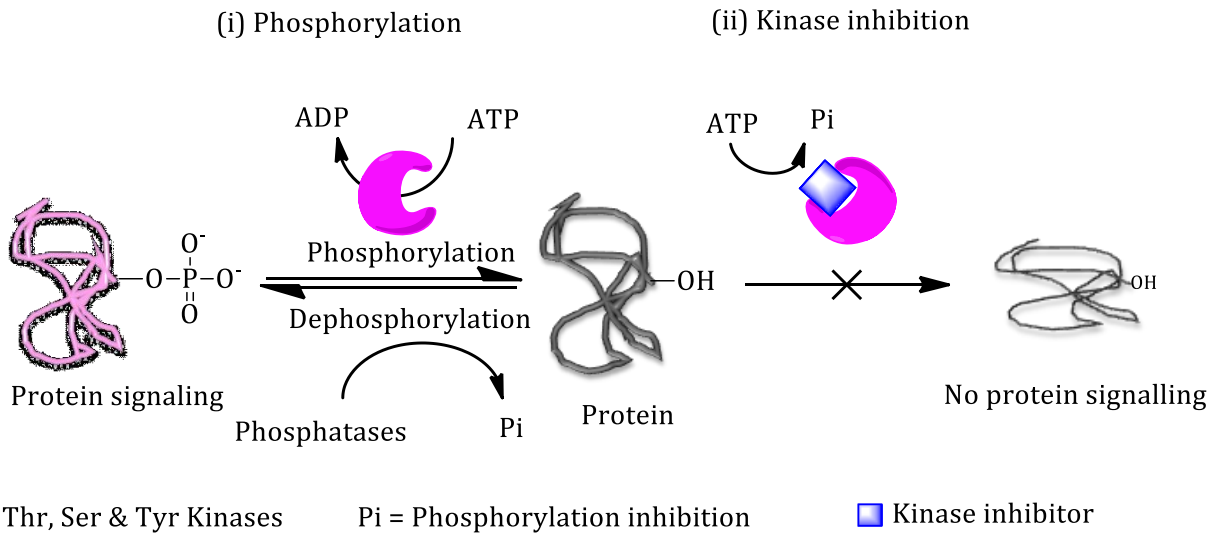

Figure 1.2 Reversible protein phosphorylation between (i) kinase and phosphatase enzymes. (ii) Kinase phosphorylation prevented by exogenous compounds such as small-molecule kinase inhibitors.

With the increased understanding of the key roles played by signalling pathways, a complementary theme to the Warburg phenomenon is called 'oncogene addiction'.[13] The subject outlines tumour dependency to a signal transduction network, which is activated by the oncogenic proteins.[13b] According to Volgestein *et al.*,[14] between two and eight mutant oncogenic proteins can sufficiently promote selective tumour proliferation advantage in a cell with about 140 intragenic mutations. These tumour-selective proliferation oncogenes are known as 'mutant driver genes', which can be grouped into twelve signalling pathways which modulate, namely, (i) cell fate, (ii) survival, and (iii) genome consistency. The rest of the genetic mutations without identifiable biological flaws are classified as 'passenger' mutations.[15] In view of the oncogene addiction aspect, tumours rely on one to several signalling pathways to execute their biochemical activities. Proof of this concept has been consolidated by disparate data sources from the literature and clinical practices using molecularly targeted therapy [inhibition of the EGFR tyrosine kinase (EGFR TK) signalling pathway].[13-14, 16]

1.3 Inhibition of the EGFR tyrosine kinase phosphorylation

Recent perspectives in developing more differentiated cancer therapy encourage the use of molecules that target specific biological pathways in mutant cells. In line with this, the tyrosine kinase family has become one of the primary targets in cancer treatment, and more than 23 small-molecule kinase inhibitors (SMKIs) are now on the market.[17] The ICI Pharmaceuticals Parke-Davies group (the present AstraZeneca) has demonstrated selective anti-tumour efficacies of 4-anilinoquinazoline compounds against EGFR TK activities.[18] The combination of high potency and good selectivity offered by these compounds makes them ideal choices for long-term clinical use. In addition, these cytotoxic agents are effective against advanced non-small-cell lung cancer (NSCLC) adenocarcinoma.[19] Examples include Gefitinib, which received an accelerated FDA approval after only two phase II trials in 2003, and Erlotinib, which was endorsed in 2004 (structures are shown in **Fig. 1.3**). They were both approved for second-line and third-line monotherapy for patients under chemotherapy.[20] Today, few 4-anilinoquinazoline molecules are clinically used against NSCLC adenocarcinomas with EGFR *activating* mutations.[21] The inventory of 4-anilinoquinazolines has since been diversely expanded with other quinazoline derivatives, the majority of which have failed in different stages

of the clinical trials. These compounds derive anti-tumour activity by occupying the ATP binding site, thereby blocking the EGFR kinase catalytic activity.[22]

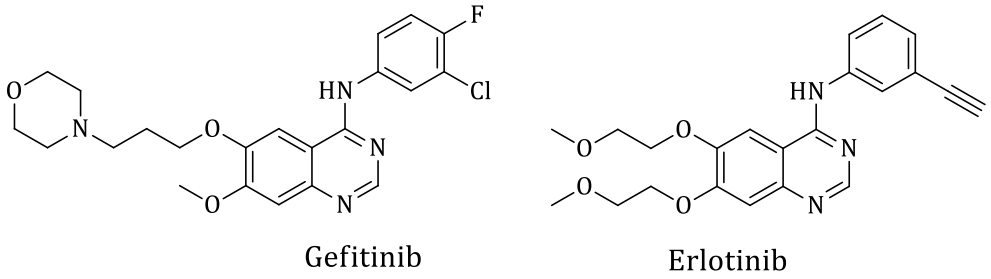

Figure 1.3 Small-molecule tyrosine kinase inhibitors based on the 4-anilinoquinazoline scaffold currently in clinical use for treatment of lung adenocarcinomas.

1.4 Acquired drug resistance to 4-anilinoquinazoline EGFR TK inhibitors

Alluding to a universal problem of mutation development in cancer, 4-anilinoquinazolines are clinically limited to NSCLC patients with EGFR *activating* mutations (EGFR L858R is a prominent mutation that positively activates signalling pathways in oncogenic proteins).[23] Gefitinib and Erlotinib are 4-anilinoquinazoline drugs that were withdrawn, due to low clinical benefits, from the US and EU markets, but not in Asia. Lung cancer patients that received treatment with these compounds either exhibited an outstanding positive or a poor response.[23] This impression has inspired genetic profiling of lung tumours according to EGFR mutations in clinical trials and has further paved the new era in the management of lung cancer. At present, lung cancer patients are tactfully stratified according to histomorphology and genetic differentiation of tumours. A compulsory screening of EGFR mutations prior to medical prescription has also been accepted as the standard clinical practice.[24] As a result, Gefitinib and Erlotinib were thus recalled into clinical practice, in 2015 and 2013 respectively, as first-line treatment drugs.[21, 25]

Because of EGFR mutations, there is a renewed interest in the clinical re-evaluation of 4-anilinoquinazoline anti-tumour agents. A series of expanded phase III clinical trials examining the acquired drug resistance in lung cancer was launched in 2009. Approximately ten phase III clinical trials comparing 4-anilinoquinazoline kinase inhibitors with chemo-regimens have been completed on a single-arm data collection

basis.[21, 25-26] There have been discrepancies across randomised clinical trial designs due to population selection criteria, study methodology and the primary end point of evaluation. Nonetheless, collective data emanating from these studies have presented improved overall tumour responses (60–80%) and progression-free survival of the patients in favour of 4-anilinoquinazolines.[21, 26-27] Head-to-head phase III trial studies on different generations of EGFR tyrosine kinase inhibitors (TKIs) have also been conducted; they are still ongoing (the FLAURA is expected to end in 2018).[21] The intention is to style a first-line therapy according to EGFR somatic mutations.

The EGFR T790M is the secondary 'gate-keeping' mutation that modestly encumbers the ATP binding pocket against quinazoline-based kinase inhibitors, thereby reducing their target affinity and anti-tumour efficacy.[28] To challenge the situation, 4-anilinoquinazolines bearing an electrophilic group at the C-7 position [see **Fig. 1.4 (a)** for structures] were designed to irreversibly occupy the ATP binding pocket.[29] The electrophilic functionality allows for the proximal covalent bond formation with the target nucleophile, cysteine thiol (Cys 797). This has permitted an effective therapeutic window for EGFR T790M in preclinical models.[28a, b] However, doses required to elicit favourable pharmacological responses have often been concomitant with adverse side effects under the clinical setting. The intrinsic reactivity of some of these electrophilic funtionalities (such as acrylamide) have been demonstrated to induce non-selective inhibition of the wild-type and mutant EGFR.[28a] Off-target reactive toxicities for this set of compounds continues to be a medically unmet challenge.

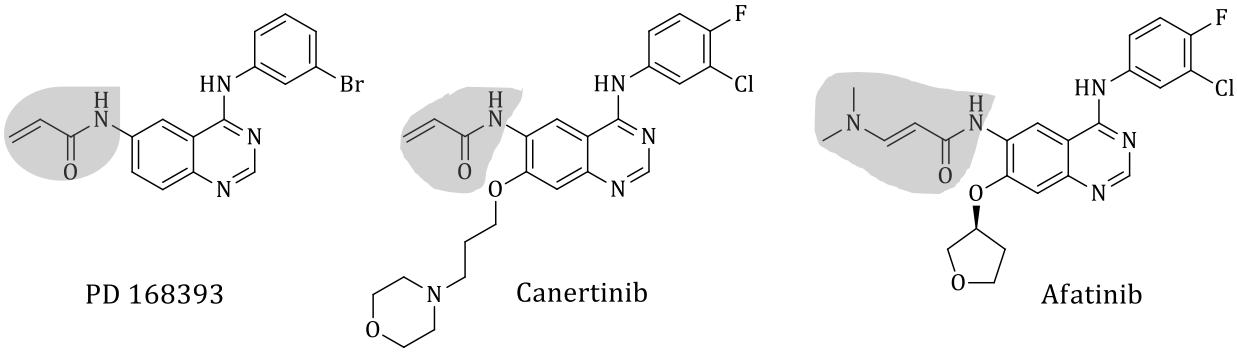

Figure 1.4 (a) Quinazoline-based kinase inhibitors targeting the EGFR T790M. The first two compounds (PD 168393 and Canertinib) have failed at different phases of clinical trials and Afatinib is an experimental drug for adenocarcinoma patients. (The acrylamide moiety is highlighted in grey.)

A different molecular approach aimed at targeting EGFR T790M has pursued a pyrimidine-based chemical scaffold of irreversible inhibitors [see **Fig. 1.4 (b)**].[30] The pyrimidines were intended to show the T790M mutant selectivity over the wild-type EGFR. However, the efficacy of pyrimidine-based compounds (third generation EGFR kinase inhibitors) was curtailed by the newly acquired EGFR C797S mutation, within 10 months of clinical use.[30-31] In EGFR C797S, the covalent bond formation between the electrophilic acrylamide group and the thiol is lost because of serine substitution of the cysteine. The next (being the 4th) generation of small molecules, which is intended for the allosteric inhibition of T790M and C797S, is in the discovery pipeline.[32] Despite this evolving genetic mutations, the ATP affinity binding assays in tumours that accrue the EGFR T790M mutation have shown that Gefitinib can still achieve low nanomolar (nM) concentration efficacies.[28a] Therefore, revisiting 4-anilinoquinazoline compounds with the intention to improve their pharmacokinetics and the therapeutic efficacy was considered to be.an instructive recourse.

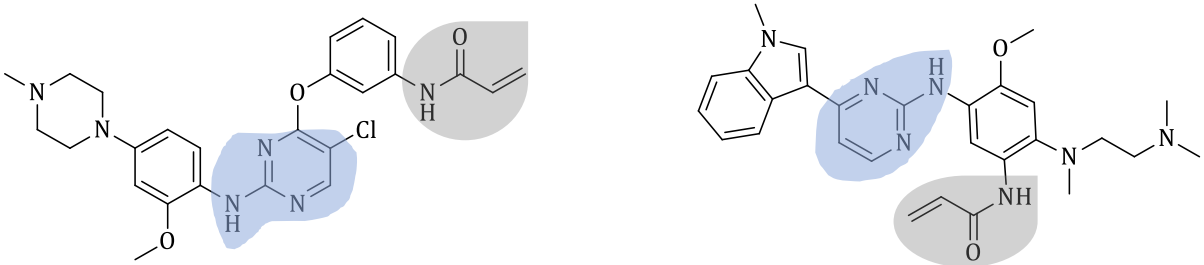

Figure 1.4 (b) EGFR T790M selective irreversible aminopyridine-based kinase inhibitors; WZ 004 is used as a conditional adjuvant drug in the EU markets and AZD 9291 is under phase III clinical studies. The parent amino-pyridine scaffold (in blue) and the electrophilic acrylamide groups (in grey) are highlighted.

1.5 Other pharmacological challenges to quinazoline-based EGFR TK inhibitors

One of the therapeutic shortcomings of quinazoline-based EGFR TKIs is low *in vivo* bioavailability. This has been established from plasma concentration levels after oral administrations.[33] The poor aqueous solubility of these compounds under physiological conditions is essentially rooted in the parent scaffold, quinazoline, itself. Efforts to address this problem for the clinical application of these compounds have been aligned

with medicinal chemistry. To date, various water solubilising groups have been successfully attached to the C-6 and/or C-7 positions of the quinazoline parent compound [see **Fig. 1.5 (a)**]. Most of the earliest quinazoline analogues had poor aqueous solubility (<1 mM) and low anti-tumour efficacy.[33a, 34] Further structure–activity relationship optimisation studies have resulted in compounds with improved IC_{50} values in the nanomolar concentration range.[33a, 34]

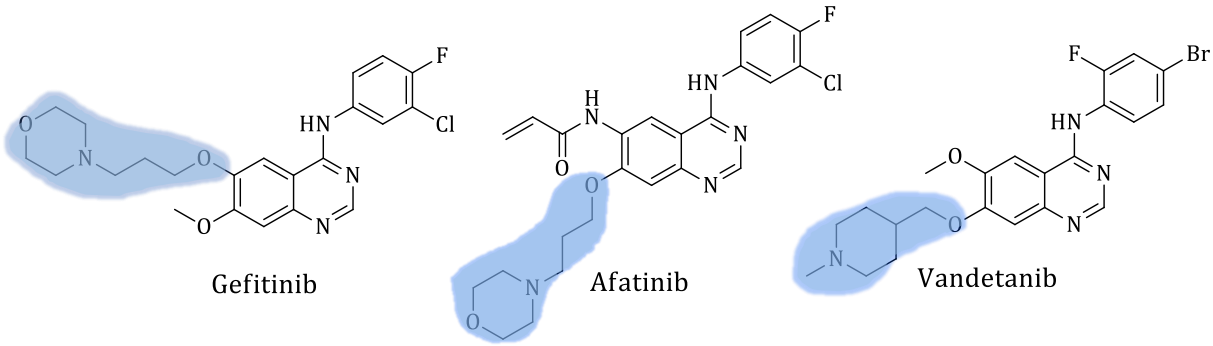

Figure 1.5 (a) Some solubilising groups (highlighted in blue) that are used to enhance the bioavailability of 4-anilinoquinazolines.

Among the most studied solubilising groups, weakly basic groups (morpholino and tertiary amino groups) and/or a variety of polyalcohol alkyl chains were found to be suitable for increasing the aqueous solubility and anti-tumour efficacy of quinazoline compounds.[34b, 35] When solubilising groups are attached to a α,β-unsaturated electrophilic acrylamide substituent in irreversible inhibitors, the anti-tumour efficacy of the compounds tends to vary.[36] These observations can be rationalised by differences in nucleophilic access to the Michael acceptor due to steric hindrance. The search for structural analogues of quinazoline with better aqueous solubility has led to a concurrent investigation of the pyridopyrimidine scaffold as an alternative.[22, 34b, 37] A pyridopyrimidine can be regarded as an aza-derivative of the quinazoline scaffold [structures shown in **Fig. 1.5 (b)**].

(i) Quinazoline derivative

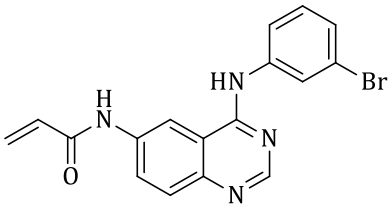

PD 168393

(ii) Aza-quinazoline derivatives

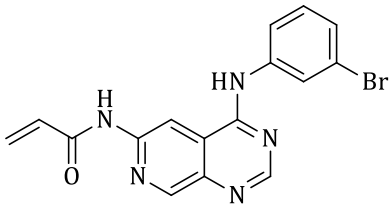

Pyrido[3,4-*d*]pyrimidine

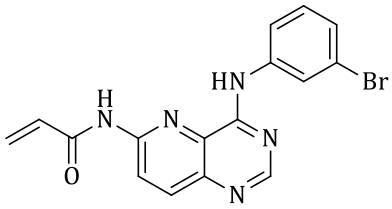

Pyrido[3,2-*d*]pyrimidine

Figure 1.5 (b) Structures of (i) 4-anilinoquinazoline derivative and (ii) aza-quinazoline analogues with conformational similarities.

Pyridopyrimidines (3,4-*d* and 3,2-*d*) with similar structural conformation to quinazolines exhibit better aqueous solubility (>10 mM) and superior anti-tumour potency to their quinazoline counterparts.[34b] In addition, the aza-quinazoline derivatives (pyrido[3,4-*d*]pyrimidines) containing α,β-unsaturated electrophilic groups (acrylamide) have higher reactivity to cysteine thiols in comparison to quinazoline compounds such as Afatinib.[36b] This implies that the formation of thiol adducts via a Michael addition reaction occurs more readily in the case of the pyridopyrimidine. In hindsight, the amide bond is less stable in irreversible pyridopyrimidines and this reduces the therapeutic efficacy of this compounds.[36b, 37] Because of this, the *in vivo* pharmacokinetics and therapeutic efficacy continues to favour quinazoline-based EGFR TKIs over the aza-quinazoline analogues. Based on the above discussion, it can be deduced that poor aqueous solubility is among the major therapeutic impediments that precludes full clinical efficacy of 4-anilinoquinazolines. Attempts improving the clinical efficacy of 4-anilinoquinazolines has included investigating the best drug administration routes.

1.6 Towards macromolecular prodrugs and tumouritropic drug delivery

The majority of studies have focused on oral intake and occasionally on intraperitoneal drug delivery.[38] The best anti-tumour efficacy results have been obtained from oral administration, especially when the compounds were formulated into fine particulate 'emulsions'.[38] From both practical and theoretical standpoints, these compounds have a good potential in lung cancer treatment. Hence, this study intends to overcome some of the therapeutic barriers and improve the anti-tumour efficacy of 4-anilinoquinazolines through the development of polymer-drug conjugates.

It was envisaged that sustained bio-distribution of SMKIs to the tumour microenvironment will minimise systemic toxicity. The commonly encountered class-specific adverse effects from 4-anilinoquinazolines include the development of grade 3/4 skin diseases such as rash, acne, and dryness, in combination with diarrhoea, vomiting, asthenia, cough, and nausea.[26a] Occasionally, treatment-related toxicity effects include liver dysfunction, intestinal lung diseases, acute respiratory distress, as well as cardiac failure.[20a, 24b, 26b] To mitigate the above adverse effects, controlled bio-distribution and delivery of 4-anilinoquinazoline anti-tumour agents can be achieved using polymer-based drug carriers. This 'Trojan horse' approach is likely to improve the EGFR mutant selectivity. This design can further accommodate both the passive and molecularly targeted kinase inhibition of tumour cells using covalently bound polymer-drug conjugates.

Relevant to this study, Wang *et al*.[39] recently entrapped a multi-target 4-anilinoquinazoline Vandetanib using amphiphilic block copolymer polyethylene glycol-polylactic acid (PEG-PLA) nanospherical encapsulation. Enhanced aqueous solubility and anti-tumour efficacy were successfully demonstrated both *in vitro* and *in vivo*. There are a number of advanced concepts that have used polymer carriers to selectively deliver therapeutic agents to diseased sites, including tumours.[40] Thus, the evolution of pharmacokinetics and dosage forms (also known as drug formulations) into drug delivery systems has the potential to achieve therapeutic benefits with minimal systemic toxicity. Drug formulations aimed at limiting drug access to systemic circulation were initiated in the late 1970s.[41] A plethora of modern water soluble drug formulations can now be illustrated in various sophisticated performances, inspired by the Ringsdorf model,[42] mostly emanating from the field of polymer chemistry. The drug delivery performances of polymeric formulations can be adjusted to conveniently minimise the shortcomings of the small-molecule therapeutic agents.

From a polymer therapeutics point of view, the formulation of polymeric prodrugs can be designed into variable architectures. The shape, size and physicochemical properties of macromolecular delivery vectors can be fine-tuned to enable optimal drug solubility, loading capacity, pharmacokinetic disposition, as well as the controlled release of drug molecules.[40a, 41a, 43] Many clinical benefits typifying the superior therapeutic indices offered by this approach have been demonstrated, over several decades. Of particular

interest in this study is the formulation of self-encapsulating micelle structures consisting of the hydrophobic 4-anilinoquinazolines and hydrophilic Poly(*N*-vinylpyrrolidone) (PVP) polymer chains (see illustration in **Fig. 1.6**). The micelle formation process is a self-organising colloidal dispersion by amphiphilic structures under energetically favourable conditions and selective solvent medium. The targeted self-organised micelles are projected to sequester the anti-tumour agents in a hydrophobic core structure. The core structure is anticipated to be sterically stabilised under physiological conditions by the highly hydrated PVP shell.

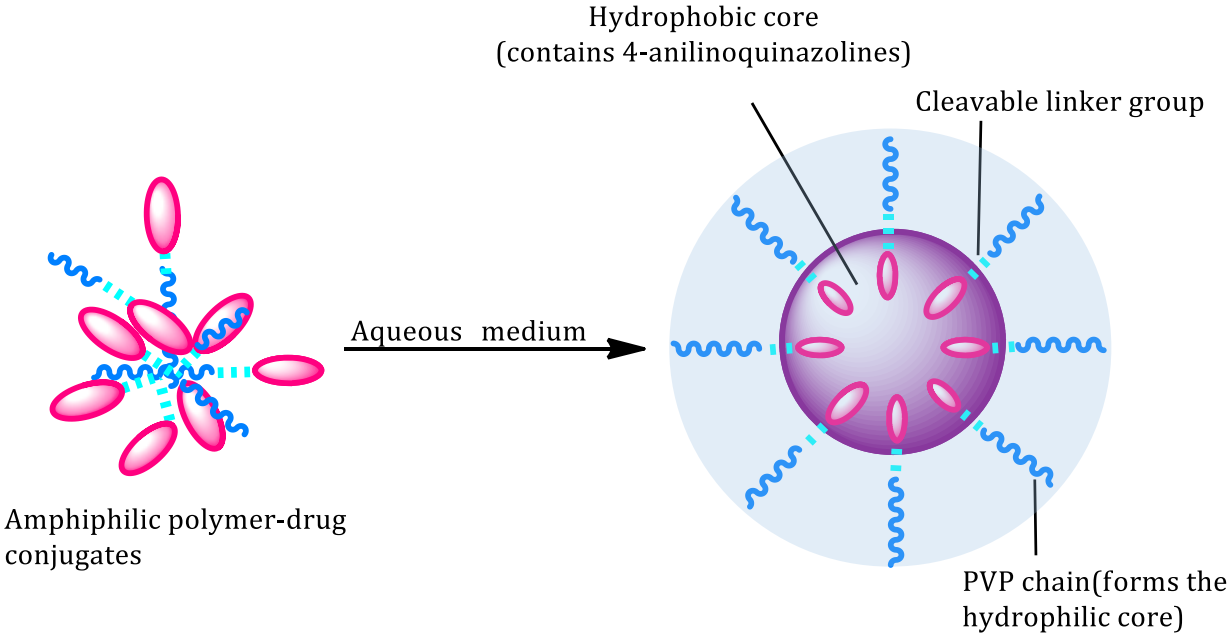

Figure 1.6 Illustration of the target structural composition and self-organised polymer-drug conjugate in aqueous medium for tumouritropic delivery.

1.7 Poly(N-vinylpyrrolidone) as a drug delivery carrier of 4-anilinoquinazolines

In addition to the formation of a hydrated PVP core that improves the aqueous solubility of 4-anilinoquinazolnes, the micellar self-organising process is known to assemble into a spherical curvature,[44] though other shapes have also been generated. The high water solubility of PVP is conferred by its five-membered ring lactam monomers, and this makes PVP a suitable drug delivery carrier under biological conditions. It is a preferred polymer of choice that offers a lyoprotectant feature,[45] which is desirable for physiological applications. PVP is also a biocompatible polymer; it has been used as a

plasma expander.[46] Beyond solubilising pharmacological agents, PVP is one of the hydrophilic polymers that has been investigated as drug carrier alternative to PEG.[47] In some instances, PVP drug conjugates have demonstrated longer circulation periods, reduced immunogenicity, and improved anti-tumour efficacy when compared to the gold standard polyethylene glycol (PEG) polymer.[48]

The PVP homopolymer is obtained through polymerisation of *N*-vinylpyrrolidone (NVP), normally under free radical polymerisation conditions. For the desired PVP application in this study, it is critical that a well-defined molecular weight, narrow molar mass distribution, and well-preserved end group functionalities of the polymer are obtained. Such merits and competencies in the reversible deactivation radical polymerisation (RDRP) of *N*-vinylpyrrolidone have been established using the reversible addition-fragmentation chain transfer (RAFT) technique.[49] This technique makes use of thiocarbonyl thio reagents, known as RAFT agents [see **Fig. 1.7 (a)**], in the presence of a radical initiator. The RAFT agents impart living characteristics to polymerisation processes between a propagating chain radical and dormant species through successive addition and fragmentation exchange of the radicals.[49a] The macromolecular design via the interchange of xanthates (MADIX) is a type of RAFT polymerisation that specifically entails the use of xanthates, and is more robust and efficient in controlling NVP polymerisation reactions.[50] According to Destarac *et al*.[50a, 51] the rate of addition of unstable propagating radicals (from less activated monomers such as NVP) to the C=S double bond is reduced by delocalisation of the non-bonded electron pairs of the xanthates. The slow exchange of radicals between the dormant and propagating chains enables efficient control of NVP polymerisation. The outstanding advantage of the RAFT/MADIX systems is the flexible design of the RAFT agents that can enable tailored telechelic PVP polymers with reactive end groups.

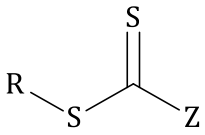

R = Homolytic leaving group; Z = Aryl, alkyl, -NR'$_2$, -OR', -SR'

Figure 1.7 (a) Generic illustration of a RAFT agent. Some polymer chain properties can be achieved by selection of the R and Z end groups at their α- and ω-ends, respectively.[49a]

The reactive end groups in a telechelic polymer confer various polymer characteristics and/or conjugation functionalities.[49a] For the purpose of this study, this feature has been employed to selectively form polymer-drug conjugates at one end of the polymer chain. Amides and esters are among the acid-labile linkers used in polymer-drug conjugates because of their ability to cleave under the acidic tumour microenvironment.[52] These linkers differ in hydrolytic stability under acidic pH. They can therefore be explored in designing pH-responsive polymer-drug conjugates. Thus, aryl esters and aryl amides are acid-labile functional groups that have been considered for hydrolysis in a tumour microenvironment as well as in the lysosomal compartment. It is projected that high vascular density and the extended permeability between endothelial cells of tumour cells will enable selective accumulation and retention of the polymer-drug conjugates.[53] This is known as the enhanced permeability and retention (EPR) effect;[54] the trapped macromolecular prodrugs can release active anti-tumour agents at this pharmacological site or can be taken up by the tumour cells via endocytosis.[55]

A poor metabolic clearance in tumour cells encourages an extended exposure of polymer-drug conjugates to the acidic environment to trigger the release of trapped anti-tumour agents. As a result, hydrolysis of the aryl amides and aryl esters is expected to occur, generating free amines and hydroxyl groups from the β-propionic ester/amide of the polymer-drug conjugate molecule [see route (i) in **Fig. 1.7 (b)**]. A more complicated view of drug release is via a *retro*-Michael addition reaction to yield an α,β-unsaturated carbonyl moiety [see route (ii) in **Fig. 1.7 (b)**]. However, such reversibility is much slower, and is supported under mildly basic conditions.[56] Hence, a different line of focus, reviewing β-elimination in a more favourable light for targeting the tumour environment, requires modification of a thiol functional group. This is not addressed in this work.

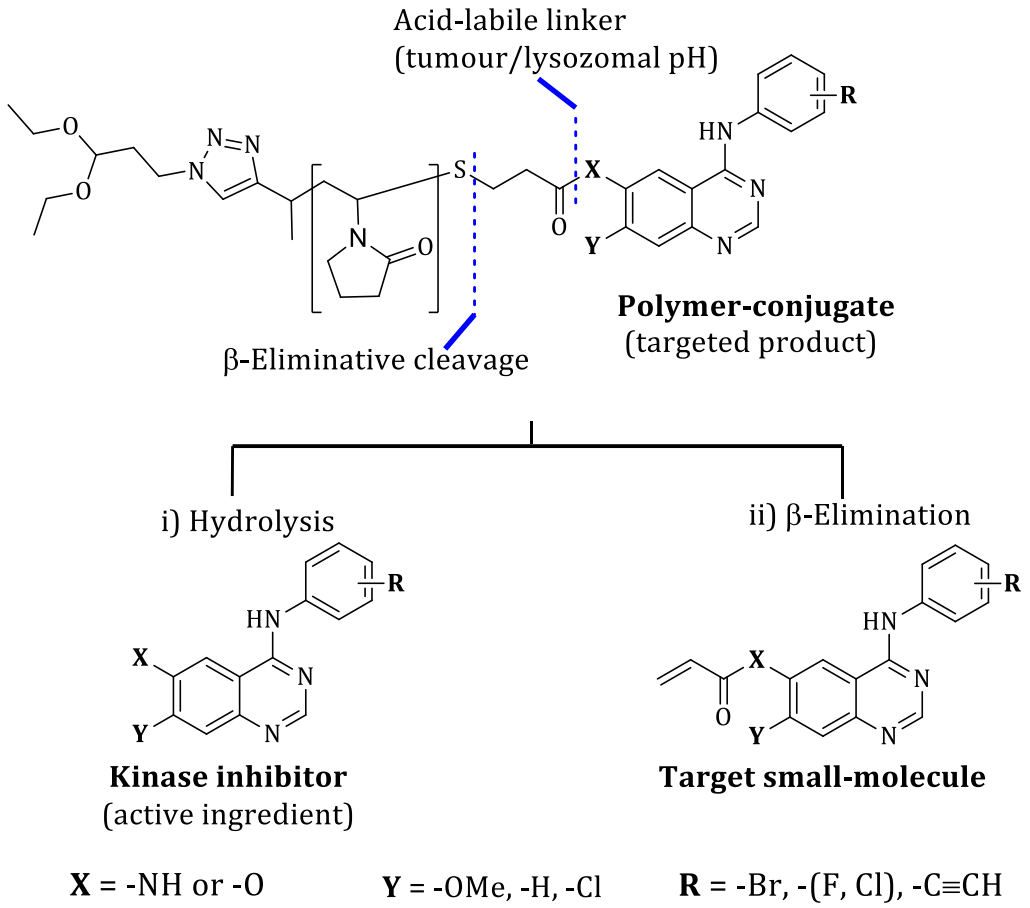

Figure 1.7 (b) Illustration of the target polymer-drug conjugate and modes of drug release.

1.8 Research objectives

In the light of the above discussion, this overall aim of this study is to overcome some of the therapeutic limitations and physiological drug delivery challenges in molecularly targeted therapy of SMKIs. The following research objectives were then formulated:

1. Develop a small library of 4-anilinoquinazoline anti-tumour agents.
2. Synthesise a linear telechelic PVP by RAFT/MADIX-mediated polymerisation.
3. Carry out the modular conjugation of PVP to 4-anilinoquinazolines via Michael addition.
4. Assemble PVP-(4-phenyl amine)quinazoline conjugates into micelles.
5. Evaluate pH-stimulated drug release and anti-tumour efficacy of polymer-drug conjugates *in vitro.*

1.9 Summary

Kinase inhibitors intercept aberrant signal transductions in mutant proteins and guarantee a differentiated cancer therapy. However, the lack of target selectivity and prevalence of EGFR mutations can lead to the requirement for increased drug doses and the possibility of severe adverse effects. Despite the ever-emerging drug resistant mutations, the clinical application of quinazoline-based TKIs is by far the most promising subclass of anti-tumour agents for NSCLC. An attempt to expedite their pharmacological efficacy using micellar drug delivery system is investigated in this study. A more detailed discussion on lung cancer studies and the mechanisms that underlie its therapeutic treatment will be discussed in the next chapter.

1.10 References

1. (a) Vineis, P.; Wild, C. P., *The Lancet* **2014,** *383*, 549-557; (b) Ferlay, J.; Soerjomataram, I.; Dikshit, R.; Eser, S.; Methers, C.; Rebelo, M.; Parkin, D. M.; Bray, F., *International Journal of Cancer* **2015,** *136*, E359-E386.

2. Sadikovic, B.; Al-Romaih, K.; Squire, J. A.; Zielenska, M., *Current Genomics* **2008,** *9*, 394-408.

3. (a) Warburg, O., *Science* **1956,** *123*, 309-314; (b) Warburg, O.; Posener, K.; Negelein, E., *Biochemische Zeitschrift* **1924,** *152*, 399-344.

4. Kroemer, G.; Pouyssegur, J., *Cancer Cell* **2008,** *13*, 472-482.

5. (a) Cairns, R. A.; Harris, I. S.; Mak, T. W., *Nature Reviews Cancer* **2011,** *11*, 85-95; (b) DeBerardinis, R. J.; Lum, J. J.; Hatzivassiliou, G.; Thompson, C. B., *Cell Metabolism* **2008,** *7*, 11-20.

6. (a) Matthews, H. R., *Pharmacology and Therapeutics* **1995,** *67*, 323-350; (b) Taylor, S. S.; Radzio-Andzelm, E.; Hunter, T., *Federation of American Societies for Experimental Biology Journal* **1995,** *9*, 1255-1266.

7. (a) Carpenter, G.; King, L.; Cohen, S., *Journal of Biological Chemistry* **1979,** *254*, 4884-4891; (b) Hunter, T.; Cooper, J. A., *Cell* **1981,** *24*, 741-752.

8. (a) Kim, S.; Lee, J.; Oh, S. J.; Nam, S. J.; Lee, J. E., *Oncology Reports* **2015,** *34*, 1611-1619; (b) Knowlden, J. M.; Hutcheson, I. R.; Jones, H. E.; Madden, T.; Gee, J. M. W.; Harper, M. E.; Barrow, D.; Wakeling, A. E.; Nicholson, R. I., *Endocrinology* **2003,** *144*, 1032-1044.

9. (a) Sainsbury, J. R.; Malcolm, A. J.; Appleton, D. R.; Farndon, J. R.; Harris, A. L., *Journal of Clinical Pathology* **1985,** *38*, 1225-1228; (b) Nicholson, R. I.; Gee, J. M. W.; Harper, M. E., *European Journal of Cancer* **2001,** *37,* 9-15.

10. Fischer, E. H.; Krebs, E. G., *Journal of Biological Chemistry* **1955,** *216*, 121-132.

11. Brunk, U.; Schellens, J.; Westermark, B., *Experimental Cell Research* **1976,** *103*, 295-302.

12. (a) Schlessinger, J., *Cell* **2002,** *110*, 669-672; (b) Hunter, T., *Cell* **2000,** *100*, 113-127.

13. (a) Settleman, J., *Current Biology* **2012,** *22*, R43-R44; (b) Weinstein, I. B., *Science* **2002,** *297*, 63-64.

14. Vogelstein, B.; Papadopoulos, N.; Velculescu, V. E.; Zhou, S.; Diaz, L. A.; Kinzler, K. W., *Science* **2013,** *339*, 1546-1558.

15. (a) Stratton, M. R.; Campbell, P. J.; Futreal, P. A., *Nature* **2009,** *458*, 719-724; (b) Bozic, I.; Gerold, J. M.; Nowak, M. A., *PLOS Computational Biology* **2016,** *12*, e1004731.

16. (a) Weinstein, I. B.; Joe, A. K., *Nature Clinical Practice Oncology* **2006,** *3*, 448-457; (b) Sharma, S. V.; Settleman, J., *Genes and Development* **2007,** *21*, 3214-3231; (c) Weinstein, I. B., *Carcinogenesis* **2000,** *21*, 857-864.

17. Wu, P.; Nielsen, T. E.; Clausen, M. H., *Drug Discovery Today* **2016,** *21*, 5-10.

18. (a) Wakeling, A. E.; Barker, A. J.; Davies, D. H.; Brown, D. S.; Green, L. R.; Cartlidge, S. A.; Woodburn, J. R., *Breast Cancer Research and Treatment* **1996,** *38*, 67-73; (b) Rewcastle, G. W.; Denny, W. A.; Bridges, A. J.; Zhou, H.; Cody, D. R.; McMichael, A.; Fry, D. W., *Journal of Medicinal Chemistry* **1995,** *38*, 3482-3487.

19. Levitzki, A., Annual Review of Pharmacology and Toxicology **2013,** *53*, 161-185.

20. (a) Fukuoka, M.; Yano, S.; Giaccone, G.; Tamura, T.; Nakagawa, K.; Douillard, J.-Y.; Nishiwaki, Y.; Vansteenkiste, J.; Kudoh, S.; Rischin, D.; Eek, R.; Horai, T.; Noda, K.; Takata, I.; Smit, E.; Averbuch, S.; Macleod, A.; Feyereislova, A.; Dong, R.-P.; Baselga, J., *Journal of Clinical Oncology* **2003,** *21*, 2237-2246; (b) Shepherd, F. A.; Rodrigues Pereira, J.; Ciuleanu, T.; Tan, E. H.; Hirsh, V.; Thongprasert, S.; Campos, D.; Maoleekoonpiroj, S.; Smylie, M.; Martins, R.; van Kooten, M.; Dediu, M.; Findlay, B.; Tu, D.; Johnston, D.; Bezjak, A.; Clark, G.; Santabárbara, P.; Seymour, L., *New England Journal of Medicine* **2005,** *353*, 123-132.

21. (a) Zhou, C.; Wu, Y.-L.; Chen, G.; Feng, J.; Liu, X.-Q.; Wang, C.; Zhang, S.; Wang, J.; Zhou, S.; Ren, S.; Lu, S.; Zhang, L.; Hu, C.; Hu, C.; Luo, Y.; Chen, L.; Ye, M.; Huang, J.; Zhi, X.; Zhang, Y.; Xiu, Q.; Ma, J.; You, C., *The Lancet Oncology* **2011,** *12*, 735-742; (b) Park, K.; Tan, E.-H.; O'Byrne, K.; Zhang, L.; Boyer, M.; Mok, T.; Hirsh, V.; Yang, J. C.-H.; Lee, K. H.; Lu, S.; Shi, Y.; Kim, S.-W.; Laskin, J.; Kim, D.-W.; Arvis, C. D.; Kölbeck, K.; Laurie, S. A.; Tsai, C.-M.; Shahidi, M.; Kim, M.; Massey, D.; Zazulina, V.; Paz-Ares, L., *The Lancet Oncology* **2016,** *17*, 577-589.

22. Fry, D. W.; Kraker, A. J.; McMichael, A.; Ambroso, L. A.; Nelson, J. M.; Leopold, W. R.; Connors, R. W.; Bridges, A. J., *Science* **1994,** *265*, 1093-1095.

23. (a) Paez, J. G.; Jänne, P. A.; Lee, J. C.; Tracy, S.; Greulich, H.; Gabriel, S.; Herman, P.; Kaye, F. J.; Lindeman, N.; Boggon, T. J.; Naoki, K.; Sasaki, H.; Fujii, Y.; Eck, M. J.; Sellers, W. R.; Johnson, B. E.; Meyerson, M., *Science* **2004,** *304*, 1497-1500; (b) Lynch, T. J.; Bell, D. W.; Sordella, R.; Gurubhagavatula, S.; Okimoto, R. A.; Brannigan, B. W.; Harris, P. L.; Haserlat,

S. M.; Supko, J. G.; Haluska, F. G.; Louis, D. N.; Christiani, D. C.; Settleman, J.; Haber, D. A., *New England Journal of Medicine* **2004,** *350*, 2129-2139.

24. (a) Travis, W. D.; Brambilla, E.; Burke, A. P.; Marx, A.; Nicholson, A. G., In *WHO classification of tumours*, International Agency for Research on Cancer: Albany, NY, 2015; Vol. 7, pp 9-122; (b) Keedy, V. L.; Temin, S.; Somerfield, M. R.; Beasley, M. B.; Johnson, D. H.; McShane, L. M.; Milton, D. T.; Strawn, J. R.; Wakelee, H. A.; Giaccone, G., *Journal of Clinical Oncology* **2011,** *29*, 2121-2127.

25. Zhou, C.; Yao, L. D., *Journal of Thoracic Oncology* **2016,** *11*, 174-186.

26. (a) Mok, T. S.; Wu, Y.-L.; Thongprasert , S.; Yang, C.-H.; Chu, D.-T.; Saijo, N.; Sunpaweravong, P.; Han, B.; Margono, B.; Ichinose, Y.; Nishiwaki, Y.; Ohe, Y.; Yang, J.-J.; Chewaskulyong, B.; Jiang, H.; Duffield, E. L.; Watkins, C. L.; Armour, A. A.; Fukuoka, M., *New England Journal of Medicine* **2009,** *361*, 947-957; (b) Miller, V. A.; Hirsh, V.; Cadranel, J.; Chen, Y.-M.; Park, K.; Kim, S.-W.; Zhou, C.; Su, W.-C.; Wang, M.; Sun, Y.; Heo, D. S.; Crino, L.; Tan, E.-H.; Chao, T.-Y.; Shahidi, M.; Cong, X. J.; Lorence, R. M.; Yang, J. C.-H., *The Lancet Oncology* **2012,** *13*, 528-538; (c) Rosell, R.; Carcereny, E.; Gervais, R.; Vergnenegre, A.; Massuti, B.; Felip, E.; Palmero, R.; Garcia-Gomez, R.; Pallares, C.; Sanchez, J. M.; Porta, R.; Cobo, M.; Garrido, P.; Longo, F.; Moran, T.; Insa, A.; De Marinis, F.; Corre, R.; Bover, I.; Illiano, A.; Dansin, E.; de Castro, J.; Milella, M.; Reguart, N.; Altavilla, G.; Jimenez, U.; Provencio, M.; Moreno, M. A.; Terrasa, J.; Muñoz-Langa, J.; Valdivia, J.; Isla, D.; Domine, M.; Molinier, O.; Mazieres, J.; Baize, N.; Garcia-Campelo, R.; Robinet, G.; Rodriguez-Abreu, D.; Lopez-Vivanco, G.; Gebbia, V.; Ferrera-Delgado, L.; Bombaron, P.; Bernabe, R.; Bearz, A.; Artal, A.; Cortesi, E.; Rolfo, C.; Sanchez-Ronco, M.; Drozdowskyj, A.; Queralt, C.; de Aguirre, I.; Ramirez, J. L.; Sanchez, J. J.; Molina, M. A.; Taron, M.; Paz-Ares, L., *The Lancet Oncology* **2012,** *13*, 239-246.

27. Gorden, K. J.; Mesbah, P.; Kolesar, J. M., *Journal of Oncology Pharmacy Practice* **2012,** *18*, 245-249.

28. (a) Yun, C.-H.; Mengwasser, K. E.; Toms, A. V.; Woo, M. S.; Greulich, H.; Wong, K.-K.; Meyerson, M.; Eck, M. J., *Proceedings of the National Academy of Sciences of the United States of America* **2008,** *105*, 2070-2075; (b) Pao, W.; Miller, V. A.; Politi, K. A.; Riely, G. J.; Somwar, R.; Zakowski, M. F.; Kris, M. G.; Varmus, H., *PLoS Medicine* **2005,** *2*, e73; (c) Godin-Heymann, N.; Ulkus, L.; Brannigan, B. W.; McDermott, U.; Lamb, J.; Maheswaran, S.; Settleman, J.; Haber, D. A., *Molecular Cancer Therapeutics* **2008,** *7*, 874-879.

29. (a) Fry, D. W.; Bridges, A. J.; Denny, W. A.; Doherty, A.; Greis, K. D.; Hicks, J. L.; Hook, K. E.; Keller, P. R.; Leopold, W. R.; Loo, J. A.; McNamara, D. J.; Nelson, J. M.; Sherwood, V.; Smaill, J. B.; Trumpp-Kallmeyer, S.; Dobrusin, E. M., *Proceedings of the National Academy of Sciences of the United States of America* **1998,** *95*, 12022-12027; (b) Wissner, A.; Johnson, B. D.; Floyd, M. B.; Kitchen, D. B. US 5760041, 02 Jun 1998, 1998.

30. Sullivan, I.; Planchard, D., *Therapeutic Advances in Respiratory Disease* **2016,** *10*, 549-565.

31. Thress, K. S.; Paweletz, C. P.; Felip, E.; Cho, B. C.; Stetson, D.; Dougherty, B.; Lai, Z.; Markovets, A.; Vivancos, A.; Kuang, Y.; Ercan, D.; Matthews, S. E.; Cantarini, M.; Barrett, J. C.; Janne, P. A.; Oxnard, G. R., *Nature Medicine* **2015,** *21*, 560-562.

32. Jia, Y.; Yun, C.-H.; Park, E.; Ercan, D.; Manuia, M.; Juarez, J.; Xu, C.; Rhee, K.; Chen, T.; Zhang, H.; Palakurthi, S.; Jang, J.; Lelais, G.; DiDonato, M.; Bursulaya, B.; Michellys, P.-Y.; Epple, R.; Marsilje, T. H.; McNeill, M.; Lu, W.; Harris, J.; Bender, S.; Wong, K.-K.; Jänne, P. A.; Eck, M. J., *Nature* **2016,** *534*, 129-132.

33. (a) Thompson, A. M.; Murray, D. K.; Elliott, W. L.; Fry, D. W.; Nelson, J. A.; Hollis Showalter, H. D.; Roberts, B. J.; Vincent, P. W.; Denny, W. A.,. *Journal of Medicinal Chemistry* **1997,** *40*, 3915-3925; (b) Tsou, H.-R.; Mamuya, N.; Johnson, B. D.; Reich, M. F.; Gruber, B. C.; Ye, F.; Nilakantan, R.; Shen, R.; Discafani, C.; DeBlanc, R.; Davis, R.; Koehn, F. E.; Greenberger, L. M.; Wang, Y.-F.; Wissner, A., *Journal of Medicinal Chemistry* **2001,** *44*, 2719-2734.

34. (a) Rewcastle, G. W.; Bridges, A. J.; Fry, D. W.; Rubin, J. R.; Denny, W. A., *Journal of Medicinal Chemistry* **1997,** *40*, 1820-1826; (b) Rewcastle, G. W.; Palmer, B. D.; Bridges, A. J.; Showalter, H. D. H.; Sun, L.; Nelson, J.; McMichael, A.; Kraker, A. J.; Fry, D. W.; Denny, W. A., *Journal of Medicinal Chemistry* **1996,** *39*, 918-928.

35. Rewcastle, G. W.; Murray, D. K.; Elliott, W. L.; Fry, D. W.; Howard, C. T.; Nelson, J. M.; Roberts, B. J.; Vincent, P. W.; Hollis Showalter, H. D.; Winters, R. T.; Denny, W. A., *Journal of Medicinal Chemistry* **1998,** *41*, 742-751.

36. (a) Smaill, J. B.; Showalter, H. D. H.; Zhou, H.; Bridges, A. J.; McNamara, D. J.; Fry, D. W.; Nelson, J. M.; Sherwood, V.; Vincent, P. W.; Roberts, B. J.; Elliott, W. L.; Denny, W. A., *Journal of Medicinal Chemistry* **2001,** *44*, 429-440; (b) Smaill, J. B.; Rewcastle, G. W.; Loo, J. A.; Greis, K. D.; Chan, O. H.; Reyner, E. L.; Lipka, E.; Showalter, H. D. H.; Vincent, P. W.; Elliott, W. L.; Denny, W. A., *Journal of Medicinal Chemistry* **2000,** *43*, 1380-1397.

37. Smaill, J. B.; Gonzales, A. J.; Spicer, J. A.; Lee, H.; Reed, J. E.; Sexton, K.; Althaus, I. W.; Zhu, T.; Black, S. L.; Blaser, A.; Denny, W. A.; Ellis, P. A.; Fakhoury, S.; Harvey, P. J.; Hook, K.; McCarthy, F. O. J.; Palmer, B. D.; Rivault, F.; Schlosser, K.; Ellis, T.; Thompson, A. M.; Trachet, E.; Winters, R. T.; Tecle, H.; Bridges, A., *Journal of Medicinal Chemistry* **2016,** *59*, 8103-8124.

38. Smaill, J. B.; Palmer, B. D.; Rewcastle, G. W.; Denny, W. A.; McNamara, D. J.; Dobrusin, E. M.; Bridges, A. J.; Zhou, H.; Showalter, H. D. H.; Winters, R. T.; Leopold, W. R.; Fry, D. W.; Nelson, J. M.; Slintak, V.; Elliot, W. L.; Roberts, B. J.; Vincent, P. W.; Patmore, S. J., *Journal of Medicinal Chemistry* **1999,** *42*, 1803-1815.

39. Wang, J.; Wang, H.; Li, J.; Liu, Z.; Xie, H.; Wei, X.; Lu, D.; Zhuang, R.; Xu, X.; Zheng, S., *ACS Applied Materials and Interfaces* **2016,** *8*, 19228-19237.

40. (a) Khandare, J.; Minko, T., *Progress in Polymer Science* **2006,** *31*, 359-397; (b) Duncan, R.; Vicent, M. J.; Greco, F.; Nicholson, R. I., *Endocrine-Related Cancer* **2005,** *12*, S189-S199.

41. (a) Maeda, H.; Matsumura, Y., Critical Reviews in Therapeutic Drug Carrier Systems **1989,** 6, 193-210; (b) Ringsdorf, H., Journal of Polymer Science: Polymer Symposia **1975,** *51*, 135-153.

42. (a) Taghizadeh, B.; Taranejoo, S.; Monemian, S. A.; Salehi Moghaddam, Z.; Daliri, K.; Derakhshankhah, H.; Derakhshani, Z., *Drug Delivery* **2015,** *22*, 145-155; (b) Estanqueiro, M.; Amaral, M. H.; Conceição, J.; Sousa Lobo, J. M., *Colloids and Surfaces B: Biointerfaces* **2015,** *126*, 631-648.

43. Maeda, H.; Ueda, M.; Morinaga, T.; Matsumoto, T., *Journal of Medicinal Chemistry* **1985,** *28*, 455-461.

44. (a) Kwon, G. S.; Kataoka, K., *Advanced Drug Delivery Reviews* **1995,** *16*, 295-309; (b) Nishiyama, N.; Kataoka, K., *Pharmacology and Therapeutics* **2006,** *112*, 630-648.

45. (a) Townsend, M. W.; Patrick P. Deluca, M. E., *PDA Journal of Pharmaceutical Science and Technology* **1988,** *42*, 190-199; (b) Gaucher, G.; Dufresne, M.-H.; Sant, V. P.; Kang, N.; Maysinger, D.; Leroux, J.-C., *Journal of Controlled Release* **2005,** *109*, 169-188.

46. Ravin , H. A.; Seligman , A. M.; Fine , J., *New England Journal of Medicine* **1952,** *247*, 921-929.

47. Knop, K.; Hoogenboom, R.; Fischer, D.; Schubert, U. S., *Angewandte Chemie International Edition* **2010,** *49*, 6288-6308.

48. (a) Kaneda, Y.; Tsutsumi, Y.; Yoshioka, Y.; Kamada, H.; Yamamoto, Y.; Kodaira, H.; Tsunoda, S.-i.; Okamoto, T.; Mukai, Y.; Shibata, H.; Nakagawa, S.; Mayumi, T., *Biomaterials* **2004,** *25*, 3259-3266; (b) Kamada, H.; Tsutsumi, Y.; Yamamoto, Y.; Kihira, T.; Kaneda, Y.; Mu, Y.; Kodaira, H.; Tsunoda, S.-I.; Nakagawa, S.; Mayumi, T., *Cancer Research* **2000,** *60*, 6416-6420; (c) Kamada, H.; Tsutsumi, Y.; Tsunoda, S.-i.; Kihira, T.; Kaneda, Y.; Yamamoto, Y.; Nakagawa, S.; Horisawa, Y.; Mayumi, T., *Biochemical and Biophysical Research Communications* **1999,** *257*, 448-453.

49. (a) Chiefari, J.; Chong, Y. K.; Ercole, F.; Krstina, J.; Jeffery, J.; Le, T. P. T.; Mayadunne, R. T. A.; Meijs, G. F.; Moad, C. L.; Moad, G.; Rizzardo, E.; Thang, S. H., *Macromolecules* **1998,** *31*, 5559-5562; (b) Nakabayashi, K.; Mori, H., *European Polymer Journal* **2013,** *49*, 2808-2838; (c) Moad, G.; Rizzardo, E.; Thang, S. H., *Australian Journal of Chemistry* **2012,** *65*, 985-1076.

50. (a) Destarac, M.; Bzducha, W.; Taton, D.; Gauthier-Gillaizeau, I.; Zard, S. Z., *Macromolecular Rapid Communications* **2002,** *23*, 1049-1054; (b) Destarac, M.; Brochon, C.; Catala, J.-M.; Wilczewska, A.; Zard, S. Z., *Macromolecular Chemistry and Physics* **2002,** *203*, 2281-2289.

51. Destarac, M.; Charmot, D.; Franck, X.; Zard, S. Z., *Macromolecular Rapid Communications* **2000,** *21*, 1035-1039.

52. (a) Gillies, E. R.; Frechet, J. M. J., *Chemical Communications* **2003,** *40*, 1640-1641; (b) Bachelder, E. M.; Beaudette, T. T.; Broaders, K. E.; Dashe, J.; Fréchet, J. M. J., *Journal of the American Chemical Society* **2008,** *130*, 10494-10495; (c) Rautio, J.; Kumpulainen, H.; Heimbach, T.; Oliyai, R.; Oh, D.; Jarvinen, T.; Savolainen, J., *Nature Reviews Drug Discovery* **2008,** *7*, 255-270.

53. (a) Oueis, E.; Nachon, F.; Sabot, C.; Renard, P.-Y., *Chemical Communications* **2014,** *50*, 2043-2045; (b) Oishi, M.; Nagatsugi, F.; Sasaki, S.; Nagasaki, Y.; Kataoka, K., *ChemBioChem* **2005,** *6*, 718-725; (c) Oishi, M.; Nagasaki, Y.; Itaka, K.; Nishiyama, N.; Kataoka, K., *Journal of the American Chemical Society* **2005,** *127*, 1624-1625.

54. Maeda, H.; Wu, J.; Sawa, T.; Matsumura, Y.; Hori, K., *Journal of Controlled Release* **2000,** *65*, 271-284.

55. (a) de Duve, C.; Wattiaux, R., *Annual Review of Physiology* **1966,** *28*, 435-492; (b) Sengupta, S.; Eavarone, D.; Capila, I.; Zhao, G.; Watson, N.; Kiziltepe, T.; Sasisekharan, R., *Nature* **2005,** *436*, 568-572.

56. Ploemen, J. H. T. M.; van Schanke, B.; Van Ommen, B.; Van Bladeren, P. J., *Cancer Research* **1994,** *54*, 915-919.

Chapter 2: Literature review

Chapter 2: Literature review

Abstract
This chapter addresses lung cancer, with focus on the current treatment options of lung tumours. A recent trend in the stratification of lung cancer patients according to EGFR genetic mutation in tumour cells is highlighted. This is the result of continuous efforts aimed to improve therapeutic responses and the overall patient survival. More importantly, the resurgence of 4-anilinoquinazoline molecules in the treatment of lung cancer patients with EGFR *activating* mutations and the clinical perspective SMKIs is discussed

2.1 Clinical staging of lung cancer and its management options

Predisposition to cancerous lung diseases is frequently the result of long-term exposure to and inhalation of carcinogens, genetic mutations, and occasionally infectious agents.[1] In addition, it is estimated that about 5–10% of individuals are vulnerable to hereditary related epigenetic causes.[2] Regardless of the cause of the disease, poor prognosis and late diagnosis remain critical setbacks for lung cancer patient survival.[3] Acquiring drug resistance is another exacerbating problem that continues to pose a series of hurdles which must be overcome to prolong patient survival. Unfortunately, lung cancer has a heterogeneous tumour composition, both morphologically and genetically.[4] Thus, lung cancer can only be strategically categorised and properly managed by different treatment modalities. Relevant to this observation, this chapter discusses a limited scope of the clinical application of 4-anilinoquinazolines in molecularly targeted kinase therapy in lung tumours.

Lung cancer is presented in different progressive stages: IA, IB, IIA, IIB, IIIA, IIIB, and IV.[5] One of the common problems is that lung cancer patients are often diagnosed at advanced disease stages (IIIB/IV) and this creates the problem of treatment refractory tumours. On these occasions, most patients are considered unfit for surgical intervention and are thus programmed into radiotherapy and/or chemotherapy. Of late, there are emerging treatment options such as the use of biological agents to trigger the immune system.[6] Most of the biological approaches are however still in their experimental stages. In the past five years, immunotherapy has begun to be an active field,[6a] after the results of the first clinical trial was made publicly available. On the other hand, molecularly targeted

therapy, designed to inhibit specific protein kinase signalling pathways, has advanced from a mere clinical approval to a genome-based personalised medicine.[4a]

2.2 Classification of lung tumours

The characterisation of lung tumours has recently been revised and expanded for thoracic oncologists.[3] For a long time, therapeutic intervention of lung cancer was solely influenced by the histological features of tumour cells. The epithelial lung tumours were categorised into small cell lung cancer (SCLC, ~15%) and NSCLC (~85%).[4b] Following recent revisions, NSCLC can be subdivided further into three groups: (i) squamous cell carcinomas, (ii) adenocarcinomas, and (iii) large cell carcinoids [see illustration in **Fig. 2.2**].[3, 5] Adenocarcinomas and squamous tumour cells are the most common lung cancer cases. Molecularly targeted kinase therapy using small molecules finds clinical application in the adenocarcinoma group.

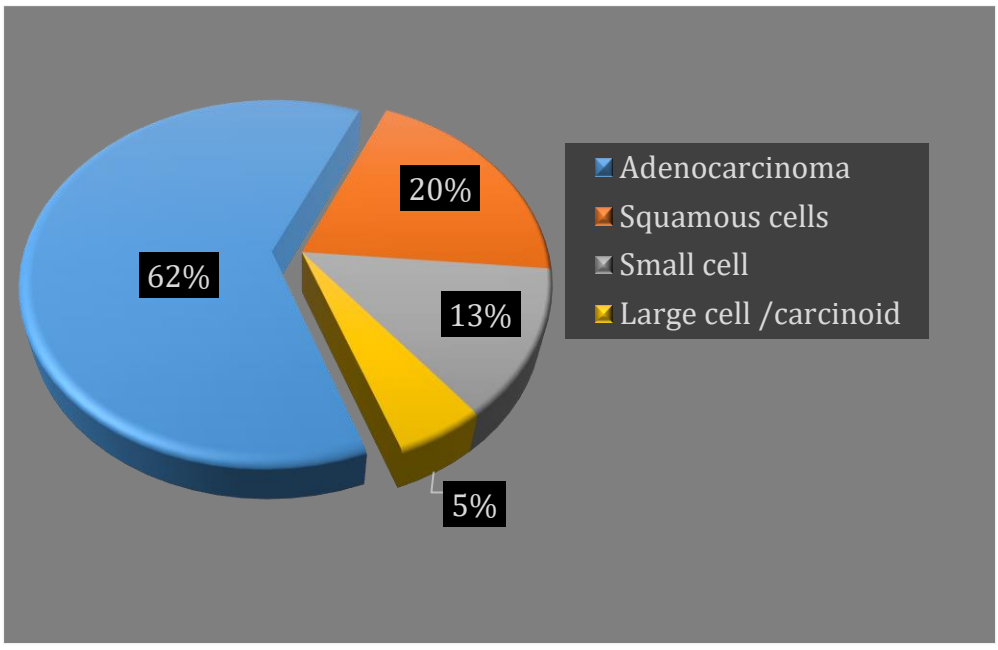

Figure 2.2 Pie chart showing an estimated distribution of different types of tumours found in lung cancer (the NSCLC group comprises adenocarcinoma, squamous cell carcinoma, and large cell carcinoma).[7]

Classification of lung tumours for the purpose of developing a treatment option is a delicate process, particularly because NSCLC tumour cells continually evolve.[8] Substantial morphological and genetic heterogeneity exists among histologically

classified tumours. As a result, immunohistochemistry (IHC) and EGFR genetic screening are now used as additional new tools in tumour classification.[3] The IHC staining is a histological companion that assists in chemical differentiation of cellular and non-cellular tissues, especially when clear cell morphology is not available.[6] Genetic screening is employed in defining EGFR mutations and to stratify patients according to a specific class of SMKIs. For the advanced medical precision of lung cancer treatment, lung tumours are fully characterised using histomorphology, and chemical and genetic differentiation.[3] The suggested treatment plans are earmarked for continuous patient biopsy during the course of treatment, where feasible.[3]

The ability to define genetic variations in tumours of identical histomorphological subgroups is important for the future success of molecularly targeted therapy of kinase inhibitors.[8a] It is generally accepted that intragenic diversity among the tumour cells occurs via distinct pathways of genetic expressions.[4a, 8b] As such, a therapeutic intervention that targets specific protein kinases (the. EGFR TK signalling pathway) can inhibit the oncoprotein function and yield anti-tumour activity.[9] This phenomenon has been reinforced by the use of 4-anilinoquinazoline compounds for clinical application in adenocarcinoma patients with EGFR *activating* mutations. NSCLC adenocarcinoma patients are distributed across many countries and account for >60% of all lung cancer cases.[5] The earlier randomised clinical studies on this group have demonstrated inconsistent therapeutic responses; therefore, genetic variation among the patients was scrutinised.[10] Following this initiative, lung cancer treatment using molecularly targeted kinase inhibition can now be used to predict >70% of favourable therapeutic responses in patients with EGFR mutations.[11]

2.3 EGFR tyrosine kinase as a therapeutic target in lung tumours

EGFR is a member of the human epidermal growth factor receptors (HER/ ErbB), a family of four oncogenic proteins, collectively known as the receptor tyrosine kinases (RTKs). The ErbB family consists of EGRF itself (also referred to as HER1), HER2/ErbB2, HER3/ErbB3, and HER4/ErbB4 homologous receptors.[12] These RTKs encode a similar structural signature of glycoproteins, which are composed of the extracellular ligand binding domain, a single transmembrane lipophilic segment, and a cytoplasmic (or

intracellular) domain. The intracellular domain is of importance as it contains the protein phosphorylation kinase region with the ATP binding pocket, which is successfully used as a therapeutic target in oncology [see the expanded phosphorylation catalysis domain in **Fig. 2.3 (i)**].[12a] EGFR is found in most cells, beyond those of epithelial origin, and has approximately 10^4–10^5 receptors per cell.[12b, 13] The EGFR gene has a full length of 170 KDa, encoded by 28 exons of segmented amino acid sequences.[14] A simplified illustration of four EGFR subunits (divided into colour-coded exons) is shown in **Fig. 2.3 (ii)**.

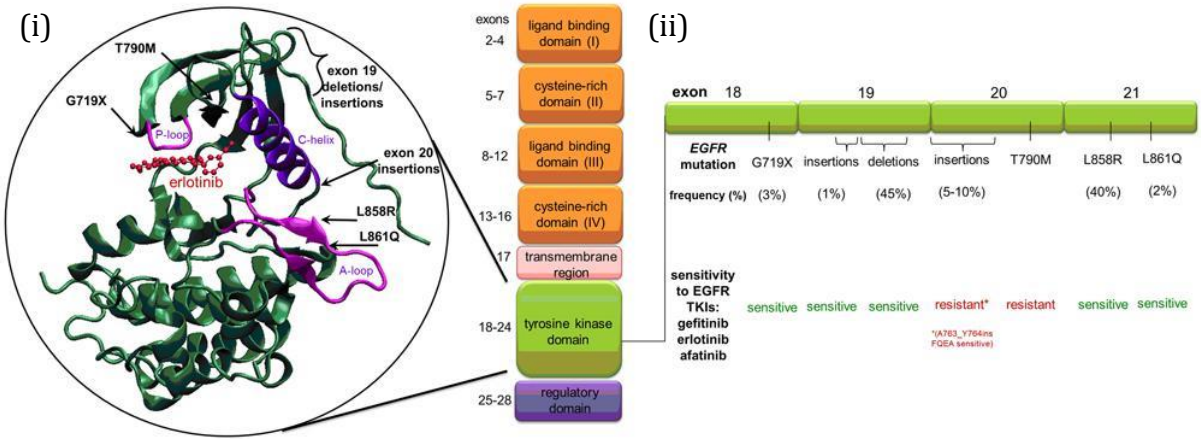

Figure 2.3 Colour-coded structural partitions of EGFR domains. The phosphorylation catalysis domain is shown in a complex with the kinase inhibitor Erlotinib, (i) enlarged to the left. (ii) The EGFR mutation hotspots are enlarged to the right [15] A more expanded view of these illustrations is discussed in later sections.

The extracellular domain of EGFR is divided into four subdomains (I–IV; colour-coded orange in **Fig. 2.3**) and, during a normal signalling process, a sequence of highly modulated biochemical reactions take place. First, the subdomains I and III act as receptor or ligand binding sites for cell surface growth factor proteins.[12a] The growth factor proteins bind to these extracellular receptor subdomains (I and III) to initiate kinase activation. Following binding of the ligands, cysteine-rich subdomains (II and IV) mediate the EGFR dimerisation processes. The EGFR-induced dimerisation process then decodes conformational changes in the intracellular kinase structure (colour-coded green). Consequently, a highly conserved amino acid sequence Asp-Phe-Gly (DFG motif) within the protein phosphorylation domain authenticates ATP to access the binding pocket in order to begin a phosphorylation process.[12] The intracellular phosphorylation

of key tyrosine residues is then mediated by the protein kinases, after which a platform for direct protein–protein interactions with the signal transducers (SH2-proteins) is created. The signal transduction processes are then set to cascade a stream of biochemical reactions to the cell nucleus, thereby modulating cell proliferation and other metabolic activities.[16]

2.4 Overcoming hyperphosphorylation in EGFR tyrosine kinases with 4-anilinoquinazolines

A controlled phosphorylation process is achieved by the balanced catalytic activity of kinases and phosphatases, through opposing phosphorylation and dephosphorylation reactions, respectively.[17] To overcome aberrant kinase phosphorylation activity, 4-anilinoquinazoline inhibitors block the intracellular phosphorylation of EGFR TK by occupying the ATP binding pocket. A closer look at the bound ATP to EGFR TK is colour-coded green in **Fig. 2.4 (i);** the ATP structure is shown in (iii).[18] Once the pocket has been occupied by anti-tumour agents like Gefitinib shown in (ii), phosphorylation reactions and downstream signal transduction cascaded via phosphotransferase channels to the cell nucleus are terminated. As a result, normal cellular processes such as cell division are put on hold. Under these conditions, tumour cells under ATP deficiency undergo autophagic self-cannibalism for limited survival, before they follow a programmed cell death.[19] In view of a so-called oncogenic addiction, these tumour cells undergo oncogenic shock and apoptosis when the signalling pathway has been shut off.

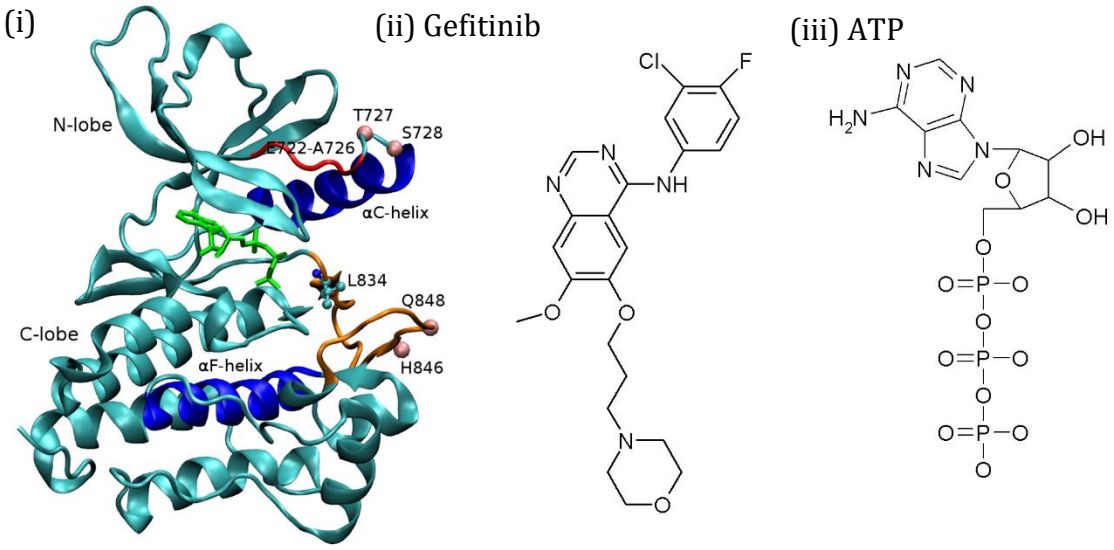

Figure 2.4 Drug-sensitive EGFR mutant (i). in complex with ATP molecule (colour-coded green), (ii) chemical structures of EGFR TK inhibitor Gefitinib and (iii) the endogenous ATP ligand are also shown next to the protein complex.[18]

2.5 Clinically significant EGFR kinase domain mutations in lung tumours

Personalised lung cancer therapy makes use of the differences between genetic profiles of tumour cells, particularly those with EGFR mutant kinases.[10b, 20] In essence, lung tumours have abundant somatic mutations in comparison with other types of cancer, ~150 intragenic mutations per tumour cell.[4a] Thus, lung tumours have a heterogeneous and non-synonymous composition of genetic mutations, which often imposes subtle structural differences in proteins (as in the EGFR kinase phosphorylation catalysis domain). Depending on EGFR mutations, which constitutively lead to a selective tumour proliferation advantage, therapeutic responses to specific conventional treatments can vary from one patient to another. For further clarification, the therapeutic influence of mutations in the EGFR catalytic domain is briefly examined [exons 18–21; see enlarged view in **Fig. 2.5 (a)**].[16a] It should be noted here that recent studies report drug-resistance-inducing mutations for the newly approved 3,4-aminopyridine class of compounds;[21] however, the emphasis here will now be on the T790M and L858R mutations, which are well studied for 4-anilinoquinazoline compounds.

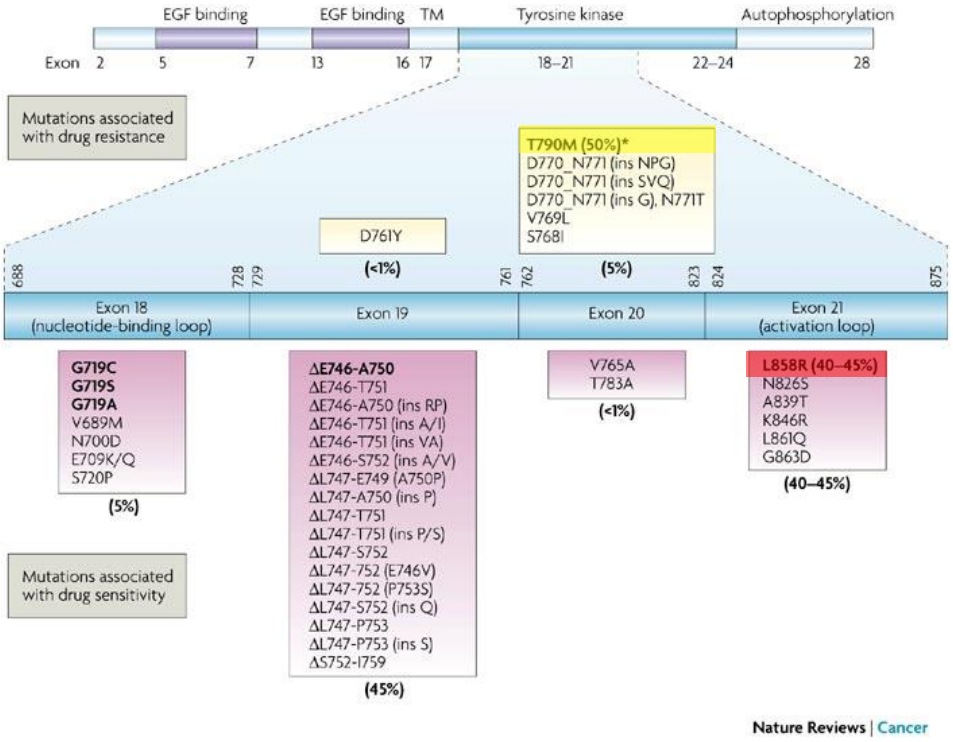

Figure 2.5 (a) Clinically significant mutations for 4-anilinoquinazoline EGFR TKIs. The mutations of interest (T790M in yellow and L858R in red) are highlighted with the more vivid colouring.[16a]

It can be deduced that EGFR mutations can vary per a given segment of amino acid sequence in lung tumours [see exons 18–21 in **Fig. 2.5 (a)**]. In exons 18 and 19, most mutations are substitutions and small amino acid deletions close to the ATP binding pocket, and mostly drug sensitising.[22] Most of these mutations (highlighted in pale purple) are drug sensitising mutations, but an important EGFR *activating* mutation is in exon 21. A missense mutation of a nucleotide substitution, a thymidine to guanidine (T→G), is known to result in further amino acid substitutions, arginine for leucine (L858R), in the activation loop (A-loop) of the ATP binding pocket. The EGFR L858R (highlighted in red) is also known as a 'gain-of-function' mutation because it activates the EGFR signalling and prolongs the ATP phosphorylation. [23] This effect has also been implicated in sensitising tumour cells to ATP-mimetic kinase inhibitors.[23a] The mechanisms elaborating on increased binding affinity of 4-anilinoquinazoline molecules in EGFR L858R have been validated through enzymatic assays and are lately supported by docking studies.[12, 21] These studies have confirmed that mutations in the A-loop affect the critical protein regions involved in ATP ligand recognition.

Another clinically relevant missense mutation is of a cytidine for thymidine (C→T) nucleotide substitution, which gives rise to the development of further auxiliary mutations in exon 20.[24] The infamous EGFR T790M mutation [highlighted with a yellow colour in **Fig. 2.5 (a)**] is caused by a substitution of the methionine for threonine amino acid at the gatekeeping position of the hydrophobic subpocket of the ATP. The presence of T790M encourages drug resistance to EGFR TKIs by causing steric clashes with the aniline ring of 4-anilinoquinazoline kinase inhibitors. This gatekeeping mutation restores the binding affinity of ATP to its binding pocket and revives a selective proliferative advantage to drug-sensitive tumours.[25,26] Further structural illustrations of this secondary mutation are shown with respect to the wild-type and mutant EGFR T790M in **Fig. 2.5 (b)**. The anchor positions such as hydrogen bonding between the 4-anilinoquinazoline N-3 and the protein hinge are lost.[27]

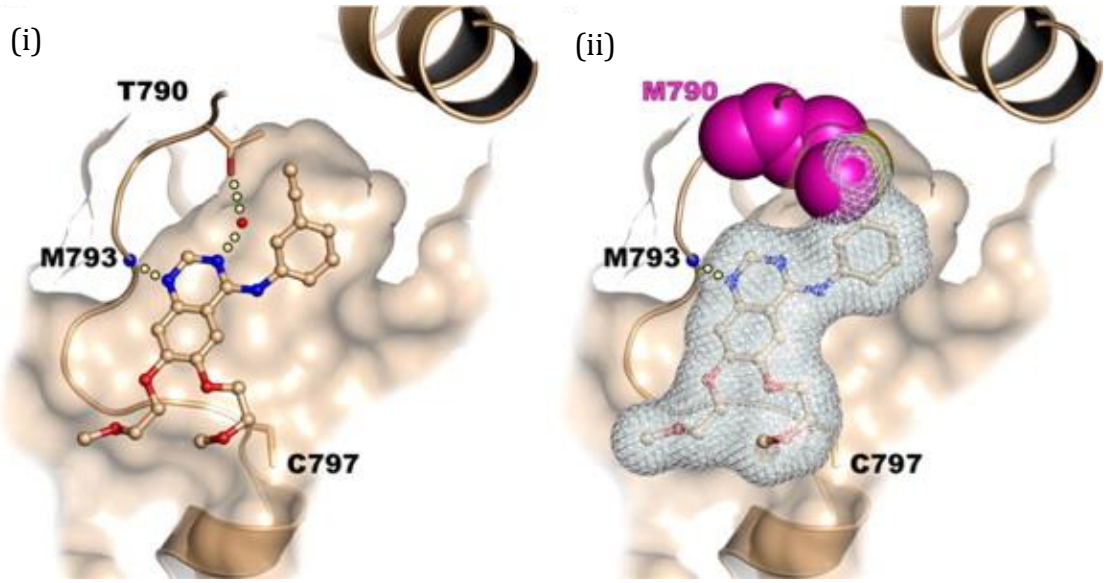

Figure 2.5 (b) Wild-type EGFR in complex with Erlotinib showing the anchoring hydrogen bond between 4-anilinoquinazolines and the protein hinge in the ATP binding pocket (i). EGFR T790M (colour-coded magenta) and its steric clash limits the aniline ring's access to the hydrophobic pocket and reduces the overall optimal binding of the whole molecule (ii).[27]

2.6 Other molecularly targeted therapies for lung cancer patients

Despite the improved tumour responses achieved in recent personalised molecularly targeted kinase therapy,[11] the presence of other oncogenic proteins such as KRAS and BRAF have been proposed to reduce the therapeutic responses in adenocarcinoma patients.[28] The coexistence of EGFR mutations with other oncogenic protein mutations has been implicated in the primary drug resistance to 4-anilinoquinazolines (refer to **Fig. 2.6** for more oncogenic protein mutations).[28a, 29] Lung cancer patients with EGFR mutations are universally represented in the adenocarcinoma histological group, but new mutation drivers have also been characterised and launched as additional therapeutic targets by the US FDA.[30] These newly discovered genetic alterations (ROS1, MET, BRAF, HER2, ALK, RET, FGFR2, PDGFR, and PIK3CA) also have a number of orphan drugs under deveopment at different clinical stages and these are combined alongside the EGFR inhibitors.[4a, 30b, 31] Most of these new targets (BRAF, KRAS, ROS1, and PIK3CA) do not contain receptors *per se*, but they stimulate tumour proliferation via downstream signalling pathways when activated by receptor growth factors, such as EGFR.[32]

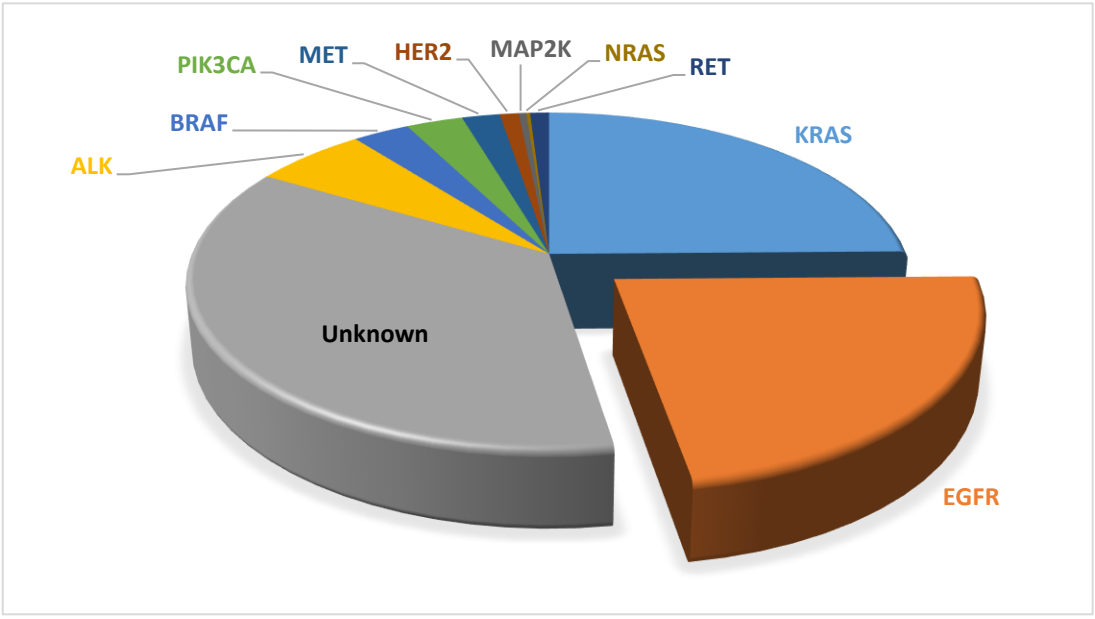

Figure 2.6 Approximate distributions of oncogenic protein mutations found in NSCLC adenocarcinoma.[30b, 33] Most of these mutations are responsible for promoting selective tumour growth advantage but they are less statistically represented across lung cancer patients in comparison to EGFR mutations.

A number of monoclonal antibodies have also been endorsed for clinical practice, especially in breast cancer.[34] The clinical efficacy of these agents in lung cancer has remained controversial, however, as they fail to prevent phosphorylation caused by EGFR mutations found in the extracellular regions.[35] However, necitumumab and pembrolizumab antibodies are currently undergoing phase III clinical trials for lung cancer patients.[36] These antibodies have demonstrated improved overall patient survival when used in a combination therapy with chemotherapy regimens in squamous cell carcinoma patients (constituting about 20% of all lung cancer cases). The general problem with combination therapy involving antibodies in lung cancer treatment is pulmonary bleeding.[37] Unlike the adenocarcinoma patients, squamous cell carcinoma (including large cell carcinoids) patients do not have EGFR mutations, and small-molecule 4-anilinoquinazolines can only be used as palliatives.[38]

2.7 Clinical perspectives for 4-anilinoquinazolines with multiple kinase targets

Targeting of multiple kinase pathways by using EGFR TKIs was accidentally discovered. Very few such inhibitors are currently under clinical pursuit. Vandetanib is an example of a multi-targeting kinase inhibitor of vascular endothelial growth factor receptor (VEGFR-2), EGFR, and RET pro-oncogene.[39] VEGFR-2 is known for stimulating angiogenesis and promoting tumour progression. The angiogenesis process is one of well-documented hallmarks of cancer.[40] For tumour cells to access nutrients from the systemic circulation, they form new micro-vessel sprouts from the existing endothelium blood vessels.[41] As a result of this, tumour cells can successfully proliferate, detach, and migrate, to establish new and distant metastasis colonies. It must be noted, however, that some quinazoline-based clinical drugs (shown in **Fig. 2.7)** are also effective angiogenic inhibitors.

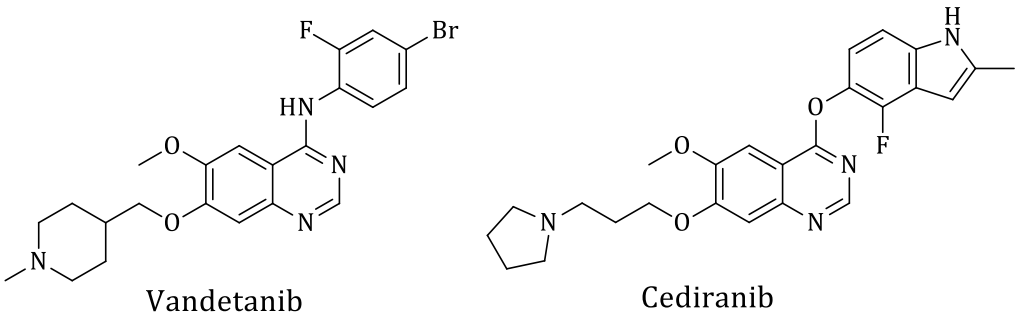

Figure 2.7 Some quinazoline-based angiogenic inhibitors with multi-kinase targeting capabilities, clinically used against RET (Vandetanib) and VEGF-2 (Cediranib).

Among lung tumours, squamous cell carcinomas are highly metastatic and undergo angiogenesis more frequently.[37] The antigiogenic drug Vandetanib possesses a broader inhibitory profile of RTKs (VEGFR-2, EGFR, and RET). It inhibits two independent key pathways of VEGFR and EGFR (together with downstream signalling RET).[39] The multiple kinase targeting capabilities of this compound might possibly delay the onset of EGFR kinase-mediated drug resistance or upregulation of alternative oncogene protein pathways. In spite of this possibility, Vandetanib doses required to elicit pharmacological responses are high, and compromise patient safety, perhaps due to its multi-kinase inhibitory effects.[42] During clinical phase I trials, favourable tumour responses were obtained with ~600 mg/day, but drug-related toxicities were also sustained beyond 300 mg/day.[42] Other pharmacokinetic irregularities included achieving minimal steady-state plasma concentrations after 1 month.[42b] Nevertheless, the encouraging overall objective responses from the lung cancer patients managed to secure further clinical studies for Vandetanib.

Unfortunately, poor patient survival in phase III clinical trials relegated this 4-anilinoquinazoline's approval from the treatment of lung cancer to medullary thyroid cancers with RET mutations.[43] It is therefore safe to conclude that RET mutations in medullary thyroid cancers have persuaded the endorsement of Vandetanib by the US FDA.[44] Late-stage thyroid tumours tend to undergo metastasis via the lymph nodes in the neck, close to sensory areas, which makes therapeutic intervention by radiotherapy or the surgeon's scalpel very challenging. Because of the new beginnings in precision medicine and genomic profiling, RET mutations are also being diagnosed in ~2% NSCLC adenocarcinoma cases.[44c, 45] The efficacy assessment of 4-anilinoquinazolines in

populations harbouring this mutation were not performed in earlier randomised clinical trials, but are now being considered for re-examination, in favour of Vandetanib.[44c]

The discussion above about Vandetanib highlights SMKIs polypharmacology in molecularly targeted therapy. Polypharmacology generally challenges the practical footing and patient safety, but inhibition of multiple targets is also considered ideal for treatment of various cancers.[46] From these multi-targeting kinase inhibitor clinical studies, the associated problem is drug-related systemic toxicities that are concomitant with either elevated doses or drug accumulation over long treatment periods.[43b] One way to overcome this limitation is to explore a more controlled drug delivery and bio-distribution of this small molecule. Thus, the emerging application of nano-delivery in this field is another promising therapeutic avenue to improve target selectivity in tumour cells.[47]

2.8 Structural basis of EGFR selectivity in 4-anilinoquinazolines

The subject of kinase selectivity dominates in the discovery of SMKIs; it is reviewed elsewhere.[48] A more formal presentation of inhibitor selectivity is usually interpreted with reference to the biology of the kinase target. Using the DrugBank database, Wu assigned 25% of the US FDA-approved SMKIs to more than 10 kinase targets.[48b] Aligned with Wu's discovery is the appreciation of a large inventory of chemical scaffolds that display ATP-competitive inhibition kinetics. Most ATP-competitive compounds have been serendipitously discovered by high-throughput screening techniques combined with a limited panel of kinase assays.[49] Over the past decade, the high-throughput screening method has become less practical because of the increased availability of purified kinases, which are prohibitively expensive for screening a large library of compounds. However, this has favoured analogue synthesis (structure-informed design). The optimum structure–activity features required for improving 4-anilinoquinazoline EGFR binding affinity are summarised in **Fig. 2.8**.[50]

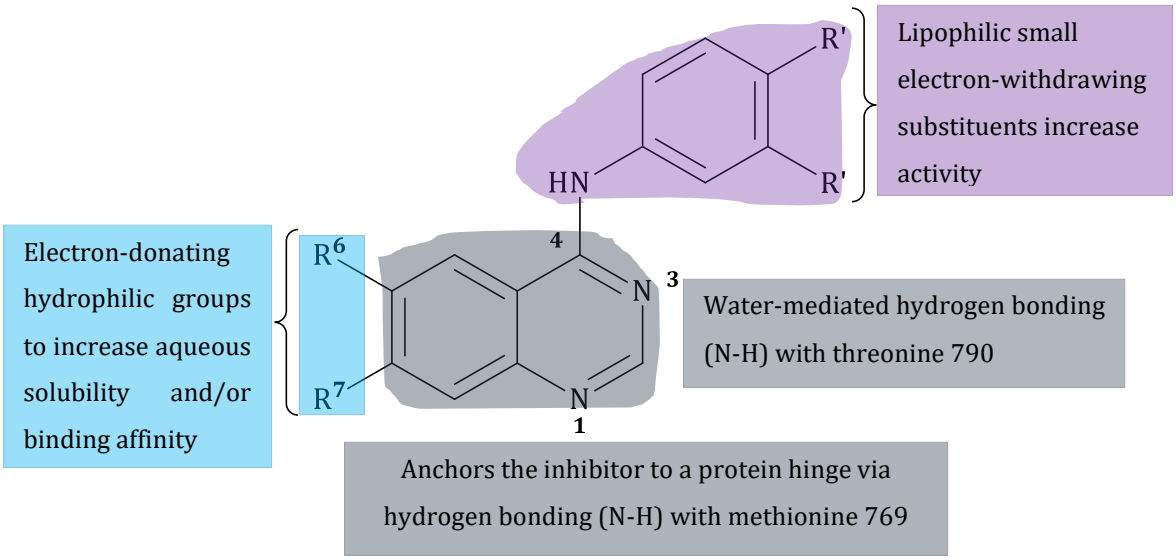

Figure 2.8 Structural basis of 4-anilinoquinazoline EGFR selectivity: the 4-aniline ring (colour-coded purple) occupies the hydrophobic subpocket, quinazoline (colour-coded blue-grey) hydrogen bonding anchors the inhibitor to the protein hinge. The C-6 and C-7 substituents (colour-coded turquoise) can be aqueous solubilising groups or stabilise the overall binding affinity.[50]

Beyond the structure-informed drug design, current efforts involve bioinformatics and molecular biology. These have added kinome-wide selectivity profiling screens for the small molecules to reveal structural complementarity between compounds and the kinase targets.[51] Studies have revealed that gatekeeping amino acids are among the critical determinants of kinase inhibitor binding affinity.[52] The gatekeeping residues occupy a unique region, located at the entrance of a hydrophobic subpocket that is usually occupied by the aniline ring of the 4-anilinoquinazolines. Thus, the identity of these residues can influence the optimal binding of ATP-mimetic compounds such as quinazoline-based kinase inhibitors.[25, 51] According to Backes *et al*.[53] small gatekeeping residues like methionine control the access to the hydrophobic subpocket of the wild-type EGFR. For instance, small gatekeeping residues like threonine offer selective access to EGFR TKIs, while bulkier substituents like methionine impart steric impediments (as in EGFR T790M).[25, 54]

2.9 Selection of 4-anilinoquinazoline compounds for further investigation

In the light of the literature discussed above, our choice of 4-anilinoquinazoline derivatives was that of EGFR SMKIs with known pharmacological activity [PD 153035, Gefitinib and Erlotinib; see **Fig. 2.9 (a)**]. Of note is that PD 153035 has low nanomolar EGFR binding affinity in enzymatic assays and poor aqueous solubility *in vivo*.[55] Although PD 153035 was already discovered in 1994,[55] this compound has not yet been evaluated against EGFR L858R/T790M mutations. Gefitinib and Erlotinib, on the other hand, show decreased potency, by two to three orders of magnitude, against drug resistant EGFR T790M in biochemical assays.[24-25, 55] Pawar *et al*.[56] have demonstrated that a 6,7-dimethoxy structural analogue of Erlotinib is more potent than Erlotinib against EGFR L858R/T790M.

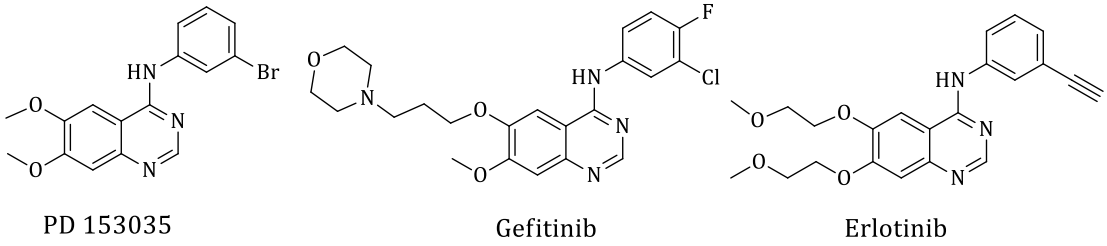

Figure 2.9 (a) Some EGFR SMKIs with known anti-tumour pharmacological activity selected to model our study of 4-anilinoquinazoline compounds.[24-25, 55]

Reflecting on the above three clinical drugs with high EGFR binding affinity and target selectivity, the 4-anilino fragment and the quinazoline skeleton attracted our interest as the core structural requirements for the study. For this class of compounds, it is known that the C-6 and C-7 positions are the optimal substitution positions to improve the solubility and anti-tumour efficacy. Our focus has mainly been to functionalise the C-6 position of these compounds with a linker group that can form covalent conjugation with a biocompatible polymer of interest, *i.e*. PVP. For drug delivery purposes, the position C-7 was intended to be used to influence the rate of drug release, should the conjugates have poor stability under physiological conditions. Hence, structural variations in 4-anilinoquinazoline compounds were formulated as shown in **Fig. 2.9 (b)**.

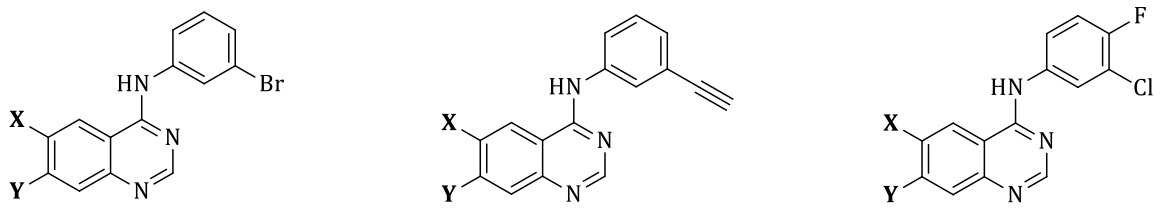

X = -OC(O)C=C, -NHC(O)C=C (Michael acceptors)
Y = -OMe, -H, -Cl

Figure 2.9 (b) Typical examples of 4-anilinoquinazoline compounds with the core structural resemblance to EGRF-selective clinical candidate drugs.

2.10 Michael acceptors in 4-anilinoquinazoline kinase inhibitors as bio-orthogonal cleavable linkers.

The 6,7-dialkoxy-substituted 4-anilinoquinazoline derivatives are potent ATP-competitive EGFR kinase inhibitors.[55, 57] With precedence set by these solubilising groups, irreversible inhibitors have also been developed by attaching a Michael acceptor electrophile at the C-7 position.[50c] The acrylamides are the most studied electrophilic fragments for irreversible inhibition. They have been proven to efficiently overcome *in vivo* competition with endogenous ATP substrates and drug resistance associated with the gatekeeping mutation (EGFR T790M).[58] The Parke-Davies group has demonstrated that the C-6 position is capable of irreversible interaction with nucleophilic cysteine residues.[50c] As a result, the C-7 position is often used for attaching water solubilising groups, while the C-6 position is substituted with Michael acceptor electrophiles [see **Fig. 2.10 (a)**] to alkylate cysteine thiols (Cys 797) adjacent to the ATP-binding pocket.[59] PD 168393 has low plasma concentration in clinical models, while Afatinib and Dacomitinib are used as clinical drugs in the EU for the treatment of NSCLC adenocarcinoma.[60]

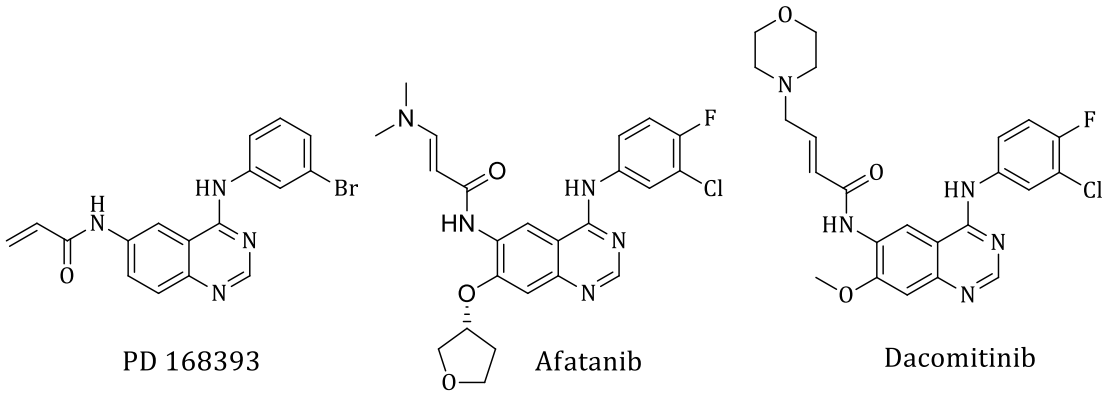

Figure 2.10 (a) Examples of EGFR cysteine targeting 4-anilinoquinazoline irreversible kinase inhibitors with the Michael acceptor at position C-6.

The above irreversible inhibitors [shown in **Fig. 2.10 (a)**] retain high binding affinity and overcome the odds of a direct steric clash with gatekeeping EGFR T790M mutation.[58] The irreversible covalent formation with the EGFR is known to prolong kinase inhibition activity at minimum drug doses, and improves efficacy.[27, 56] In hindsight, reversible ATP-competitive EGFR kinase inhibition activity is well tolerated by normal cells,[48a] but the irreversible covalent formation with 4-anilinoquinazoline results in indiscriminate tumour to non-tumour off-targeting effects. As a result, lung cancer patients under treatment with 4-anilinoquinazoline irreversible inhibitors experience drug-related toxicities due to non-selective inhibition of the wild-type EGFR.[61] This problem underlines the need for improved targeting methods, such as the differential delivery of irreversibly binding anti-tumour agents.

Irreversible covalent inhibitors are often avoided; they have been persistently rejected by the pharmaceutical industries when it comes to treating chronic diseases. This is because continuous exposure to covalent bond forming drugs is associated with increased risks of protein modifications, mutagen formation, and idiosyncratic immune responses.[62] Fortunately, some reviewers have emphasised the risks and therapeutic benefits of covalently binding drugs, which brought about the revival of irreversible kinase inhibitors.[63]

Our line of synthesis in this study is to develop irreversible inhibitors, but use the cysteine-trapping electrophilic group as a linker to the polymer. The strategy is to form a covalent bond to an α,β-unsaturated carbonyl electrophilic moiety via the Michael addition reaction.[64] With this in mind, our synthetic goal is to target 4-

anilinoquinazolines with an acrylamide or acrylate functionality, as shown in **Fig. 2.10 (b)** [*revisited in Chapter 03*].

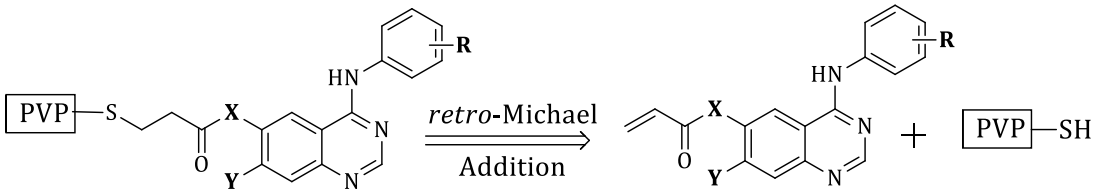

Polymer-drug conjugate
(final product)

Target small molecule
(irreversible kinase inhibitor)

X = -NH or -O **Y** = -OMe, -H, -Cl

R = 4-Anilino substituent(s) -Br, -(F, Cl) and -C≡CH

Figure 2.10 (b) 4-Anilinoquinazolines with acrylamide or acrylate functionality targeted in our synthesis.

2.11 Summary

Lung cancer has low overall patient survival rates because it becomes symptomatic in the late progression stages. At the stage of primary diagnosis, lung tumours have undergone several genetic variations, and this presents a huge difficulty in managing lung cancer treatment. As a result, the treatment landscape in lung cancer is finally shifting towards genetically informed molecularly targeted kinase therapies. This chapter has reflected on the clinical application of 4-anilinoquinazoline kinase inhibitors (reversible and irreversible) against lung tumours. Molecularly targeted kinase therapy is a rapidly evolving field, with new emerging targets and anti-tumour agents alongside EGFR TKIs; however, the discussion has been restricted to 4-anilinoquinazoline molecules.

Our study addresses the use of 4-anilinoquinazoline irreversible inhibitor kinase inhibitors to develop polymer-drug conjugates. These irreversible kinase inhibitors are able to form polymer conjugates under Michael addition conditions, thus creating bio-orthogonal cleavable linkers under a suitable environment of tumour cells. Thus, the synthesis of SMKIs is discussed in the next chapter.

2.12 References

1. Vineis, P.; Wild, C. P., *The Lancet* **2014,** *383*, 549-557.

2. Nagy, R.; Sweet, K.; Eng, C., *Oncogene* **2004,** *23*, 6445-6470.

3. Travis, W. D.; Brambilla, E.; Nicholson, A. G.; Yatabe, Y.; Austin, J. H. M.; Beasley, M. B.; Chirieac, L. R.; Dacic, S.; Duhig, E.; Flieder, D. B.; Geisinger, K.; Hirsch, F. R.; Ishikawa, Y.; Kerr, K. M.; Noguchi, M.; Pelosi, G.; Powell, C. A.; Tsao, M. S.; Wistuba, I., *Journal of Thoracic Oncology* **2015,** *10*, 1243-1260.

4. (a) Vogelstein, B.; Papadopoulos, N.; Velculescu, V. E.; Zhou, S.; Diaz, L. A.; Kinzler, K. W., *Science* **2013,** *339*, 1546-1558; (b) Zugazagoitia, J.; Enguita, A. B.; Nuñez, J. A.; Iglesias, L.; Ponce, S., *Journal of Thoracic Disease* **2014,** *6*, S526-S536.

5. Travis, W. D.; Brambilla, E.; Burke, A. P.; Marx, A.; Nicholson, A. G., In *WHO classification of tumours*, International Agency for Research on Cancer: Albany, NY, 2015; Vol. 7, pp 9-122.

6. (a) Holt, G. E.; Podack, E. R.; Raez, L. E., *Therapy* **2011,** *8*, 43-54; (b) Massarelli, E.; Papadimitrakopoulou, V.; Welsh, J.; Tang, C.; Tsao, A. S., *Translational Lung Cancer Research* **2014,** *3*, 53-63.

7. Bunn, P. A. In *Current status of advanced lung cancer therapy*, 13th International lung cancer congress, Huntington Beach CA, Huntington Beach CA, 2012.

8. (a) CLCGP; NGM, *Science Translational Medicine* **2013,** *5*, 153-209; (b) Kadara, H.; Scheet, P.; Wistuba, I. I.; Spira, A. E., *Cancer Prevention Research* **2016,** *9*, 518-527.

9. Settleman, J., *Current Biology* **2012,** *22*, R43-R44.

10. (a) Fukuoka, M.; Yano, S.; Giaccone, G.; Tamura, T.; Nakagawa, K.; Douillard, J.-Y.; Nishiwaki, Y.; Vansteenkiste, J.; Kudoh, S.; Rischin, D.; Eek, R.; Horai, T.; Noda, K.; Takata, I.; Smit, E.; Averbuch, S.; Macleod, A.; Feyereislova, A.; Dong, R.-P.; Baselga, J., *Journal of Clinical Oncology* **2003,** *21*, 2237-2246; (b) Sharma, S. V.; Settleman, J., *Genes and Development* **2007,** *21*, 3214-3231; (c) Shepherd, F. A.; Rodrigues Pereira, J.; Ciuleanu, T.; Tan, E. H.; Hirsh, V.; Thongprasert, S.; Campos, D.; Maoleekoonpiroj, S.; Smylie, M.; Martins, R.; van Kooten, M.; Dediu, M.; Findlay, B.; Tu, D.; Johnston, D.; Bezjak, A.; Clark, G.; Santabárbara, P.; Seymour, L., *New England Journal of Medicine* **2005,** *353*, 123-132.

11. (a) Gazdar, A. F., *Oncogene* **2009,** *28*, S24-S31; (b) Gazdar, A. F., *Cancer Metastasis Reviews* **2010,** *29*, 37-48.

12. (a) Schlessinger, J., *Cell* **2002,** *110*, 669-672; (b) Carpenter, G.; King, L.; Cohen, S., *Journal of Biological Chemistry* **1979,** *254*, 4884-4891.

13. Hunter, T.; Cooper, J. A., *Cell* **1981,** *24*, 741-752.

14. Reiter, J. L.; Threadgill, D. W.; Eley, G. D.; Strunk, K. E.; Danielsen, A. J.; Schehl Sinclair, C.; Pearsall, R. S.; Green, P. J.; Yee, D.; Lampland, A. L.; Balasubramaniam, S.; Crossley, T. D.; Magnuson, T. R.; James, C. D.; Maihle, N. J., *Genomics* **2001,** *71*, 1-20.

15. Jorge, S.; Kobayashi, S. S.; Costa, D. B., *Brazilian Journal of Medical and Biological Research* **2014,** *47*, 929-939.

16. (a) Sharma, S. V.; Bell, D. W.; Settleman, J.; Haber, D. A., *Nature Reviews Cancer* **2007,** *7*, 169-181; (b) Pawson, T.; Schlessingert, J., *Current Biology* **1993,** *3*, 434-442.

17. Johnson, L. N.; Lowe, E. D.; Noble, M. E. M.; Owen, D. J., *FEBS Letters* **1998,** *430*, 1-11.

18. Wan, S.; Wright, D. W.; Coveney, P. V., *Molecular Cancer Therapeutics* **2012,** *11*, 2394-2400.

19. DeBerardinis, R. J.; Lum, J. J.; Hatzivassiliou, G.; Thompson, C. B., *Cell Metabolism* **2008,** *7*, 11-20.

20. Weinstein, I. B.; Joe, A. K., *Nature Clinical Practice Oncology* **2006,** *3*, 448-457.

21. (a) Wang, S.; Cang, S.; Liu, D., *Journal of Hematology and Oncology* **2016,** *9*, 1-7; (b) Wang, S.; Tsui, S. T.; Liu, C.; Song, Y.; Liu, D., *Journal of Hematology and Oncology* **2016,** *9*, 59.

22. Guimarães, C. R. W.; Rai, B. K.; Munchhof, M. J.; Liu, S.; Wang, J.; Bhattacharya, S. K.; Buckbinder, L., *Journal of Chemical Information and Modeling* **2011,** *51*, 1199-1204.

23. (a) Yun, C. H.; Boggon, T. J.; Li, Y.; Woo, M. S.; Greulich, H.; Meyerson, M.; Eck, M. J., *Cancer Cell* **2007,** *11*, 217-227; (b) Carey, K. D.; Garton, A. J.; Romero, M. S.; Kahler, J.; Thomson, S.; Ross, S.; Park, F.; Haley, J. D.; Gibson, N.; Sliwkowski, M. X., *Cancer Research* **2006,** *66*, 8163-8171.

24. Fujii, A.; Harada, T.; Iwama, E.; Ota, K.; Furuyama, K.; Ijichi, K.; Okamoto, T.; Okamoto, I.; Takayama, K.; Nakanishi, Y., *Cancer Genetics* **2015,** *208*, 271-278.

25. Yun, C.-H.; Mengwasser, K. E.; Toms, A. V.; Woo, M. S.; Greulich, H.; Wong, K.-K.; Meyerson, M.; Eck, M. J., *Proceedings of the National Academy of Sciences of the United States of America* **2008,** *105*, 2070-2075.

26. Godin-Heymann, N.; Ulkus, L.; Brannigan, B. W.; McDermott, U.; Lamb, J.; Maheswaran, S.; Settleman, J.; Haber, D. A., *Molecular Cancer Therapeutics* **2008,** *7*, 874-879.

27. Michalczyk, A.; Klüter, S.; Rode, H. B.; Simard, J. R.; Grütter, C.; Rabiller, M.; Rauh, D., *Bioorganic and Medicinal Chemistry* **2008,** *16*, 3482-3488.

28. (a) Tissot, C.; Couraud, S.; Tanguy, R.; Bringuier, P.-P.; Girard, N.; Souquet, P.-J., *Lung Cancer* **2016,** *91*, 23-28; (b) Dearden, S.; Stevens, J.; Wu, Y. L.; Blowers, D., *Annals of Oncology* **2013,** *24*, 2371-2376.

29. Pao, W.; Wang, T. Y.; Riely, G. J.; Miller, V. A.; Pan, Q.; Ladanyi, M.; Zakowski, M. F.; Heelan, R. T.; Kris, M. G.; Varmus, H. E., *PLoS Medicine* **2005,** *2*, e17.

30. (a) Parsons, A.; Daley, A.; Begh, R.; Aveyard, P., *The British Medical Journal* **2010,** *340*, b5569; (b) Pao, W.; Girard, N., *The Lancet Oncology* **2011,** *12*, 175-180.

31. (a) Jorge, S. E. D. C.; Kobayashi, S. S.; Costa, D. B., Epidermal growth factor receptor (EGFR) mutations in lung cancer: preclinical and clinical data. *Brazilian Journal of Medical and Biological Research* **2014,** *47*, 929-939; (b) Imielinski, M.; Berger, A. H.; Hammerman, P. S.; Hernandez, B.; Pugh, T. J.; Hodis, E.; Cho, J.; Suh, J.; Capelletti, M.; Sivachenko, A.; Sougnez, C.; Auclair, D.; Lawrence, M.; Stojanov, P.; Cibulskis, K.; Choi, K.; de Waal, L.; Sharifnia, T.; Brooks, A.; Greulich, H.; Banerji, S.; Zander, T.; Seidel, D.; Leenders, F.; Ansén, S.; Ludwig, C.; Engel-Riedel, W.; Stoelben, E.; Wolf, J.; Goparju, C.; Thompson, K.; Winckler, W.; Kwiatkowski, D.; Johnson, B. E.; Jänne, P. A.; Miller, V. A.; Pao, W.; Travis, W. D.; Pass, H.; Gabriel, S.; Lander, E.; Thomas, R. K.; Garraway, L. A.; Getz, G.; Meyerson, M., *Cell* **2012,** *150*, 1107-1120; (c) Yamamoto, H.; Toyooka, S.; Mitsudomi, T., *Lung Cancer* **2009,** *63*, 315-321.

32. (a) Boch, C.; Kollmeier, J.; Roth, A.; Stephan-Falkenau, S.; Misch, D.; Grüning, W.; Bauer, T. T.; Mairinger, T., *British Medical Journal (Open)* **2013,** *3*, e002560; (b) Arrieta, O.; Cardona, A. F.; Martín, C.; Más-López, L.; Corrales-Rodríguez, L.; Bramuglia, G.; Castillo-Fernandez, O.; Meyerson, M.; Amieva-Rivera, E.; Campos-Parra, A. D.; Carranza, H.; Gómez de la Torre, J. C.; Powazniak, Y.; Aldaco-Sarvide, F.; Vargas, C.; Trigo, M.; Magallanes-Maciel, M.; Otero, J.; Sánchez-Reyes, R.; Cuello, M., *Journal of Thoracic Oncology* **2015,** *10*, 838-843.

33. Cheng, L.; Alexander, R. E.; MacLennan, G. T.; Cummings, O. W.; Montironi, R.; Lopez-Beltran, A.; Cramer, H. M.; Davidson, D. D.; Zhang, S., *Modern Pathology* **2012,** *25*, 347-369.

34. (a) Reck, M.; Rodríguez-Abreu, D.; Robinson, A. G.; Hui, R.; Csőszi, T.; Fülöp, A.; Gottfried, M.; Peled, N.; Tafreshi, A.; Cuffe, S.; O'Brien, M.; Rao, S.; Hotta, K.; Leiby, M. A.;

Lubiniecki, G. M.; Shentu, Y.; Rangwala, R.; Brahmer, J. R., *New England Journal of Medicine* **2016,** *375*, 1823-1833; (b) Schiller, J. H., *The Lancet Oncology* **2015,** *16*, 738-739.

35. Harley, J. D.; Hsuan, J. J.; Waterfield, M. D., *Oncogene* **1989,** *4*, 273-283.

36. (a) Thatcher, N.; Hirsch, F. R.; Luft, A. V.; Szczesna, A.; Ciuleanu, T. E.; Dediu, M.; Ramlau, R.; Galiulin, R. K.; Bálint, B.; Losonczy, G.; Kazarnowicz, A.; Park, K.; Schumann, C.; Reck, M.; Depenbrock, H.; Nanda, S.; Kruljac-Letunic, A.; Kurek, R.; Paz-Ares, L.; Socinski, M. A., *The Lancet Oncology* **2015,** *16*, 763-774; (b) Langer, C. J.; Gadgeel, S. M.; Borghaei, H.; Papadimitrakopoulou, V. A.; Patnaik, A.; Powell, S. F.; Gentzler, R. D.; Martins, R. G.; Stevenson, J. P.; Jalal, S. I.; Panwalkar, A.; Yang, J. C.-H.; Gubens, M.; Sequist, L. V.; Awad, M. M.; Fiore, J.; Ge, Y.; Raftopoulos, H.; Gandhi, L., *The Lancet Oncology* **2016,** *17*, 1497-1508.

37. Johnson, D. H.; Fehrenbacher, L.; Novotny, W. F.; Herbst, R. S.; Nemunaitis, J. J.; Jablons, D. M.; Langer, C. J.; III, R. F. D.; Gaudreault, J.; Damico, L. A.; Holmgren, E.; Kabbinavar, F., *Journal of Clinical Oncology* **2004,** *22*, 2184-2191.

38. (a) Hirsch, F. R.; Herbst, R. S.; Gandara, D. R., *The Lancet Oncology* **2015,** *16*, 872-873; (b) Cappuzzo, F.; Ciuleanu, T.; Stelmakh, L.; Cicenas, S.; Szczésna, A.; Juhász, E.; Esteban, E.; Molinier, O.; Brugger, W.; Melezínek, I.; Klingelschmitt, G.; Klughammer, B.; Giaccone, G., *The Lancet Oncology* **2010,** *11*, 521-529.

39. Wedge, S. R.; Ogilvie, D. J.; Dukes, M.; Kendrew, J.; Chester, R.; Jackson, J. A.; Boffey, S. J.; Valentine, P. J.; Curwen, J. O.; Musgrove, H. L.; Graham, G. A.; Hughes, G. D.; Thomas, A. P.; Stokes, E. S. E.; Curry, B.; Richmond, G. H. P.; Wadsworth, P. F.; Bigley, A. L.; Hennequin, L. F., *Cancer Research* **2002,** *62*, 4645-4655.

40. Hanahan, D.; Weinberg, Robert A., *Cell* **2011,** *144*, 646-674.

41. (a) Cox, G.; Jones, J. L.; Walker, R. A.; Steward, W. P.; O'Byrne, K. J., *Lung Cancer* **2000,** *27*, 81-100; (b) Holmes, K.; Roberts, O. L.; Thomas, A. M.; Cross, M. J., *Cellular Signalling* **2007,** *19*, 2003-2012.

42. (a) Holden, S. N.; Eckhardt, S. G.; Basser, R.; de Boer, R.; Rischin, D.; Green, M.; Rosenthal, M. A.; Wheeler, C.; Barge, A.; Hurwitz, H. I., *Annals of Oncology* **2005,** *16*, 1391-1397; (b) Tamura, T.; Minami, H.; Yamada, Y.; Yamamoto, N.; Shimoyama, T.; Murakami, H.; Horiike, A.; Fujisaka, Y.; Shinkai, T.; Tahara, M.; Kawada, K.; Ebi, H.; Sasaki, Y.; Jiang, H.; Saijo, N., *Journal of Thoracic Oncology* **2006,** *1*, 1002-1009.

43. (a) Natale, R. B.; Bodkin, D.; Govindan, R.; Sleckman, B. G.; Rizvi, N. A.; Capó, A.; Germonpré, P.; Eberhardt, W. E. E.; Stockman, P. K.; Kennedy, S. J.; Ranson, M., *Journal of Clinical Oncology* **2009,** *27*, 2523-2529; (b) Lee, J. S.; Hirsh, V.; Park, K.; Qin, S.; Blajman,

C. R.; Perng, R.-P.; Chen, Y.-M.; Emerson, L.; Langmuir, P.; Manegold, C., *Journal of Clinical Oncology* **2012,** *30*, 1114-1121.

44. (a) Klein, J. D.; Christopoulos, A.; Ahn, S. M.; Gooding, W. E.; Grandis, J. R.; Kim, S., *Head and neck* **2012,** *34*, 1269-1276; (b) DeLellis, R. A., *Journal of Surgical Oncology* **2006,** *94*, 662-669; (c) Kohno, T., *Translational Cancer Research* **2016,** *4*, S237-S239.

45. Takeuchi, K.; Soda, M.; Togashi, Y.; Suzuki, R.; Sakata, S.; Hatano, S.; Asaka, R.; Hamanaka, W.; Ninomiya, H.; Uehara, H.; Lim Choi, Y.; Satoh, Y.; Okumura, S.; Nakagawa, K.; Mano, H.; Ishikawa, Y., *Nature Medicine* **2012,** *18*, 378-381.

46. (a) Zhou, Y.; Zhang, Y.; Zou, H.; Cai, N.; Chen, X.; Xu, L.; Kong, X.; Liu, P., *Scientific Reports* **2015,** *5*, 8629; (b) Fabian, M. A.; Biggs, W. H.; Treiber, D. K.; Atteridge, C. E.; Azimioara, M. D.; Benedetti, M. G.; Carter, T. A.; Ciceri, P.; Edeen, P. T.; Floyd, M.; Ford, J. M.; Galvin, M.; Gerlach, J. L.; Grotzfeld, R. M.; Herrgard, S.; Insko, D. E.; Insko, M. A.; Lai, A. G.; Lelias, J.-M.; Mehta, S. A.; Milanov, Z. V.; Velasco, A. M.; Wodicka, L. M.; Patel, H. K.; Zarrinkar, P. P.; Lockhart, D. J., A small molecule-kinase interaction map for clinical kinase inhibitors. *Nature Biotechnology* **2005,** *23*, 329-336.

47. Wang, J.; Wang, H.; Li, J.; Liu, Z.; Xie, H.; Wei, X.; Lu, D.; Zhuang, R.; Xu, X.; Zheng, S., *ACS Applied Materials and Interfaces* **2016,** *8*, 19228-19237.

48. (a) Zhang, J.; Yang, P. L.; Gray, N. S., *Nature Reviews Cancer* **2009,** *9*, 28-39; (b) Wu, P.; Nielsen, T. E.; Clausen, M. H., *Drug Discovery Today* **2016,** *21*, 5-10.

49. (a) Barker, A. J.; Davies, D. H. 1992; (b) Ward, W. H. J.; Cook, P. N.; Slater, A. M.; Davies, D. H.; Holdgate, G. A.; Green, L. R., *Biochemical Pharmacology* **1994,** *48*, 659-666.

50. (a) Rewcastle, G. W.; Palmer, B. D.; Bridges, A. J.; Showalter, H. D. H.; Sun, L.; Nelson, J.; McMichael, A.; Kraker, A. J.; Fry, D. W.; Denny, W. A., *Journal of Medicinal Chemistry* **1996,** *39*, 918-928; (b) Garuti, L.; Roberti, M.; Bottegoni, G., *Current Medicinal Chemistry* **2010,** *17*, 2804-2821; (c) Fry, D. W.; Bridges, A. J.; Denny, W. A.; Doherty, A.; Greis, K. D.; Hicks, J. L.; Hook, K. E.; Keller, P. R.; Leopold, W. R.; Loo, J. A.; McNamara, D. J.; Nelson, J. M.; Sherwood, V.; Smaill, J. B.; Trumpp-Kallmeyer, S.; Dobrusin, E. M., *Proceedings of the National Academy of Sciences of the United States of America* **1998,** *95*, 12022-12027.

51. Smyth, L. A.; Collins, I., *Journal of Chemical Biology* **2009,** *2*, 131-151.

52. Kobayashi , S.; Boggon , T. J.; Dayaram , T.; Jänne , P. A.; Kocher , O.; Meyerson , M.; Johnson , B. E.; Eck , M. J.; Tenen , D. G.; Halmos , B., *New England Journal of Medicine* **2005,** *352*, 786-792.

53. Backes, A. C.; Zech, B.; Felber, B.; Klebl, B.; Müller, G., *Expert Opinion on Drug Discovery* **2008,** *3*, 1409-1425.

54. Pao, W.; Miller, V. A.; Politi, K. A.; Riely, G. J.; Somwar, R.; Zakowski, M. F.; Kris, M. G.; Varmus, H., *PLoS Medicine* **2005,** *2*, e73.

55. Fry, D. W.; Kraker, A. J.; McMichael, A.; Ambroso, L. A.; Nelson, J. M.; Leopold, W. R.; Connors, R. W.; Bridges, A. J., *Science* **1994,** *265*, 1093-1095.

56. Pawar, V. G.; Sos, M. L.; Rode, H. B.; Rabiller, M.; Heynck, S.; van Otterlo, W. A. L.; Thomas, R. K.; Rauh, D., *Journal of Medicinal Chemistry* **2010,** *53*, 2892-2901.

57. Bridges, A. J.; Zhou, H.; Cody, D. R.; Rewcastle, G. W.; McMichael, A.; Showalter, H. D. H.; Fry, D. W.; Kraker, A. J.; Denny, W. A., *Journal of Medicinal Chemistry* **1996,** *39*, 267-276.

58. Kwak, E. L.; Sordella, R.; Bell, D. W.; Godin-Heymann, N.; Okimoto, R. A.; Brannigan, B. W.; Harris, P. L.; Driscoll, D. R.; Fidias, P.; Lynch, T. J.; Rabindran, S. K.; McGinnis, J. P.; Wissner, A.; Sharma, S. V.; Isselbacher, K. J.; Settleman, J.; Haber, D. A., *Proceedings of the National Academy of Sciences of the United States of America* **2005,** *102*, 7665-7670.

59. Tsou, H.-R.; Mamuya, N.; Johnson, B. D.; Reich, M. F.; Gruber, B. C.; Ye, F.; Nilakantan, R.; Shen, R.; Discafani, C.; DeBlanc, R.; Davis, R.; Koehn, F. E.; Greenberger, L. M.; Wang, Y.-F.; Wissner, A., *Journal of Medicinal Chemistry* **2001,** *44*, 2719-2734.

60. Garuti, L.; Roberti, M.; Bottegoni, G., *Current Medicinal Chemistry* **2011,** *18*, 2981-2994.

61. (a) Sequist, L. V.; Soria, J. C.; Goldman, J. W.; Wakelee, H. A.; Gadgeel, S. M.; Varga, A.; Papadimitrakopoulou, V.; Solomon, B. J.; Oxnard, G. R.; Dziadziuszko, R.; Aisner, D. L.; Doebele, R. C.; Galasso, C.; Garon, E. B.; Heist, R. S.; Logan, J.; Neal, J. W.; Mendenhall, M. A.; Nichols, S.; Piotrowska, Z.; Wozniak, A. J.; Raponi, M.; Karlovich, C. A.; Jaw-Tsai, S.; Isaacson, J.; Despain, D.; Matheny, S. L.; Rolfe, L.; Allen, A. R.; Camidge, D. R., *The New England Journal of Medicine* **2015,** *372*, 1700-1709; (b) Cross, D. A. E.; Ashton, S. E.; Ghiorghiu, S.; Eberlein, C.; Nebhan, C. A.; Spitzler, P. J.; Orme, J. P.; Finlay, M. R. V.; Ward, R. A.; Mellor, M. J.; Hughes, G.; Rahi, A.; Jacobs, V. N.; Brewer, M. R.; Ichihara, E.; Sun, J.; Jin, H.; Ballard, P.; Al-Kadhimi, K.; Rowlinson, R.; Klinowska, T.; Richmond, G. H. P.; Cantarini, M.; Kim, D.-W.; Ranson, M. R.; Pao, W., *Cancer Discovery* **2014,** *4*, 1046-1061.

62. (a) Nakayama, S.; Atsumi, R.; Takakusa, H.; Kobayashi, Y.; Kurihara, A.; Nagai, Y.; Nakai, D.; Okazaki, O., *Drug Metabolism and Disposition* **2009,** *37*, 1970-1977; (b) Ikeda, T., *Drug Metabolism and Pharmacokinetics* **2011,** *26*, 60-70.

63. (a) Singh, J.; Petter, R. C.; Baillie, T. A.; Whitty, A., *Nature Reviews Drug Discovery* **2011,** *10*, 307-317; (b) Potashman, M. H.; Duggan, M. E., *Journal of Medicinal Chemistry* **2009,** *52*, 1231-1246.

64. Singha, N. K.; Gibson, M. I.; Koiry, B. P.; Danial, M.; Klok, H.-A., *Biomacromolecules* **2011,** *12*, 2908-2913.

Chapter 3: Synthesis of small molecules

Chapter 3: Synthesis of small molecules

Abstract
This chapter focuses on the synthesis of 4-anilinoquinazoline small molecules containing the electrophilic Michael acceptor (an acrylamide or an acrylate) in the C-6 position. The quinazolin-4(3*H*)-one skeleton was used as the template for the synthesis of 4-anilinoquinazoline derivatives. The synthetic approaches and characterisation methods used in the preparation of quinazoline compounds are discussed.

3.1 Synthesis of quinazolin-4(3H)-one

Alkaloids containing a quinazoline structure are compounds of interest for diverse medicinal applications.[1] The 4-oxo-derivative of quinazoline, which is more correvtly cited as quinazolin-4(3*H*)-one, is an important intermediate in the synthesis of 4-anilinoquinazoline small-molecule TKIs. The medicinal application of this skeleton has had some noteworthy, but rather inflexible, synthetic advances. An exhaustive review on different synthetic methods and the classification of quinazoline derivatives is available in literature.[2] Among the prominent investigators who synthesised quinazolinone and quinazoline motifs were Niemenstowski in the late 1800s and Gabriel in early 1900s.[3]

To date, the Niementowski protocol continues to be among the most attractive routes in the synthesis of the quinazolin-4(3*H*)-one moieties. This simple procedure is based on the thermally promoted formal condensation and cyclisation between a bifunctional 2-aminobenzoic acid derivative and an amide (refer to **Fig. 3.1**).[3a] The quinazolin-4(3*H*)-ones formed under these conditions are known to exist in tautomeric forms, which interconvert through a proton shift. The amidic acid and amide constitutional isomer forms are the most stable and commonly encountered prototropic tautomers. The formation of the amidic acid isomer is usually influenced by the acidic pH of the reaction medium, but the amide isomer is the thermodynamically more favourable isomer. Apart from the long-standing use of the Niementowski reaction, an appealing alternative is a two-step transformation process of 2-aminobenzonitrile into 4-anilinoquinazolines via a Dimroth-type of rearrangement reaction.[4] However, a challenge to the application of this method is commercial scarcity of suitably substituted 2-aminobenzonitrile synthons.

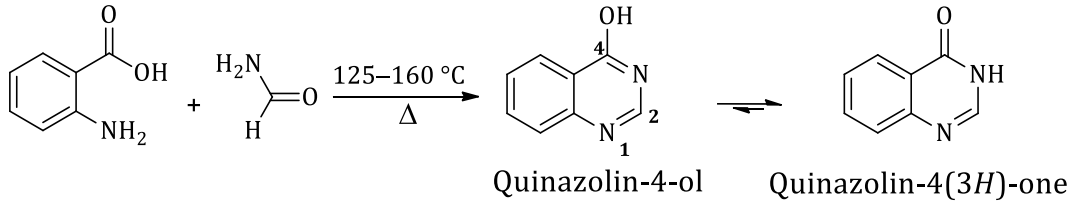

Figure 3.1 The Niementowski synthesis of quinazolinones. The amidic acid and amide quinazolinone isomers are shown.

The focus in this chapter is the preparation of 4-anilinoquinazoline moieties. Here, the required quinazolin-4(3*H*)-one intermediates were prepeared via the Niementowski approach. Despite the widespread application of quinazoline derivatives, most of the starting materials required for the synthesis of these compounds are either commercially unavailable or only available at significant cost. Hence, most the synthetic intermediates reported in this work were prepared in-house. After carefully examining the chemistry of quinazoline compounds, it was concluded that creating the substituted quinazolin-4(3*H*)-one skeleton served as a good starting point for our synthetic studies.

3.2 Towards the synthesis of substituted 4-anilinoquinazoline compounds

In line with developing polymer-drug conjugates via covalent bonding, the foremost evaluations of the final products would involve assessing the chemistry of the linker groups (the hydrolytic stability). The intention would be to establish the pharmacokinetic drug release profile, recovery of anti-tumour agents, and ultimately anti-tumour efficacy of the conjugates.[5] The synthetic requirements for constructing C-6-substituted quinazoline derivatives were twofold: (i) the first synthetic route was directed at generating compounds with amide linker groups, and (ii) the other route was directed at compounds that would form the ester linkage. The two end products are shown in **Fig. 3.2**.

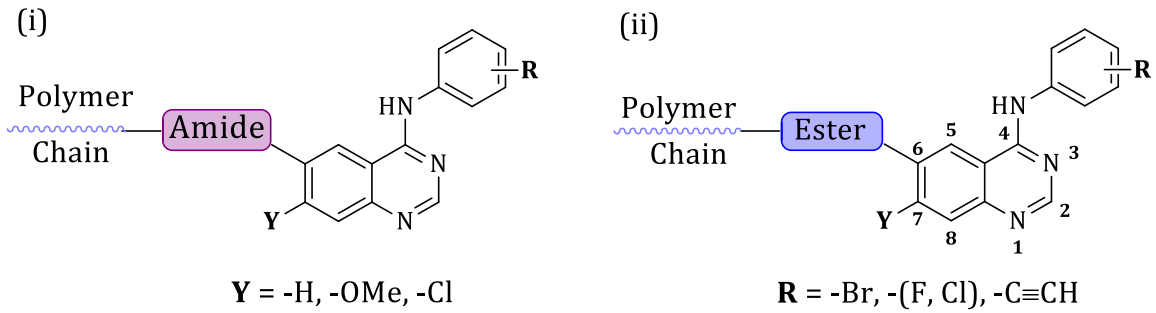

Y = -H, -OMe, -Cl

R = -Br, -(F, Cl), -C≡CH

Figure 3.2 The end products in the synthesis of polymer-bound 4-anilinoquinazoline anti-tumour agents.

In view of these final products, the rate at which the consigned drug load would be released from the polymer chain (assembled into micelles) was also important. One way to control the hydrolytic cleavage of the acid-labile group on the aromatic ring was to perturb the overall electron density around the quinazoline ring by either adding electron-withdrawing or -donating groups to the C-7 position. Methoxy substituents in 4-anilinoquinazoline anti-tumour agents are generally known to improve anti-tumour efficacy as electron donors.[6] They have also been used to influence drug release rates in covalently conjugated molecules with aromatic systems by enhancing cleavage of the linkers in mild acidic environments.[7]

Thus, 7-methoxy-substituted quinazoline derivatives were synthesised with the intention to promote the cleavage of quinazoline acid-labile linkers. On the contrary, electron-withdrawing groups were meant to slow down the rate of drug release.[8] The chloro group was selected based on its availability as one of the synthetic intermediates during the synthesis of quinazolinone derivatives. However, the 7-chloroquinazolinone intermediates for ester derivatives were not prepared as synthetic difficulties were encountered in the final steps of 7-chloro-substituted 4-anilinoquinazolines.

3.3 Synthesis of 6-nitroquinazolin-4(3H)-one derivatives

The requirement for preparing 6-aminoquinazolin-4(3*H*)-one derivatives could be achieved by either (i) applying the Niementowski protocol to 2-amino-5-nitrobenzoic acid and formamide, or (ii) nitration of quinazolin-4(3*H*)-one via electrophilic aromatic substitution [see **Fig. 3.3 (a)**].[9] The synthetic plan appeared straightforward; however, 2-

methylaniline was the starting material that was available (prepared in-house). Thus, one of the preliminary steps turned out to be the preparation of the 2-amino-5-nitrobenzoic acid precursor for the direct synthesis of 6-nitroquinazolin-4(3*H*)-one.

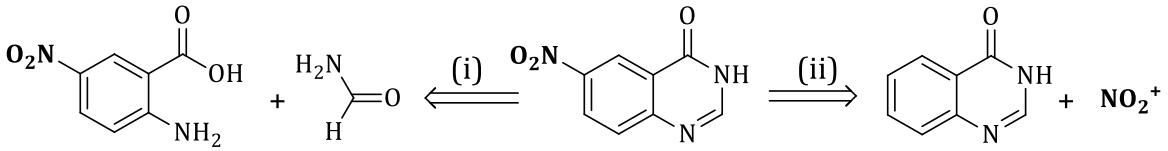

2-Amino-5-nitrobenzoic acid (precursor 1)

Quinazolin-4(*3H*)-one (precursor 2)

Figure 3.3 (a) Synthetic pathways towards 6-nitroquinazolin-4(3*H*)-one via (i) the Niementowski protocol and (ii) electrophilic aromatic substitution.

The planned synthetic steps of 2-amino-5-nitrobenzoic acid are shown in **Fig. 3.3 (b)**. It was envisaged that aniline would be protected as the *N*-acetamide (***1***) to enable selective *para*-directed nitration, thus affording compound ***2***.[10] Oxidation of the aryl methyl group of ***2*** followed by amide bond hydrolysis of ***3*** would yield the required precursor ***1***.

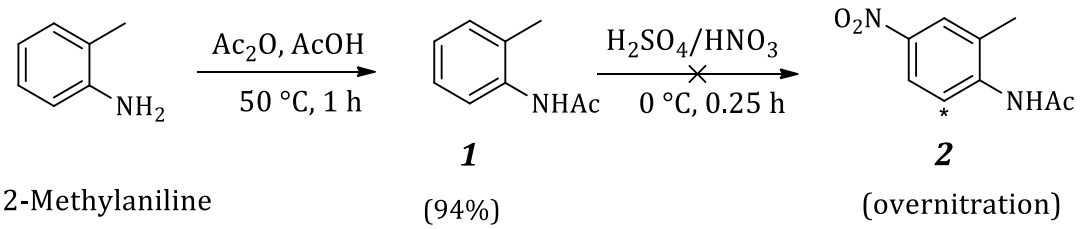

2-Methylaniline

1

(94%)

2

(overnitration)

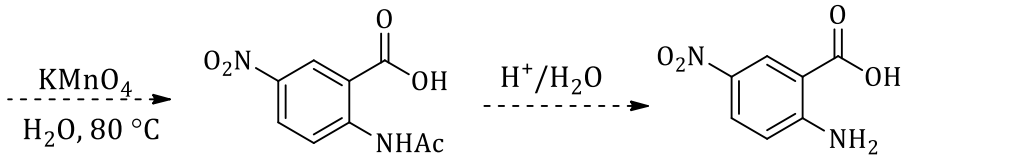

3

2-Amino-5-nitrobenzoic acid

Figure 3.3 (b) Attempted preparation of 5-nitrobenzoic acid from 2-methylaniline as starting material. (*Potential additional nitration position in compound ***2***.)

With regards to the preparation plan in **Fig. 3.3 (b)**, *N*-acylation of 2-methylaniline was carried out using acetic anhydride in acetic acid solvent, affording *N*-(2-methylphenyl)acetamide (***1)*** in good yield (94%). Unaware of the difficulties associated with controlling the nitration reaction for substituted acetanilide moieties, efforts to introduce the nitro group regioselectively at low temperatures using dilute HNO_3 (40%

max.) were unsuccessful. The presence of activating or deactivating substituents on the aromatic system usually defines the reaction conditions, but the major problem here was finding the optimum conditions for selective nitration. Because overnitration took place, it was decided to follow route (ii) in **Fig. 3.3 (a)**, using ***1*** as starting material, for the preparation of quinazolin-4(3 *H*)-one.[9] Continuation of the synthesis is shown in **Fig. 3.3 (c)**.

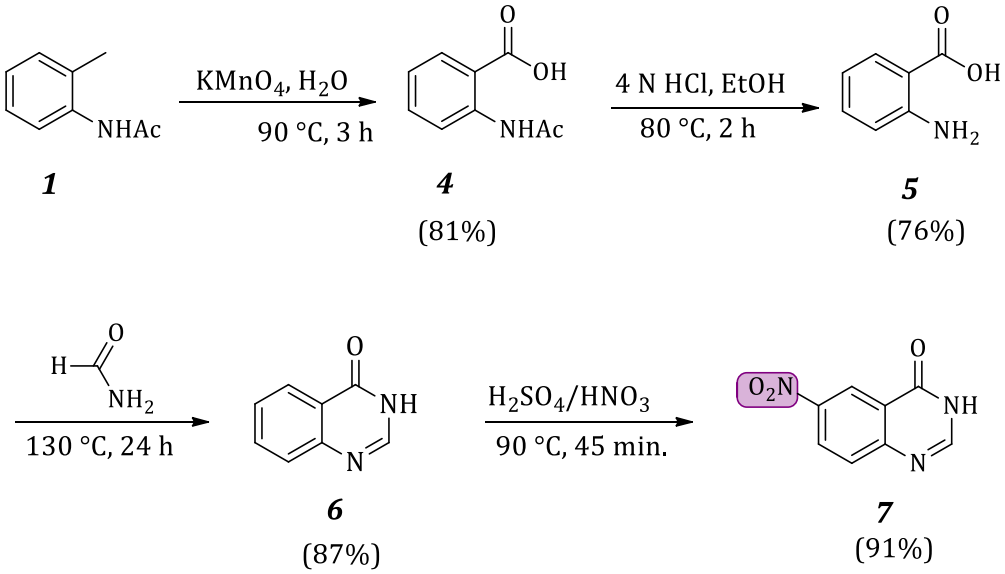

Figure 3.3 (c) Synthetic steps towards 6-nitroquinazoline-4(3*H*)-one (***7***).

With this adjustment in the synthetic plan, transformation of the aryl methyl group into the carboxylic acid was accomplished through oxidation with aqueous potassium permanganate; it afforded compound ***4*** in good yield.[11] The amine functionality was unmasked from *N*-acetamide with 4 N HCl solution in 96% ethanol. Next, the anthranilic acid (***5***) was converted into quinazolin-4(3*H*)-one (***6***) under the Niementowski reaction conditions.[3a] The nitration of **6** using mixed acids (96% H_2SO_4/99% HNO_3) led to the regioselective placement of the nitro group at the C-6 position, to afford 6-nitroquinazolin-4(3*H*)-one (***7***) in good yield. The ^{1}H NMR spectroscopic data of ***7*** matched the literature,[12] thus confirming the expected structure.

3.4 Synthesis of 7-methoxy-substituted 6-nitroquinazolin-4(3H)-one moiety

It was next decided to use 4-fluoro-1-methyl-2-nitrobenzene starting material for the 7-methoxy-substituted analogues. The attempted synthetic route is presented in **Fig. 3.4 (a)**.

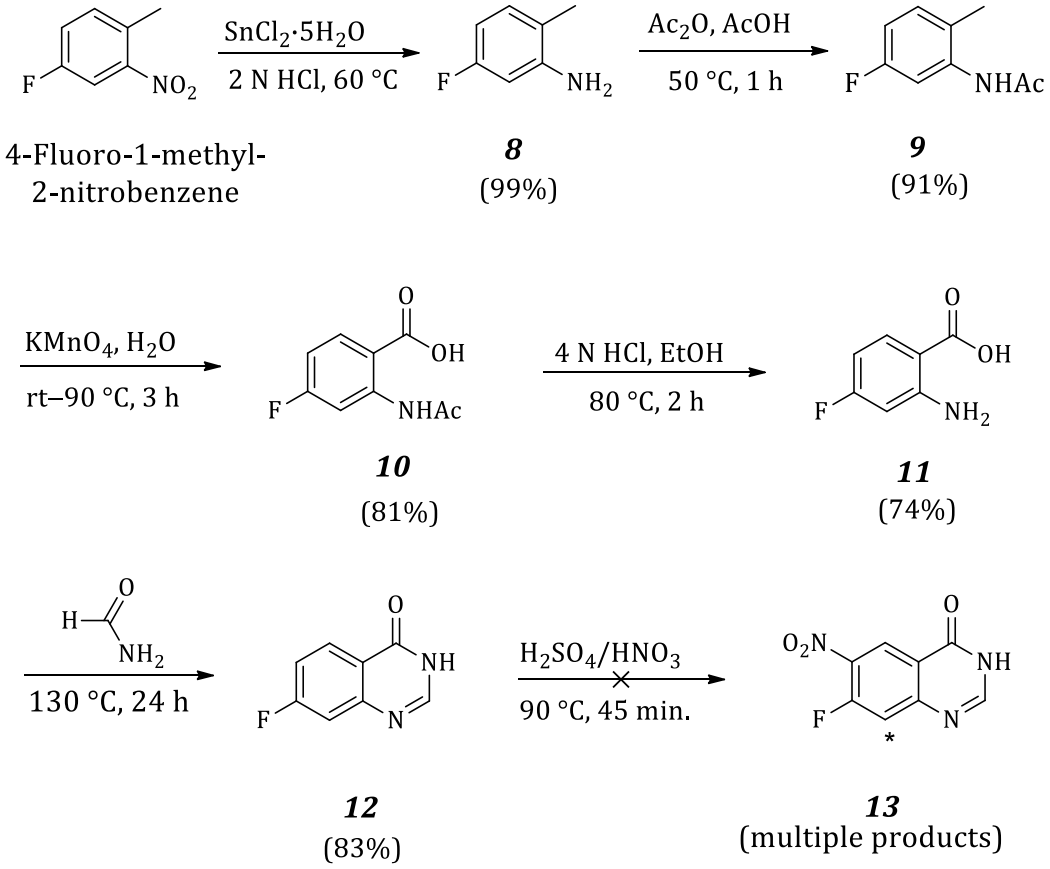

Figure 3.4 (a) Attempted synthesis of 7-methoxy-6-nitroquinazolin-4(3*H*)-one from 4-fluoro-1-methyl-2-nitrobenzene as the starting material. (*Position with high likelihood for additional nitration.)

The synthetic steps commenced by reducing the aryl nitro group in 4-fluoro-1-methyl-2-nitrobenzene with tin(II)chloride under acidic conditions, affording the aniline ***8*** in excellent yield.[13] The downside to tin reduction experiments was the formation of insoluble hydroxides in aqueous media upon the neutralisation work-up procedure. Luckily, primary amines were extracted at pH 10, where tin hydroxides formed reversible soluble complexes: $Sn(OH)_{4(s)} + 2OH^-_{(aq)} \Leftrightarrow [Sn(OH)_6]^{2-}_{(aq)}$.[14] Apart from the difficulty in the work-up, the synthetic process continued smoothly through the usual oxidation, hydrolysis, and Niementowski quinazolinone synthesis until the attempted nitration of

7-fluoroquinazolin-4(3*H*)-one (***12***) offered no prospect of further progress. Unlike the previously encountered regioselective nitration of quinazolin-4(3*H*)-one (***6***), nitration of ***12*** generated a mixture of products that were insufficiently soluble for purification by normal chromatography. Alternative nitration reactions under ambient conditions (in $NaNO_3/NH_4OAc$ and Ac_2O/HNO_3) were also unproductive. We were then forced to resort to using alternate purification methods, such as crystallisation. Although boiling the compounds in ammonium hydroxide/acetone seemed to be a promising solvent combination, unfortunately no reasonably pure compounds were isolated.

A partial view of enlarged ^{1}H NMR spectra of products of the attempted synthesis of the fluoro-substituted quinazolinones ***12–13*** is given in **Fig. 3.4 (b)**. From the proton spectra of ***12***, the proton splitting pattern fully resembles that of the expected 7-fluoroquinazolin-4(3*H*)-one. The usual first-order proton splitting of the *tri*-substituted aromatic ring was made more complex by the fluorine coupling. Beside the usual proton coupling in the *ortho*- and *meta*-positions, fluorine seemed to couple with every available proton of the quinazoline ring, including long range C-2 coupling, which is common for nitrogen-containing heterocycles.[15] For instance, the expected doublet of doublets of *H-6* appeared as doublets of a triplet because of the differences in both *ortho* and *meta* aromatic chemical environments, but this was also accompanied by a fluorine coupling. The observed signal duplicities were equally upheld by ^{13}C NMR spectroscopy in the adjacent positions to the fluoro group (C-6, C-7, and C-8 had $^1J_{C\text{-}F}$ = 251 Hz, $^2J_{C\text{-}F}$ = 24 Hz, and $^2J_{C\text{-}F}$ = 22 Hz, respectively). However, similar distinctions were impossible after the nitration of ***12*** as the overlapping peaks coalesced into one another. It was then decided to attempt the S_NAr displacement of the fluoro group and purify the compounds of interest later. Unfortunately, these attempts were fruitless, and the final products were not successfully purified.

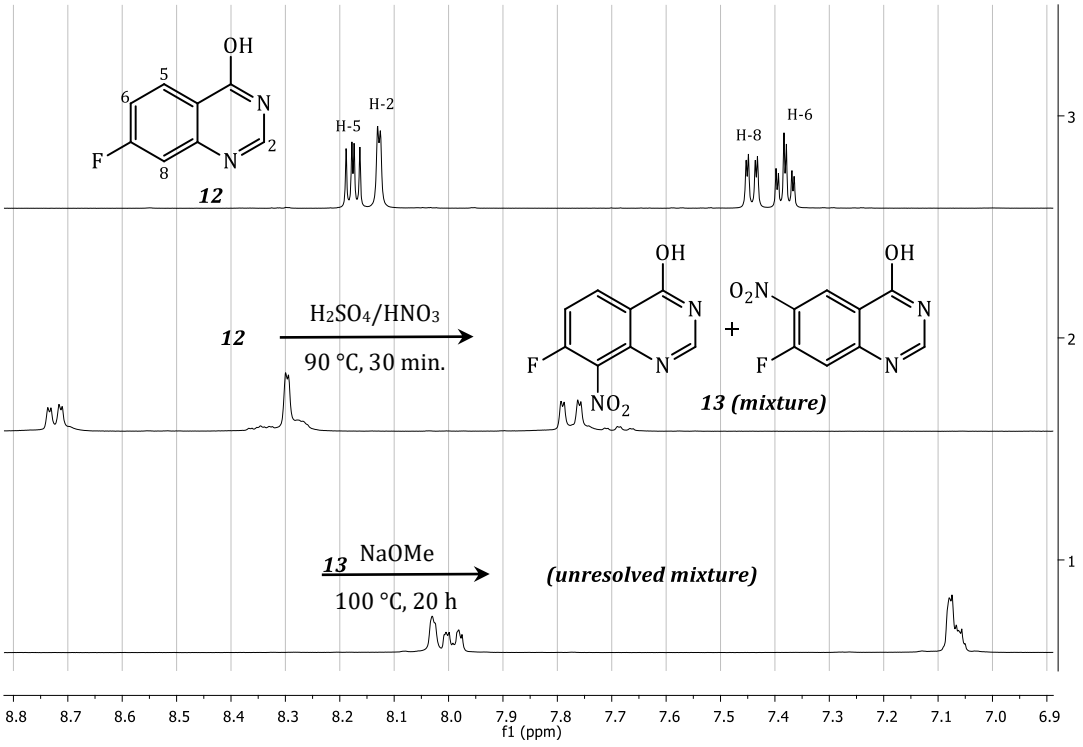

Figure 3.4 (b) ^{1}H NMR spectra of 7-fluoroquinazoline, its transformation via the nitration reaction, and attempted nucleophilic displacement of the fluoro group.

This impasse persuaded us to consider using a different starting material, or perhaps one with a larger halogen substituent (I>Br>Cl>F), to sterically impede nitration at the C-8 position. It should however be mentioned here that positional selectivity of nitration is essentially sensitive to the nature of the substituting agent, and not necessarily to steric hindrances.[16] Trying to merge this idea with the affordability of the starting material required us to create sufficient quantities of nitrated product and re-examine possible purification methods. For this purpose, 2-amino-4-chlorobenzoic acid was selected as the affordable starting material that should decisively reveal the outcome of the nitration reaction without additional peak splitting. The synthetic steps, analogous to in the preparation of ***12***, were followed using 2-amino-4-chlorobenzoic acid. See **Fig. 3.4 (c)**.

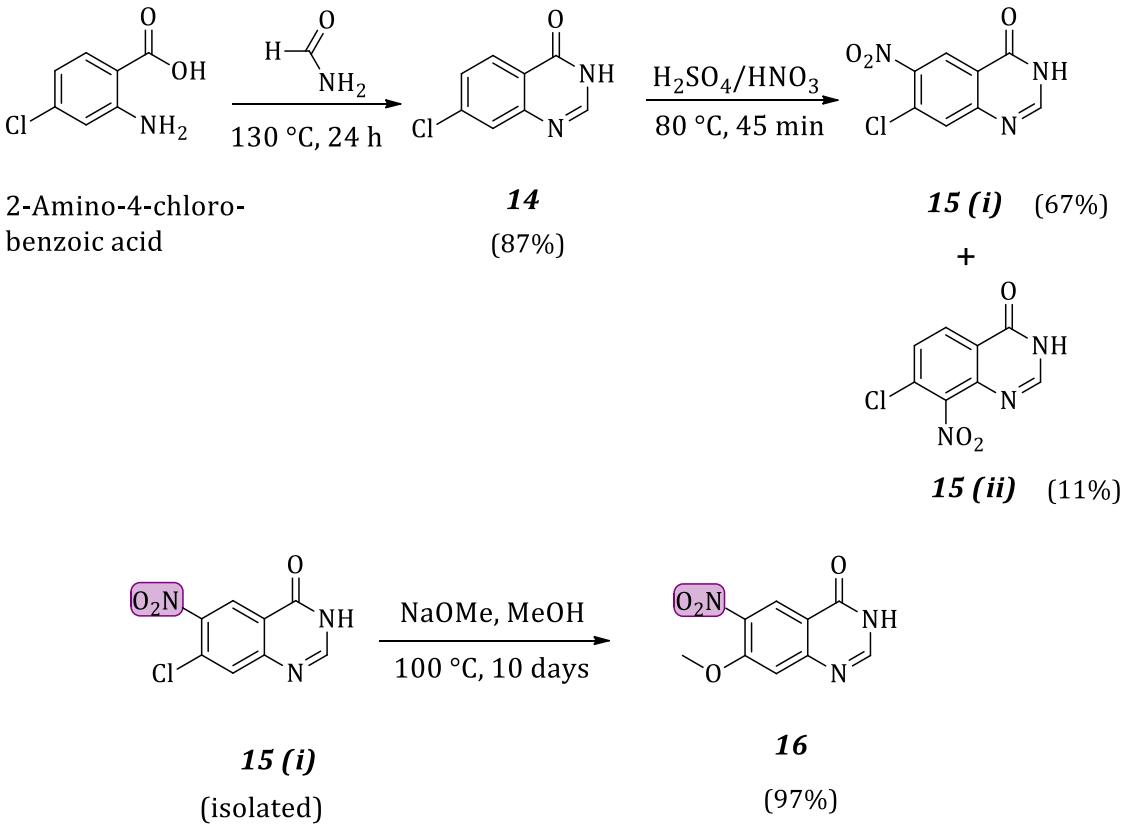

Figure 3.4 (c) Synthesis of 7-choro-6-nitroquinazolin-4(3*H*)-one [***15 (i)***] and 7-methoxy-6-nitroquinazolin-4(3*H*)-one (***16***).

The Niementowski quinazolinone synthesis was once again employed to obtain ***14***,[17] which was then nitrated to afford a crude mixture of ***15 (i)*** and ***15 (ii)*** in 85–93% yield. Safety precautions were exercised when conducting the nitration using mixed fuming acids (H_2SO_4/HNO_3) at elevated temperatures (90 °C). The synthetic scale was restricted to 500 mg and the product was accumulated to approximately 4 g, ground into a fine powder, mixed with silica gel, and then packed onto a pre-loaded column.

Based on the earlier crystallisation attempts, it was duly noted that nitrated quinazolinones were partially soluble in acetone. As a result, careful choice of the mobile phase for chromatographic purification consisted of 2% acetone in dichloromethane (DCM) to 100% acetone. The eluent was continuously collected in fractions from a drip-fed column, concentrated, and then monitored by a thin layer chromatography (TLC) until isolates of pure ***15 (i)*** and ***15 (ii)*** were obtained in yields of 67% and 11%, respectively. The compounds were confirmed by ^{1}H NMR spectroscopy based on the splitting pattern of the benzene ring protons. For instance, for ***15 (i)*** the benzene protons

appeared as distinct singlets, but doublets were observed for ***15 (ii)***. The partial ^{1}H NMR spectra displaying a crude mixture of ***15 (i)*** and ***15 (ii)*** prior to purification and ***15 (i)*** thereafter are shown in **Fig. 3.4 (d)**.

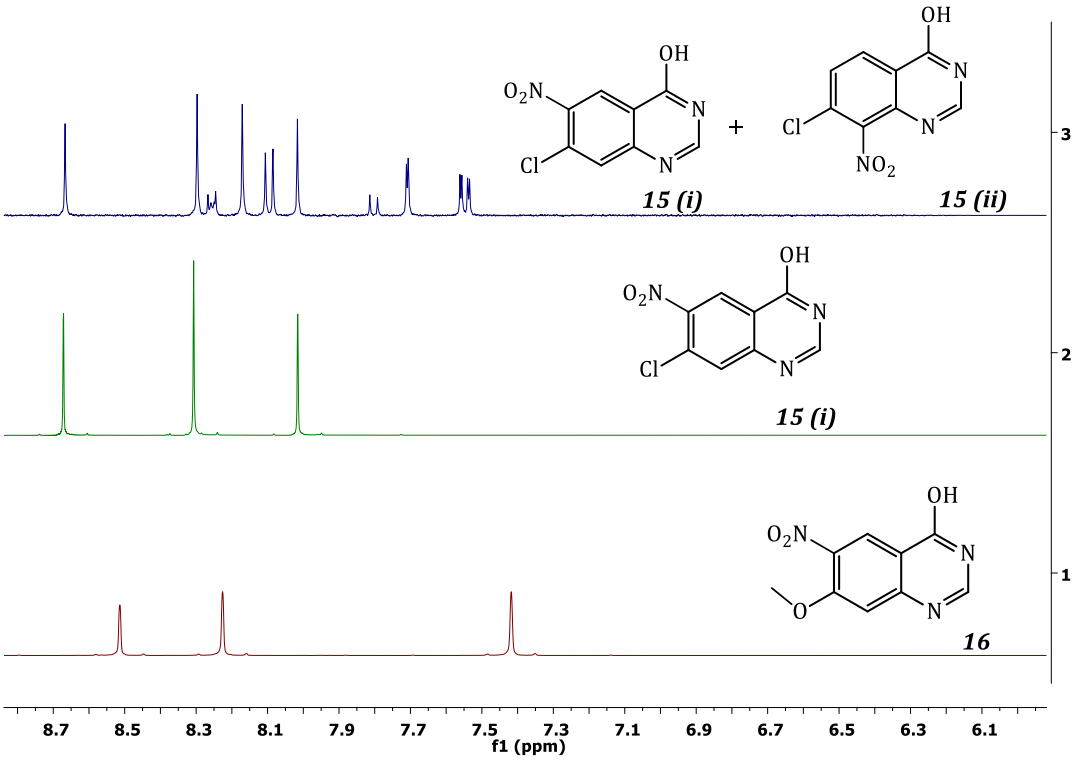

Figure 3.4 (d) ^{1}H NMR spectra showing a crude mixture of ***15 (i)*** and ***15 (ii)***, purified ***15 (i)***, and ***16*** after nucleophilic aromatic substitution of the chloro group with the methoxy group.

Compound ***15 (i)*** turned out to be a valuable intermediate for the preparation of 4-anilinoquinazoline derivatives containing an electron-withdrawing chloro group in the *ortho*-position. Thus some of this material was reserved for future use, while the rest was utilised for further preparation of ***16***. According to the literature procedure,[18] the methoxydechlorination reaction of the quinazoline activated by the nitro-group has been conveniently conducted under pressure in a sealed glass tube. However, we did not have a completely closed system and the reaction was carried out under inert conditions using in-house prepared sodium methoxide [$2Na_{(s)} + 2MeOH_{(l)} \rightarrow 2NaOMe_{(l)} + H_{2(g)}$]. The reaction was heated to reflux at 100 °C and completed after 10 days. After removing excess methanol solvent *in vacuo,* the crude product was neutralised with 50% aqueous

acetic acid. The obtained precipitate was rinsed with cold water and dried, to afford ***16*** as a pure product in an excellent yield of 97%. As was anticipated, substitution of the chloro group with the methoxy group was also demonstrated by the change in chemical environment of the aryl protons to lower frequencies (from 8.23ppm to 7.42 ppm) in the ^{1}H NMR spectra [see **Fig. 3.4 (d)**].

3.5 Synthesis of C-6 hydroxyquinazolin-4(3H)-one analogues.

At this point, preparation of the quinazolin-4(3*H*)-one derivatives intended for use in the synthesis of the amide linker group was successfully completed. Their respective analogues with the ability to form ester bonds were then prepared. Considering that the 6-nitroquinazolines were already available, a shortcut to the synthesis of 6-hydroxy analogues was via conversion of the nitro functional group (see an example in **Fig. 3.5**) to the amine. Thus, subjecting 6-aminoquinazolin-4(3*H*)-ones to the Sandmeyer–Gattermann substitution reaction would potentially result in the formation of diazonium salts,[19] which could be treated with oxygen-based nucleophiles. However, poor solubility of these quinazolinones and instability of the corresponding diazonium salts under the required experimental conditions were prohibitive factors, hence this route was abandoned.

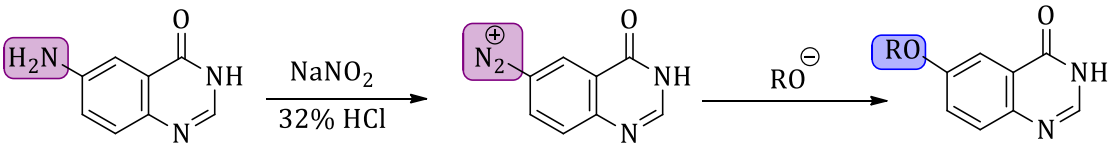

Figure 3.5 Proposed Sandmeyer–Gattermann type of aromatic substitution reaction for the synthesis of 6-hydroxyquinazolines from 6-aminoquinazoline derivatives.

3.6 Synthesis of 6-hydroxyquinazolin-4(3H)-one derivatives.

Because of the instability of the quinazolinone diazonium salts, the possibility of transforming 5-bromoanthranilate ***19 (i)*** to a 6-bromoquinazolinone (***20***) was considered [see **Fig. 3.6 (a)**]. The nucleophilic displacement of the aryl bromine with methoxide compounds or transition metal-catalysed reactions would yield the required compound ***21***.[20]

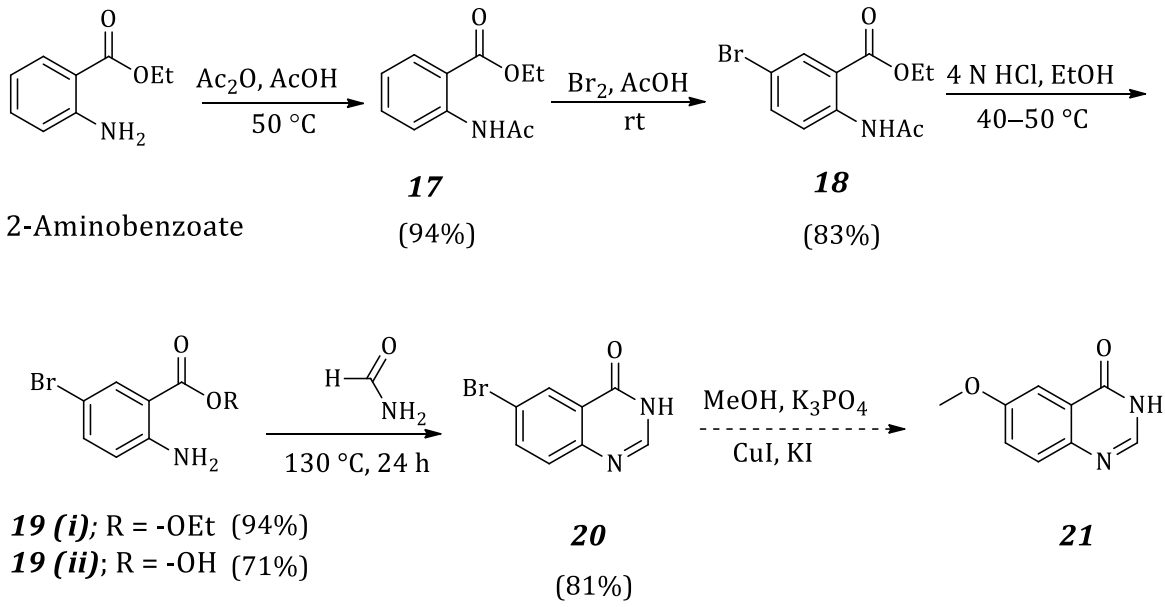

Figure 3.6 (a) Synthesis of 6-methoxyquinazolin-4(3*H*)-one via aromatic nucleophilic substitution of 6-bromoquinazolin-4(3*H*)-one [***19 (i)***].

With this plan in mind, *N*-acetamide ***17*** was prepared from ethyl 2-aminobenzoate precursor and halogenated with molecular bromine *in situ* [$KBrO_{3(s)} + HOAc_{(l)} +$ (48%) $5HBr_{(aq)} \rightarrow 3Br_{2(l)} + 3H_2O_{(aq)} + KOAc_{(aq)}$] to afford ***18*** in good yield. In order to avoid aqueous work-up problems associated with zwitterionic compounds, selective hydrolysis of the amide group under mild reaction conditions was investigated. Treatment of ***18*** with 4 N ethanolic potassium hydoxide solution provided exclusive ester hydrolysis within 2 h at room temperature. It turned out that the selectivity could be achieved to give the amine by using a 4 N ethanolic HCl solution to afford compound ***19 (i)*** as the only product. Further conversion of ***19 (i)*** into 5-bromoquinazolin-4(3*H*)-one (***20***) was achieved in reasonably good yields. At this point, ***20*** was exposed to nucleophilic debromination conditions in an attempt to form 6-methoxyquinazoline-4(3*H*)-one (***21***). As in most Ullman reaction conditions,[21] copper-assisted cross-coupling with oxygen-based nucleophiles required higher temperatures and prolonged reaction periods, but the yields were disappointingly low. Further attempts investigated the aromatic Finkelstein variation method with a domino halide-exchange reaction, involving catalytic potassium iodide at 110 °C in dry 1,4-dioxane solvent.[22] Unfortunately these attempts were not successful.

It was then decided that commercial 2-amino-5-hydroxybenzoic acid would be an economically viable alternative for synthesizing 6-hydroxyquinazoline, in comparison with the attempted 5-methoxy derivative shown in **Fig. 3.6 (a)**. The revised synthetic strategy commenced with 2-amino-5-hydroxybenzoic acid under the Niementowski reaction conditions, affording 6-hydroxyquinazolin-4(3*H*)-one (***22***) in 76% yield [see **Fig. 3.6 (b)**]. Protection of the hydroxyl group in ***22*** produced the acetoxyquinazolinone (***23***) in 79% yield.

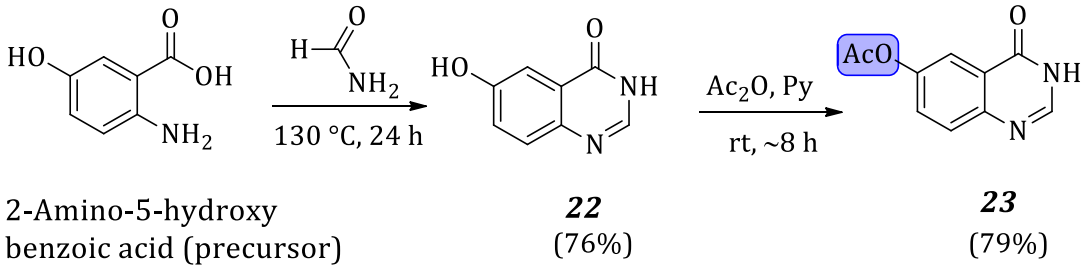

2-Amino-5-hydroxy benzoic acid (precursor)

22 (76%)

23 (79%)

Figure 3.6 (b) Preparation of acetyl-protected 6-hydroxyquinazolin-4(3*H*)-one (***23***).

According to most literature methods,[23] *O*-acylation of hydroxy-substituted quinazolinones occurs under Dakin–West reaction conditions.[24] Under these conditions, excess pyridine solvent and higher temperature (100–150 °C) were required to initiate acylation reactions, perhaps to account for the limited solubility of quinazolinones. In some cases, the acquired acetoxyquinazolinones have been further used without any purification.[23] However, these literature conditions were not useful the obtained end product consisted of a mixture of compounds, probably due to mixed *O*- and *N*-acylations, and decompositions.

Upon consideration of the Steglich esterification,[25] we learned that 4-dimethylaminopyridine (DMAP) significantly promotes the reaction rate by creating highly reactive acyl intermediates, especially if the alcohol is a poor nucleophile. However, our combination of catalytic DMAP and Ac_2O resulted in the gelation of the reaction mixture, to the already poorly soluble ***22***. As a result, excess Ac_2O and a molar equivalent of pyridine were used to obtain a clear solution, which was then stirred overnight at room temperature. Product ***23*** was obtained in 79% yield [see **Fig. 3.6 (b)**].

To confirm the regioselective acylation, the ^1H NMR spectra of ***23***, its former unprotected hydroxyl moiety ***22***, and the bromoquinazolinone (***20***) were compared [see **Fig. 3.6 (c)**].

It could be deduced from the spectra that the highly solvent interchangeable amide/amidic acid proton [4(3*H)* and/or 4-OH tautomers] exhibited a broad singlet in all the compounds in a high frequency region (11–13 ppm). In comparison, the presence of this exchangeable proton in ***23*** indicated exclusive acylation of the hydroxyl group. In addition, the absence of a hydroxyl peak signal at 10.2 ppm in ***23*** relative to ***22*** unambiguously corroborated the expected functional group transformation. This observation was further substantiated by the existence of the methyl protons of the acetyl group in ***23*** at 2.32 ppm. The net influence of electronegativity and/or van der Waals deshielding effects was also evident among the compounds when the aromatic protons were taken into consideration.

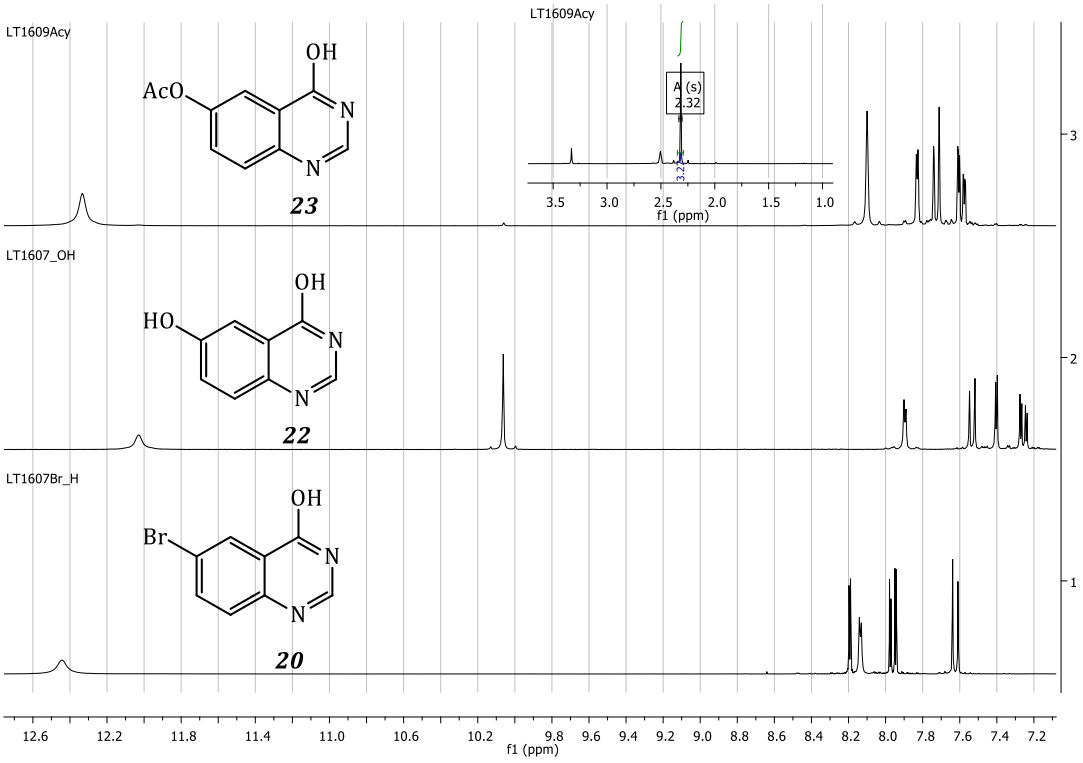

Figure 3.6 (c) ^{1}H NMR spectra of 6-bromoquinazolin-4(3*H*)-one (***20***), and its derivatives 6-hydroxyquinazolin-4(3*H*)-one (***22***) and 6-acetoxyquinazolin-4(3*H*)-one (***23***).

3.7 Synthesis of 7-methoxy-substituted 6-hydroxyquinazolin-4(3H)-one

Having obtained the first 6-hydroxyquinazolin-4(3*H*)-one intermediate, the 7-methoxy-substituted analogue **(*29*)** was prepared next. According to the literature,[26] preparation of this intermediate is related to the synthesis of Gefinitib, which is via selective

demethylation of 6,7-dimethoxyquinazolin-4(3*H*)-one (***27***), as depicted in **Fig. 3.7 (a)**. Our synthesis commenced with conversion of 3,4-dihydoxybenzoic acid into methyl 3,4-dimethoxy benzoate (***24***) using modified Williamson etherification conditions.[27] The methyl 4,5-dimethoxy-2-nitrobenzoate [***25 (i)***] was obtained after attempting a few different experimental conditions for the moderately reactive aromatic molecule.[28] Besides the likely *para*-directed nitration, whose incoming nitro group's inductive influence must sufficiently inhibit further nitrations, di-nitrated product ***25 (ii)*** was also formed. The compounds were isolated by chromatographic methods. Product ***25 (ii)*** was further elucidated by a combination of ($^{1}J_{C\text{-}H}$) HSQC and ($^{2,3}J_{C\text{-}H}$) HMBC NMR spectroscopic methods.

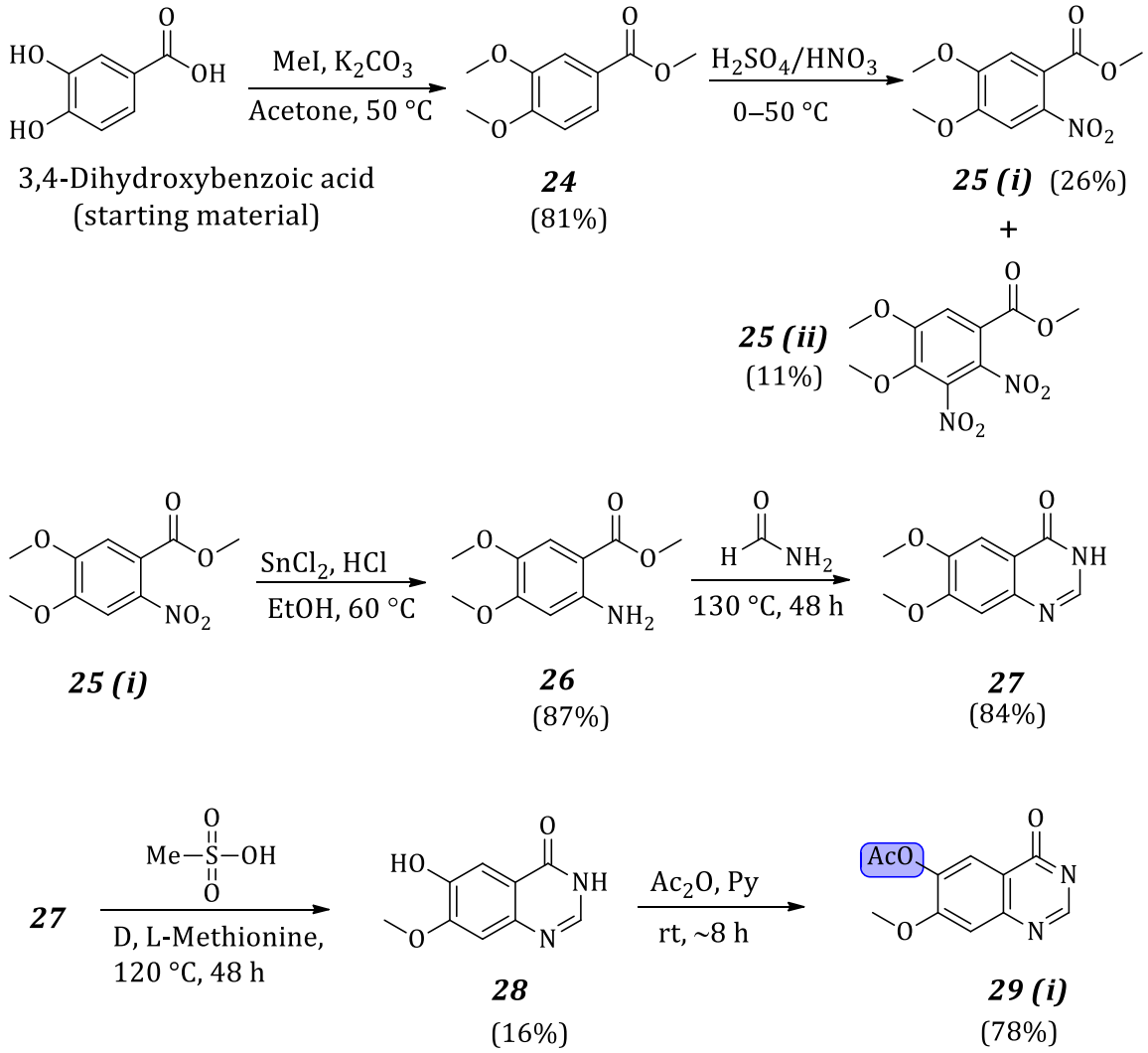

Figure 3.7 (a) Synthesis of a 7-methoxy-substituted quinazolin-4(3*H*)-one derivative (***29***) via selective demethylation of 6,7-dimethoxyquinazolin-4(3*H*)-one (***28***).

Based on ^{1}H NMR spectroscopic analysis, the two structures, ***25 (i)*** and ***25 (ii)*** were easily identified by peak multiplicities or signal splitting patterns. Moreover, the location of the second nitro substituent in ***25 (ii)*** was also confirmed. In doing so, it was obvious that only one singlet could be identified in the aromatic region (except the $CDCl_3$ solvent peak); thus a $^{1}J_{CH}$ correlation NMR experiment (HSQC) would conclusively identify the carbon to which the proton was bound. Further $^{2}J_{CH}$ and $^{3}J_{CH}$ correlations over multiple bonds from the HMBC were used to ascertain the two neighbouring carbons on either side of the aromatic ring, during which a mutual correlation between the methoxy and ethyl ester groups was also established. The resulting gradient selection of the HSQC and HMBC correlations are summarised by the interpreted structure shown in **Fig. 3.7 (b)**.

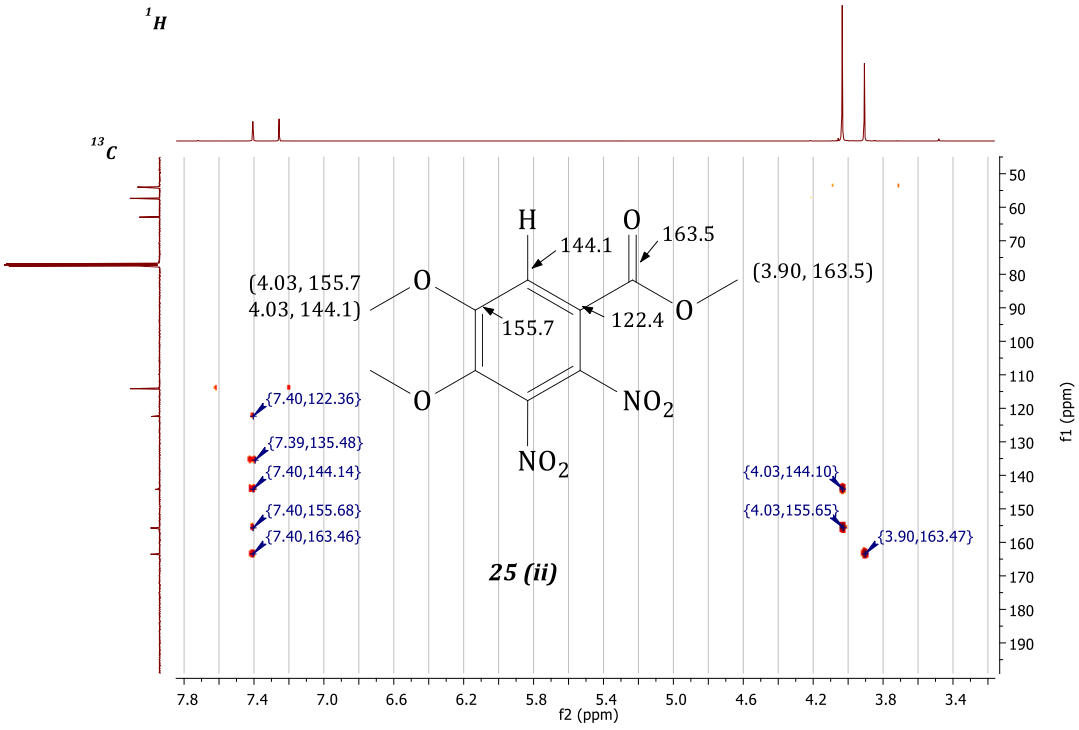

Figure 3.7 (b) Structural elucidation of over-nitrated ***25 (ii)*** via J_{CH} correlations (only HMBC spectroscopic analysis is displayed).

For the purified ***25 (i)***, tin(II)chloride was used to selectively reduce the nitro group. Product ***26*** was obtained in good yield. Cyclisation of ***26*** into ***27*** was achieved under the Niementwoski method with formamide. As in the conversion of isovaniliic acid from 3,4-dimethoxybenzoic acid by acidolysis,[29] the electron-rich methoxy group at the C-6 position of ***27*** accepts acidic protons more readily to enable selective hydrolysis. With

this in mind, selective hydroxylation of the C-6 aryl methyl ether by means of methane sulfonic acid and the methionine salt was carried out, but with little success.[26] The recommended experimental periods for demethylations were found to be inadequate in most cases and the reaction was gradually extended from 16 h to 48 h. Despite the meticulous experimental executions, including the freeze-pump-thaw cycles to exclude moisture, prolonged reaction periods resulted in over-demethylation. As a result, only small quantities of pure ***28*** were recovered. *O*-acylation was carried out to obtain the acetoxyquinazolinone ***29 (i)***. The NMR spectroscopic analysis to determine the selectivity of this reaction will be discussed later, in *Section 3.13*, where ***28*** was coupled to a 4-aniline substrate.

Since we were only able to obtain low quantities of pure ***28*** (73 mg), it was decided to attempt the demethylation of 6,7-dimethoxy-4-anilinoquinazolines instead.[30] Thus, using compound ***27***, 6,7-dimethoxy-4-anilinoquinazoline derivatives were then prepared as shown in **Fig. 3.7 (c)**. Generally, compounds ***30–32*** were obtained in sufficient gram quantities and good purity. Attempted selective hydroxydemethylation of these compounds under microwave conditions,[30] and conventional heating, were unfortunately ineffective. Among these three compounds, the alkynyl aniline moiety (***30***) demonstrated high sensitivity and rapid decomposition in the attempted demethylation experiments. On the other hand, the halo-substituted anilines proved to be more stable and robust to undergo demethylation without significant decomposition. The end products were very impure. Chromatographic isolations and re-purification efforts were unsuccessful.

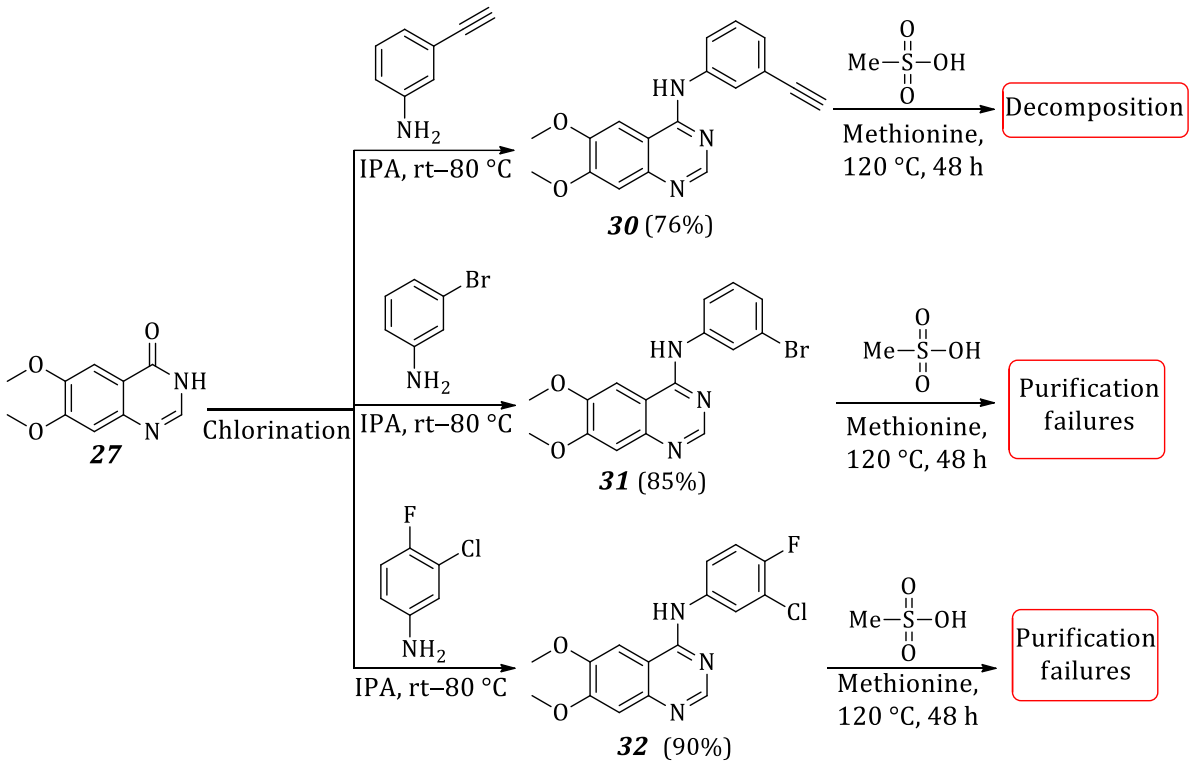

Figure 3.7 (c) Attempted microwave-assisted and conventional heating hydroxyl-demethylation of 6,7-dimethoxy-4-anilinoquinazolines (***30–32***).

As efforts to obtain 7-methoxy-substituted 6-hydroxyquinazoline derivatives were unrewarding thus far, it was decided to carry on with creating a library of 4-anilinoquinazoline compounds using the available quinazolinone materials.

3.8 Creating the C-6 acrylamide-substituted 4-anilinoquinazolines

At this point, commercially acquired aniline substrates had to be appended on the C-4 position of quinazolinone intermediates [see **Fig. 3.8 (a)**]. To carry out the S_NAr substitution with poor nucleophilic anilines, the quinazolinone C-4 position is usually activated by halogenation under acidic conditions using phosphorus(V) oxychloride ($POCl_3$).[31] In some cases, direct C-N coupling has been achieved by means of phosphonium-mediated reagents (pyBOP) under basic conditions.[32]

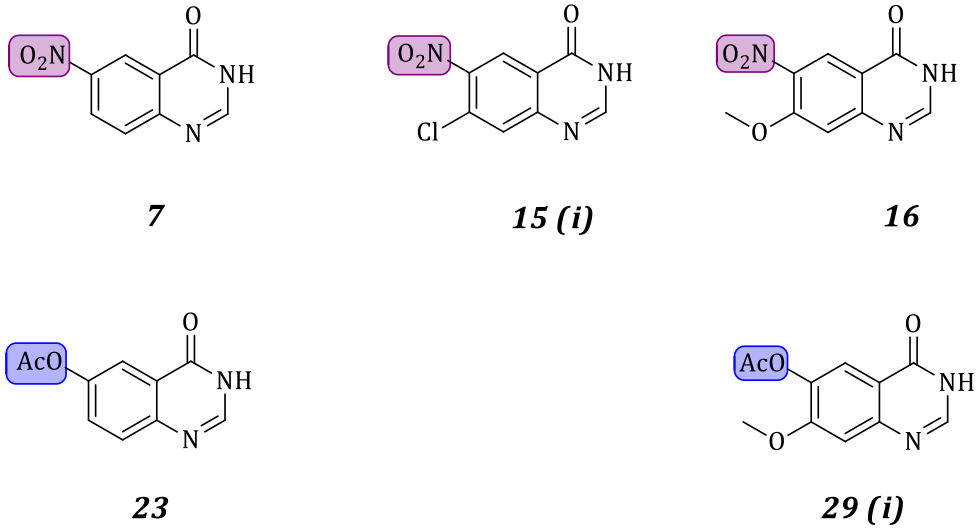

7 ***15 (i)*** ***16***

23 ***29 (i)***

Figure 3.8 (a) The C-6-substituted quinazoline-4(3*H*)-ones for the preparation of 4-anilinoquinazoline compounds.

The formation of the quinazolinone amidic acid tautomer (4-OH) can be influenced by the pH of reaction medium. This allows for facile activation of the C-4 position by means of chlorodehydroxylation using $POCl_3$.[31] The 4-chloro intermediates from the nitroquinazolin-4(3*H*)-one derivatives [***7***, ***15 (i)***, and ***16***] were treated with selected aniline substrates to undergo S_NAr *N*-arylation and compounds ***34–42*** were obtained [see **Fig. 3.8 (b)**]. These intermediates (***34–42***) were then subjected to different reducing agents to obtain the C-6 amino functionality ***43–51***. The aminoquinazolines (***43–51***) were found amenable to form the required α,β-unsaturated olefinic amide linkers ***52–58*** under Schotten–Baumann *N*-acylation conditions.[33] The resultant acrylamide-bearing 4-anilinoquinazolines (***52–58***) would then inevitably undergo Michael addition reaction with thiol-terminated polymers to create the desired end products. A more elaborate discussion on the synthesis follows in the next section.

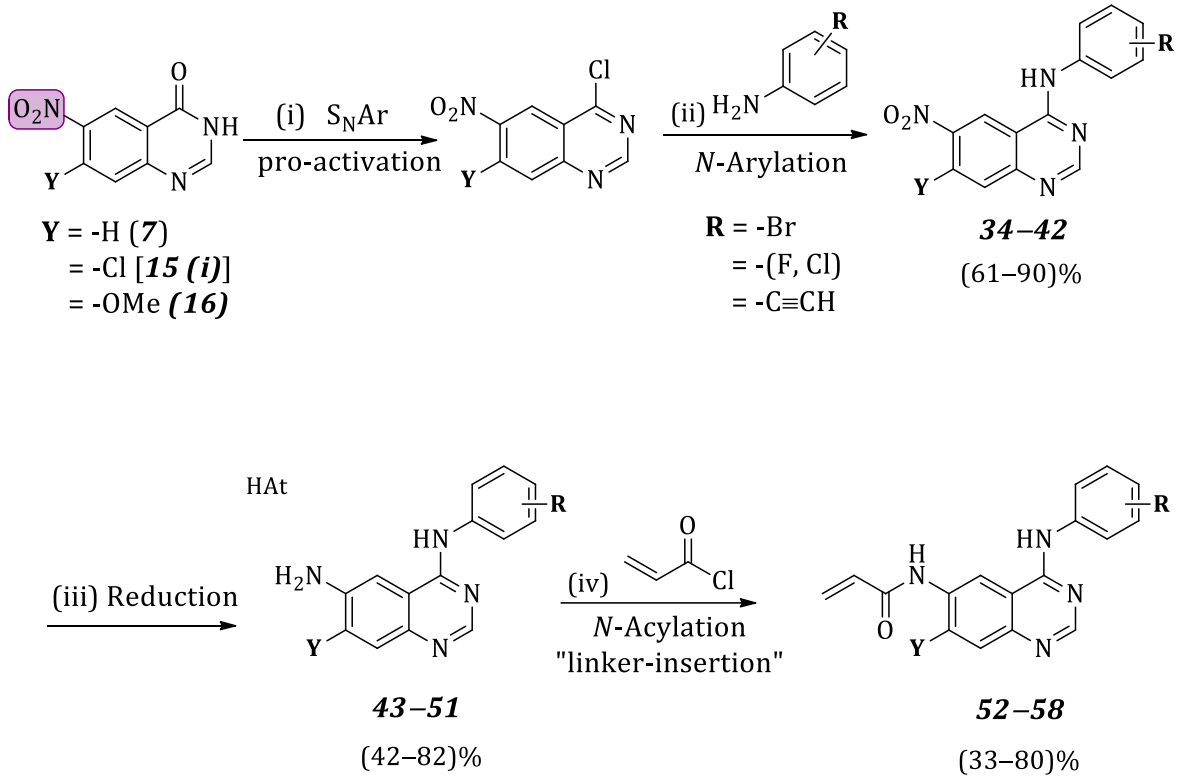

Figure 3.8 (b) Generic example for creating 4-anilinoquinazolines with acrylamide linkers (***52–58***).

*3.9 S_NAr amination of 6-nitroquinazolin-4(3H)-one derivatives (**34–42**)*

Activation of 7-nitroquinazolin-4(3*H*)-one compounds (*e.g.* ***7***) for S_NAr, to enable facile transformation into *N*-heteroaromatic chlorides (such as ***33***), was achieved with $POCl_3$ in the presence of Hünig's base. However, it must be noted that most chlorinating agents, including $POCl_3$, are extremely moisture sensitive, which makes them difficult to handle. During the work-up, it emerged that 4-chloro-activated quinazoline derivatives are prone to reversible hydrolysis to their initial starting materials. Because of this instability, *N*-arylation reactions were sequentially performed on freshly chlorinated products, as illustrated in **Fig. 3.9 (a)**. For a quinazolinone ***7***, successful chlorination was confirmed by ^1H NMR spectroscopic analysis of ***33***. The obtained proton spectrum unambiguously showed the absence of the quinazolinone proton, which is usually observed at 11.5–12.5 ppm [see **Fig. 3.6 (c)**]. *N*-heteroaromatic chloride intermediates [***15 (i)*** and ***16***] were then coupled with their respective aniline compounds without further characterisation.

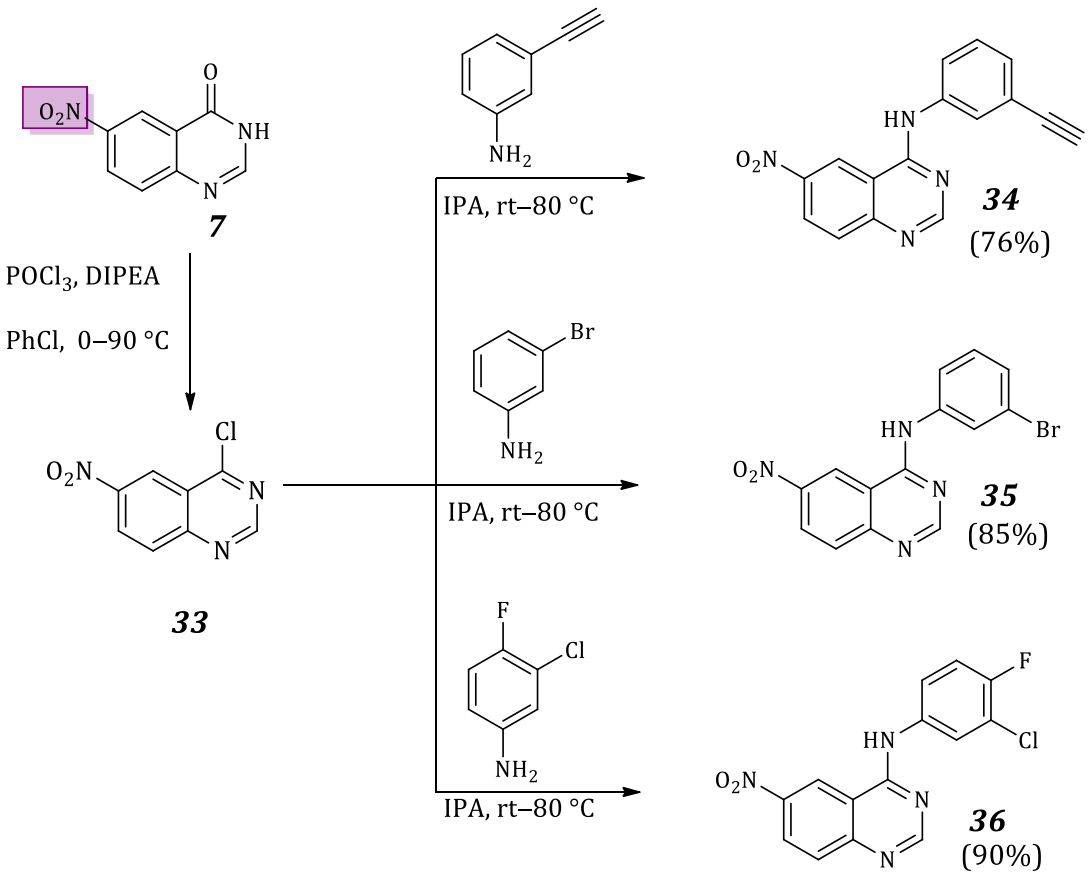

Figure 3.9 (a) Synthesis of 4-anilinoquinazoline derivatives (***34–36***) via acid-catalysed S_NAr with anilines.

Upon installation of the anilines onto the *N*-heteroaromatic chloride (***33***), additional aromatic signals were observed in the ^1H NMR spectra. The amidine C-4 protons of ***34–36*** appeared rather flat on the baseline (~11.5–12.5 ppm) due to a rapid solvent exchange with the DMSO solvent. In addition to this, quinazoline protons generally exhibited a slight shift (1–1.5 ppm) in the direction of higher frequency values. An additional six compounds were developed from ***15 (i)*** and ***16*** using the same experimental approach. The chemical structures of these analogues (***37–42***) are shown in **Fig. 3.9 (b)**.

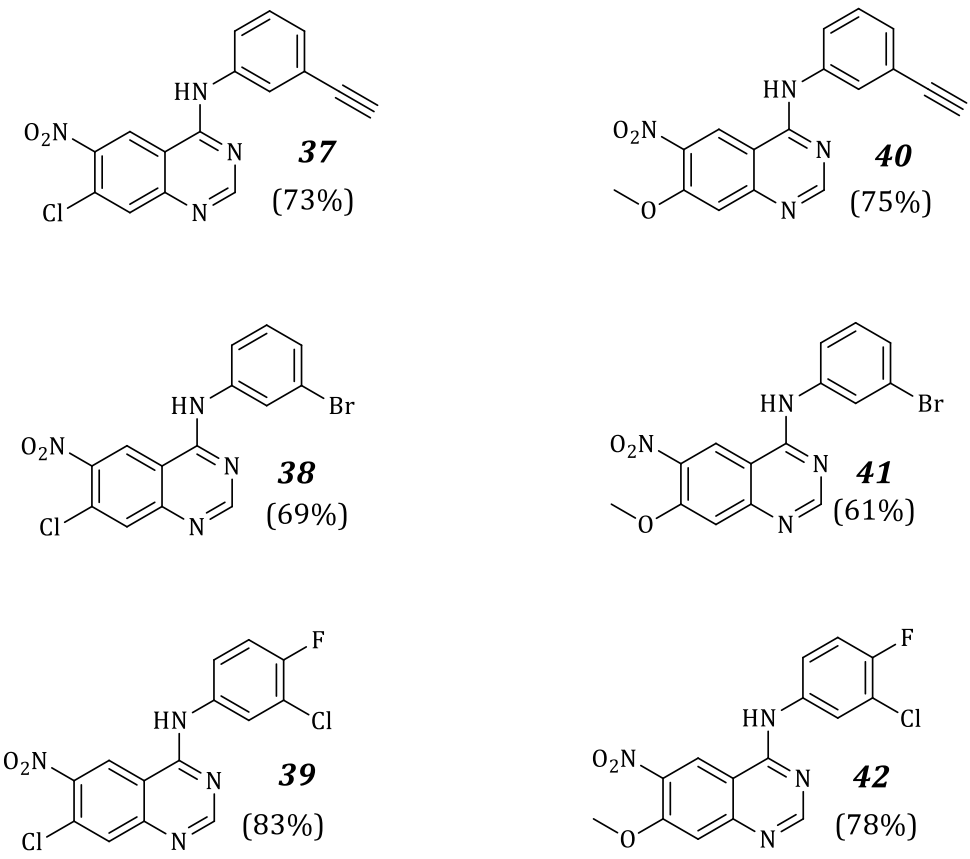

Figure 3.9 (b) The 6-nitro-4-anilinoquinazoline compounds (***37–42***) developed from 7-chloro- and 7-methoxyquinazolin-4(3*H*)-ones via S_NAr *N*-arylation.

*3.10 Reduction of 6-nitro-4-anilinoquinazolines (**43–51**)*

The 6-nitro-4-anilinoquinazolines (***34–42***) were then subjected to different Lewis acids in an attempt to acquire the C-6 amino functionality via reduction of the nitro group. Although tin(II)chloride was found to reduce the compounds selectively, the problem of forming stable tin(IV)hydroxides precipitates under neutral aqueous conditions compelled us to consider other reducing agents. Molecular hydrogenation under palladium catalysis was another attractive method that reduced the nitro group, followed by a simple filtration work-up. However, an unexpected problem with this method was an occasional reductive dehalogenation, probably via oxidative insertion of palladium on the aniline aromatic ring. Although the observed aryl dehalogenation resembled that of the Buchwald–Hartwig reaction,[34] it usually happens at elevated temperatures in the presence of amine-based nucleophiles. Unfortunately, this seems to be a common

occurrence under mild reaction conditions as well, especially in alcohol (ethanol) solvents.[35]

Ultimately, $Fe_{(s)}/NH_4Cl$ in aqueous ethanol proved to be a universal reducing agent for compounds ***34–42***. Eventually, after successfully carrying out the reduction, a small library of the C-6 amino-substituted 4-anilinoquinazoline compounds was developed. Their chemical structures are shown in **Fig. 3.10**. Because the nitro group was converted to the amine, a new broad singlet integrating for two protons at 5.35–5.81 ppm was observed in the ^1H NMR spectra of compounds ***43–51***.

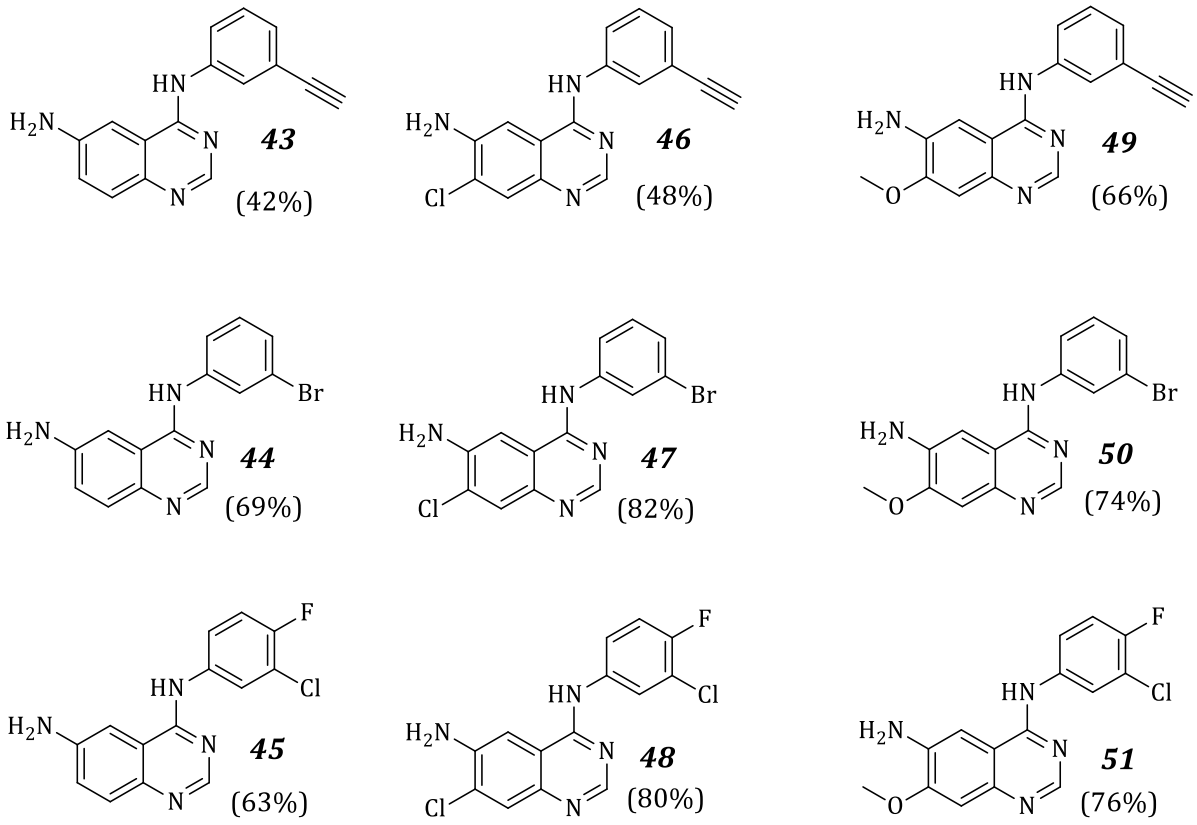

Figure 3.10 The C-6 amino-substituted 4-anilinoquinazoline compounds ***43–51***.

*2.11 The C-6 amidation of 4-anilinoquinazolines, linker insertion (**52–58**)*

According to our intended application of the polymer-bound small molecules, the C-6 amino-substituted 4-anilinoquinazolines were treated with acryloyl chloride in the presence of Hünig's base to form the acrylamides [see **Fig. 3.11 (a)**]. Among the 4-anilinoquinazoline derivatives, the C-7 chloro analogues performed poorly in the

acylation reactions. In most cases, there was no observed reaction progress, perhaps due to steric effect, also known as the *ortho* effect.[8, 36] A final library of 4-anilinoquinazolines with the acrylamide functional group was then created with the compounds shown in **Fig. 3.11 (a)**.

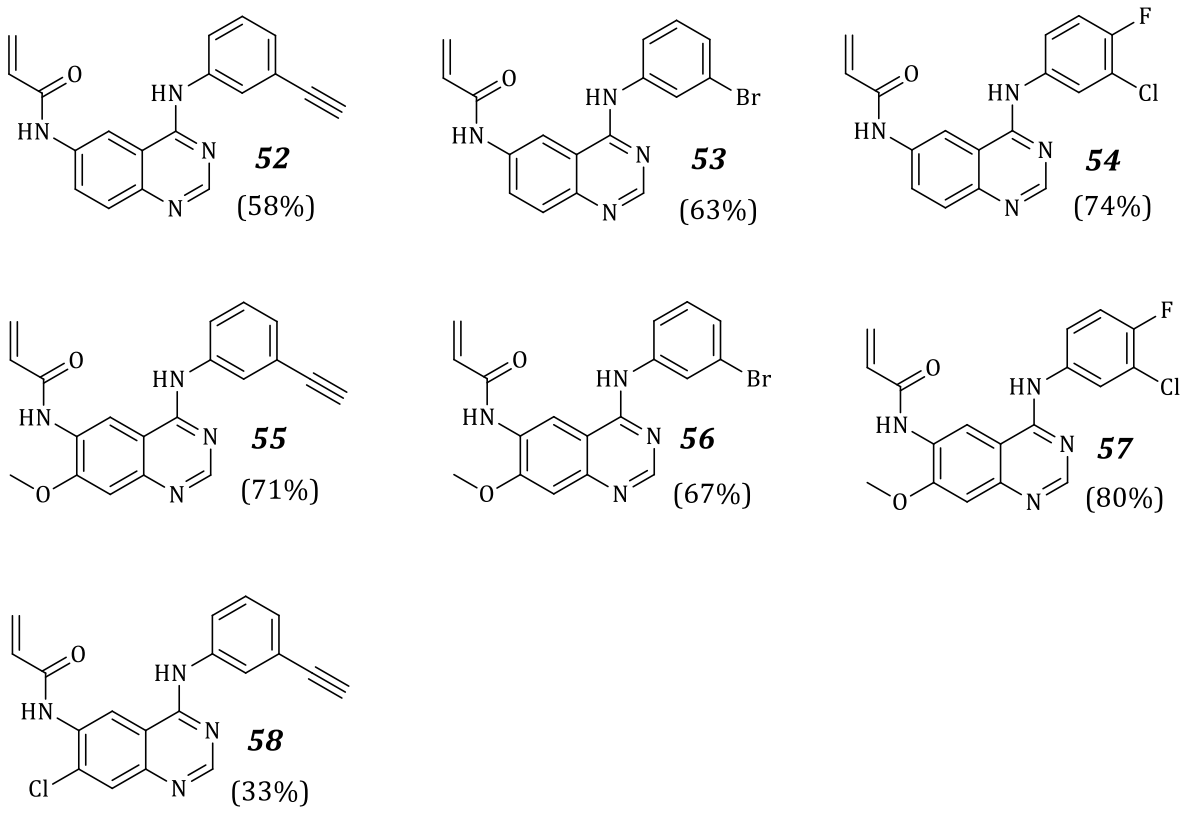

Figure 3.11 (a) Small library of 4-anilinoquinazolines with the acrylamide linker functionality (***52***–***58***).

Structural elucidation of these compounds (***52***–***58***), using ^{1}H and ^{13}C NMR spectroscopy, and MS. Upon insertion of the Michael acceptor, the C-6 amino functionality was modified into the amide. Ordinarily, the broad aryl amine singlet at 5.35–5.81 ppm (in DMSO) converts to a singlet at ~10 ppm, integrating for one proton. The newly introduced α,β-unsaturated alkene groups were observed in the range 5.8–6.5 ppm. Apart from the distinctive proton splitting patterns of this alkene, terminal protons were precisely differentiated by their *J* coupling values. In general, the *trans* coupling ($J \cong 17$ Hz) was always larger than that of the *cis* ($J \cong 10$ Hz) hydrogens. In addition, the molecular masses of the synthesised compounds were determined within the 5 ppm range by MS.[37] In rare

cases, atoms with strong isotopic influence [^{79}Br (50.69) and ^{81}Br (49.31)] were observed displaying two parent peaks; see the mass spectrum of ***53*** in **Fig. 3.11 (b)**. The compounds were analysed in positive ionisation mode, $[M+H]^+$, and the isotopic peaks of ***53*** clearly resembled the isotopic abundances of bromine. Occasionally, the amide bond cleaved during MS analysis, but a cone voltage of 15 V was used to analyse most 4-anilinoquinazolines without additional fragmentations.

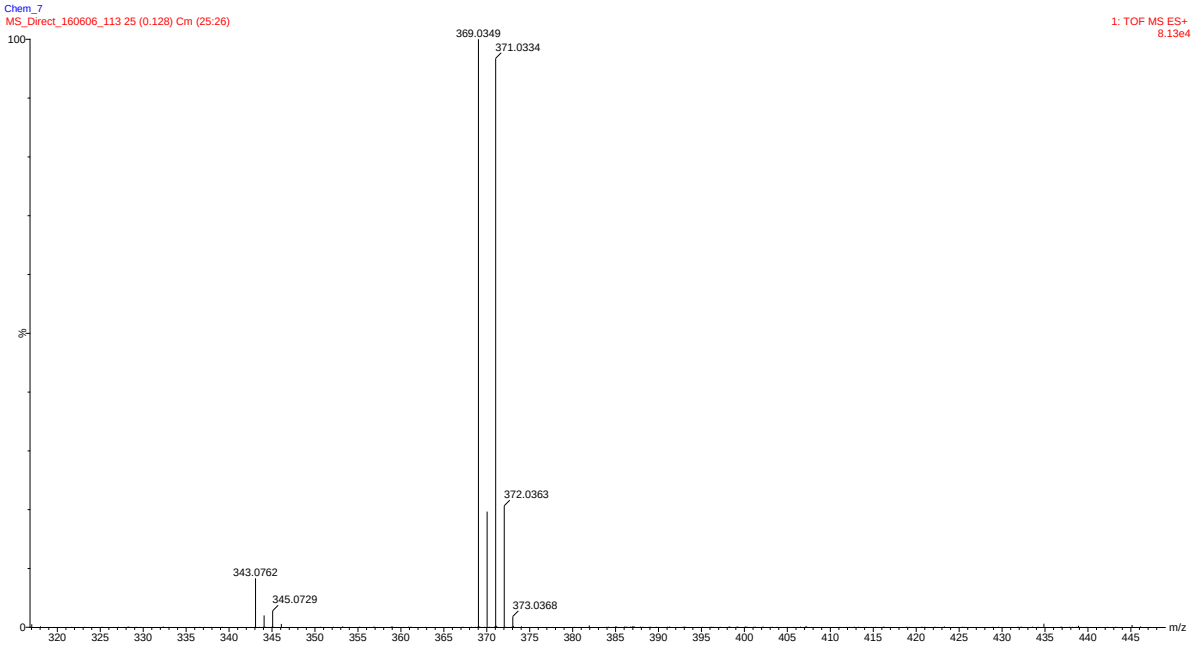

Figure 3.11 (b) Mass spectrum of ***53*** showing isotopic influence in molecular mass determination.

Some of the final compounds were intended for biological evaluation (anti-tumour efficacy) and it was critical for their chemical purities to be known. Chemical purities were evaluated with a Synapt ultra-performance liquid chromatography-tanderm mass spectroscopy (UPLC-MS) instrument at various ultraviolet (UV) wavelengths ($\lambda_{max.}$). The chromatogram for ***53,*** as an example, is shown in **Fig. 3.11 (c)**. Good chemical purity was evident (close to 95%).

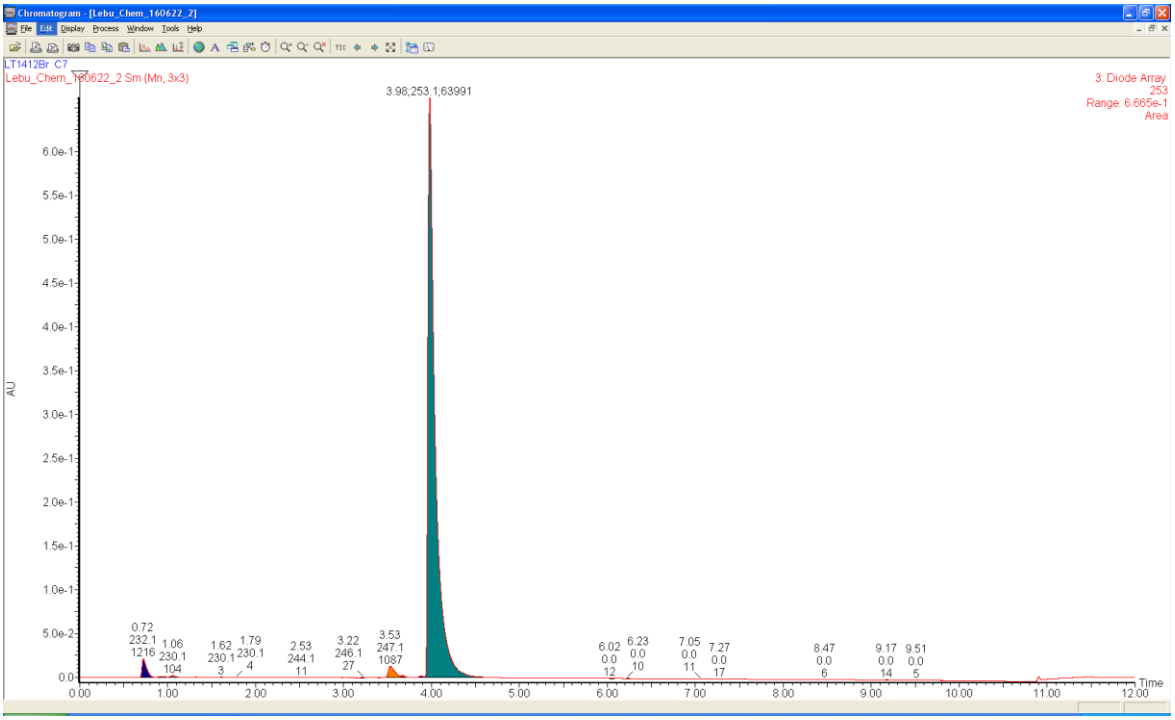

Figure 3.11 (c) Chromatogram of ***53***, displaying chemical purity ($\lambda_{max.}$ 253 nm).

3.12 Towards the C-6 acrylate-substituted 4-anilinoquinazolines for polymer-conjugation

The next efforts were then directed at creating 4-anilinoquinazoline analogues containing an acrylate functionality. The acetoxyquinazolinone intermediates ***23*** and ***29 (i)*** were thus used to develop the second library of 4-anilinoquinazolines. The general synthetic procedure for these compounds was analogous to that of the acrylamides ***52***–***58***, except that the hydroxyl groups were deprotected through hydrolysis of the acetyl protecting group. A generic synthetic route towards acrylates is given in **Fig. 3.12 (a)**.

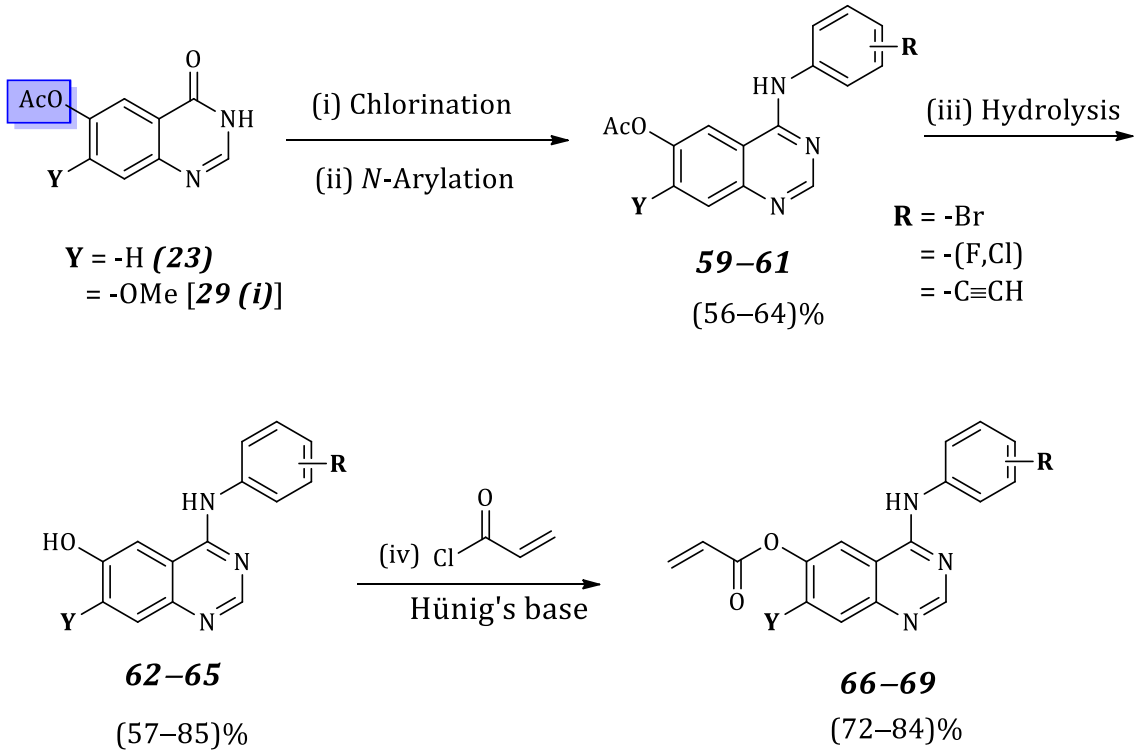

Figure 3.12 (a) A generic synthetic route for the synthesis of acrylate-substituted 4-anilinoquinazoline compounds (***66–69***).

3.13 Preparation of the C-6 hydroxy-substituted 4-anilinoquinazolines

The 4-anilinoquinazolines (***59–61***) were obtained with the acetate still group intact in most cases after the S_NAr *N*-arylation of activated acetoxyquinazolinones. In cases where small quantities of hydroxyl deprotection had occurred, a few drops of ammonium hydroxide were added to complete the hydrolysis process. Because there was a limited quantity of ***28***, it was decided to synthesise one 7-methoxy-substituted analogue. The overall set of 4-anilinoquinazolin-6-ol derivatives (***62–65***) is presented in **Fig. 3.13 (a)**.

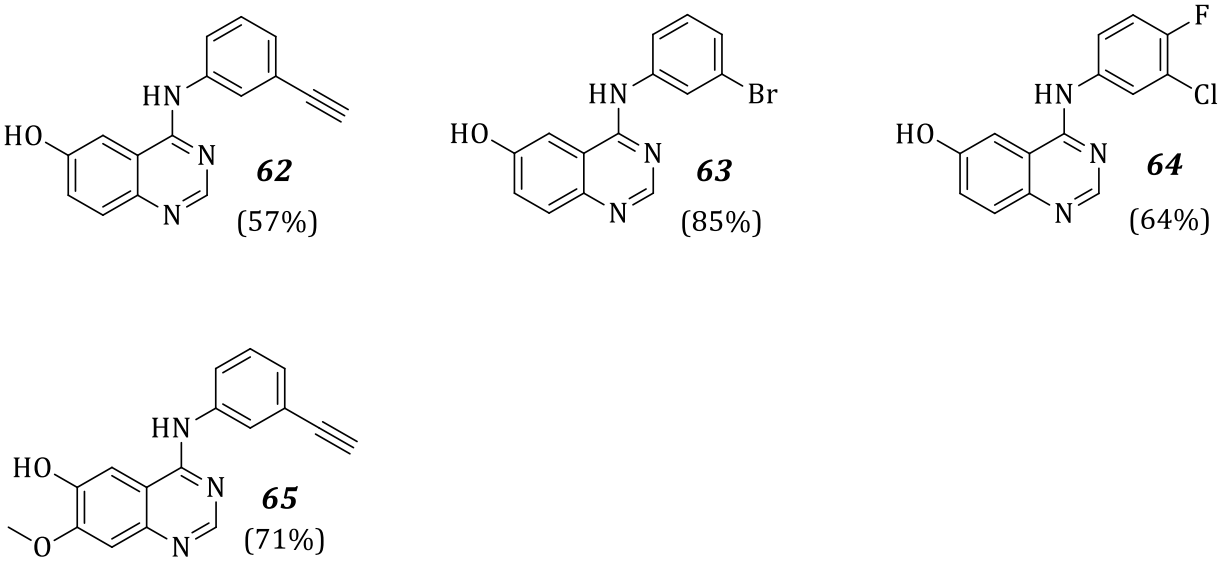

Figure 3.13 (a) The hydroxyl-substituted 4-anilinoquinazoline compounds (***62***–***65***).

Most importantly, compound ***65*** in **Fig. 3.13 (b)** was synthesised from low quantities of the acetoxyquinazoline ***29 (i),*** which was synthesised via selective demethylation route of ***27*** to afford ***28*** in poor yield (16%). The above compounds (***62***–***65***) were also analysed using the previously encountered NMR spectroscopic methods. In addition, heteronuclear NMR correlations (HSQC and HMBC) were used to acquire the full structural assignment of ***65***. Once again, the carbons with proton attachments were obtained from $^{1}J_{CH}$ HSQC and the carbon skeleton of the molecule was confirmed by $^{2,3}J_{CH}$ HMBC spectroscopic analysis. Based on these analyses, it was concluded that demethylation via acidolysis had occurred at the C-6 position of 6,7-dimethoxyquinazolin-4(3*H*)-one (***27***).

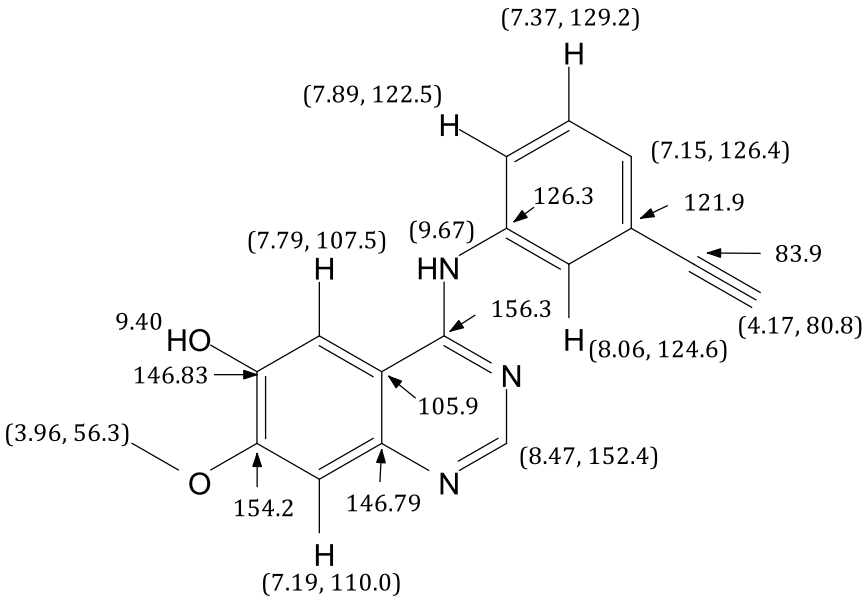

Figure 3.13 (b) Structural elucidation of 4-analinoquinazoline (***65***), synthesised via selective demethylation route of 6,7-dimethoxyquinazolinone (***27***), determined using HSQC and HMBC NMR .

3.14 The C-6 esterification of 4-anilinoquinazolines, linker insertion

At this point, it was possible to complete the synthesis of the small molecule 4-anilinoquinazolines by sequentially attaching the acrylate functionality via *O*-acylation. Thus, the acrylate library consisted of four compounds, shown in **Fig. 3.14**.

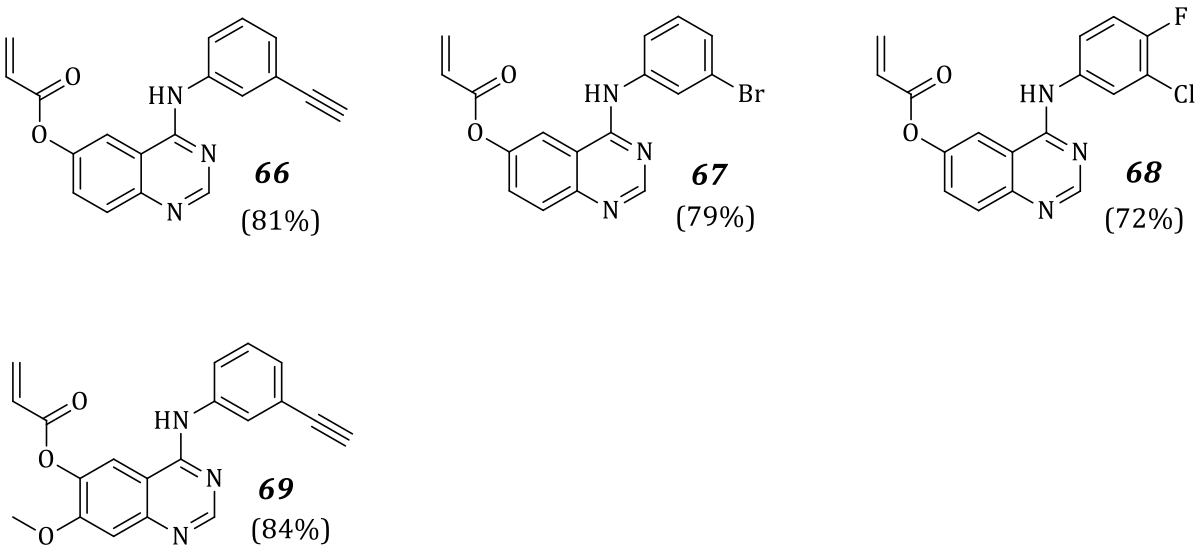

Figure 3.14 Library of C-6 acrylate-substituted 4-anilinoquinazoline final compounds ***66–69***.

3.15 Summary

A library of 4-anilinoquinazoline tyrosine kinase inhibitor small molecules composed acrylamide and acrylate electrophilic groups was successfully developed after the synthesis of quinazolinone intermediates that were prepared via the Niementowski protocol. These intermediates exhibited poor solubility, however, except in strong acids or bases, and this was found to be one of the barriers to their synthetic manipulation. Despite this setback, the required 4-anilinoquinazoline derivatives were obtained in reasonable yields and high chemical purities, which then allowed for their further conjugation with the PVP polymer. The polymerisation and conjugation of the selected 4-anilinoquinazoline compounds shown in **Fig. 3.15** will be addressed in the next chapter.

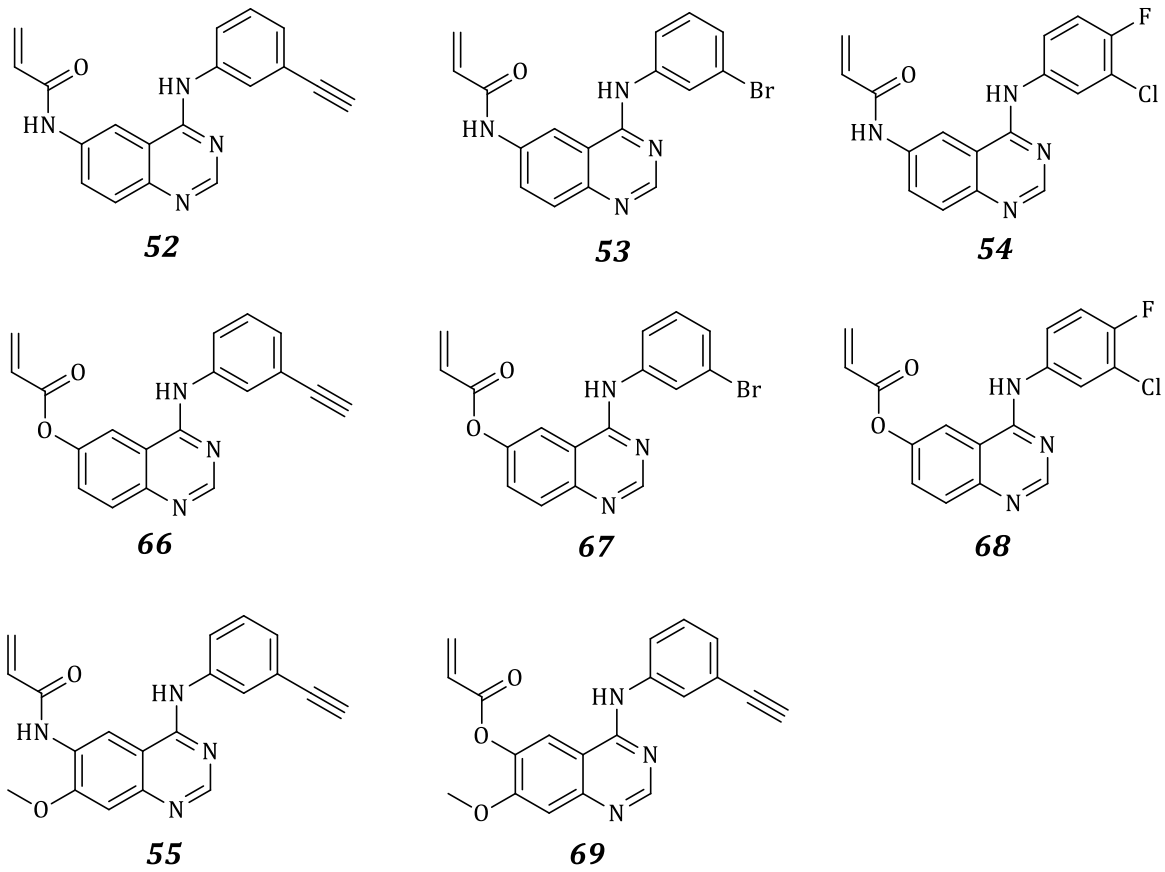

Figure 3.15 The 4-anilinoquinazoline compounds selected for further studies in developing the polymer conjugates.

3.16 References

1. (a) D'yakonov, A. L.; Telezhenetskaya, M. V., *Chemistry of Natural Compounds* **1997,** *33*, 221-267; (b) Khan, I.; Zaib, S.; Batool, S.; Abbas, N.; Ashraf, Z.; Iqbal, J.; Saeed, A., *Bioorganic and Medicinal Chemistry* **2016,** *24*, 2361-2381; (c) McGrath, N. A.; Brichacek, M.; Njardarson, J. T., *Journal of Chemical Education* **2010,** *87*, 1348-1349.

2. (a) Connolly, D. J.; Cusack, D.; O'Sullivan, T. P.; Guiry, P. J., *Tetrahedron* **2005,** *61*, 10153-10202; (b) Khan, I.; Ibrar, A.; Ahmed, W.; Saeed, A., *European Journal of Medicinal Chemistry* **2015,** *90*, 124-169.

3. (a) Niementowski, S.; Orzechowski, B., *Berichte der Deutschen Chemischen Gesellschaft* **1895,** *28*, 2809-2822; (b) Gabriel, S., *Berichte der Deutschen Chemischen Gesellschaft* **1903,** *36*, 800-813.

4. (a) Tsou, H.-R.; Mamuya, N.; Johnson, B. D.; Reich, M. F.; Gruber, B. C.; Ye, F.; Nilakantan, R.; Shen, R.; Discafani, C.; DeBlanc, R.; Davis, R.; Koehn, F. E.; Greenberger, L. M.; Wang, Y.-F.; Wissner, A., *Journal of Medicinal Chemistry* **2001,** *44*, 2719-2734; (b) Engel, J. D., *Biochemical and Biophysical Research Communications* **1975,** *64*, 581-586.

5. Ohya, Y.; Kuroda, H.; Hirai, K.; Ouchi, T., *Journal of Bioactive and Compatible Polymers* **1995,** *10*, 51-66.

6. Rewcastle, G. W.; Palmer, B. D.; Bridges, A. J.; Showalter, H. D. H.; Sun, L.; Nelson, J.; Michael, A.; Kraker, A. J.; Fry, D. W.; Denny, W. A., *Journal of Medicinal Chemistry* **1996,** *39*, 918-928.

7. Gillies, E. R.; Frechet, J. M. J., *Chemical Communications* **2003,** *40*, 1640-1641.

8. Nishioka, T.; Fujita, T.; Kitamura, K.; Nakajima, M., *Journal of Organic Chemistry* **1975,** *40*, 2520-2525.

9. Morley, J. S.; Simpson, J. C. E., *Journal of Chemical Society* **1947**, 360-366.

10. Moodie, R. B.; Thomas, P., N.; Schofield, K. S., *Journal of Chemical Society, Perkin Transactions II* **1977**, 1693-1705.

11. Steck, E., A; Fletcher, L., T, *Journal of the American Chemical Society* **1947,** *70*, 439-440.

12. Kulkarni, S. S.; Singh, S.; Shah, J. R.; Low, W.-K.; Talele, T. T., *European Journal of Medicinal Chemistry* **2012,** *50*, 264-273.

13. Bellamy, F. D.; Ou, K., *Tetrahedron Letters* **1984,** *25*, 839-842.

14. Proust, L., *Annales de Chimie et de Physique* **1798,** *28*, 213.

15. (a) Doddrell, D.; Jordan, D.; Riggs, N. V.; Wells, P. R., *Journal of the Chemical Society, Chemical Communications* **1972,** *20*, 1158-1158; (b) Barfield, M.; Walter, S. R.; Clark, K. A.; Gribble, G. W.; Haden, K. W.; Kelly, W. J.; Le Houllier, C. S., *Organic Magnetic Resonance* **1982,** *20*, 92-101.

16. Olah, G. A.; Narang, S. C.; Olah, J. A.; Lammertsma, K., *Proceedings in National Academy of Sciences of the United States of America* **1982,** *79*, 4487-4494.

17. Tobe, M.; Isobe, Y.; Tomizawa, H.; Matsumoto, M.; Obara, F.; Nagasaki, T.; Hayashi, H., *Bioorganic and Medicinal Chemistry Letters* **2001,** *11*, 545-548.

18. Bridges, A. J.; Zhou, H.; Cody, D. R.; Rewcastle, G. W.; McMichael, A.; Showalter, H. D. H.; Fry, D. W.; Kraker, A. J.; Denny, W. A., *Journal of Medicinal Chemistry* **1996,** *39*, 267-276.

19. García Martínez, A.; de la Moya Cerero, S.; Osío Barcina, J.; Moreno Jiménez, F.; Lora Maroto, B., *European Journal of Organic Chemistry* **2013,** *2013*, 6098-6107.

20. Lino, T.; Sasaki, Y.; Bamba, M.; Mitsuya, M.; Ohno, A.; Kamata, K.; Hosaka, H.; Maruki, H.; Futamura, M.; Yoshimoto, R.; Ohyama, S.; Sasaki, K.; Chiba, M.; Ohtake, N.; Nagata, Y.; Eiki, J.-i.; Nishimura, T., *Bioorganic and Medicinal Chemistry Letters* **2009,** *19*, 5531-5538.

21. Lindley, J., *Tetrahedron* **1984,** *40*, 1433-1456.

22. Klapars, A.; Buchwald, S. L., *Journal of the American Chemical Society* **2002,** *124*, 14844-14845.

23. (a) Li, R.-D.; Zhang, X.; Li, Q.-Y.; Ge, Z.-M.; Li, R.-T., *Bioorganic and Medicinal Chemistry Letters* **2011,** *21*, 3637-3640; (b) Lin, S.; Li, Y.; Zheng, Y.; Luo, L.; Sun, Q.; Ge, Z.; Cheng, T.; Li, R., *European Journal of Medicinal Chemistry* **2017,** *127*, 442-458.

24. Buchanan, G. L., *Chemical Society Reviews* **1988,** *17*, 91-109.

25. Neises, B.; Steglich, W., *Angewandte Chemie International Edition in English* **1978,** *17*, 522-524.

26. (a) Gibson, K. H.; Grundy, W.; Godfrey, A. A.; Woodburn, J. R.; Ashton, S. E.; Curry, B. J.; Scarlett, L.; Barker, A. J.; Brown, D. S., *Bioorganic and Medicinal Chemistry Letters* **1997,** *7*, 2723-2728; (b) Barker, A. J.; Gibson, K. H.; Grundy, W.; Godfrey, A. A.; Barlow, J. J.; Healy, M. P.; Woodburn, J. R.; Ashton, S. E.; Curry, B. J.; Scarlett, L.; Henthorn, L.; Richards, L., *Bioorganic and Medicinal Chemistry Letters* **2001,** *11*, 1911-1914.

27. (a) Asano, T.; Yoshikawa, T.; Usui, T.; Yamamoto, H.; Yamamoto, Y.; Uehara, Y.; Nakamura, H., *Bioorganic and Medicinal Chemistry* **2004,** *12*, 3529-3542; (b) Williamson, A., *Philosophical Magazine* **1850,** *37*, 350-356.

28. Coppola, G. M.; Schuster, H. F., *Journal of Heterocyclic Chemistry* **1989,** *26*, 957-964.

29. Cardwell, D.; Robinson, R., *Journal of the Chemical Society, Transactions* **1915,** *107*, 255-259.

30. Fredrikson, A.; Stone-Elander, S., *Journal of Labelled Compounds and Radiopharmaceuticals* **2002,** *45*, 529-538.

31. Arnott, E. A.; Chan, L. C.; Cox, B. G.; Meyrick, B.; Phillips, A., *Journal of Organic Chemistry* **2011,** *76*, 1653-1661.

32. Wan, Z.-K.; Wacharasindhu, S.; Levins, C. G.; Lin, M.; Tabei, K.; Mansour, T. S., *Journal of Organic Chemistry* **2007,** *72*, 10194-10210.

33. (a) Baumann, E., *Berichte der Deutschen Chemischen Gesellschaft* **1886,** *19*, 3218-3222; (b) Schotten, C., *Berichte der Deutschen Chemischen Gesellschaft* **1884,** *17*, 2544-2547.

34. Hartwig, J. F., *Angewandte Chemie International Edition* **1998,** *37*, 2046-2067.

35. (a) Marques, C. A.; Selva, M.; Tundo, P., *Journal of Organic Chemistry* **1995,** *60*, 2430-2435; (b) Arcadi, A.; Cerichelli, G.; Chiarini, M.; Vico, R.; Zorzan, D., *European Journal of Organic Chemistry* **2004,** *2004*, 3404-3407.

36. Fujita, T.; Nishioka, T., In *Progress in Physical Organic Chemistry*, John Wiley & Sons, Inc.: New Jersy, 2007; Vol. 12, pp 49-89.

37. Brenton, A. G.; Godfrey, A. R., *Journal of the American Society for Mass Spectrometry* **2010,** *21*, 1821-1835.

Chapter 4: Polymerisation and synthesis of polymer-drug conjugates

Chapter 4: Polymerisation and synthesis of polymer-drug conjugates

Abstract

This chapter addresses the synthesis of a PVP polymer by RAFT/MADIX polymerisation, ω-end group modification, and modular PVP conjugation with the 4-anilinoquinazoline small molecules. It further addresses the morphological characterisation of the subsequent polymer-drug conjugates using various analytical techniques. Synthesis and characterisation are discussed.

4.1 Introduction

The core objective was the development of polymeric-drug conjugates, *i.e*. polymeric prodrugs, for the drug delivery of 4-anilinoquinazoline kinase inhibitors to target sites. Therapeutic limitations of quinazoline-derived anti-tumour agents are well established,[1] but a recent advance in the treatment of lung cancer has demonstrated accelerated approval of kinase inhibitors that exhibit reactive toxicity properties.[2] While intentions are to develop curative therapy and overcome drug resistance, the occurrence of adverse drug reactions (ADRs) has remained one of the critical challenges that requires immediate attention in this field.[3] In view of this problem, a micellar drug delivery system was developed to improve the therapeutic efficacy and minimise ADRs. To achieve the desired delivery structure, it is critical that the polymer designed for this purpose must be well defined.

4.2 Reversible deactivation radical polymerisation of N-vinylpyrrolidone

A number of synthetic characteristics of reversible deactivation radical polymerisation (RDRP) methods, formerly referred to as controlled/living radical polymerisation (the three main techniques being nitrogen-mediated polymerisation (NMP), atom radical transformation (ATRP), and reversible addition-fragmentation chain transfer (RAFT), have been extensively studied.[4] Their capabilities in and limitations to achieving good control in polymerisation of less activated vinyl monomers such as NVP have been established.[5] Synthesis of well-defined PVP with predictable molecular weight and low dispersity is best controlled by the RAFT/MADIX polymerisation technique.[4, 6] The optimal synthetic protocol for NVP polymerisations requires the following: (i) design of

RAFT agents (also referred to as chain transfer agents) aligned with the monomer reactivity, and (ii) optimization of reaction conditions.[4b]

In line with this concept, Klumperman and co-workers have demonstrated the utility of triazole-derived RAFT agents to form good leaving groups for a variety of monomers, including NVP, using RAFT/MADIX polymerisations.[7] Besides establishing the potential utility of triazole-based leaving groups, Pound *et al*.[8] methodically explored RAFT/MADIX polymerisation of NVP using *O*-ethyl xanthates. In their studies,[8] a number of unexpected side reactions were determined during polymerisation. One of the highlights of their work was establishing the optimum reaction conditions (temperature ≤ 60 °C) that are essential to retaining the unstable xanthate ω-end group. The xanthate end groups are susceptible to several chemical modifications; they readily undergo the thermally stimulated Chugaev elimination reaction during polymerisation, thus resulting in the formation of olefin-terminated PVP end groups.[9] In the present study, preservation of the ω-end group is particularly important for the ensuing conjugation of bioactive 4-anilinoquinazoline molecules. Informed by these developments, the RAFT/MADIX-mediated synthesis of α,ω-heterotelechelic PVP using a triazole-based RAFT agent is discussed in this chapter.

4.3 Preparation of RAFT agent

The general synthetic strategy for the preparation of triazole-based RAFT agents was adapted from Akeroyd *et al*.[7] [see **Fig. 4.3 (a)**]. Using an alkyne moiety as the starting material, the but-3-yn-2-ol hydroxyl group was activated to form a tosylate leaving group in ***70***.[10] Treatment of ***70*** with the *O*-ethyl xanthate salt of potassium effected the nucleophilic displacement of the tosylate group, at room temperature,[7] affording (***71***) in good yield. At this point, the ω-end thiocarbonyl thio functionality was successfully substituted onto the alkyne precursor, and an azide functionality was thus required to create the triazole group. Therefore, a copper(II)-catalysed diazotransfer reaction between 1-amino-2,2-diethoxypropane and 1*H*-imidazole-1-sulfonyl azide was carried out first, affording the corresponding 3-azido-1,1-diethoxypropane (***73***).[11] The copper(II)-promoted [3+2] Huisgen cycloaddition reaction was then performed between

the functionalised alkyne ***71*** and azido ***73*** to afford the desired RAFT agent (***74)*** in good yield. More recently, Reader *et al.*[12] highlighted the topological arrangement of ***74*** for α,ω-heterochelic functionality to favour orthogonal end group modifications. This feature is of interest in bio-conjugation as it allows for the chain-end-oriented binding,[13] thus enabling one-to-one attachments in prodrug formulations. This study focused on the ω-end functionality.

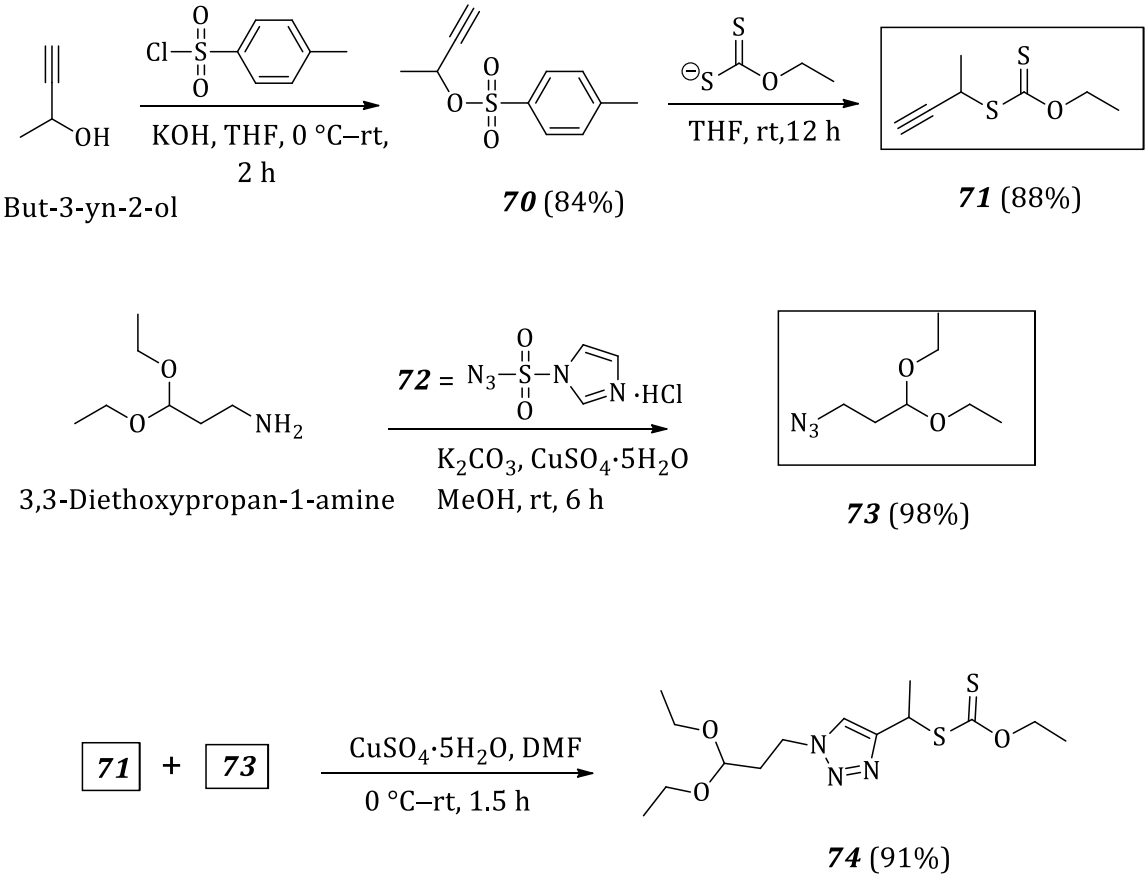

Figure 4.3 (a) Outline for the preparation of a RAFT agent (***74***) with a triazole moiety for RAFT/MADIX-mediated polymerisation. The ω-end alkyne and the α-end azide groups (in rectangles) can be functionalised with various substrates.[7]

^{1}H NMR analysis of the RAFT agent provided the opportunity to determine the degree of polymerisation (DP_n) and the number average molecular weight (M_n) of a polymer. For polymers with high end group fidelity, the number of monomers in a polymer chain can be determined by comparing clearly defined proton signals from the RAFT agent with those that can be distinguished from the repeating unit.[14] Thus, ^{1}H NMR spectroscopy

remains one of the most important tools for polymer characterisation. The ^{1}H NMR spectrum of the RAFT agent used for the polymerisation of NVP is depicted in **Fig. 4.3 (b)**. Other useful techniques include relative measurements of M_n by size-exclusion chromatography (SEC) and more absolute measurements by mass spectrometry (MS), specifically matrix assisted laser desorption ionization-time of flight mass spectrometry (MALDI-TOF MS).[14-15] Owing to the common problem of thermal degradation of polymers during volatilisation, as well as MS sensitivity bias to dispersity,[16] emphasis is now placed on ^{1}H NMR and SEC analytical methods throughout our polymerisation experiments.

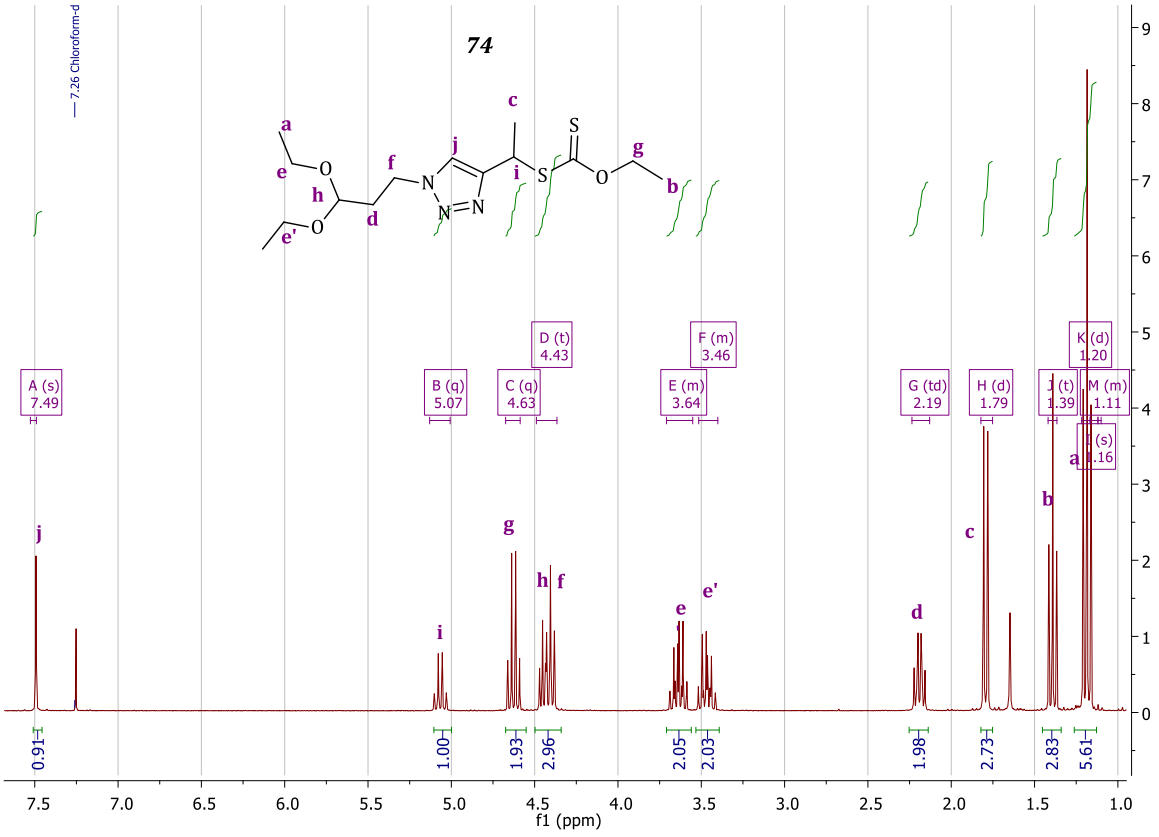

Figure 4.3 (b) ^{1}H NMR spectrum of the RAFT agent used for NVP polymerisation.

4.4 RAFT/MADIX-mediated polymerisation of NVP

The efficacy of ***74*** in controlling NVP polymerisation under various reaction conditions was determined earlier, by Klumperman and co-workers.[12] It was established that NVP polymerisations were achieved at 60% monomer conversion at various DP_ns. Thus, using

these optimised experimental conditions, a baseline assessment of ***74*** for controlling polymerisations was revisited, as outlined in **Table 4.4**.

Table 4.4 RAFT/MADIX polymerisation of NVP; experimental conditions: [RAFT agent, ***74***]/[AIBN] is 4; temperature, 60 °C; solvent, THF

Entry	[NVP]:[*74*]:[AIBN]	Time (h)	$M_{n,\ theory}$[a] (g/mol)	$M_{n,\ SEC}$[b] (g/mol)	$M_{n,\ NMR}$[c] (g/mol)	$Đ$
1	45:1:0.25	9	nd	1007	1790	1.08
2	45:1:0.25	15	nd	1529	2012	1.14
3	45:1:0.25	17	nd	1524	2234	1.14
4	45:1:0.25	24	3343	1536	2123	1.14
5	40:1:0.25	24	3011	1361	1330	1.15

[a] $M_{n,theor} = M_{n,\mathrm{RAFT}} + \left([M_{n,\mathrm{NVP}}]_\circ \times M_{r,\mathrm{NVP}} \times \alpha\right)/\left([M_{n,\mathrm{RAFT(74)}}]_\circ\right)$, α = 60% estimated monomer (NVP) conversions.[12]
[b] M_n determined by SEC in DMAc relative to PMMA standards
[c] M_n determined by ^{1}H NMR ($M_{n,\mathrm{NMR}} = M_{r,\mathrm{NVP}} \times DP_n$) + $M_{r,RAFT(74)}$

The SEC analyses for polymerisations were obtained using a refractive index (RI) detector. From **Table 4.4**, **entries 1–4,** the $M_{n,\ SEC}$ values indicate that polymerisations of NVP ended at reaction times of < 15 h. This conclused is based on general RDRP polymerisation behaviour, in which M_n increases in a linear fashion with monomer consumption, *i.e.* $DP_n = \frac{[M]_\circ - [M]_t}{[RAFT]}$. The DP_n is used to define the size of a polymer by the number of monomer (NVP) repeat units in a polymer molecule and a closer look at **entries 2–4** reveal no increase in $M_{n,\ SEC}$ values. The overall efficiency of the RAFT agent performance in controlling NVP polymerisations was in agreement with the previously reported data, for which the 4-methyl-1,2,3-triazole leaving group showed improved living character in the presence of the radical stabilising methyl group.[6, 11] The polydispersity indices ($Đ \leq 1.15$) of PVP indicated narrow molecular weight distributions. However, it was noted that monomer conversions were lower than expected,[12] and the consistent polydispersity values after the polymerisation reaction had stopped (beyond 15 h) were ascribed to solvent participation in reducing the viscosity of the reaction medium. SEC-DRI chromatograms (DRI: differential refractive index) of PVP are shown in **Fig. 4.4 (a)**.

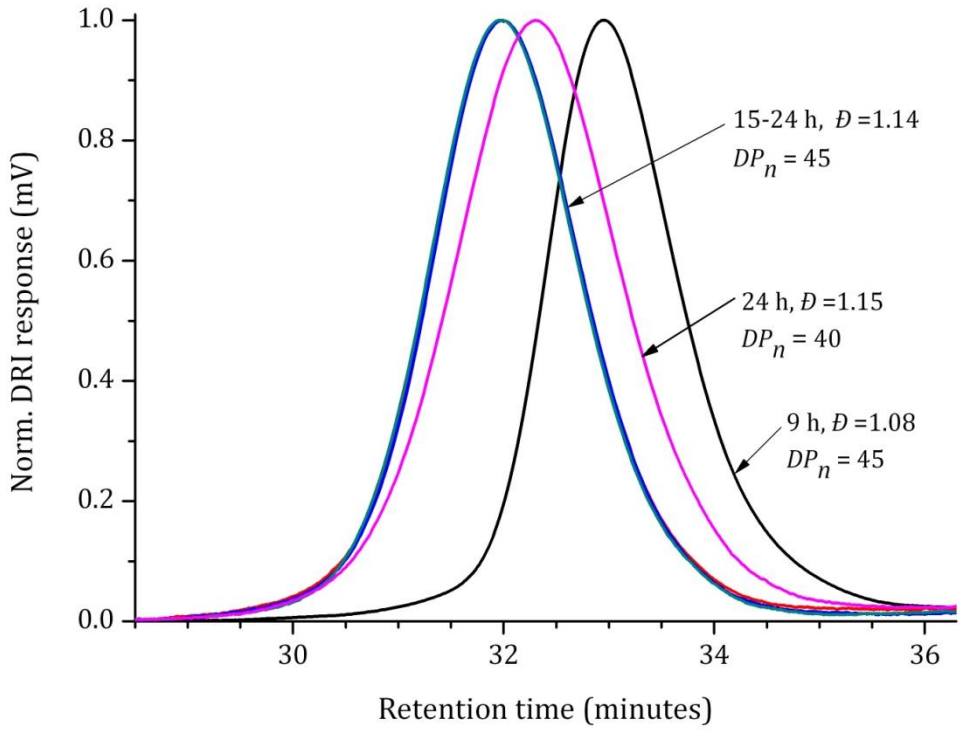

Figure 4.4 (a) Normalised SEC-DRI chromatograms of PVP samples, **entries 1–5** from **Table 4.4.**

The ^{1}H NMR end group analysis was used in parallel with SEC to obtain comparable results. The end group protons of the RAFT agent from the α-end were distinguished and their integral values were compared to those of identifiable NVP repeating unit [see **Fig. 4.4 (b)**]. The ratios of these protons were deduced, and the experimental DP_n and $M_{n,NMR}$ were then determined. There were systemic deviations in $M_{n,SEC}$ because of the hydrodynamic volume differences between PVP and the poly(methyl methacrylate) (PMMA) standards used for the calibration. Nonetheless, the thermally unstable *O*-ethyl xanthate functional group was mostly preserved throughout polymerisation reactions. This was established by comparing the end groups α-(***f*** + ***h***) and ω-(***g***) in **Fig. 4.4 (b),** which were approximated to 3:2, as expected. It was thus reckoned that modification of the ω-chain end would lead to the facile introduction of 4-anilinoquinazoline small molecules.

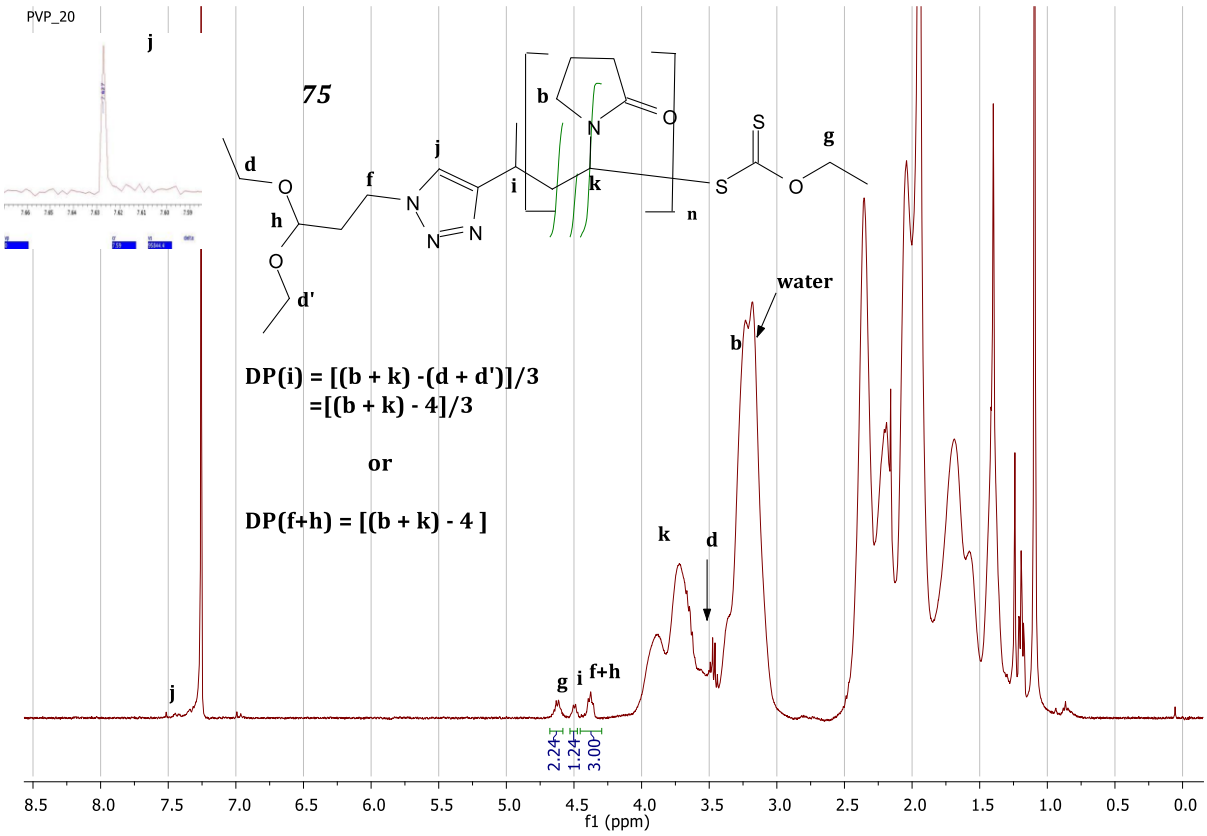

Figure 4.4 (b) ^{1}H NMR spectrum of end-group functionalised PVP polymer, ***75***.

4.5 End group modification of RAFT/MADIX-mediated PVP polymer

In pursuit of polymer-drug conjugates, the first step of transformation involved conversion of the thiocarbonyl thio end group into the thiol functionality.[13a, 17] A general presentation of the synthetic strategy is illustrated in **Fig. 4.5 (a)**. The thiocarbonyl thio end groups can undergo several transformations according to the intended use of the final product.[17] Of particular interest was creating a thiol-terminated PVP. The aminolysis reaction was used to achieve quantitative results. Use of different reducing agents to achieve similar thioamidation reactions with differing probabilities of side reactions has been reviewed elsewhere.[17]

Hence, ***75*** was suspended in acetone, the solution was treated with cyclohexyl amine and then stirred at room temperature, to afford ***76*** in good yield. The bulky cyclohexyl amine was purposely employed with the intention to mitigate base-promoted elimination side

reactions. In doing so, preservation of the end group functionality during the aminolysis reaction was also realised. No additional purification steps were required, other than precipitation of the polymer in diethyl ether.

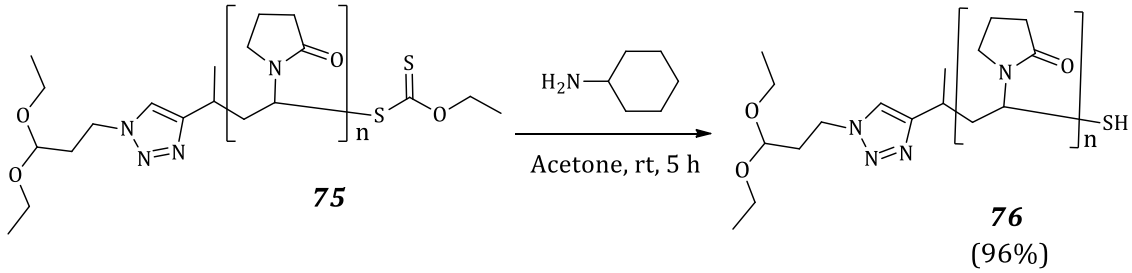

75 ***76*** (96%)

Figure 4.5 (a) Transformation of *O*-ethyl xanthate end group into a thiol end group via an aminolysis reaction.

A successful *O*-ethyl xanthate end group transformation was ascertained by ^{1}H NMR; it was discovered that characteristic methylene protons of the *O*-ethyl xanthate end group had disappeared at 4.63 ppm [refer to **Fig. 4.5 (b)**].

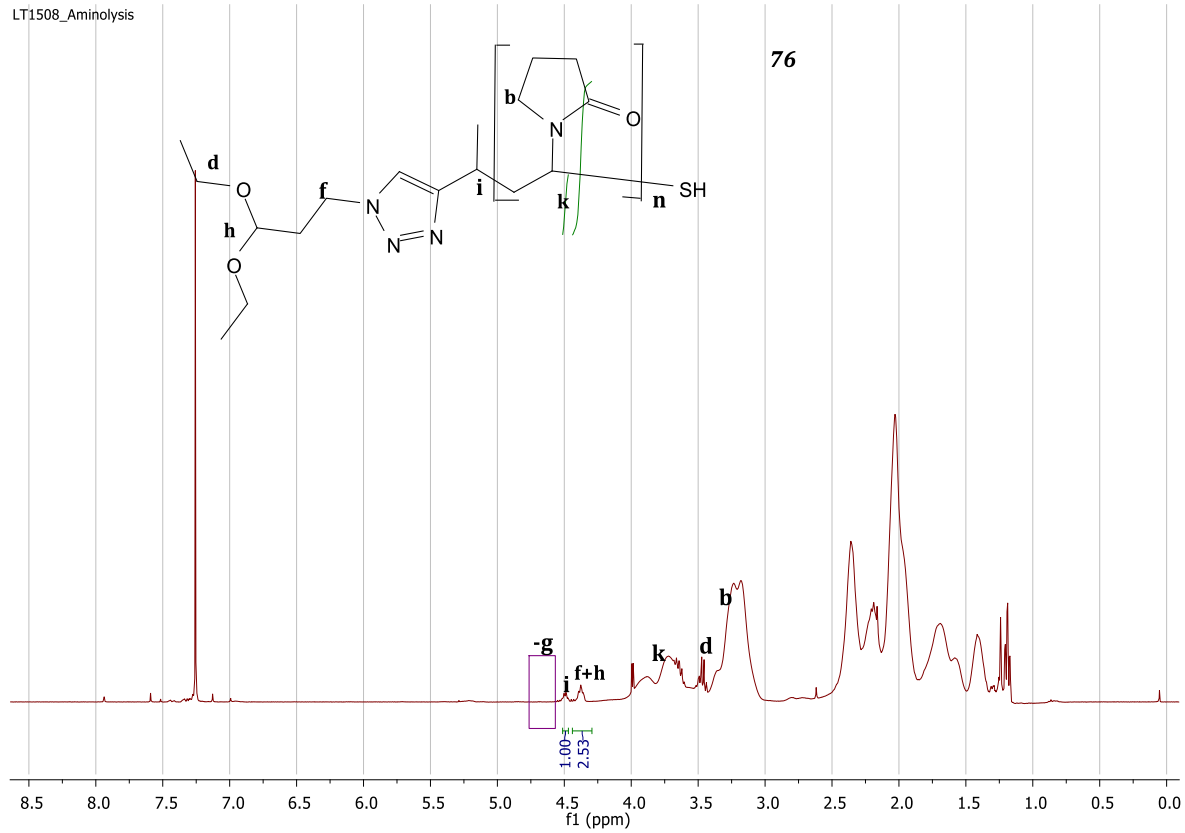

Figure 4.5 (b) ^{1}H NMR spectra of thiol-terminated PVP (***76***) prepared via an aminolysis reaction. Disappearance of the previously distinguished *O*-ethyl xanthate protons has been highlighted by a rectangle.

Besides using ^{1}H NMR data, a more accurate detection of *O*-ethyl xanthate modification was obtained with SEC-UV analysis. The xanthate chromophore absorption band (SC=S, $\lambda_{max.}$ = 280 nm) in ***75*** was overlapped by the UV absorbance of ***76***. Because of the xanthate transformation into a thiol end group, no corresponding UV absorbance signal was observed for ***76*** at this wavelength [see **Fig. 4.5 (c)**].

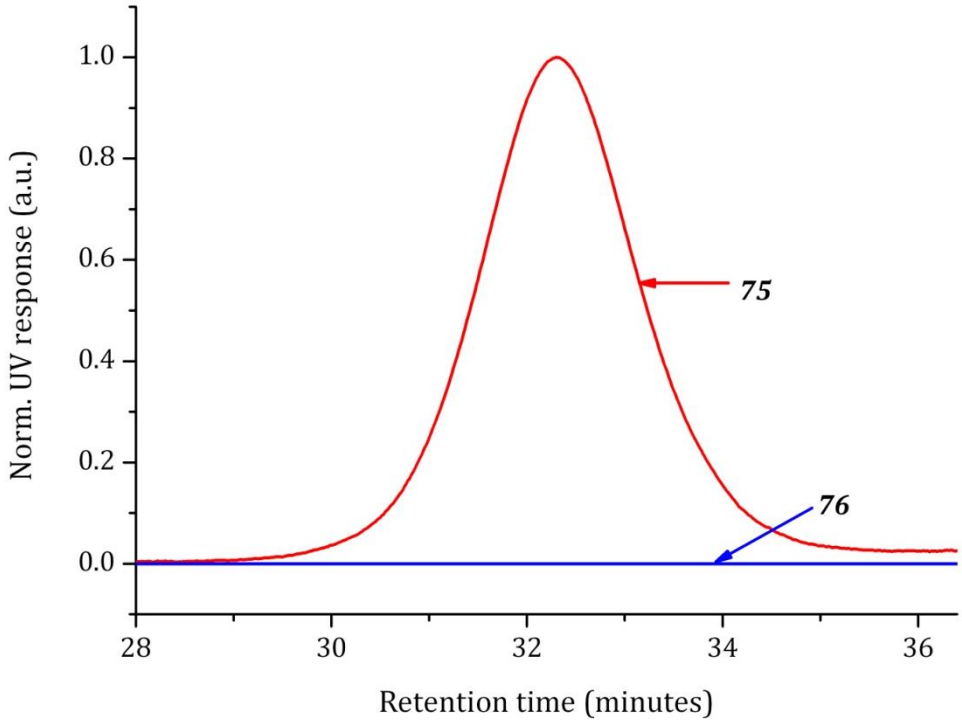

Figure 4.5 (c) The SEC-UV response (λ_{max}.= 280 nm) showing transformation of a xanthate SC=S end group to a thiol (***75*** to ***76***). The UV responses were normalised to smooth the plots.

Besides the *O*-ethyl xanthate transformation to a thiol group, formation of disulfide bridges due to a thiol oxidative coupling side reaction was expected. This was not a major concern as it could be lessened by performing the reaction under inert conditions or perhaps including phosphines, which are known to reduce alkyl disulfides.[18] Other commonly used methods to prevent the formation of alkyl disulfides make use of the Ellman procedure,[19] which is generally referred to as thiol-trapping in polymer chemistry, or capping agents. Keeping the possibility of disulphide formation in mind, SEC-DRI chromatograms for ***75*** and ***76*** were overlaid as shown in **Fig. 4.5 (d).** The RI response of ***76*** was then examined for doubling of M_n or shouldering. Nevertheless, only broadening of the baseline in the direction of higher molecular weight (shorter elution time) was observed; this gave rise to the increased poly dispersity index ($Đ$ =1.20).

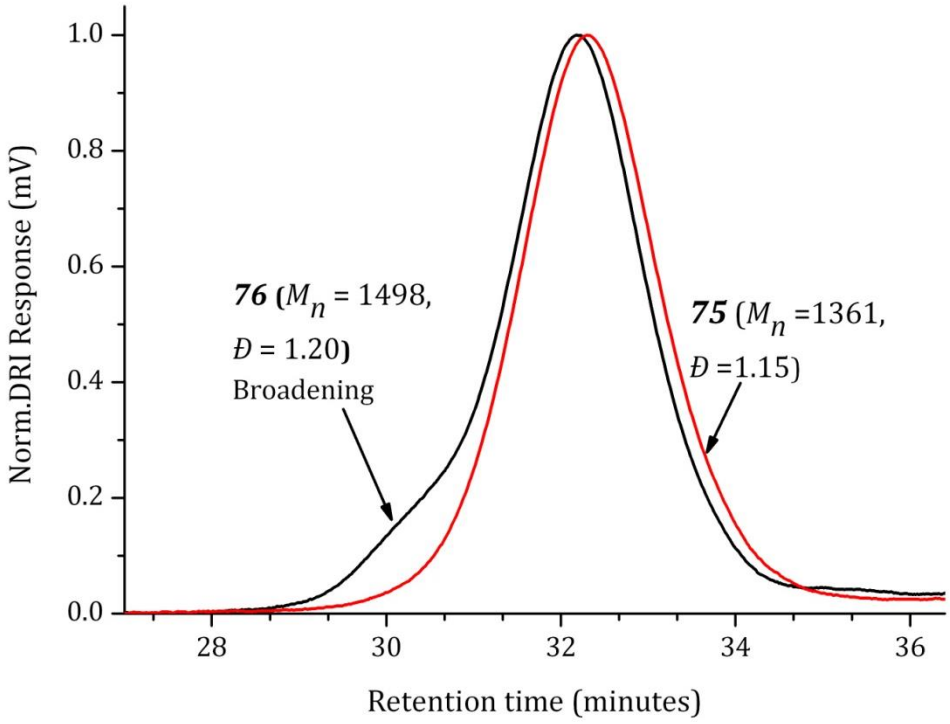

Figure 4.5 (d) SEC-DRI chromatograms of ***75*** and (***76***). Peak broadening towards shorter elution time suggests doubling of the PVP chain length due to disulfide formation.

From overall polymerisation results, it appeared that PVP polymers of predetermined molecular weights were successfully obtained. The ^{1}H NMR and SEC analyses demonstrated controlled polymerisation reactions. More importantly conservation of end group functionalities was also observed. Following the aminolysis reaction, it was further observed that ***76*** existed as a thiol-terminated PVP polymer. This permitted the facile development of polymer conjugates via 1,4-conjugated addition to the small molecules containing α,β-unsaturated electrophilic groups.

4.6 Synthesis of PVP-(4-phenyl amine)quinazoline conjugates

In previous work,[12, 20] similar conjugation reactions have been carried out under aqueous solution or very polar solvents, which were normally basified by organic bases. This is in agreement with Edwards and Pearson's views of enhancing overall nucleophilicity.[21] Thiol groups could then exist in solution as more reactive thiolates under these conditions. Among the studied organic bases, Li *et al.*[20] have demonstrated primary and

tertiary amines as efficient catalysts for phosphines, when preventing alkyl disulfides formation. In cases where alkyl disulfides have already been formed, only 30% could be successfully reduced under mild conditions in under 4 h, thus requiring intervention of thermally promoted disulphide reductions.[22] On the other hand, Levison *et al*.[23] have developed efficient water soluble phosphines such as tris(2-carboxyethyl)phosphine (TCEP) for the mild reduction of alkyl disufides under biological conditions and it works well without generating reactive by-products. TCEP oxidises readily in aqueous bases to form phosphine oxides, irreversibly,[18] but its hydrogen chloride salt is very stable in air, which makes it easier to manipulate.

Presented with these options, thiol-terminated PVP polymer and 4-anilinoquinazoline compounds were conjugated to form polymer-bound SMKIs. A modulated Michael addition reaction was used to form covalent bonds between these two substrates.[13a, 20, 24] A representative example of the conjugation reaction, with its conditions, is shown in **Fig. 4.6 (a)**. With an 1.2 molar equivalent excess of 4-anilinoquinazoline to PVP polymer in DMF solvent, the reaction mixture was basified with 25% NH_4OH in the presence of TCEP·HCl as the reducing agent, to afford PVP-(4-phenyl amine)quinazoline conjugates in good yields.

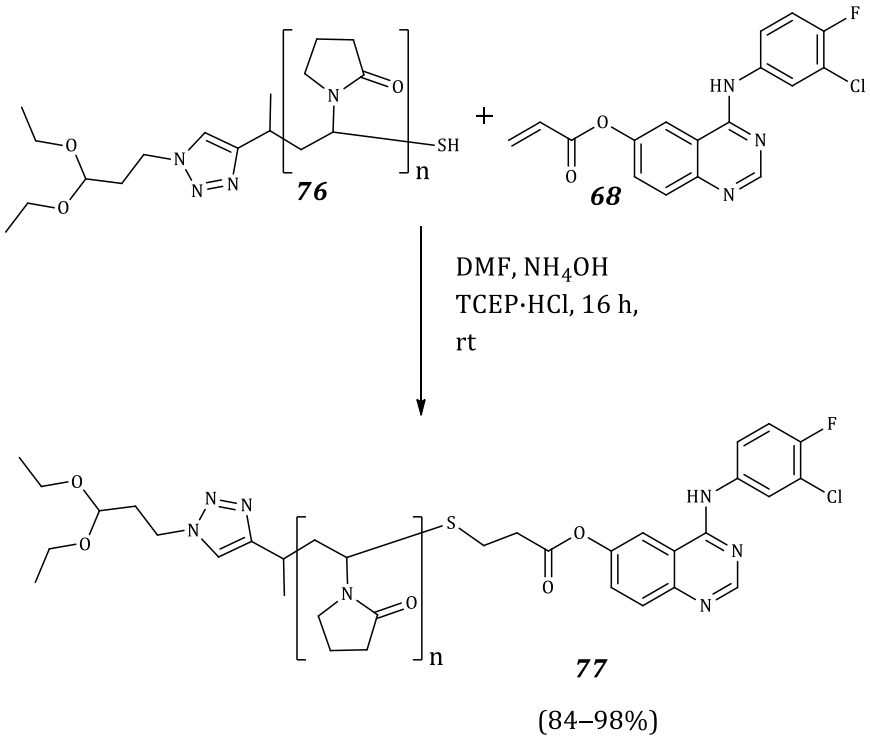

Figure 4.6 (a) Preparation of covalently bonded PVP-(4-phenyl amine)quinazoline conjugates via the 1,4-conjugated Michael addition reaction.

At the end of the reaction, ***77*** was subjected to purification by dialysis; excess 4-anilinoquinazoline was removed. The dialysis procedure was guided by membrane tolerance to organic solvents according to the manufacturer's specifications. Dialysis solvent composition was 10% ethanol in deionised water for the first 24 h, followed by 100% deionised water for another 24 h. At the end of dialysis, ***77*** was recovered as a suspension in deionised water: it was frozen in liquid nitrogen and freeze-dried. ^{1}H NMR analysis of ***77*** showed successful conjugation of polymer to a small molecule in a 1:1 ratio [see **Fig. 4.6 (b)**]. The PVP methine proton integration at 4.5 ppm was used to calculate the number of aromatic protons (1:9) that corresponded to 4 anilinoquinazoline and a triazole. Moreover, disappearance of the Michael acceptor olefin signals at 5.80–6.60 ppm further confirmed positive conjugation.

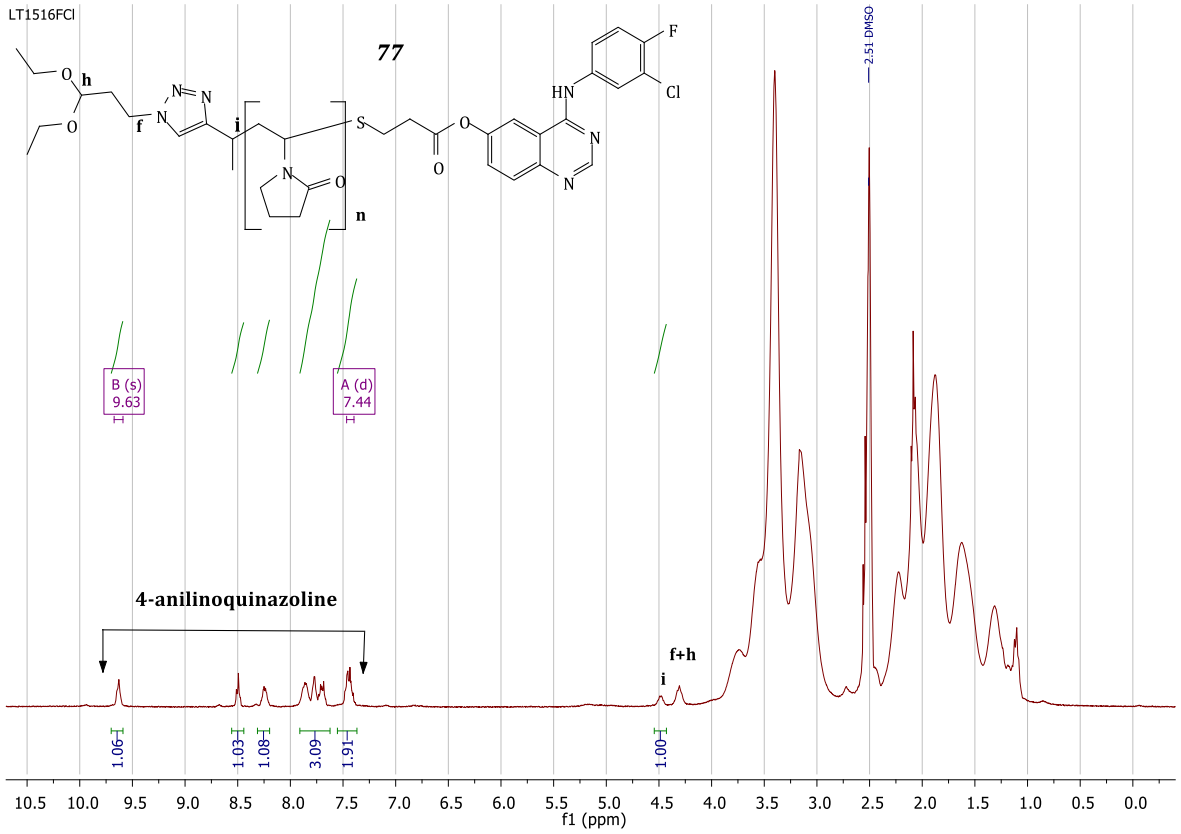

Figure 4.6 (b) ^{1}H NMR spectra showing end group analysis for the PVP-(4-phenyl amine)quinazoline conjugate (***77***).

The ^{1}H NMR results were further confirmed by SEC analysis using both a RI detector and the UV wavelength corresponding to 4-anilinoquinazoline. Thus, an ultraviolet-visible (UV-Vis) scan was performed in *N,N*-dimethylacetamide (DMAc) to determine the absorption bands ($\lambda_{max.}$) of the conjugated 4-anilinoquinazoline. The absorption bands of ***77*** showed two absorption bands at approximately 290 nm and 350 nm, as shown in **Fig. 4.6 (c)**.

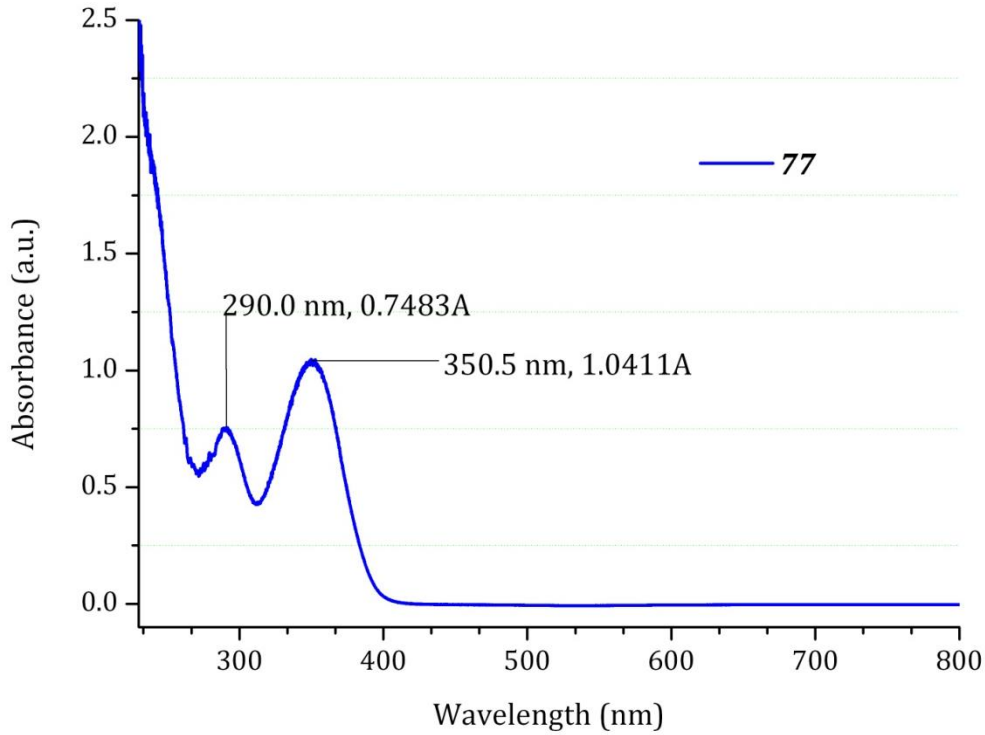

Figure 4.6 (c) UV-Vis spectrum of the PVP-(4-phenyl amine)quinazoline conjugate (***77***).

The absorption band at λ = 350 nm was then selected for the SEC-UV analysis of the conjugates in DMAc ($\lambda_{max.}$ ~260 nm), where the solvent interference was considered minimal. The SEC-UV chromatogram of ***77*** obtained is shown in **Fig. 4.6 (d)**. Two additional conjugates (***78*** and ***79***) were added for comparison purposes. The chemical structures are shown in *Section 4.8* of this chapter. A closer look at the SEC-UV chromatograms revealed minor peaks close to the baseline, which could suggest that the conjugates were interacting with the SEC column.

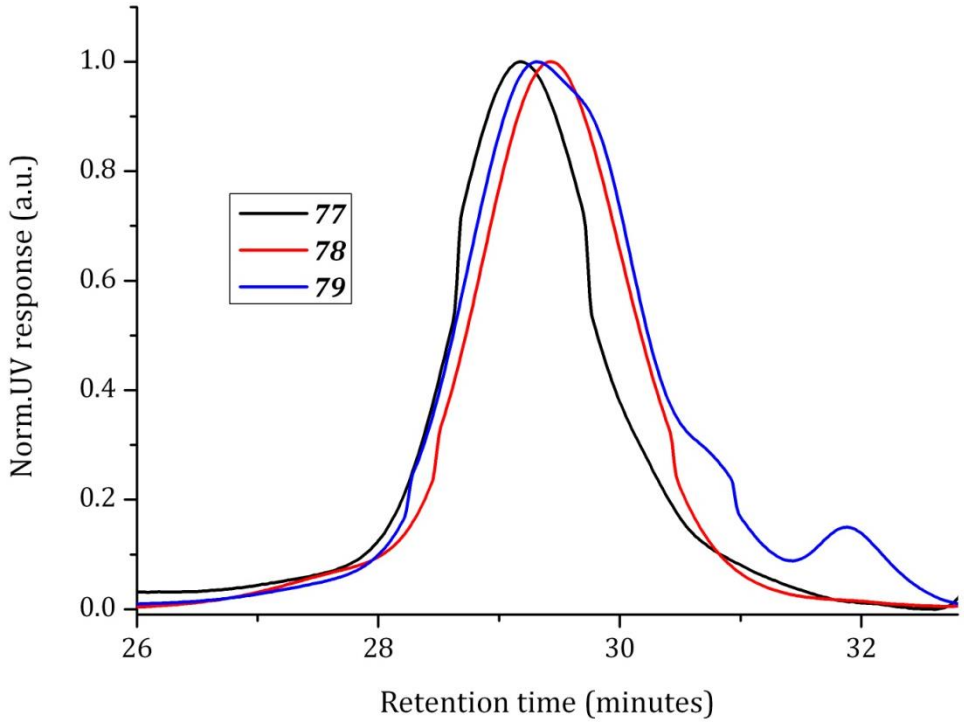

Figure 4.6 (d) SEC-UV chromatograms (λ_{max} = 350 nm) of PVP-(4-phenyl amine)quinazoline conjugates (***77***, ***78***, and ***79***) in DMAc solvent.

Besides having these SEC-UV results in hand, SEC-DRI results were also obtained. The chromatograms shouldering towards higher molecular weight positively indicated successful conjugation. All the SEC analyses were performed at a concentration of 1.3×10^{-3} M and the obtained M_n values are as shown in **Fig. 4.6 (e)**. In the light of these results, it was considered useful to attempt to induce particle self-assembly in a selective solvent and then assess the resultant aggregation morphologies.

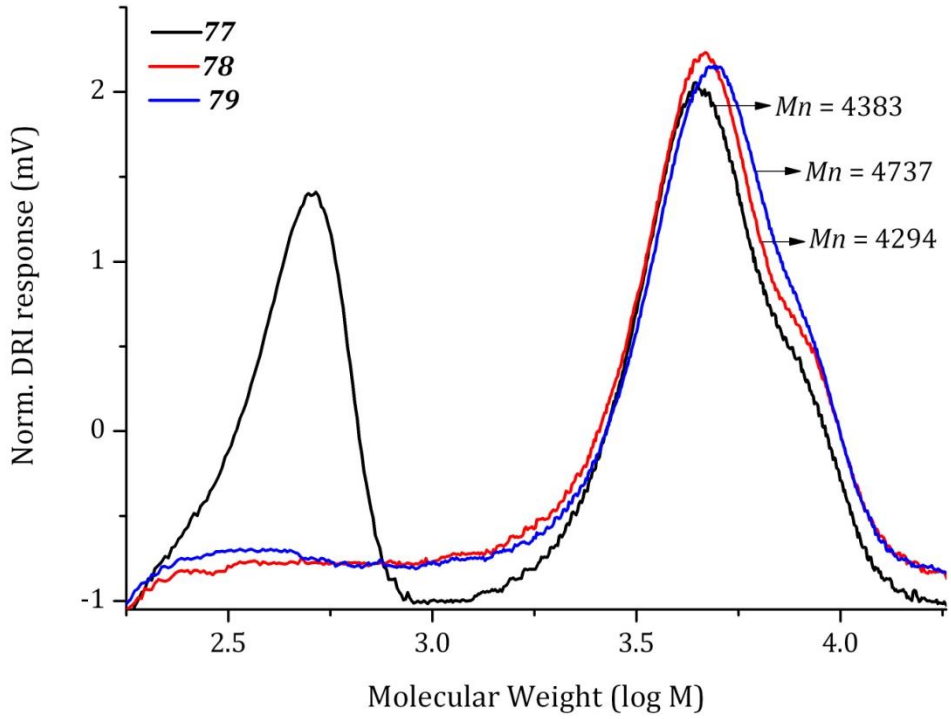

Figure 4.6 (e) SEC-DRI chromatograms of PVP-(4-phenyl amine)quinazoline conjugates (***77***, ***78***, and ***79***).

4.7 Micelle formation and characterisation

The self-organising behaviour of amphiphilic conjugates was studied in aqueous solutions. To initiate self-assembly, a complete dissolution of the conjugates (*e.g.* ***77***) was investigated in different aprotic solvents; DMSO was determined as a common solvent. Thus, the conjugates were dissolved in DMSO and solvent composition was changed by gradual addition of a more selective aqueous solvent. The high miscibility of DMSO with water proved to be instrumental, as DMSO was easily displaced through dialysis in deionised water.

These amphiphilic conjugates were expected to arrange themselves into organised assemblies of micelles.[25] Thus, a solution of ***77*** was prepared in DMSO (1 mg/mL) and serially diluted with deionised water in a drop-wise fashion, while swirling, into different concentrations. The particle size distribution of resulting turbid colloidal suspensions were then analysed by a dynamic light scattering (DLS) technique. DLS measures the scattered light intensity from a laser passing through the colloidal solution as a function

of time (Brownian motion) and this is correlated to the hydrodynamic size of the particles by the Stokes–Einstein equation.[26] The obtained DLS results showing particle size distribution of the conjugates at different concentrations are shown in **Fig. 4.7 (a)**. It was determined that in the concentration range 10^{-6} to 10^{-5} M, the conjugates self-organised into uniformly distributed sizes of 123–130 nm, while at 10^{-4} M concentration the conjugates seemed to generate more than one aggregate state.

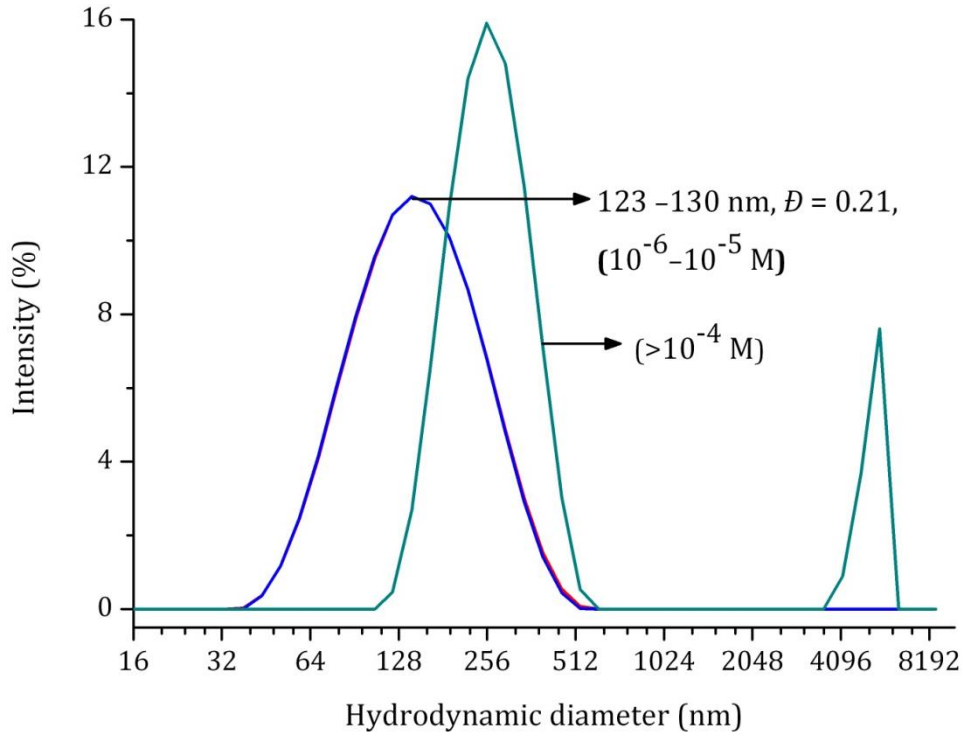

Figure 4.7 (a) Particle size distribution plots of PVP-(4-phenyl amine)quinazoline conjugates (***77***) obtained by DLS.

With the promising DLS data showing narrowly dispersed ($Đ$ = 0.21) particle distributions, we decided to characterise the shape of the aggregates. Thus, imaging the particles by scanning transmission electron microscopy (STEM) and confocal microscopy (CM) were considered. Thus, sample preparations for STEM were done at a concentration of 3×10^{-5} M and immobilised on carbonised copper grids (3×) for drying. The self-organised polymer-drug conjugates were expected to retain their aqueous morphological state because PVP exhibits both cryoprotectant and lyoprotectant properties.[27] The sample preparation methods involved freeze-drying, slow solvent evaporation at room temperature, and drying under vacuum at 37 °C. Unfortunately, the particle sizes and

morphology determinations of all samples viewed using STEM were generally unsuccessful due to a lack of imaging contrast and resolution. It was then realised that the use of confocal fluorescence imaging microscopy may be worthwhile.

The 4-anilinoquinazoline derivatives are known fluorescent kinase inhibitors for confocal microscopy imaging,[28] but they require high UV excitation energy [see the UV-Vis spectrum in **Fig. 4.6 (c)**]. They could be expected to fluoresce in the blue to green region. Although this property is not favourable for imaging at the Central Analytical Facility (CAF) at Stellenbosch University, due to the unavailability of a UV laser, attempted imaging of the conjugates (*e.g.* ***77***) was nonetheless carried out, using the violet laser at 405 nm. A vague auto-fluorescence in the green region was seen.

It was decided to study the structure of the self-assembled particles in the presence of Nile red, a common lipophilic fluorophore dye used in cell imaging.[29] Its fluorescence (excitation at 515–560 nm and emission >590 nm) properties are influenced by the existence of the hydrophobic and hydrophilic environment in self-organised particles.[29] The dye tends to accumulate in the hydrophobic environment. Hence, this lipophilic behaviour was used to successfully image quinazoline conjugates with the violet laser.

In preparation of CM samples, solutions of conjugate were made up in the presence of 1 mol% Nile red and again immobilized on a carbonised copper grid at room temperature. The dried samples were then visualised using two wavelength regions (violet-blue and golden-red), independently. Each imaging wavelength captured individual fluorescences (of conjugates or of Nile red). These independent images overlapped. The overlaid images were then used to reveal the morphology of the self-assembled particles according to composition. The violet to blue region wavelength captured the auto-fluorescence of polymer-drug conjugates, while the golden-red region filmed the Nile red fluorescence. These two visuals were then overlaid to define the shape of the self-assembled particles.

With reference to the 3D images shown in **Fig. 4.7 (b)**, the overall spherical colloidal dispersion of the particles is demonstrated by image (i) with the yellow dot at the centre. The images (ii) and (iii) are the result of auto-fluorescence of 4-anilinoquinazolines and Nile red, respectively. It can be deduced from these images [(ii) and (iii)] that self-assembled particles were unambiguously observed according to their composition.

Indeed, merging of the two independent fluorescence colours from (ii) and (iii) produced the yellow colour which is observed in image (iv), also seen in image (i). Various visual perspectives were also explored [(v) and (vi)] and cross-sectioning was utilised to show preferential accumulation of Nile red inside the hydrophobic core segment of the 4-anilinoquinazolines. This was more visible in image (v). Overall, the images demonstrated the anticipated self-assembling behaviour of the amphiphilic polymer-drug conjugates in solution to form spherical micelles. CM measurements of the particle size were however not performed due to only a limited magnification option being available.

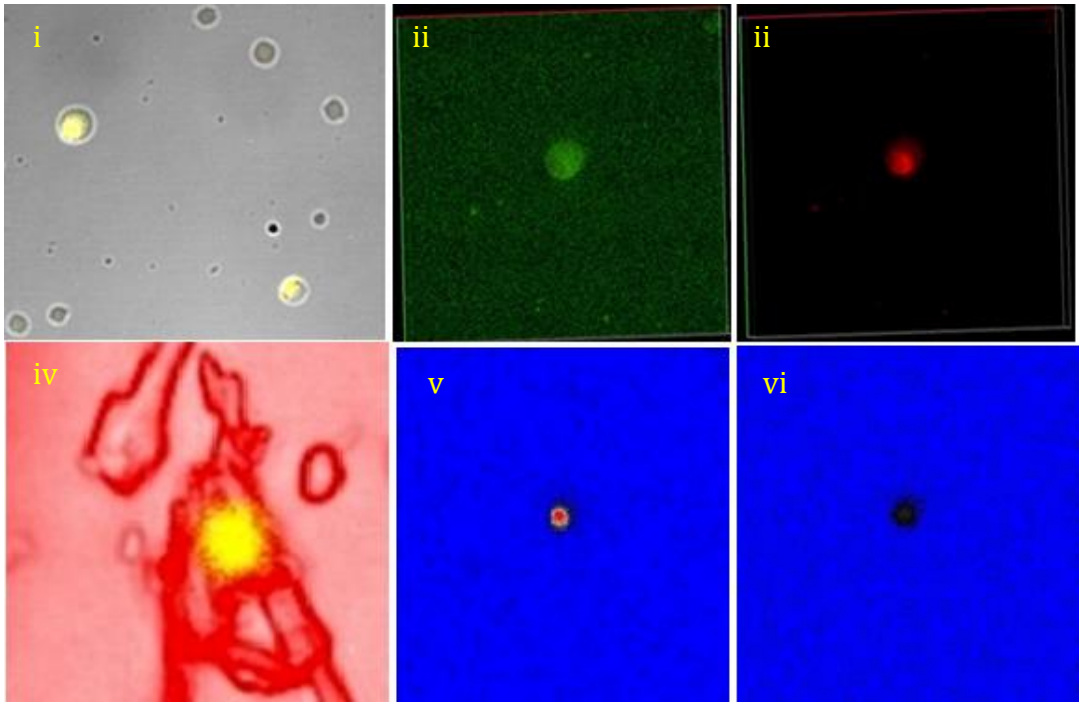

Figure 4.7 (b) Confocal microscopy imaging of self-assembled PVP-(4-phenyl amine)quinazoline conjugate (***77***) stained with Nile red. The particles were visualised as follows: (i) a broader perspective of self-assembled particles showing circular shapes in 2D, (ii) autofluorescence of conjugates, (iii) fluorescence by Nile red, and (iv)–(vi) overlaid images, through fluorescence at different wavelengths, ~450–600 nm.

The very same sample, on a copper grid, was carefully used for further imaging by STEM, but without success. It was hoped that the Nile red stain at the centre of these globular

particles would enhance the relative contrast and result in an improved view of the particles. However, ultimately, the different imaging modes were exhausted and increased magnifications that were meant to enhance the resolution often resulted in focus loss and blurred images. Selected STEM images are shown in **Fig. 4.7 (c)**.

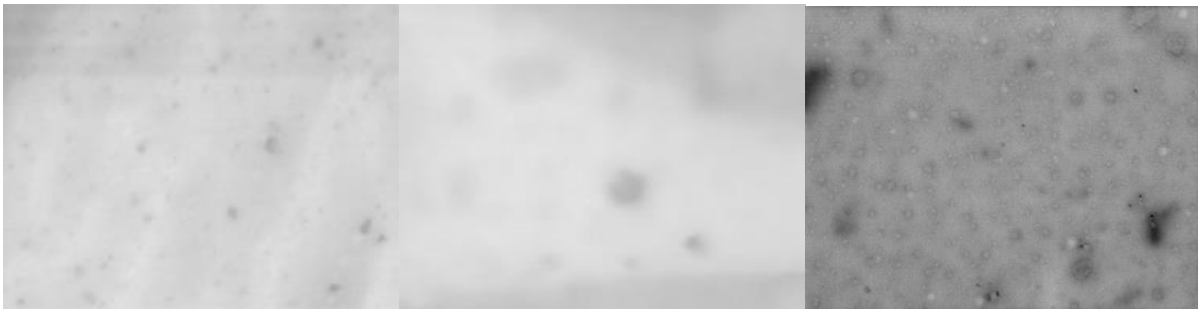

Figure 4.7 (c) Selected STEM images of self-assembled PVP-(4-phenyl amine)quinazoline conjugates.

Furthermore, qualitative methods such as ^{1}H NMR analysis were instrumental in demonstrating the self-organising effect of the particles into micelles in both DMSO and water solvents. The illustrative behaviour of the conjugates in solutions involved the disappearance of characteristic peaks assigned to the hydrophobic core (4-anilinoquinazolines) while only the outer hydrophilic segments (PVP chain) were selectively revealed after micelle formation. An example of this observation is depicted by the ^{1}H NMR spectra in **Fig. 4.7 (d)**. The two spectra demonstrate polymer-drug conjugates in unimolecular arrangement and micelle aggregation state in DMSO solvent.

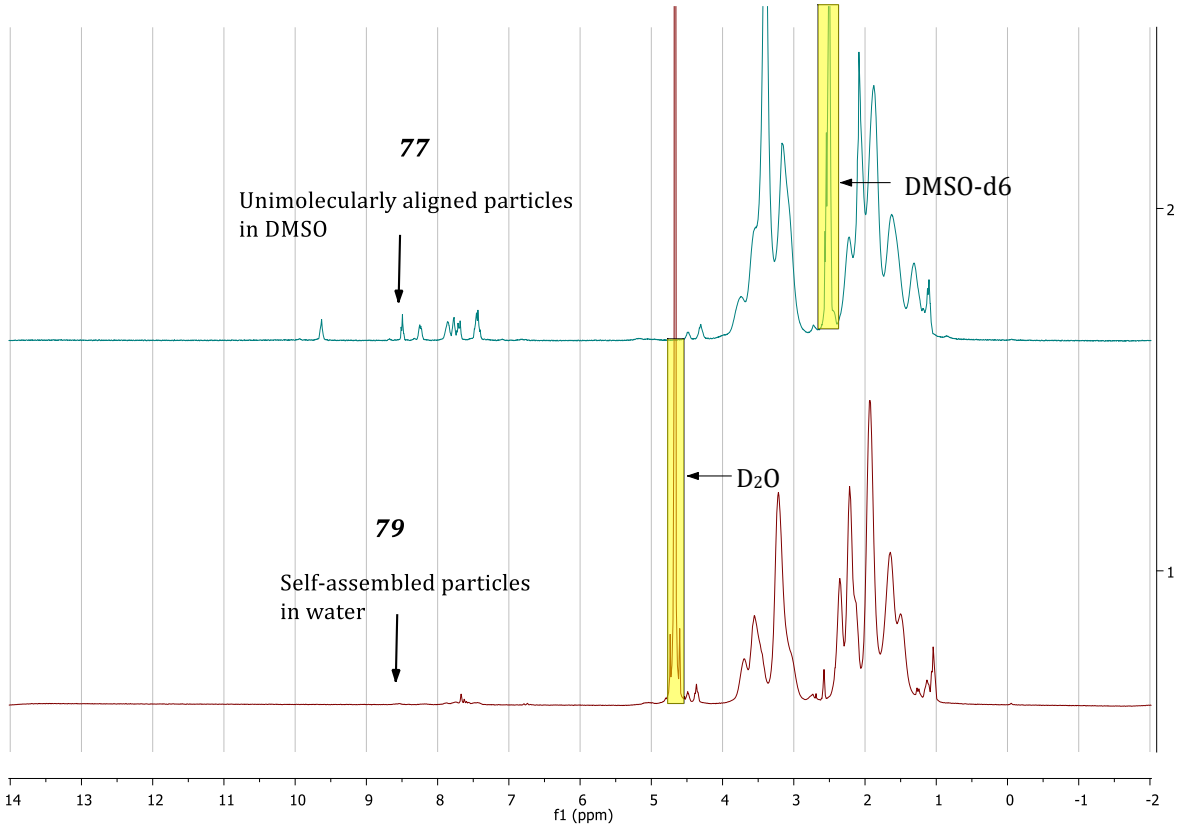

Figure 4.7 (d) The influence of the aggregation state of PVP-(4-phenyl amine)quinazoline conjugates (***77***, ***78***, and ***79***) on the appearance of ^{1}H NMR spectra in different solvents (DMSO and water).

After using all the above-mentioned analytical methods (DLS, CM, STEM, SEC, and ^{1}H NMR), the strengths and weakness of each method were identified during characterisation of the conjugates. Eventually, this enabled us to logically establish, finally, the morphology of the aqueously dispersed particles. The particle size distribution and dispersity were obtained from DLS and the shape of the particles was visualised by CM imaging.

4.8 Summary

RDRP of NVP using the RAFT/MADIX technique on a triazole-based RAFT agent was utilised to successfully obtain well-defined PVP polymers. These PVP polymers demonstrated highly controlled polymerisation with low dispersity values ($Đ \leq 1.15$) and

well-preserved end group functionalities. Transformation of the *O*-ethyl xanthate was performed by an aminolysis reaction to form thiol-terminated PVP, which was then coupled to 4-anilinoquinazoline conjugates via an 1,4-conjugated Michael addition reaction. The formed conjugates were then dissolved in DMSO and dialysed in water to induce micelle formation. The morphology of the self-assembled particles was established using various analytical tools. Eventually, a total of eight PVP-(4-phenyl amine)quinazoline conjugates were prepared and formulated into micellar structures. See **Fig. 4.8**. A preliminary drug release and anti-tumour efficacy study of the two conjugates (highlighted on cleavable linkers) was performed *in vitro*. This, and the effect of the linker chemistry in drug release and the biological efficacy of these conjugates will be discussed in *Chapter 05*.

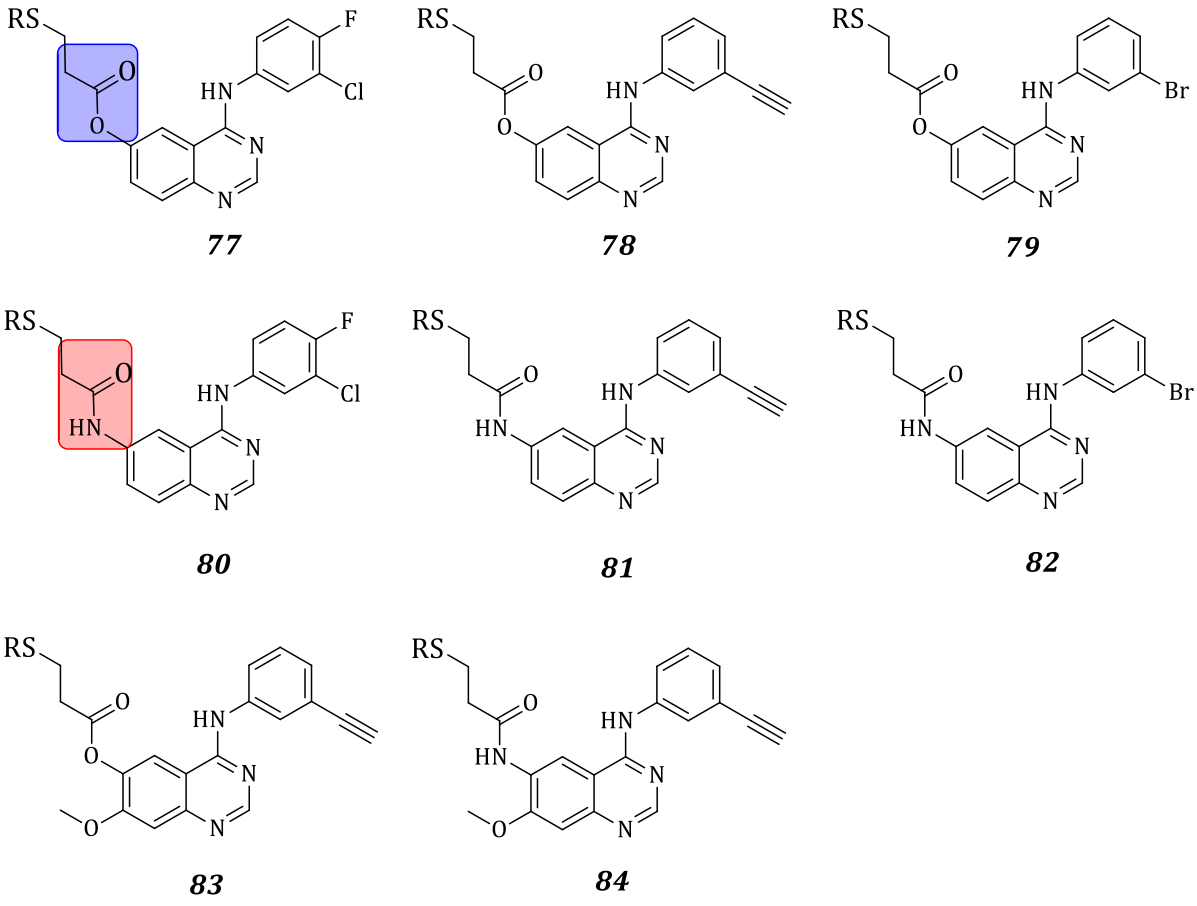

Figure 4.8 PVP-(4-phenyl amine)quinazoline conjugates realised in this study. The *R* group represents the PVP polymer chain. The difference between the two test conjugates is highlighted on the linker group.

4.9 References

1. (a) Rewcastle, G. W.; Bridges, A. J.; Fry, D. W.; Rubin, J. R.; Denny, W. A., *Journal of Medicinal Chemistry* **1997,** *40*, 1820-1826; (b) Thompson, A. M.; Murray, D. K.; Elliott, W. L.; Fry, D. W.; Nelson, J. A.; Hollis Showalter, H. D.; Roberts, B. J.; Vincent, P. W.; Denny, W. A., *Journal of Medicinal Chemistry* **1997,** *40*, 3915-3925.

2. (a) Liu, R.; Yu, X.; Wallqvist, A., *Journal of Cheminformatics* **2015,** 7, 4; (b) Schultz, T. W.; Yarbrough, J. W.; Hunter, R. S.; Aptula, A. O., *Chemical research in toxicology* **2007,** *20*, 1359-1363.

3. Liebler, D. C.; Guengerich, F. P., *Nature Reviews in Drug Discovery* **2005,** *4*, 410-420.

4. (a) Chiefari, J.; Chong, Y. K.; Ercole, F.; Krstina, J.; Jeffery, J.; Le, T. P. T.; Mayadunne, R. T. A.; Meijs, G. F.; Moad, C. L.; Moad, G.; Rizzardo, E.; Thang, S. H., *Macromolecules* **1998,** *31*, 5559-5562; (b) Moad, G.; Rizzardo, E.; Thang, S. H., *Australian Journal of Chemistry* **2012,** *65*, 985-1076.

5. Nakabayashi, K.; Mori, H., *European Polymer Journal* **2013,** *49*, 2808-2838.

6. Keddie, D. J.; Moad, G.; Rizzardo, E.; Thang, S. H., *Macromolecules* **2012,** *45*, 5321-5342.

7. Akeroyd, N.; Pfukwa, R.; Klumperman, B., *Macromolecules* **2009,** *42*, 3014-3018.

8. Pound, G.; Eksteen, Z.; Pfukwa, R.; McKenzie, J. M.; Lange, R. F. M.; Klumperman, B., Journal of Polymer Science Part A: *Polymer Chemistry* **2008,** *46*, 6575-6593.

9. Gagosz, F.; Zard, S. Z., *Organic Letters* **2003,** *5*, 2655-2657.

10. Hastings, C. J.; Fiedler, D.; Bergman, R. G.; Raymond, K. N., *Journal of the American Chemical Society* **2008,** *130*, 10977-10983.

11. Goddard-Borger, E. D.; Stick, R. V., *Organic Letters* **2007,** *9*, 3797-3800.

12. Reader, P. W.; Pfukwa, R.; Jokonya, S.; Arnott, G. E.; Klumperman, B., *Polymer Chemistry* **2016,** *7*, 6450-6456.

13. (a) Lima, V.; Jiang, X.; Brokken-Zijp, J.; Schoenmakers, P. J.; Klumperman, B.; Van Der Linde, R., *Journal of Polymer Science Part A: Polymer Chemistry* **2005,** *43*, 959-973; (b) Roth, P. J.; Jochum, F. D.; Zentel, R.; Theato, P., *Biomacromolecules* **2010,** *11*, 238-244.

14. Izunobi, J. U.; Higginbotham, C. L., *Journal of Chemical Education* **2011,** *88*, 1098-1104.

15. (a) Watson, J. T.; Sparkman, O. D., *Introduction to mass spectrometry: Instrumemtation, applications and strategies for data interpretation*. Wiley: Chichester, 2007; Vol. 4; (b) Räder, H. J.; Schrepp, W., *Acta Polymerica* **1988,** *49*, 272-293.

16. (a) Vergne, M. J.; Hercules, D. M.; Lattimer, R. P., *Journal of chemical education* **2006,** *84*, 81-90; (b) Zhu, H.; Yalcin, T.; Li, L., *Journal of the American Society for Mass Spectrometry* **1998,** *9*, 275-281.

17. Moad, G.; Rizzardo, E.; Thang, S. H., *Polymer International* **2011,** *60*, 9-25.

18. Burns, J. A.; Butler, J. C.; Moran, J.; Whitesides, G. M., *The Journal of Organic Chemistry* **1991,** *56*, 2648-2650.

19. (a) Ellman, G. L., *Archives of Biochemistry and Biophysics* **1958,** *74*, 443-450; (b) Ellman, G. L., *Archives of Biochemistry and Biophysics* **1959,** *82*, 70-77.

20. Li, G.-Z.; Randev, R. K.; Soeriyadi, A. H.; Rees, G.; Boyer, C.; Tong, Z.; Davis, T. P.; Becer, C. R.; Haddleton, D. M., *Polymer Chemistry* **2010,** *1*, 1196-1204.

21. Edwards, J. O.; Pearson, R. G., *Journal of the American Chemical Society* **1962,** *84*, 16-24.

22. Humphrey, R. E.; Potter, J. L., *Analytical Chemistry* **1965,** 37, 164-165.

23. Levison, M. E.; Josephson, A. S.; Kirschenbaum, D. M., *Experientia* **1969,** *25*, 126-127.

24. (a) Lowe, A. B., *Polymer Chemistry* **2014,** *5*, 4820-4870; (b) Roth, P. J.; Kessler, D.; Zentel, R.; Theato, P., *Journal of Polymer Science Part A: Polymer Chemistry* **2009,** *47*, 3118-3130.

25. (a) Kwon, G. S.; Kataoka, K., *Advanced Drug Delivery Reviews* **1995,** *16*, 295-309; (b) Nishiyama, N.; Kataoka, K., *Pharmacology and Therapeutics* **2006,** *112*, 630-648.

26. Edward, J. T., *Journal of Chemical Education* **1970,** *47*, 261.

27. (a) Gaucher, G.; Dufresne, M.-H.; Sant, V. P.; Kang, N.; Maysinger, D.; Leroux, J.-C., *Journal of Controlled Release* **2005,** *109*, 169-188; (b) Ravin , H. A.; Seligman , A. M.; Fine , J., *New England Journal of Medicine* **1952,** *247*, 921-929.

28. Wilson, J. N.; Liu, W.; Brown, A. S.; Landgraf, R., *Organic and Biomolecular Chemistry* **2015,** *13*, 5006-5011.

29. Greenspan, P.; Mayer, P. E.; Fowler, S. D., *The Journal of Cell Biology* **1985,** *100*, 965-973.

Chapter 5: Drug release and *in vitro* anti-tumour activity of polymer-drug conjugates

Chapter 5: Drug release and *in vitro* anti-tumour activity of polymer-drug conjugates

Abstract

This chapter describes a study on drug release and biological evaluation of two amphiphilic polymer-drug conjugates. These conjugates comprised a PVP polymer attached to cytotoxic 4-anilinoquinazoline anti-tumour agent through acid-labile linkers (an ester and an amide). The drug release profiles of the active ingredient were studied under various pH conditions. Based on the outcome of this study, pH-selective drug release profiles showing favourable chemical stabilities were obtained. The second part of this chapter focuses on the biological assessment of anti-tumour efficacy in carcinoma cells. These preliminary biological studies demonstrated comparable anti-tumour efficacy between conjugated molecules and 'free 4-anililoquinazolines', with similar mechanisms of anti-tumour activity.

5.1 Introduction

Formulation of polymer-drug conjugates into a pH-responsive micellar delivery system to target a tumour microenvironment has promising therapeutic potential for cancer treatment.[1] This type of colloidal drug carrier system is known to have tumouricidal effects that are underlined by enhanced bio-distribution and release of cytotoxic agents in the acidic environment of tumour cells.[2] While this has proven to be explicitly tumouritropic,[3] it also offers an interesting opportunity to improve target specificity of the SMKIs. Because of these features, micelle formulations for drug delivery has the potential to overcome a number of therapeutic barriers found in conventional molecularly targeted cancer therapy.

In assembling these conjugates, emphasis was placed on the critical role that each component plays in influencing the anti-tumour efficacy.[4] Thus, the hydrolytic stability of the linkers (ester and amide) and anti-tumour efficacy of two conjugates were evaluated under physiologically relevant conditions, and will be discussed.

Chapter 5: Drug release and *in vitro* anti-tumour activity of polymer-drug conjugates

5.2 Assessment of drug release from the conjugates

Drug release profiles of the conjugates were established *in vitro* by measuring the hydrolytic stability of the linker groups under a set of conditions. During the process, self-assembled micelle conjugates were subjected to conditions mimicking the endosomal pH (5.6) and normal physiological pH (7.4) over a period of 24 h. A typical reaction showing hydrolysis of the acid-labile ester linker is shown in **Fig. 5.2 (a)**.

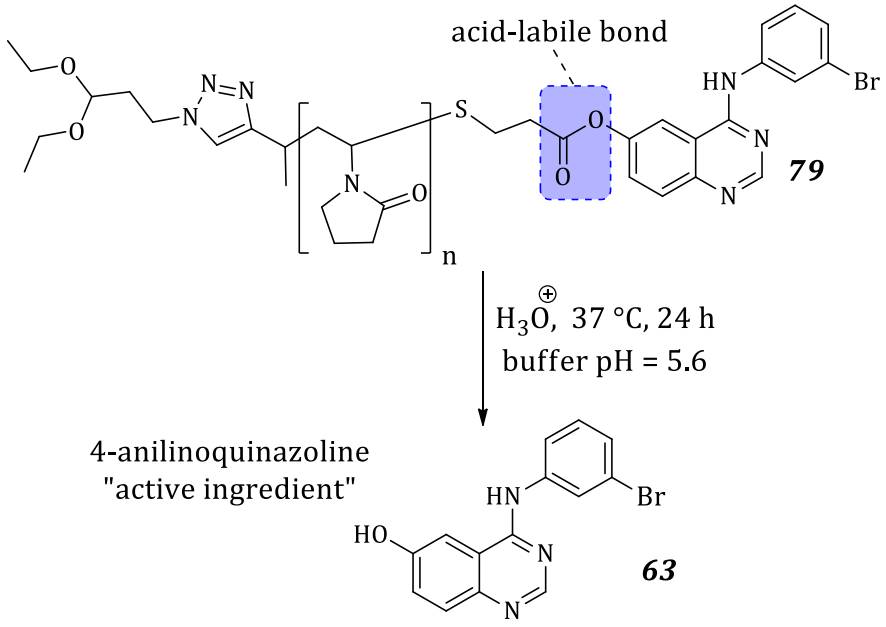

Figure 5.2 (a) Hydrolysis of the acid-labile ester linker in PVP-(4-phenyl amine)quinazoline conjugate (***79***) at pH 5.6.

In conducting the hydrolysis of self-assembled PVP-(4-phenyl amine)quinazoline conjugates, a 0.1 M potassium acetate buffer was prepared to a predetermined pH of 5.6 using the Henderson–Hasselbalch equation:[5] $pH = \mathrm{p}Ka + log\frac{[A^-]}{[HA]}$. The buffering effect is well known to result from a reversible reaction equilibrium, when the concentrations of the proton donor and its conjugate base are equal. Thus, equimolar (0.2 M) solutions of acetic acid ($\mathrm{p}K_a$ = 4.75) and potassium acetate were prepared using deionised water, HOAc (11.55 mL/L), and KOAc (19.6 g/L), in separate volumetric flasks. To achieve a 0.1 M buffer concentration and the desired pH, HOAc (35.8 mL) and KOAc (264.2 mL)

solutions were mixed to a volume of 300 mL and then diluted to a final volume of 600 mL using deionised water. Based on the above equation, the pH is dependent on the ratio of buffer components. The solutions were mixed under mechanical stirring to ensure homogeneity. The buffer solutions (2×300 mL) were then equilibrated to a constant temperature (37 °C). To initiate the hydrolysis process, preconditioned dialysis membranes [Float-A-Lyzer G2; pore size rating/molecular weight cut-off (MWCO) 500–1000] were charged with freshly prepared conjugates (1.0×10^{-3} M) then immersed into equilibrated buffer solutions under gentle stirring (200 rpm).

The amount of the drug released was followed quantitatively using UV-Vis analysis ($\lambda_{max.}$ = 350 nm). The initial absorbance intensities were recorded as [A_o] corresponding to time t_o = 0 h, and the reaction progress was monitored at regular time intervals of ~2 h for 10 h, then 18 h, and 24 h. The recorded absorbance values were measured against a blank buffer solution. It was projected that as the hydrolysis occurred, the released small molecules would diffuse from the semi-permeable membrane (Float-A-Lyzer G2) into the dialysate across the concentration gradient. This procedure thus allowed for selective molecular separation, during which hydrated PVP polymer was trapped inside the membrane as the free 4-anilinoquinazoline chromophores diffused into the solution. The analytical samples were withdrawn from dialysis membranes with a seleable screw-cap. The reactions were interrupted to measure the absorbance. By applying the Beer–Lambert law in our UV-Vis analyses,[6] the measured absorbance values were expected to decrease as the molar concentration of the chromophores decreased. A decrease in the absorbance during hydrolysis at the acidic pH of 5.6 was observed for both the ester and the amide bonds. One example to illustrate the decreasing absorbance of ***79*** as ***63*** is released into the dialysate solution is shown in **Fig. 5.1 (b)**.

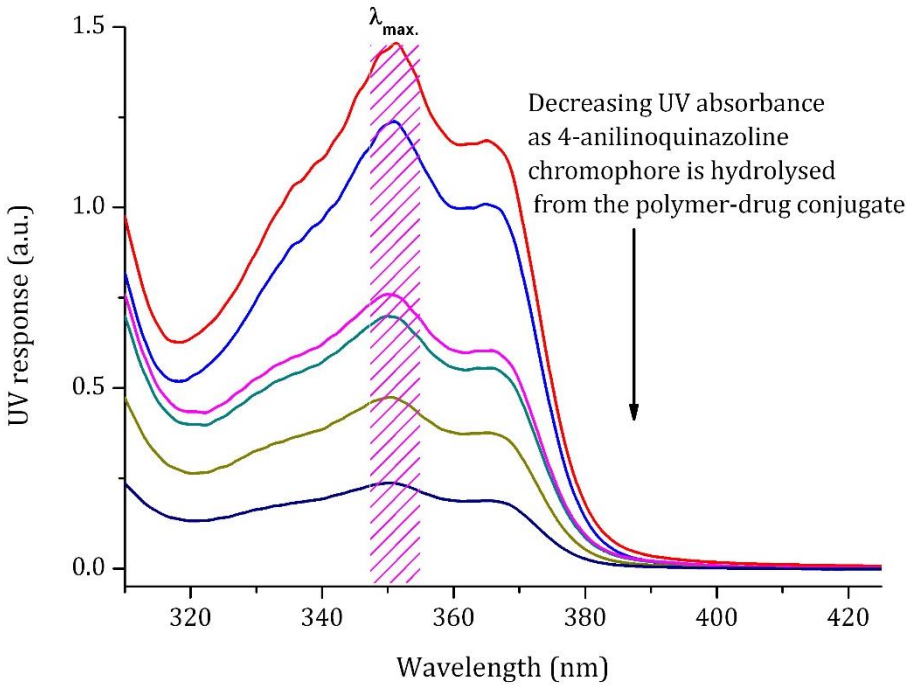

Figure 5.2 (b) UV-Vis spectra of ***79*** showing decreasing UV absorbance during hydrolysis as ***63*** is released into the buffer solution at pH 5.6.

The dialysate was changed three times to ensure the movement of 4-anilinoquinazolines from the dialysis membrane into the buffer solution against the concentration gradient. Then 0.1 M potassium phosphate buffer solutions at pH 7.4 were prepared using a method similar to that used to prepare the acetate buffers at pH 5.6. While acetate ions have strong buffering capacity under acidic conditions. (buffer range = pK_a±1.0), the phosphate buffers have pK_a 7.21, and work well from pH 5.8–8.0.[7] The overall hydrolysis drug release studies at pHs 5.6 and 7.4 were plotted as a function of time, as shown in **Fig. 5.2 (c)**.

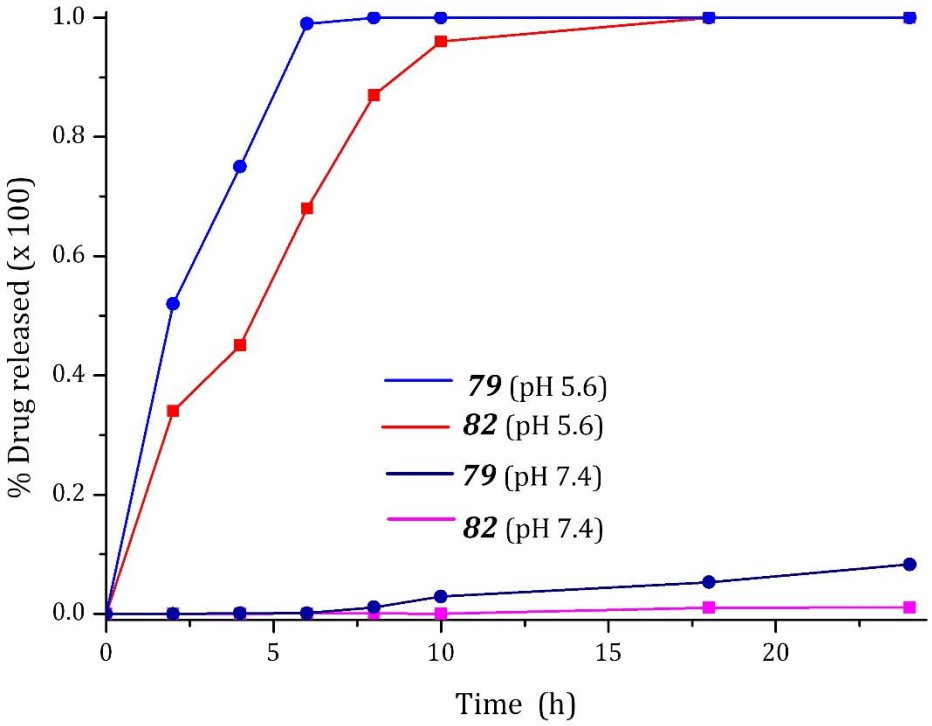

Figure 5.2 (c) Drug release profiles of polymer-drug conjugates showing the amide and ester linker group hydrolysis at pH 5.6 and 7.4.

With reference to the pre-established multiple aggregation states of PVP-(4-phenyl amine)quinazolines for the concentration of 10^{-3} M, the UV-Vis spectroscopic absorbance for the amount of released 4-anilinoquinazoline chromophores was calculated as the percentage of drug released ($\% \, drug \, release = \frac{([A_\circ]-[A_t])}{[A_\circ]} \times 100$). It can be observed from **Fig. 5.2 (c)** that the hydrolysis reactions were sensitive to the reaction pH. It was evident that both linker groups showed high chemical stability at pH 7.4, while they were hydrolysed within ~12 h at the endosomal pH of 5.6. This confirmed that the two linkers were suitable for the selective delivery of compounds into acidic tumour environments. More importantly, they hydrolyse within the cell cycle doubling time of tumour cells.[8]

The observed pH sensitivity profiles were also attributable to the proton-trapping ability of the 4-anilinoquinazoline interior, *i.e.* the hydrophobic core of the formed micelles. The proton-trapping effect exhibited by the hydrophobic core was expected to stimulate hydrolytic cleavage of the conjugates and micelle dissociation. In some micelle-based drug delivery systems, the pH-trapping effect has been induced by incorporating

poly(histidine) or imidazole rings to form the basic hydrophobic core in amphiphilic block polymers.[9] In our case, the ester linker group was cleaved earlier (after ~5 h), but the amide bond hydrolysis was much slower (~12 h).

The hydrolytic products of PVP-(4-phenyl amine)quinazoline conjugates at pH 5.6 were analysed by MS. This experiment was also in line with the earlier hypothesis in *Chapter 02*, namely, that β-propionic ester/amide linker groups are likely to undergo hydrolytic cleavage instead of β-elimination under acidic conditions. To confirm this hypothesis, two additional reactions were performed at pH 5.6 [3-mg-scale polymer-drug conjugates in 1 mL acetate buffer solution at 37 °C in reaction flasks]. After 24 h, crude hydrolytic products were dialysed in deionised water for 12 h, and dialysates were collected and freeze-dried. Using liquid chromatography-mass spectroscopy (LC-MS) analytical technique, the identity of released compounds is usually confirmed by matching the retention time and *m/z* of the known molecules with the hydrolysed compounds. Unfortunately, only the MS results were successfully obtained as the samples bound strongly to the column packing, perhaps due to PVP polymer contamination. MS results of the dialysates showed *m/z* values which were consistent hydrolysis [see structures of ***63*** and ***44*** in **Fig. 5.2 (d)**]. These results verified our hypothesis—none agreed with the β-elimination reaction. However, the overall concentration of compounds was very low and no purification was performed before MS analysis.

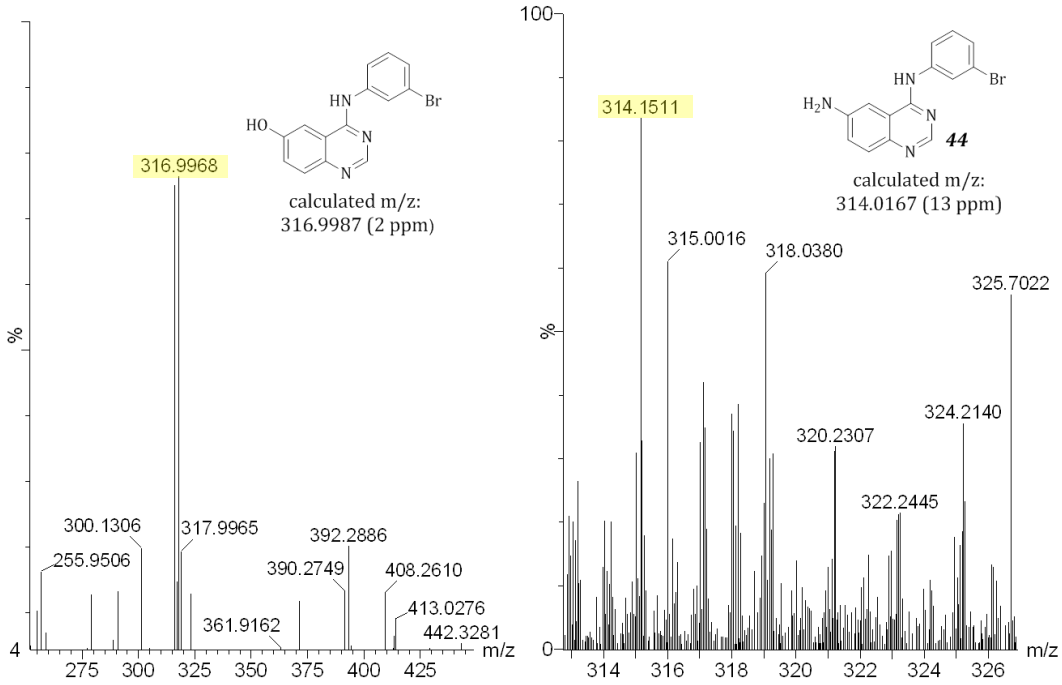

Figure 5.2 (d) MS results of ***63*** and ***44*** obtained from hydrolysis of ***79*** and ***82,*** respectively at pH 5.6. Experimental $[M+H]^+$ values are highlighted in pale yellow and the calculated *m/z* values are shown under the chemical structures.

The overall drug release results showed the successful recovery of 4-anilinoquinazolines under an acidic pH of 5.6, which favours selective tumouritropic drug delivery. With the obtained chemical stability at the physiological pH of 7.4, micellar-encupsulated anti-tumour agents were expected to have prolonged plasma half-life *in vivo*. The MS results further confirmed that drug release was solely as a result of hydrolytic cleavage. Because of hydrolytic cleavage, active ingredients obtained from polymer-drug conjugates were expected to inhibit EGFR kinase activity via a reversible ATP-competitive mechanism. It was thus considered suitable to carry out *in vitro* biological assessment of the anti-tumour efficacy of selected PVP-(4-phenyl amine)quinazolines. Bioassays were performed by the research group of Daniel Rauh (Prof) at Technical University of Dortmund, Germany.

5.3 Evaluation of anti-tumour activity

The anti-tumour activities of PVP-(4-phenyl amine)quinazoline conjugates (***77*** and ***78***) and 4-anilinoquinaolines (***45***, ***54***, ***64,*** and ***68***) were evaluated on wild-type and EGFR mutant epithelial cells (A431 and H1975, respectively). These human epidermoid carcinoma cell variants are known to possess a large number of EGFRs and are universally used to study the EGFR overexpression in protein kinase activities.[10] EGFR phosphorylation activity is highly overexpressed in A431 carcinomas, while H1975 cells carry mutant EGFR L858R/T790M.[10c] Both cell lines are found in lung tissues of NSCL patients with adenocarcinoma. They were used to determine the efficacy of conjugates against EGFR phosphorylation and drug resistance which is induced by secondary mutations.

In assessing the anti-tumour efficacy of 4-anilinoquinazolines in cell cultures, the CellTiter-Glo luminescent cell viability assay was used. Thus, the polymer-drug conjugates (***77*** and ***78***) and 4-anilinoquinazolines (***45***, ***54***, ***64***, and ***68***) were dissolved in DMSO in the concentration range 14 nM to 30 μM, along with the conventional drugs Gefitinib, Afatinib, WZ 004, and Osimertinib as the reference compounds (see **Table 5.3**). The free PVP polymer, DMSO solvent, and staurosporine were used as negative controls. The preconditioned cells (A431 and H1975) were treated with EGFR kinase inhibitors and incubated for 96 h prior to luminescence measurements. Based on bioassay protocols, inhibition of EGFR kinase activity was correlated to the reduction of cell proliferation by quantifying the amount of ATP in cells.[11] The presence of metabolic activity in cells usually requires ATP, whose measurable luminescent signal is directly proportional to the number of viable cells per culture.[12] Measurements were carried out in duplicate and cell seeding (150 cells/well) was replicated in at least two plates. The luminescence signal intensity was recorded on a Perkin Elmer Envision microplate reader at 500 ms integration time for which the Z'-factor ≥0.5 was obtained. The 50% of maximum effective concentration (EC_{50}) values of the compounds were determined using the Quatro Software suite.

Table 5.3 EC_{50} determination of PVP-(4-phenyl amine)quinazoline conjugates and small molecules on wild-type EGFR (A431 cells) and double-mutant EGFR L858R/T790M (H1975 cells)

Entry	Compound identity	Chemical structure	EC_{50} (μM)	
			$EGFR^{WT}$	$EGFR^{L858R/T790M}$
1	Gefitinib	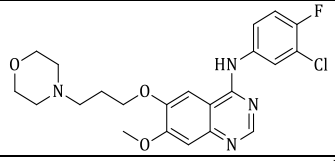	1.71±0.79	10.73±2.55
2	Afatinib	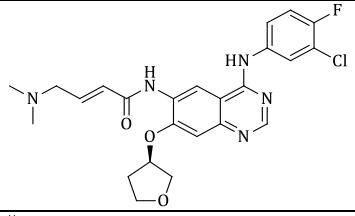	0.63±0.31	0.65±0.11
3	WZ 004	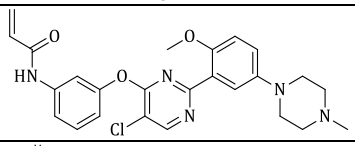	2.14±0.44	0.10±0.04
4	Osimertinib	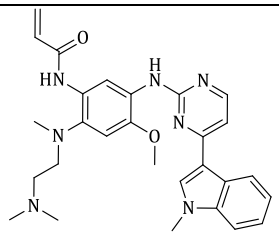	0.76±0.34	0.04±0.08
5	PVP	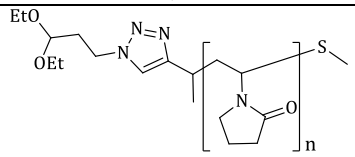	30.00	30.00
6	***77***	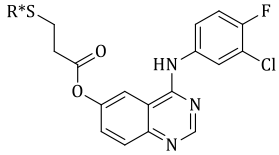	12.82±2.47	30.00
7	***64***	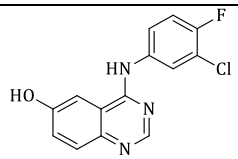	10.75±3.37	30.00
8	***68***	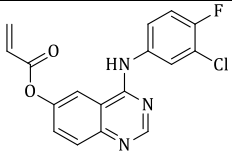	4.13±0.07	18.41±5.82

9	***78***	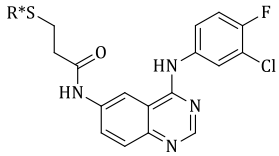	5.85±3.15	7.99±3.62
11	***45***	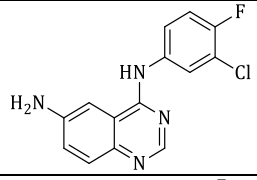	21.26±11.71	30.00
12	***54***	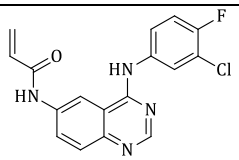	0.30±0.05	0.59±0.25

R*S = PVP polymer chain

With reference to the EC_{50} values in **Table 5.3, entries 1–4**, it can be seen that the standard drugs maintained low micromolar EGFR kinase inhibition on both wild-type and mutant EGFR over 4 days of incubation. During this period, cells experiencing no EGFR inhibition were expected to grow exponentially with respect to their doubling cell-cycle times. Under such conditions (see the negative control in **entry 5**) the maximum concentration value (30 μM) was obtained, demonstrating that no measurable effective dose was obtained. Looking closely at Gefitinib (**entry 1**) showed a diminishing anti-tumour activity against mutant EGFR L858R/T790M. In previous studies,[13] this effect has been ascribed to the T790M steric clash in the hydrophobic region of the ATP binding pocket. The T790M is common for 4-anilinoquinazoline reversible kinase inhibitors, but Afatinib (**entry 2**) is an irreversible kinase inhibitor, which has been proven by good efficacy against both EGFR variants. This is attributed to the acrylamide functionality that forms covalent bonds with the Cys 797 thiol of the EGFR target.[14] Although Afatanib received the first FDA approval in 2013 against NSCLC adenocarcinoma patients with EGFR T790M, it is still considered as an experimental drug due to dose-limiting adverse effects.[15] The third generation amino pyrimidine irreversible inhibitors,[16] **entries 3 and 4**, demonstrated superior efficacy over 4-anilinoquinazolines on EGFR L858R/T790M.

Proceeding to entries ***6***–***8***, it is evident that polymer-bound conjugate (***77***) and the small molecules (***64*** and ***68***) exhibited threefold lower anti-tumour activities on wild-type EGFR in comparison to Gefitinib (**entry 1**). Based on the hydrolysis reaction profiles, it

was determined that active anti-tumour agents released from polymer conjugates are expected to display reversible kinase inhibition efficacies that are similar to Gefitinib.[17] It was however disappointing to see the ester conjugate (***77***) displaying no activity against mutant EGFR. In view of this outcome, it was hypothesised that the reduced anti-tumour efficacy for the acrylate derivative (***68***) was also attributable to the cleavage of ester functionality, thus averting the compound's mode of action from irreversible to reversible kinase inhibition mechanisms. The loss of acrylate functionality leading to less potent substrates in irreversible kinase inhibition has also been observed by Denny and co-workers.[18] One of the reasons why the acrylate functionality was used in our studies was to achieve the release of cytotoxic anti-tumour agents with a lesser hydrolytically stable ester linker group, should the amides have unfavourable physiological stability.

Looking at **entries 9–12**, the polymer-drug conjugate ***78*** demonstrated a better anti-tumour inhibitory profile on both EGFR cell variants. From drug release studies, it could be suggested that the conjugates of the amide linker group had better sustained release profiles, thus ensuring sizeable drug doses over prolonged periods, in comparison with the ester linkers. On the other hand, the free amine ***45*** had notably low anti-tumour activity; it was considered to be an outlier among the other amino compounds (***78*** and ***54***). It was however interesting to note that polymer-drug conjugate ***78*** exhibited similar anti-tumour activity profiles to the gold standard ATP-competitive Gefitinib (**entry 1**). Of even further interest was to note that compound ***54*** displayed good anti-tumour efficacy on wild-type and double mutant EGFR. The anti-tumour efficacy of this C-6 acrylamide-substituted quinazoline (***54*)** was similar to that of Afatinib (**entry 2**). Afatinib is traded under the name Gilotrif® after its second FDA approval in 2016 as a front-line treatment option for advanced squamous cell lung cancer.[19] These results (with polymer-drug conjugate ***78*** and the free drug ***54***) warrant further investigation of the amide-based polymer-drug conjugates.

Based on the bioassay results, it was significant to obtain anti-tumour activity for the polymer bound 4-anilinoquinazoline molecules. The active ingredients released from the conjugates have demonstrated comparable bioactivity profiles with their small-molecule counterparts (except ***45***) possessing the same anti-tumour inhibitory mechanism. One of

the outstanding results was that the anti-tumour efficacy of the amide-linked polymer-drug conjugate (***78***) resembled that of Gefitinib, which was anticipated to have the same mechanism of kinase inhibition. Moreover, acrylamide-bearing ***54*** also displayed a similar irreversible kinase inhibition pattern to Afatinib, the first quinazoline-based drug against squamous cell lung cancer. Although anti-tumour agents released from the conjugates were expected to have improved anti-tumour efficacy, it must be emphasised that the present bioassay experiments do not address the effects of limited solubility and bioavailability of 4-anilinoquinazolines, as all the compounds were solubilized in DMSO solvent.

5.4 Summary

The two PVP-(4-phenyl amine)quinazoline conjugates composed of the PVP polymer and 4-anilinoquinazoline anti-tumour agents linked by the acid-labile groups (ester and amide) were evaluated *in vitro*. Based on the obtained drug release profiles, polymer-drug conjugates demonstrated selective hydrolysis at acidic pH, which is a requirement for targeting tumour cells. Furthermore, MS analysis of the dialysates supported an acid-catalysed hydrolysis mechanism, thus ascribing the active ingredients released from the polymer conjugates to a reversible EGFR kinase inhibition mechanism. Finally, the bioassay assessments of the polymer conjugates on EGFR kinase inhibition in A431 cells and double-mutant EGFR L858R/T790M in H1975 cells revealed anti-tumour efficacy that corresponds to reversible EGFR kinase inhibition. Attempts to upgrade the conjugates into irreversible EGFR kinase inhibitors will be briefly addressed in the section on future work, in *Chapter 07*.

5.5 References

1. (a) Lin, X.; Zhang, Q.; J.R., R.; Stewart, D. R.; Nowotnik , D. P., *European Journal of Cancer.* **2004,** *40*, 291–297; (b) Gillies, E. R.; Frechet, J. M. J., *Chemical Communications* **2003,** *40*, 1640-1641.

2. (a) Liu, Y.; Wang, W.; Yang, J.; Zhou, C.; Sun, J., *Asian Journal of Pharmaceutical Sciences* **2013,** *8*, 159-167; (b) Li, R.; Xie, Y., *Journal of Controlled Release* **2017,** *251*, 49-67.

3. Lee, E. S.; Gao, Z.; Bae, Y. H., *Journal of Controlled Release* **2008,** *132*, 164-170.

4. Ohya, Y.; Kuroda, H.; Hirai, K.; Ouchi, T., *Journal of Bioactive and Compatible Polymers* **1995,** *10*, 51-66.

5. (a) Haenderson, J. L., *American Journal of Physiology* **1908,** *21*, 173-179; (b) Hasselbalch, K. A., *Biochemische Zeitschrift* **1917,** *78*, 112-144.

6. (a) Beer, A., *Annalen der Physik und Chemie* **1852,** *86*, 78-88; (b) Peiponen, K.-E.; Vartiainen, E. M.; Asakura, T., *Dispersion, complex analysis and optical spectroscopy: classical theory*. Springer Science & Business Media: Heidelberg, 1998; Vol. 147.

7. Mohan, C., Buffers: *In* A guide for the preparation and use of buffers in biological systems. Calbiochem Biochemicals: California, 2006; p 4-30.

8. (a) Sherr, C. J., *Science* **1996,** *274*, 1672; (b) Schoelch, M. L.; Regezi, J. A.; Dekker, N. P.; Irene, O. L.; McMillan, A.; Ziober, B. L.; Le, Q. T.; Silverman, S.; Fu, K. K., *Oral Oncology* **1999,** *35*, 333-342.

9. (a) Oh, K. T.; Lee, E. S.; Kim, D.; Bae, Y. H., *International Journal of Pharmaceutics* **2008,** *358*, 177-183; (b) Bae, Y.; Nishiyama, N.; Fukushima, S.; Koyama, H.; Yasuhiro, M.; Kataoka, K., *Bioconjugate Chemistry* **2005,** *16*, 122-130.

10. (a) Carpenter, G.; King, L.; Cohen, S., *Nature* **1978,** *276*, 409-410; (b) Carpenter, G.; King, L.; Cohen, S., *Journal of Biological Chemistry* **1979,** *254*, 4884-4891; (c) Walter, A. O.; Sjin, R. T. T.; Haringsma, H. J.; Ohashi, K.; Sun, J.; Lee, K.; Dubrovskiy, A.; Labenski, M.; Zhu, Z.; Wang, Z.; Sheets, M.; Martin, T. S.; Karp, R.; van Kalken, D.; Chaturvedi, P.; Niu, D.; Nacht, M.; Petter, R. C.; Westlin, W.; Lin, K.; Jaw-Tsai, S.; Raponi, M.; Dyke, T. V.; Etter, J.; Weaver, Z.; Pao, W.; Singh, J.; Simmons, A. D.; Harding, T. C.; Allen, A., *Cancer Discovery* **2013,** *3*, 1404-1415.

11. Crouch, S. P. M.; Kozlowski, R.; Slater, K. J.; Fletcher, J., *Journal of Immunological Methods* **1993,** *160*, 81-88.

12. Lundin, A.; Hasenson, M.; Persson, J.; Pousette, Å., *Methods in Enzymology* **1986,** *133*, 27-42.

13. Michalczyk, A.; Klüter, S.; Rode, H. B.; Simard, J. R.; Grütter, C.; Rabiller, M.; Rauh, D., *Bioorganic and Medicinal Chemistry* **2008,** *16*, 3482-3488.

14. Garuti, L.; Roberti, M.; Bottegoni, G., *Current Medicinal Chemistry* **2011,** *18*, 2981-2994.

15. (a) Sequist, L. V.; Soria, J. C.; Goldman, J. W.; Wakelee, H. A.; Gadgeel, S. M.; Varga, A.; Papadimitrakopoulou, V.; Solomon, B. J.; Oxnard, G. R.; Dziadziuszko, R.; Aisner, D. L.; Doebele, R. C.; Galasso, C.; Garon, E. B.; Heist, R. S.; Logan, J.; Neal, J. W.; Mendenhall, M. A.; Nichols, S.; Piotrowska, Z.; Wozniak, A. J.; Raponi, M.; Karlovich, C. A.; Jaw-Tsai, S.; Isaacson, J.; Despain, D.; Matheny, S. L.; Rolfe, L.; Allen, A. R.; Camidge, D. R., *The New England Journal of Medicine* **2015,** *372*, 1700-1709; (b) Cross, D. A. E.; Ashton, S. E.; Ghiorghiu, S.; Eberlein, C.; Nebhan, C. A.; Spitzler, P. J.; Orme, J. P.; Finlay, M. R. V.; Ward, R. A.; Mellor, M. J.; Hughes, G.; Rahi, A.; Jacobs, V. N.; Brewer, M. R.; Ichihara, E.; Sun, J.; Jin, H.; Ballard, P.; Al-Kadhimi, K.; Rowlinson, R.; Klinowska, T.; Richmond, G. H. P.; Cantarini, M.; Kim, D.-W.; Ranson, M. R.; Pao, W., *Cancer Discovery* **2014,** *4*, 1046-1061.

16. Smaill, J. B.; Gonzales, A. J.; Spicer, J. A.; Lee, H.; Reed, J. E.; Sexton, K.; Althaus, I. W.; Zhu, T.; Black, S. L.; Blaser, A.; Denny, W. A.; Ellis, P. A.; Fakhoury, S.; Harvey, P. J.; Hook, K.; McCarthy, F. O. J.; Palmer, B. D.; Rivault, F.; Schlosser, K.; Ellis, T.; Thompson, A. M.; Trachet, E.; Winters, R. T.; Tecle, H.; Bridges, A., *Journal of Medicinal Chemistry* **2016,** *59*, 8103-8124.

17. Palmer, B. D.; Trumpp-Kallmeyer, S.; Fry, D. W.; Nelson, J. M.; Showalter, H. D. H.; Denny, W. A., *Journal of Medicinal Chemistry* **1997,** *40*, 1519-1529.

18. Smaill, J. B.; Showalter, H. D. H.; Zhou, H.; Bridges, A. J.; McNamara, D. J.; Fry, D. W.; Nelson, J. M.; Sherwood, V.; Vincent, P. W.; Roberts, B. J.; Elliott, W. L.; Denny, W. A., *Journal of Medicinal Chemistry* **2001,** *44*, 429-440.

19. Boehringer-ingelheim https://www.boehringer-ingelheim.us/press-release/fda-approves-gilotrifr-afatinib-new-oral-treatment-option-patients-squamous-cell (accessed 23 August 2016).

Chapter 5: Drug release and *in vitro* anti-tumour activity of polymer-drug conjugates

Chapter 6: Experimental methods and characterisation data

Chapter 6 Experimental methods and .characterisation data

Abstract
This chapter contains description of experimental procedures that were used during the course of synthesis of small molecules and polymerisation reactions. Descriptive analytical methods and characterisation techniques will be outlined throughout the main text.

6.1 General remarks

a) Synthesis

Analytical grade solvents and reagents were purchased from Sigma Aldrich and dried using conventional distillation prior to use. Unless stated otherwise, moisture sensitive reactions were performed under an inert nitrogen atmosphere. Stabiliser free NVP was distilled under reduced pressure and α,α′-azobisisobutyronitrile (AIBN) radical initiator was recrystallized twice from ethanol, dried under high vacuum and kept under argon atmosphere.

Preparative column chromatography separations were performed on a silica gel column (70–230 mesh size, ASTM, Fluka). Reactions and separations were monitored by TLC on pre-coated aluminium silica gel plates (60F254 Merck) and the developed TLCs were viewed under UV lamp (254 nm) or visualised after staining. The melting points were recorded using the open capillary method on a Lasany melting point apparatus. Only the compounds with definite melting points, which did not undergo decomposition before melting, were recorded. Organic solvents were evaporated on a Büchi rotary evaporator equipped with a diaphragm pump and aqueous solvents were removed on a lyophilizer after they were frozen in liquid nitrogen. Polymer-drug conjugates were dialysed using the Spectra/Por Float-A-Lyzer G2, biotech grade, cellulose ester membrane with screw-on caps and MWCO 500-1000.

b) Instrumentation

The nuclear magnetic resonance (NMR) spectroscopy (^{1}H and ^{13}C, $^{1}J_{C\text{-}H}$ HSQC, $^{2,3}J_{C\text{-}H}$ HMBC) data were recorded on Varian Unity Inova spectrometers. All the spectra were obtained on a 5 mm dual broad band PFG probe at 25 °C. The chemical shifts (δ) were reported in ppm relative to internal solvent peaks. The coupling constant (*J*) values were

assigned in hertz (Hz), and the standardised signals splitting abbreviations have been used throughout the text.

The average molar masses (M_n) and polydispersity indices ($Đ$) of PVP homopolymer were obtained by size exclusion chromatography (SEC), at the Polymer Science Laboratories, Stellenbosch University. A 100 µL injection volumes of PVP samples (2 mg/mL) were analysed at a flow rate of 1 mL/minute at $\lambda_{max.}$ 280 nm or 350 nm with DMAc as a mobile phase, which was calibrated with PMMA standards. The SEC set up consisted of a Waters 717 auto-sampler coupled to a Shimadzu LC-10AT pump, PSS GRAM (50 × 8.0 mm, 10 µm) guard-column, PSS GRAM (300 × 8.0 mm, 10 µm, 100 Å) column and a Waters differential refractometer (Waters 2414) in a series with a dual wavelength UV detector (Waters 2487).

The size distributions were recorded by intensity, Z-average diameter and polydispersity index ($Đ$), on Dynamic Light Scattering using a Malvern Zetasizer Nano ZS 100. The samples were measured in triplicates and the data was generated using the Zeta Sizer software. Imaging of the self-assembled polymer-drug conjugates was performed on scanning transmission electron microscope (STEM) and confocal microscope, using Zeiss Evo MA15VP and Carl Zeiss LSM 780 fluorescence microscope, respectively. The UV-VIS chromatograms were recorded by Specord 210 plus UV VIS and the absorbance wavelengths were obtained in nanometers (nm).

The mass spectra were recorded on a Waters Synapt G2 UPLC-MS instrument using the positive ionization mode (ESI^+) at a cone voltage of 15 volts. The chemical purity of the compounds were also determined on the Waters Synapt G2 UPLC-MS that is equipped with an Acquity UPLC/UV detector, a Phenomenex kinetix phenyl hexyl column, and a programmable binary elution system at a mobile phase flow rate of 0.4 mL/min. The mobile phase consisted of a 1% formic acid:acetonitrile (A:B) and a snapshot showing the solvent system is provided in the supporting information. All the NMR spectroscopy, LC-MS, STEM and confocal analyses were carried out at the CAF, Stellenbosch University.

*6.2 Synthesis of the small molecule 4-anilinoquinazolines (**1–69**)*

*N-(2-Methylphenyl)acetamide (**1**)*

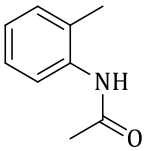

Compound ***1*** was prepared by acylation of 2-methylaniline as reported by Steck and Fletcher.[1] A solution of 2-methylaniline (1.89 g, 17.7 mmol), acetic anhydride (Ac_2O, 4 mL), and acetic acid (AcOH, 5 mL) was warmed to 50 °C with stirring for 1 h. The reaction was then quenched by emptying the flask contents into ice water (~30 mL), and white prismatic needles crushed out of the aqueous solution. The aqueous solution was decanted and the prismatic needles were then filtered, rinsed with cold water, and dried to afford pure compound ***1*** in 94% yield (2.49 g). The melting point was 96–98 °C [lit.[2] 105–108 °C]; ^{1}H NMR (300 MHz, DMSO) δ 9.26 (br s, 1H), 7.39 (d, J = 7.6 Hz, 1H), 7.25–6.98 (m, 3H), 2.19 (s, 3H), 2.05 (s, 3H); ^{13}C NMR (75 MHz, DMSO) δ 168.5, 136.9, 131.9, 130.6, 126.2, 125.4, 125.3, 23.7, 18.3. The ^{1}H NMR spectrum resembled literature data.[3]

*2-Acetamidobenzoic acid (**4**)*

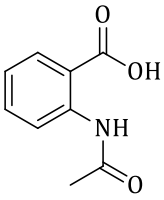

Compound ***4*** was synthesized by following the literature procedure with minor modifications to the reaction conditions.[1] The *N*-(2-methylphenyl)acetamide (1.30 g, 8.71 mmol), $KMnO_4$ (1.85 g, 11.7 mmol), and $MgSO_4$ (1.27 g, 10.1 mmol) were dissolved in water (100 mL) with stirring at a room temperature. The reaction was warmed to 75 °C under continuous stirring until the vigorous bubbling of the reaction had subsided. The reaction temperature was then raised to 90 °C for 3 h during which the purple solution ($KMnO_4$) changed colour to a brown suspension (MnO_2). The brown suspension was filtered off while still hot and the MnO_2 cake was rinsed with hot water (~50 mL) in order to obtain a clear aqueous filtrate. The filtrate was cooled into the ice-bath and titrated to pH 4 using 32% HCl. The aqueous solution was decanted and the remaining white needles were dried to obtain a pure product in 81% yield (1.27 g). The melting point was 181–183 °C [lit.[4] 184–186 °C]; ^{1}H NMR (300 MHz, DMSO) δ 13.55 (br s, 1H), 11.05 (s, 1H), 8.46 (dd, J = 7.5, 1.0 Hz, 1H), 8.00–7.93 (m, 1H), 7.61–7.51 (m, 1H), 7.14(ddd [appeared as dt], $J_1 = J_2$ =7.9, 1.2 Hz, 1H), 2.13 (s, 3H);^{13}C NMR (75 MHz, DMSO) δ 168.9, 167.9, 140.2, 133.4, 130.5, 122.0, 119.4, 115.9, 24.0. The ^{1}H NMR spectrum matched literature data.[5]

*2-Aminobenzoic acid (**5**)*

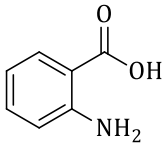

A solution of ***4*** (1.80 g, 10.1 mmol) in 96% ethanolic HCl (10 mL, 4 N) was heated to reflux at 80 °C for 2 h.[1] At the end of the reaction, the solution was concentrated *in vacuo* to obtain a brown HCl salt product. The salt was recrystallized from ethanol to obtain ***5*** as a beige powder in 76% yield (1.56 g). The melting point was 144–146 °C [lit.[6] 145 °C]; ^{1}H NMR (300 MHz, DMSO) δ 8.50 (br s, 2H), 7.68 (dd, *J* = 8.1, 1.7 Hz, 1H), 7.21 (ddd, *J* = 8.5, 5.7, 1.7 Hz, 1H), 6.73 (dd, *J* = 8.5, 1.2 Hz, 1H), 6.50 (ddd, *J* = 8.1, 7.0, 1.2 Hz, 1H); ^{13}C NMR (75 MHz, DMSO) δ 170.0, 152.0, 134.2, 131.6, 116.8, 115.0, 110.0. Alternative hydrolysis with 4 N KOH in 96% ethanol gave the identical product but in a poorer yield of 54%. The ^{1}H NMR spectrum was identical to literature data.[7]

*Quinazolin-4(3H)-one (**6**)*

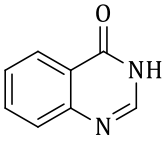

Preparation of compound ***6*** was carried out by following the literature method.[8] 2-Aminobenzoic acid (2.50 g, 18.2 mmol) was added to formamide (15 mL) at room temperature and the reaction mixture was stirred at 130 °C for 24 h. The reaction contents were poured into ice-cold water (~120 mL) and the product was allowed to precipitate out of the solution. The precipitate was recovered by filtration, rinsed with cold water, and 4-hydroxyquinazoline precipitate was isolated in 91% yield after drying (2.41 g). The melting point was 215–217 °C [lit.[9] 214–216 °C]; ^{1}H NMR (400 MHz, DMSO) δ 12.24 (s, 1H), 8.12 (dd, *J* = 7.9, 1.2 Hz, 1H), 8.09 (s, 1H), 7.84–7.78 (m, 1H), 7.66 (d, *J* = 7.9 Hz, 1H), 7.55–7.48 (m, 1H);^{13}C NMR (101 MHz, DMSO) δ 161.4, 149.4, 146.0, 135.0, 127.9, 127.4, 126.5, 123.3. The ^{1}H NMR spectra was in agreement with the literature data.[8]

*6-Nitroquinazolin-4(3H)-one (**7**)*

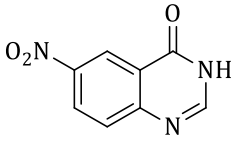

Preparation of compound ***7*** was carried out by following the literature procedure.[10] Quinazolin-4(3*H*)-one (500 mg, 3.42 mmol) was dissolved in mixed fuming acids (1:1 by volume, H_2SO_4/HNO_3; 4 mL) and the reaction mixture was stirred at 90 °C for 45 min. The reaction was quenched

by pouring the hot reaction mixture into ice-cold water (~50 mL) and the yellow precipitate was formed. The precipitate was collected by filtration, rinsed with cold water and dried to obtain 6-nitroquinazolin-4(3*H*)-one (0.60 g) as a yellow powder in 91% yield. The melting point was 273–275 °C [lit.[11] 275–276 °C]; ^{1}H NMR (400 MHz, DMSO) δ 11.41 (br s, 1H), 8.80 (d, *J* = 9.0 Hz, 1H), 8.55 (dd, *J* = 9.0, 2.7 Hz, 1H), 8.34 (s, 1H), 7.87 (d, *J* = 9.0 Hz, 1H); ^{13}C NMR (75 MHz, DMSO) δ 160.8, 149.3, 143.0, 136.8, 129.5, 127.7, 123.8, 122.6; MS (ESI$^+$) *m/z* 192.0403 was calculated for $C_8H_5N_3O_3$ [M + H]$^+$ and 192.0429 (-2.60 ppm) was determined experimentally. The ^{1}H NMR spectra closely resembled the literature data.[12]

*4-Fluoro-2-methylaniline (**8**)*

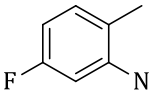

Synthesis of compound ***8*** was performed by adapting to the literature procedure,[13] with minor modifications. A solution of 4-fluoro-2-nitrotoluene (2.60 g, 16.8 mmol) and $SnCl_2$ (14.7 g, 77.7 mmol) in 96% ethanolic HCl (2 N) was maintained at 60 °C with stirring for 2 h. The solvent was then removed *in vacuo* and the residue was diluted with water (10 mL) and DCM (30 mL), and then basified to pH 10 with 4 N aqueous KOH. The product was extracted from the milky white aqueous solution into DCM (3 × 30 mL), after which the organic extract was dried over $MgSO_4$, and concentrated to obtain the crude product. The product was purified by chromatography to afford a pale yellow liquid in 99% yield (2.08 g). ^{1}H NMR (400 MHz, $CDCl_3$) δ 6.96 (ddd [appeared as dt] $^4J_{H\text{-}H}$ = 0.7, $^3J_{H\text{-}H}$ = $^3J_{F\text{-}H}$ = 8.0 Hz, 1H), 6.42–6.34 (m, 2H), 3.67 (br s, 2H), 2.11 (s, 3H); ^{13}C NMR (101 MHz, $CDCl_3$) δ 163.7 (d, $^1J_{C\text{-}F}$= 242.4 Hz), 146.1, 131.4, 117.9, 105.0 (d, $^2J_{C\text{-}F}$ = 21.2 Hz), 101.9 (d, $^2J_{C\text{-}F}$ = 26.3 Hz), 16.9. The ^{1}H NMR closely resembled the literature data.[14]

*N-(5-Fluoro-2-methylphenyl)acetamide (**9**)*

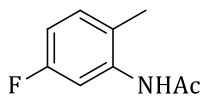

Compound ***9*** was prepared from compound ***8*** (2.00 g, 16.0 mmol) by adapting to the procedure used in the synthesis of compound ***1***.[1] The *N*-(5-fluoro-2-methylphenyl)acetamide was obtained in 91% yield (2.43 g). The melting point was 134–136 °C [lit.[15] 133–135 °C]; ^{1}H NMR (300 MHz, $CDCl_3$) δ 7.78–7.69 (m, 1H),

7.17–7.02 (m, 2H), 6.83–6.72 (m, 1H), 2.22 (br s, 6H); ^{13}C NMR (75 MHz, $CDCl_3$) δ 168.3, 162.9 (d, $^1J_{C\text{-}F}$ = 267.8 Hz), 136.8, 131.1, 123.2, 111.5 (d, $^2J_{C\text{-}F}$ = 24.0 Hz), 109.9 (d, $^2J_{C\text{-}F}$ = 25.5 Hz), 24.5, 17.1. The ^{1}H NMR data was in agreement with literature data.[16]

*2-Acetamido-4-fluorobenzoic acid (**10**)*

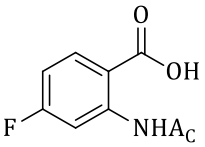

In a similar manner to the synthetic procedure reported for compound ***4***,[1] compound ***10*** acid was prepared from acid hydrolysis of *N*-(5-fluoro-2-methylphenyl)acetamide (2.01 g, 12.0 mmol). 2-Acetamido-4-fluorobenzoic acid ***10*** was obtained as an off-white powder in 82% yield (1.93 g). The melting point was 208–209 °C [lit.[1] 209–209.5 °C]; ^{1}H NMR (600 MHz, DMSO) δ 11.63 (s, 1H), 8.34 (dd, $^3J_{H\text{-}F}$ = 12.3 Hz, $^4J_{H\text{-}H}$ = 2.7 Hz, 1H), 8.05 (dd, $^3J_{H\text{-}H}$ = 8.8 Hz, $^3J_{H\text{-}F}$ = 6.9 Hz, 1H), 6.95 (ddd [appeared as dt] , $^3J_{H\text{-}H}$ = $^3J_{H\text{-}F}$ = 8.4 Hz, $^4J_{H\text{-}H}$ = 2,7 Hz, 1H), 2.15 (s, 3H); ^{13}C NMR (151 MHz, DMSO) δ 169.4 (2C), 165.5 (d, $^1J_{C\text{-}F}$ = 249.2 Hz), 143.5 (d, $^3J_{C\text{-}F}$ = 13.0 Hz), 134.2 (d, $^3J_{C\text{-}F}$ = 11.2 Hz), 109.8 (d, $^2J_{C\text{-}F}$ = 21.1 Hz, 2C), 106.0 (d, $^2J_{C\text{-}F}$ = 28.7 Hz), 25.1. The ^{1}H NMR data was in agreement with the literature.[5]

*2-Amino-4-fluorobenzoic acid (**11**)*

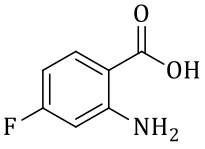

Compound ***10*** (2.02 g, 10.3 mmol) was treated in a similar fashion to synthesis of compound ***5*** under acidic medium to afford ***11*** as a beige powder in 74% yield (1.18 g). The melting point was 193–194 °C [lit.[1] 192.5–193 °C]; ^{1}H NMR (600 MHz, DMSO) δ 7.73 (ddd, [appeared as td] $^3J_{H\text{-}H}$ =11.9, $^3J_{H\text{-}F}$ = 7.2 Hz, $^4J_{H\text{-}H}$ = 2.6 Hz, 1H), 6.87 (br s, 2H), 6.51 (dd, $J_{H\text{-}F}$ = 11.9 Hz, $^4J_{H\text{-}H}$ = 2.6 Hz, 1H), 6.31 (ddd, [appeared as dt, $^3J_{H\text{-}F}$ =11.9 Hz, $^3J_{H\text{-}H}$ = 7.2 Hz, $^4J_{H\text{-}H}$ = 2.6 Hz, 1H); ^{13}C NMR (100 MHz, DMSO) δ 171.8, 169.5 (d, $^1J_{C\text{-}F}$ = 240.1 Hz), 156.3 (d, $^3J_{C\text{-}F}$ = 13.1 Hz), 136.9 (d, $^3J_{C\text{-}F}$ = 11.5 Hz), 105.1 (d, $^2J_{C\text{-}F}$ = 22.0 Hz), 104.0, 103.8 (d, $^2J_{C\text{-}F}$ = 24.0 Hz).

*7-Fluoroquinazolin-4(3H)-one (**12**)*

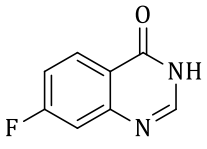

Compound ***12*** was obtained in 83% yield (1.76 g) following treatment of compound ***11*** (2.01 g, 12.9 mmol) with formamide (25 mL) as in the preparation of ***6***.[8] The melting point was 258–259 °C [lit.[17] 260.1–261 °C]; ^{1}H NMR (600 MHz, DMSO) δ 12.33 (br s, 1H), 8.18 (ddd [appeared as dt], $^{3}J_{H\text{-}H}$ =8.4, $^{3}J_{H\text{-}F}$ = 6.4, $^{4}J_{H\text{-}H}$ = 2.4 Hz , 1H), 8.13 (br d, J = 2.9 Hz, 1H), 7.44 (dd, $^{3}J_{H\text{-}F}$ = 10.1 Hz, $^{4}J_{H\text{-}H}$ = 2.5 Hz, 1H), 7.38 (ddd [appeared as dt], $^{3}J_{H\text{-}H}$ =$^{3}J_{H\text{-}F}$ = 8.7 Hz, $^{4}J_{H\text{-}H}$ = 2.5 Hz, 1H); ^{13}C NMR (75 MHz, DMSO) δ 167.7 (d, $^{1}J_{C\text{-}F}$ = 250.7 Hz), 160.5, 151.2 (d, $^{3}J_{C\text{-}F}$ = 13.1 Hz), 147.3, 129.4 (d, $^{3}J_{C\text{-}F}$ = 10.8 Hz), 120.1, 115.8 (d, $^{2}J_{C\text{-}F}$ = 24.2 Hz), 112.8 (d, $^{2}J_{C\text{-}F}$ = 22.7 Hz). The ^{1}H NMR spectrum matched the literature data.[12]

*7-Chloroquinazolin-4(3H)-one (**14**)*

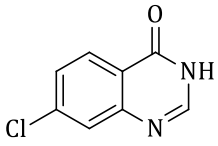

In a similar fashion to a preparation of ***6***,[8] compound ***14*** was obtained from treatment of 2-amino-4-chlorobenzoic acid (2.03 g, 11.7 mmol) with formamide (25 mL). A free flowing light-brown powder of ***14*** was obtained in 87% yield (1.84 g). The melting point was 249–250 °C [lit.[18] 249–252 °C]; ^{1}H NMR (400 MHz, DMSO) δ 12.37 (br s, 1H), 8.12 (s, 1H), 8.09 (d, J = 8.5 Hz, 1H), 7.71 (d, J = 2.1 Hz, 1H), 7.54 (dd, J = 8.5, 2.1 Hz, 1H); ^{13}C NMR (75 MHz, DMSO) δ 160.8, 149.2, 148.3, 140.0, 128.9, 128.2, 126.3, 122.0. The ^{1}H NMR data resembled the literature.[12]

*7-Chloro-6-nitroquinazolin-4(3H)-one [**15 (i)**]*

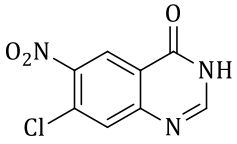

Using the same procedure for the synthesis of 6-nitoquinazolin-4(*3H*)-one (***7***),[10] compound ***15 (i)*** was obtained from nitration of 7-Chloroquinazoline (500 mg, 2.78 mmol) in fuming HNO_3/H_2SO_4 (4 mL) for 1 h at 80°C. Due to multiple products formation for this particular nitration reaction, further purification was performed by means of chromatography to afford ***15 (i)*** as a light yellow product in 67% overall yield. The melting point was 222–224 °C [lit.[19] 300–303 °C]; ^{1}H NMR (300 MHz, DMSO) δ 12.79 (br s, 1H), 8.67 (s, 1H), 8.31 (s, 1H), 8.01 (s, 1H); ^{13}C NMR (75 MHz, DMSO) δ 160.8, 149.2, 148.3, 140.0, 128.9, 128.2, 126.3, 122.0. The NMR data was identical to one reported in the literature.[20]

*7-Chloro-8-nitroquinazolin-4(3H)-one [**15 (ii)**]*

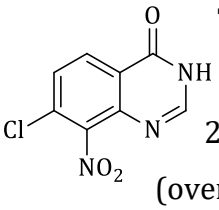

The compound was isolated as a by-product from preparation of ***15 (i)*** above at an estimated quantitative yield of 11%. The melting point was 230–232 °C; ^{1}H NMR (300 MHz, DMSO) δ 12.84 (br s, 1H), 8.28 (overlapping s, 1H), 8.28 (overlapping d, *J* = 8.7 Hz, 1H), 7.82 (d, *J* = 8.7 Hz, 1H); ^{13}C NMR (75 MHz, DMSO) δ 159.8, 156.3, 154.6, 150.5, 126.0, 119.8, 116.2, 115.9.

*7-Methoxy-6-nitroquinazolin-4(3H)-one (**16**)*

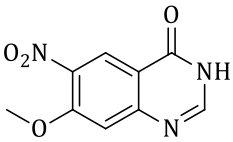

Under inert reaction conditions, $Na_{(s)}$ (0.51 mg, 22.2 mmol), was added to a freshly dried methanol (MeOH, 40 mL) reaction flask, placed in the ice-bath. After all the sodium had dissolved, the NaOMe solution was degassed, transferred to a reaction flask containing ***15 (i)*** (500 mg, 2.22 mmol), and the reaction mixture was heated to reflux at 100 °C. After 10 days, excess MeOH was removed *in vacuo* and the concentrate was quenched with ice cold water, and neutralised with 50% aqueous AcOH (20 mL) to form a yellow precipitate. The precipitate was filtered, rinsed with cold water, and dried to obtain a pure product in 97% yield (476 mg). Decomposition occurred during melting point determinations [lit.[21] 287 °C]; ^{1}H NMR (300 MHz, DMSO) δ 12.50 (br s, 1H), 8.51 (s, 1H), 8.23 (s, 1H), 7.42 (s, 1H), 4.04 (s, 3H); ^{13}C NMR (75 MHz, DMSO) δ 160.1, 156.5, 153.6, 149.3, 138.8, 124.2, 115.7, 111.0, 57.8. The ^{1}H NMR data was in agreement with the literature.[20]

*Ethyl 2-acetamidobenzoate (**17**)*

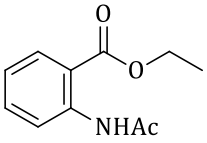

Compound ***17*** was synthesized from ethyl 2-aminobenzoate (5.05 g, 29.9 mmol) by utilizing the same procedure that has been reported in the preparation of ***1***. Ethyl 2-acetamidobenzoate was obtained as a crystalline precipitate in 94% yield (5.90 g). The melting point was 62–64 °C [lit.[22] 63–65 °C]; ^{1}H NMR (400 MHz, DMSO) δ 10.53 (s, 1H), 8.19 (d, *J* = 8.4 Hz, 1H), 7.88 (dd, *J* = 7.9, 1.6 Hz, 1H), 7.60–7.54 (m, 1H), 7.20–7.12 (m, 1H), 4.29 (q, *J* = 7.1 Hz, 2H), 2.09 (s, 3H), 1.30 (t, *J* = 7.1 Hz, 3H); ^{13}C NMR (75 MHz, DMSO) δ 168.9, 167.5, 140.1, 134.2, 130.9, 123.5,

121.6, 118.5, 61.6, 25.0, 14.4. The ^{1}H NMR spectrum was in agreement with the literature data.[23]

*Ethyl 2-acetamido-5-bromobenzoate (**18**)*

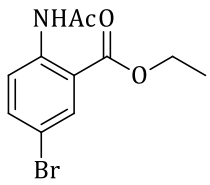

To a suspension of ethyl 2-acetamidobenzoate (4.68 g, 28.4 mmol) and $KBrO_3$ (3.02 g, 18.9 mmol) in acetic acid (80 mL) was added 48% HBr (5 mL) using a dripping funnel over 15 minutes. The reaction was stirred at a room temperature during which a permanent orange precipitate was formed. The reaction was continued for another 15 min before the flask contents were emptied into ice-cold water (250 mL). The yellow precipitate was filtered and the residual bromine was washed off with 10% $Na_2S_2O_4$ (50 mL) to afford ***18*** as a white precipitate in 83% yield (6.72 g). The measured melting point was 128–130 °C [lit.[24] 120 °C]; ^{1}H NMR (300 MHz, DMSO) δ 10.49 (s, 1H), 8.14 (d, *J* = 8.9 Hz, 1H), 7.97 (d, *J* = 2.5 Hz, 1H), 7.77 (dd, *J* = 8.9, 2.5 Hz, 1H), 4.32 (q, *J* = 7.1 Hz, 2H), 2.12 (s, 3H), 1.33 (t, *J* = 7.1 Hz, 3H); ^{13}C NMR (75 MHz, DMSO) δ 169.0, 166.2, 139.1, 136.7, 132.9, 123.9, 120.8, 115.1, 62.0, 24.9, 14.4. The ^{1}H NMR spectrum was in agreement with the literature data.[24]

*Ethyl 2-amino-5-bromobenzoate [**19 (i)**]*

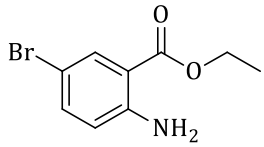

Compound ***19*** was obtained as result of selective amide hydrolysis in ***18*** (2.55g, 8.91 mmol) by adapting to acidic reaction conditions reported in preparation of compound ***5***,[1] but this time at 50 °C. After chromatographic purification, compound ***19*** was produced in 94% yield (2.04 g). The melting point was 83–83 °C [lit.[25] 80–81 °C]; ^{1}H NMR (300 MHz, DMSO) δ 7.77 (d, *J* = 2.5 Hz, 1H), 7.38 (dd, *J* = 8.9, 2.5 Hz, 1H), 6.79 (d, *J* = 8.9 Hz 1H), 6.09 (s, 4H), 4.25 (q, *J* = 7.1 Hz), 1,29 (t, *J* = 7.1 Hz, 1H); ^{13}C NMR (75 MHz, DMSO) δ 166.6, 150.7, 136.8, 132.7, 119.5, 111.0, 105.4, 60.8, 14.6. The ^{1}H NMR spectrum was identical to that of the literature data.[25]

*2-Acetamido-5-bromobenzoic acid [**19 (ii)**]*

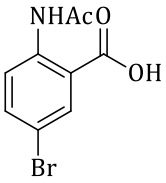

This compound was obtained as result of selective ester group hydrolysis of ***18*** under mild (50 °C) basic conditions Thus, ethyl 2-acetamido-5-bromobenzoate (1.03 g, 3.61 mmol) was dissolved in 4 N ethanolic KOH solution (15 ml) and the reaction was stirred at 50 °C for 2 h. The excess solvent was then removed *in vacuo*, the crude product was then diluted with cold water (30 mL), acidified to pH 5 with 4 N HCl, before it was extracted into DCM (3 × 40 mL). The organic extracts were dried over $MgSO_4$, concentrated and the crude product was purified by chromatography. Compound ***19 (ii)*** was obtained as a white solid in 71% yield (0.66 g). The melting point was 220–221 °C [lit.[25] 219–221 °C]; ^{1}H NMR (300 MHz, DMSO) δ 10.96 (s, 1H), 8.40 (d, *J* = 9.0 Hz, 1H), 8.03 (d, *J* = 2.5 Hz, 1H), 7.75 (dd, *J* = 9.0, 2.5 Hz, 1H), 2.13 (s, 3H); ^{13}C NMR (75 MHz, DMSO) δ 169.1, 168.5, 140.4, 136.9, 133.5, 122.6, 119.3, 114.4, 25.4. The ^{1}H NMR spectrum matched the literature data.[25]

*6-Bromoquinazolin-4(3H)-one (**20**)*

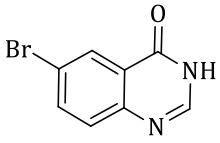

Compound ***20*** was prepared from ethyl 2-amino-5-bromobenzoate (2.01 g, 8.24 mmol) and formarmide (20 mL) using similar experimental conditions reported for **6**,[8] but at 140 °C. Compound ***20*** was obtained as a light brown powder in 81% yield (1.58 g). The melting point was 268–270 °C [lit.[26] 273–274°C]; ^{1}H NMR (300 MHz, DMSO) δ 12.44 (br s, 1H), 8.19 (d, *J* = 2.3 Hz, 1H), 8.14 (d, *J* = 3.1 Hz, 1H), 7.96 (dd, *J* = 8.7, 2.3 Hz, 1H), 7.62 (d, *J* = 8.7 Hz, 1H); ^{13}C NMR (75 MHz, DMSO) δ 160.1, 148.2, 146.5, 137.6, 130.1, 128.4, 124.7, 119.7. The ^{1}H NMR data corresponded to literature.[26]

*6-Hydroxyquinazolin-4(3H)-one (**22**)*

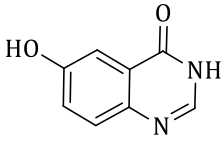

Compound ***22*** was prepared from 2-amino-5-hydroxybenzoic acid (2.00 g, 13.1 mmol) by adapting to a synthetic method for compound ***6***.[8] Compound ***22*** was obtained as a grey powder in 76% yield (1.61 g). The melting point was 214–218 °C [lit.[12] 300 °C]; ^{1}H NMR (300 MHz, DMSO) δ 12.03 (br s, 1H), 10.06 (s, 1H), 7.90 (d, *J* = 3.2 Hz, 1H), 7.53 (d, *J* = 8.8 Hz, 1H), 7.40 (d, *J* = 2.9 Hz,

1H), 7.26 (dd, *J* = 8.8, 2.9 Hz, 1H); ^{13}C NMR (75 MHz, DMSO) δ 160.9, 158.5, 156.6, 142.6, 129.3, 124.1, 109.2 (2C). The ^{1}H NMR spectrum was identical to that reported in the literature.[12]

*4-Oxo-3,4-dihydroquinazolin-6-yl acetate (**23**)*

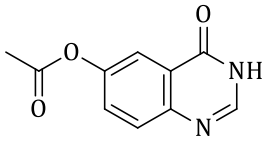

6-Hydroxyquinazolin-4(3*H*)-one (1.50 g, 9.26 mmol) was dissolved in Ac_2O (15 mL), pyridine (4 mL) was added and the reaction mixture was stirred at a room temperature overnight. The reaction was quenched by emptying the reaction contents into ice-water (30 mL). The formed precipitate was filtered, rinsed with cold water and dried to obtain a beige precipitate in 79% yield (1.49 g). The melting point was 220–222 °C; ^{1}H NMR (300 MHz, DMSO) δ 12.33 (br s, 1H), 8.10 (s, 1H), 7.83 (br d, *J* = 2.6 Hz, 1H), 7.73 (d, *J* = 8.8 Hz, 1H), 7.61–7.56 (m, 1H), 2.31 (s, 3H); ^{13}C NMR (75 MHz, DMSO) δ 169.7, 160.7, 149.0, 147.0, 145.6, 129.3, 129.2, 123.7, 118.3, 21.3. The ^{1}H NMR was in agreement with the reported literature data.[27]

*Methyl-3,4-dimethoxybenzoate (**24**)*

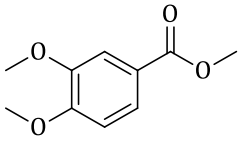

To a suspension of, K_2CO_3 (11.2 g, 81.3 mmol) in acetone (120 mL) placed over the ice bath was added 3,4-dihydrobenzoic acid (5.00 g, 32.5 mmol) and then methyl iodide (7.40 mL, 119 mmol) in a drop-wise fashion with stirring. The reaction was continued at 50 °C for 3 h, before excess K_2CO_3 was filtered off and the organic solvent removed *in vacuo* to obtain a yellow viscous liquid. The viscous liquid was diluted with DCM (40 mL) and washed with 10% $Na_2S_2O_4$ (40 mL) and then water (40 mL × 2). The organic extract was dried over $MgSO_4$, and evaporated *in vacuo* to afford a colourless liquid. Chromatographic purification afforded 81% yield of methyl-3,4-dimethoxybenzoate (5.13 g), which solidified upon storage. The melting point was 60–62 °C [lit.[28] 58–60 °C]; ^{1}H NMR (300 MHz, $CDCl_3$) δ 7.70 (dd, *J* = 8.4, 2.0 Hz, 1H), 7.56 (d, *J* = 2.0 Hz, 1H), 6.91 (d, *J* = 8.4 Hz, 1H), 3.96 (overlapping s, 3H), 3.95 (overlapping s, 3H), 3.92 (s, 3H); ^{13}C NMR (75 MHz, $CDCl_3$) δ 162.1, 148.2, 143.8, 118.8,

117.9, 107.2, 105.5, 51.3 (2C), 47.2. The ^{1}H NMR spectrum was in agreement with the literature.[29]

*Methyl 4,5-dimethoxy-2-nitrobenzoate [**25 (i)**]*

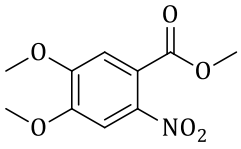

A reaction flask containing methyl 3,4-dimethoxybenzoate (1.06 g, 5.92 mmol) was placed in the ice bath and to this was added 65% HNO_3 (8 mL) in a drop-wise fashion over 10 min. The reaction was continued for another 20 min and the final temperature of the ice bath was 6 °C. The reaction mixture was poured into the ice-water (150 mL) and the resulting precipitate was filtered, rinsed with cold water and dried to obtain a yellow powder. The crude product was suspended in DCM and purified by chromatography to yield ***25 (i)*** in 26%. The melting point was 142–143 °C [lit.[30] 127–128 °C]; ^{1}H NMR (400 MHz, $CDCl_3$) δ 7.45 (s, 1H), 7.08 (s, 1H), 3.98 (overlapping s, 3H), 3.97 (overlapping s, 3H), 3.91 (s, 3H); ^{13}C NMR (100 MHz, $CDCl_3$) δ 166.5, 152.7, 150.6, 141.5, 121.8, 111.0, 107.2, 56.9, 56.8, 53.5; MS (ESI^{+}) *m/z* 264.1872 was calculated for $C_{10}H_{11}NO_6$ $[M+Na]^{+}$ and 264.1872 was determined experimentally.

*Methyl 4,5-dimethoxy-2,3-dinitrobenzoate [**25 (ii)**]*

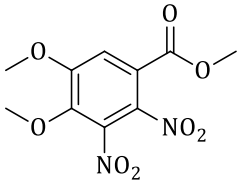

The over-nitration by-product was isolated with an estimated yield of 11% (0.15 g). The melting was 131–133 °C [lit.[31] 133–134 °C]; ^{1}H NMR (400 MHz, $CDCl_3$) δ 7.41 (s, 1H), 4.03 (s, 6H), 3.91 (s, 3H); ^{13}C NMR (100 MHz, $CDCl_3$) δ 163.5, 155.7, 144.2, 122.4, 114.2, 63.0, 57.4, 54.0; $^{1}J_{C\text{-}H}$ HSQC NMR (400, $CDCl_3$) δ (7.41, 114.1), (4.05, 62.9), (4.03, 57.27), (3.91, 53.9); $^{2,3}J_{C\text{-}H}$ HMBC NMR (400, $CDCl_3$) δ (7.41; 163.5), (7.41, 155.5), (7.41, 144.1), (7.41, 135.5), (7.41, 122.4}, (4.03, 144.1), (4.03, 155.6), (3.90,153.5); MS (ESI^{+}) *m/z* 309.1648 was calculated for $C_{10}H_{10}N_2O_8$ $[M+Na]^{+}$ and 309.1661 (-3.17 ppm) was determined experimentally.

*Methyl 2-amino-4,5-dimethoxybenzoate (**26**)*

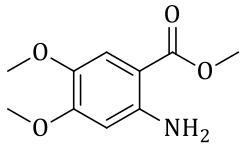

Compound ***26*** was synthesized from compound ***25 (i)*** (0.35 g, 1.45 mmol) by adapting to the literature procedure described for preparation of compound ***8***.[13] Chromatographic purification of the crude afforded a desired compound in 87% yield (0.27 g). The melting point was 128–130 °C [lit.[32] 130–132 °C]; ^{1}H NMR (600 MHz, $CDCl_3$) δ 7.29 (s, 1H), 6.14 (s, 1H), 5.57 (br s, 2H), 3.86 (s, 3H), 3.85 (s, 3H), 3.82 (s, 3H); ^{13}C NMR (150 MHz, $CDCl_3$) δ 170.8, 157.4, 149.7, 143.2, 115.3, 104.7, 102.0, 59.0, 58.4, 53.9; MS (ESI^+) *m/z* 212.0917 was calculated for $C_{10}H_{13}NO_4$ $[M+H]^+$ and 212.0915 (0.90 ppm) was determined experimentally. The ^{1}H NMR was identical to the one reported in the literature.[33]

*6,7-Dimethoxyquinazolin-4(3H)-one (**27**)*

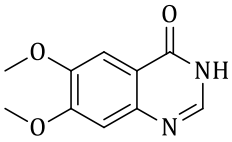

Compound ***27*** was acquired from methyl 2-amino-4,5-dimethoxybenzoate (0.40 g, 1.56 mmol) using the literature method reported in the synthesis of compound ***6***.[8] 6,7-Dimethoxyquinazolin-4(3*H*)-one was obtained as a beige powder (0.28 g, 84% yield). The melting point was 294–296 °C [lit.[33] 300–302 °C]; ^{1}H NMR (300 MHz, DMSO) δ 12.07 (s, 1H), 7.99 (s, 1H), 7.44 (s, 1H), 7.13 (s, 1H), 3.90 (s, 3H), 3.87 (s, 3H); ^{13}C NMR (75 MHz, DMSO) δ 160.5, 154.9, 149.0, 145.3, 144.3, 116.1, 108.5, 105.4, 56.4, 56.2. The ^{1}H NMR was identical to the literature report.[33]

*6-Hydroxy-7-methoxyquinazolin-4(3H)-one (**28**)*

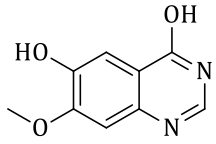

Demethylation procedure was carried out according to Knesl *et al.*[34] with degassing modification to the procedure. Thus, methane sulfonic acid (4 mL) was added to 6,7-dimethoxyquinazolin-4(3*H*)-one (0.50 g, 2.43 mmol) and D,L-methionine (0.40 g, 2.50 mmol) and the contents were subjected to three cycles of freeze-pump-thaw degassing. The reaction mixture was heated to reflux at 120 °C with stirring for 48 h, then cooled to a room temperature and the contents were poured into ice-cold water (20 mL). It was then slowly neutralized with 40% aqueous NaOH solution over the ice bath, the resultant pale grey precipitate was filtered, washed

with cold water and dried to afford ***28*** in 16% yield (73 mg). The melting point was 214–216 °C [lit.[33] 300 °C]; ^{1}H NMR (300 MHz, DMSO) δ 11.67 (br s, 1H), 9.78 (br s, 1H), 7.88 (s, 1H), 7.36 (s, 1H), 7.07 (s, 1H), 3.88 (s, 3H); ^{13}C NMR (75 MHz, DMSO) δ 160.5, 154.4, 147.2, 144.2, 143.4, 116.5, 109.1, 108.6, 56.3. The ^{1}H NMR data was in agreement with the literature.[33]

*7-Methoxy-4-oxo-3,4-dihydroquinazolin-6-yl acetate [**29 (i)**]*

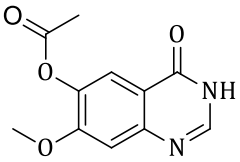

A crude sample of 6-hydroxy-7-methoxyquinazolin-4(3*H*)-one demethylation experiments (1.00 g, 5.21 mmol) was dissolved in pyridine (2.5 mL) and Ac_2O (5 mL, 52.8 mmol) and the resulting suspension was stirred at a room temperature overnight. The reaction was quenched by adding flask contents into ice-cold water (50 mL). The floating impurities were decanted off and the settled precipitate was then filtered, rinsed with ice-cold water, and dried to obtain a free flowing light-brown powder. Chromatographic purification of the *O*-acylated compounds on a silica gel column using gradient elution of 5% acetone in DCM to 100% acetone produced two positively identified products as ***29 (i)*** and ***29 (ii)*.**

Campound ***29 (i)*** was obtained as a beige solid in approximated quantitative yield of 14% (163 mg). The melting point was 298–300 °C [lit.[33] 303–305 °C]; ^{1}H NMR (300 MHz, DMSO) δ 12.20 (s, 1H), 8.09 (s, 1H), 7.75 (s, 1H), 7.28 (s, 1H), 3.92 (s, 3H), 2.30 (s, 3H); ^{13}C NMR (75 MHz, DMSO) δ 169.1, 160.4, 156.5, 149.3, 146.4, 139.3, 119.5, 116.1, 109.6, 56.9, 20.9. The ^{1}H NMR data was identical to those reported in the literature.[33]

*4-Oxo-3,4-dihydroquinazoline-6,7-diyl diacetate [**29 (ii)**]*

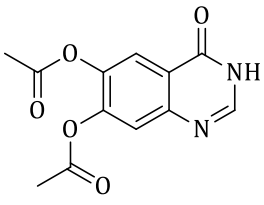

One of the collected fractions proved this compound to be a by-product constituting about 3% quantitative yield. ^{1}H NMR (300 MHz, DMSO) δ 12.40 (br s, 1H), 8.13 (s, 1H), 7.96 (s, 1H), 7.60 (s, 1H), 2.34 (overlapping s, 3H), 2.32 (overlapping s, 3H); ^{13}C NMR (75 MHz, DMSO) δ 168.8, 168.4, 160.2, 148.0, 147.5, 146.7, 141.3, 122.1, 121.3, 120.9, 20.9 (2C).

*A general method for synthesis of 6,7-dimethoxy-substituted 4-anilinoquinazolines (**30**–**32**).*

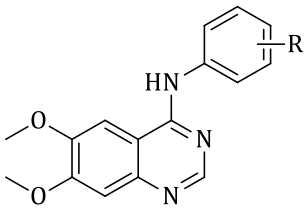

A representative procedure for the synthesis of 6,7-dimethoxy-(4-anilino)quinazolines is described.[35] Under inert atmospheric conditions, a suspension of 6,7-dimethoxyquinazolin-4(3*H*)-one (500 mg, 2.43 mmol), chlorobenzene (5 mL) and Hunig's base (0.42 mL, 2.43 mmol)was kept in the ice bath. To this cooled suspension was dispensed $POCl_3$ (10 mL) through the dripping funnel in a drop wise fashion under continuous stirring for 0.5 h. The reaction mixture was then heated to reflux at 80 °C for 3 h and excess $POCl_3$ and the solvent were distilled off at 60 °C under vacuum. The resultant beige solid was dried further under high vacuum for 1 h. This semi-dried product was dissolved in isopropyl alcohol (IPA, 30 mL) and a suitable aryl amine (1.3 molar equivalents) was then added. The reaction mixture shortly precipitated before turning into a solution at 60 °C with stirring. The reaction was continued for 2 h during which a permanent precipitate rematerialized. The precipitate was cooled, filtered, rinsed with cold IPA (15 mL) and dried to obtain almost pure product that was purified further by chromatographic methods.

*N-(3-Ethynylphenyl)-6,7-dimethoxyquinazolin-4-amine (**30**)*

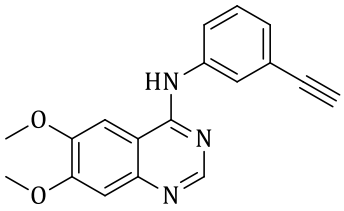

Compound ***30*** was obtained as a white precipitate in 76% yield (0.56 g). The melting point was 182–184 °C [lit.[36] 290–292 °C]; ^{1}H NMR (300 MHz, DMSO) δ 9.49 (s, 1H), 8.51 (s, 1H), 8.00 (s, 1H), 7.91 (d, J = 8.4 Hz, 1H), 7.83 (s, 1H), 7.41 (dd [appeared as a t], $J_1 = J_2$ = 8 Hz, 1H), 7.25–7.19 (m, 2H), 4.20 (s, 1H), 3.97 (s, 3H), 3.94 (s, 3H); ^{13}C NMR (75 MHz, DMSO) δ 156.6, 154.8, 153.2, 149.4, 147.5, 140.3, 129.3, 126.8, 125.2, 123.0, 122.2, 109.3, 107.7, 102.2, 84.0, 81.0, 56.7, 56.3; MS (ESI$^+$) *m/z* 306.1237 was calculated for $C_{18}H_{15}N_3O_2$ [M+H]$^+$and 306.1237 was determined experimentally; LC chemical purity was 98.4%.

*N-(3-Bromophenyl)-6,7-dimethoxyquinazolin-4-amine (**31**)*

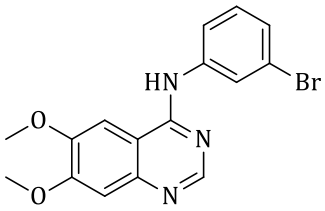

Compound ***31*** was obtained as a white precipitate in 85% yield (0.74 g). The melting point was 173–174°C [lit.[37] 188–189 °C]; ^{1}H NMR (300 MHz, DMSO) δ 9.53 (s, 1H), 8.53 (s, 1H), 8.17–8.13 (m, 1H), 7.91–7.86 (m, 1H), 7.83 (s, 1H), 7.36 (dd [appeared as a t], $J_1 = J_2$ = 8 Hz, 1H), 7.30–7.25 (m, 1H), 7.21 (s, 1H), 3.97 (s, 3H), 3.94 (s, 3H); ^{13}C NMR (75 MHz, DMSO) δ 156.4, 154.8, 153.1, 149.5, 147.6, 141.8, 130.8, 126.0, 124.4, 121.6, 121.0, 109.4, 107.7, 102.2, 56.7, 56.3; MS (ESI$^+$) *m/z* 360.0342 was calculated for $C_{16}H_{14}BrN_3O_2$ $[M+H]^+$ and 360.0339 (0.3 ppm) was determined experimentally; LC chemical purity was 96.3%.

*N-(3-Chloro-4-fluorophenyl)-6,7-dimethoxyquinazolin-4-amine (**32**)*

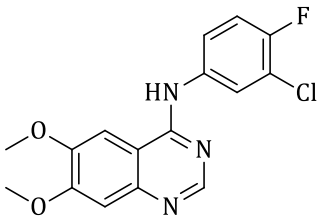

Compound ***32*** was obtained as a white precipitate in 90% yield (0.73 g). The melting point was 196–198 °C [lit.[38] 273–275 °C]; ^{1}H NMR (300 MHz, DMSO) δ 8.78 (s, 1H), 7.74 (s, 1H), 7.36 (dd, J = 6.8, 2.6 Hz, 1H), 7.09–7.00 (m, 2H), 6.68 (dd [appeared as a t], $^{3}J_{H\text{-}F} = {}^{3}J_{H\text{-}H}$ = 9.2 Hz, 1H), 6.44 (s, 1H), 3.20 (s, 3H), 3.18 (s, 3H); ^{13}C NMR (75 MHz, DMSO) δ 155.7, 154.1, 152.3, 148.7 (d, $^{1}J_{C\text{-}F}$ = 252.7 Hz), 146.8, 136.5, 123.1, 122.0, 121.9, 118.6 (d, $^{2}J_{C\text{-}F}$ = 25.2 Hz), 116.2, (d, $^{2}J_{C\text{-}F}$ = 21.8 Hz) 108.5, 106.9, 101.4, 55.9, 55.6. The ^{1}H NMR was in agreement with the literature data. [38] MS (ESI$^+$) *m/z* 334.0753 was calculated for $C_{16}H_{13}ClFN_3O_2$ $[M+H]^+$ and 334.0751 (0.20 ppm) was determined experimentally; LC chemical purity was 99.1%.

*General synthesis of the 6-nitro(4-anilino)quinazoline derivatives (**34–42**)*

The synthesis of 6-nitro(4-anilino)quinazoline derivatives was carried out according to a described representative procedure in general synthesis of compounds ***30–32***. A once off NMR analysis was performed on the crude intermediate, 4-chloro-6-nitroquinazoline (***33***), as presented next. All of the resulting 6-nitro(4-anilino)quinazoline compounds were obtained as bright yellow powdery precipitates.

*4-Chloro-6-nitroquinazoline (**33**)*

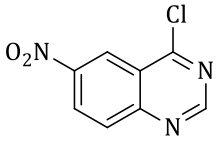

The intermediate ***33*** was analysed without quantifying the yield. ^{1}H NMR (400 MHz, DMSO) δ 8.78 (d, *J* = 2.6 Hz, 1H), 8.52 (dd, *J* = 9.0, 2.7 Hz, 1H), 8.29 (s, 1H), 7.84 (d, *J* = 9.0 Hz, 1H); ^{13}C NMR (101 MHz, DMSO) δ 160.9, 153.6, 149.7, 145.6, 129.7, 128.9, 123.4, 122.6. The ^{1}H NMR data was in agreement with the values reported in literature.[39]

*N-(3-Ethynylphenyl)-6-nitroquinazolin-4-amine (**34**)*

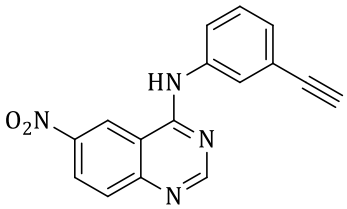

Compound ***34*** was obtained in 76% yield (0.58 g). The melting point was 232–234 °C [lit.[40] 271–272 °C]; ^{1}H NMR (300 MHz, DMSO) δ 10.42 (s, 1H), 9.62 (d, *J* = 2.4 Hz, 1H), 8.74 (s, 1H), 8.52 (dd, *J* = 9.0, 2.4 Hz, 1H), 8.04–8.01 (m, 1H), 7.94–7.91 (m, 1H), 7.91–7.88 (m, 1H), 7.42 (dd [appeared as a t], $J_1 = J_2 = 9.0$ Hz, 1H), 7.31–7.25 (m, 1H), 4.23 (s, 1H); ^{13}C NMR (75 MHz, DMSO) δ 159.1, 158.0, 153.5, 145.0, 139.2, 130.0, 129.5, 127.9, 127.1, 125.9, 123.6, 122.3, 121.2, 114.8, 83.7, 81.3. The ^{1}H NMR spectrum closely resembled the reported the literature data.[40]

*N-(3-Bromophenyl)-6-nitroquinazolin-4-amine (**35**)*

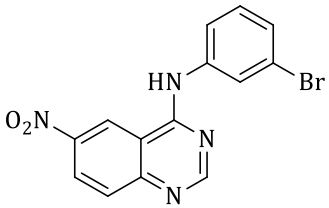

Compound ***35*** was afforded in 85% yield (0.77 g). The melting point was 244–246 °C [lit.[40] 282–283 °C]; ^{1}H NMR (300 MHz, DMSO) δ 11.95 (s, 1H), 9.90 (d, *J* = 2.2 Hz, 1H), 9.02 (s, 1H), 8.76 (dd, *J* = 9.2, 2.3 Hz, 1H), 8.17 (d, *J* = 9.2 Hz, 1H), 8.08 (m, 1H), 7.84–7.79 (m, 1H), 7.56–7.51 (overlapping m, 1H); 7.47 (overlapping dd, $J_1 = J_2 = 8.0$ Hz, 1H); ^{13}C NMR (75 MHz, DMSO) δ 160.4, 154.7, 146.1, 138.9, 131.2, 129.6, 129.5, 127.1, 124.2 (2C), 123.6, 122.2, 121.7, 114.3. The ^{1}H NMR spectrum closely resembled the literature data.[40]

*N-(3-Chloro-4-fluorophenyl)-6-nitroquinazolin-4-amine (**36**)*

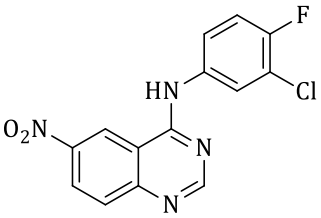

Compound ***36*** was obtained in 90% yield (0.75 g). The melting point was 254–256 °C [lit.[40] 289–281 °C]; ^{1}H NMR (300 MHz, DMSO) δ 12.13 (br s, 1H), 9.91 (d, *J* = 2.3 Hz, 1H), 9.02 (s, 1H), 8.76 (dd, *J* = 9.3, 2.1 Hz, 1H), 8.18 (d, *J* = 9.3 Hz, 1H), 8.07 (dd, *J* = 6.9, 2.4 Hz, 1H), 7.79 (ddd, $^{3}J_{H\text{-}H}$ = 9.3, $^{4}J_{H\text{-}F}$ = 4.4, $^{4}J_{H\text{-}H}$ = 2.6 Hz, 1H), 7.57 (dd [appeared as a t], $^{3}J_{H\text{-}F}$ = $^{3}J_{H\text{-}H}$ = 9.3 Hz, 1H);^{13}C NMR (75 MHz, DMSO) δ 160.5, 156.2 (d, $^{1}J_{C\text{-}F}$ = 246.3 Hz), 154.5, 146.1, 134.4, 129.8, 126.8, 125.5, 124.4, 123.9, 122.2, 119.9 (d, $^{2}J_{C\text{-}F}$ = 19.6 Hz), 117.6 (d, $^{2}J_{C\text{-}F}$ = 21.9 Hz), 114.2. The ^{1}H NMR spectrum closely resembled the literature data.[40]

*7-Chloro-N-(3-ethynylphenyl)-6-nitroquinazolin-4-amine (**37**)*

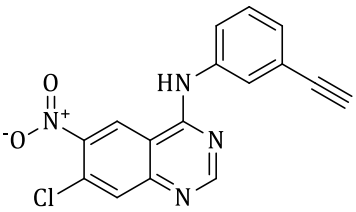

Compound ***37*** was obtained in 73% yield (0.53 g). The melting point was 216–218 °C; ^{1}H NMR (300 MHz, DMSO) δ 10.30 (s, 1H), 9.42 (d, *J* = 5.3 Hz, 1H), 8.73 (d, *J* = 5.4 Hz, 1H), 8.07–7.96 (m, 2H), 7.86 (m, 1H), 7.58–7.34 (m, 1H), 7.34–7.22 (m, 1H), 4.20 (s, 1H); ^{13}C NMR (75 MHz, DMSO) δ 158.7, 158.5, 152.3, 144.6, 139.0, 130.8, 129.5, 129.4, 128.1, 125.8, 123.4 (2C), 122.4, 113.8, 83.7, 81.3; MS (ESI^{+}) *m/z* 325.0487 was calculated for $C_{16}H_9ClN_4O_2$ $[M+H]^{+}$ and 325.0480 (0.70 ppm) was determined experimentally.

*N^{4}-(3-Bromophenyl)-7-chloro-6-nitroquinazolin-4-amine (**38**)*

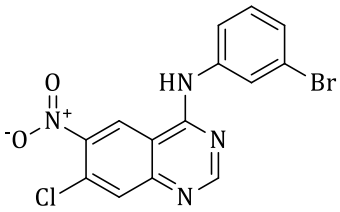

Compound ***38*** was obtained in 69% yield (0.58 g). The melting point was 222–224 °C; ^{1}H NMR (300 MHz, DMSO) δ 10.34 (s, 1H), 9.43 (s, 1H), 8.77 (s, 1H), 8.16 (s, 1H), 8.10 (s, 1H), 7.88–7.84 (m, 1H), 7.43–7.34 (m, 2H); ^{13}C NMR (75 MHz, DMSO) δ 158.6, 158.4, 152.3, 144.7, 140.4, 131.0, 130.9, 129.5, 127.5, 125.1, 123.4, 121.7, 121.6, 113.8.

*7-Chloro-N-(3-chloro-4-fluorophenyl)-6-nitroquinazolin-4-amine (**39**)*

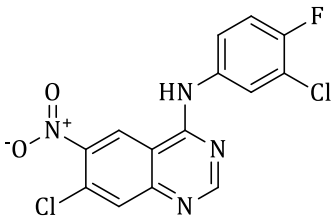

Compound ***39*** was obtained in 83% yield (0.65 g). The melting point was 244–246 °C; ^{1}H NMR (300 MHz, DMSO) δ 10.37 (br s, 1H), 9.39 (s, 1H), 8.74 (s, 1H), 8.13 (dd, *J* = 6.8, 2.4 Hz, 1H), 8.09 (s, 1H), 7.81–7.75 (m, 1H), 7.47 (dd [appeared as a t], $^{3}J_{H\text{-}H} = {}^{3}J_{H\text{-}F}$ = 9.0 Hz, 1H); ^{13}C NMR (75 MHz, DMSO) δ 158.6, 158.4, 155.9 (d, $^{1}J_{C\text{-}F}$ = 240.8 Hz), 152.2, 144.6, 135.9, 130.9, 129.5, 124.6, 123.4, 123.3, 119.6 (d, $^{2}J_{C\text{-}F}$ = 19.0 Hz), 117.4 (d, $^{2}J_{C\text{-}F}$ = 21.8 Hz), 113.7. MS (ESI^{+}) *m/z* 353.0003 was calculated for $C_{14}H_7Cl_2FN_4O_2$ $[M+H]^+$ and 353.000 (-0.3 ppm) was experimentally found.

*N-(3-Ethynylphenyl)-7-methoxy-6-nitroquinazolin-4-amine (**40**)*

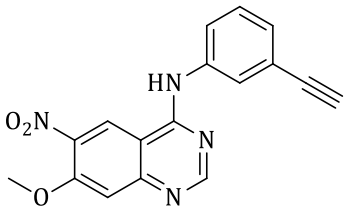

Compound ***40*** was obtained in 75% yield (0.54 g). The melting point was 178–180 °C [lit.[41] 213–218 °C with decomposition]; ^{1}H NMR (300 MHz, DMSO) δ 10.11 (br s, 1H), 9.26 (s, 1H), 8.68 (s, 1H), 8.03 (s, 1H), 7.88 (d, *J* = 8.2 Hz, 1H), 7.48 (s, 1H), 7.43 (dd [appeared as a t], $J_1 = J_2$= 7.9 Hz, 1H), 7.26 (d, *J* = 7.7 Hz, 1H), 4.22 (s, 1H), 4.07 (s, 3H); ^{13}C NMR (75 MHz, DMSO) δ 158.4, 157.9, 154.9, 153.9, 139.2, 129.5, 127.7, 125.6, 123.3 (2C), 122.3 (2C), 110.2, 108.5, 83.8, 81.2, 57.6. The ^{1}H NMR data was in agreement with the published data.[42]

*N-(3-Bromophenyl)-7-methoxy-6-nitroquinazolin-4-amine (**41**)*

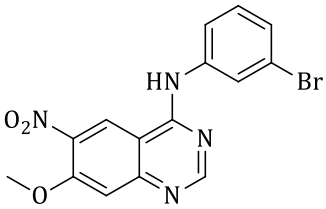

Compound ***41*** was obtained in 61% yield (0.52 g). The melting point was 188–190 °C [lit.[21] 206–207.5 °C]; ^{1}H NMR (300 MHz, DMSO) δ 10.11 (s, 1H), 9.25 (s, 1H), 8.69 (s, 1H), 8.17 (s, 1H), 7.90–7.85 (m, 1H), 7.49 (d, *J* = 3.4 Hz, 1H), 7.44–7.27 (m, 2H), 4.06 (s, 3H); ^{13}C NMR (75 MHz, DMSO) δ 158.2, 157.8, 155.0, 153.8, 140.8, 139.2, 130.8, 126.9, 124.8, 122.3, 121.6, 121.2, 110.1, 108.5, 57.6. The ^{1}H NMR spectrum was in agreement with literature data.[42]

*N-(3-Chloro-4-fluorophenyl)-7-methoxy-6-nitroquinazolin-4-amine (**42**)*

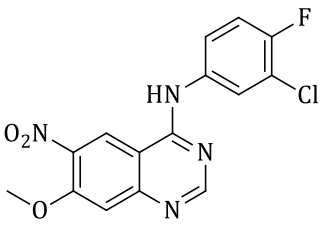

Compound ***42*** was obtained in 78% yield (0.62 g). The melting point was 238–240 °C [lit.[17] 292–293 °C]; ^{1}H NMR (300 MHz, dmso) δ 10.09 (s, 1H), 9.17 (s, 1H), 8.64 (s, 1H), 8.13 (dd, J = 6.8, 2.6 Hz, 1H), 7.81–7.73 (ddd, $^{3}J_{H\text{-}H}$ = 9.1 Hz, $^{4}J_{H\text{-}F}$ = 4.3 Hz, $^{4}J_{H\text{-}H}$ =2.7 Hz, 1H), 7.43 (dd [appeared as a t], J = 8.3 Hz, 2H), 4.04 (s, 3H);^{13}C NMR (75 MHz, DMSO) δ 157.5, 157.1, 155.0 (d, $^{1}J_{C\text{-}F}$ = 246.0 Hz), 154.3, 153.0, 138.4, 135.5, 123.5, 122.2, 121.5, 118.6 (d, $^{2}J_{C\text{-}F}$ = 20.6 Hz), 116.5 (d, $^{2}J_{C\text{-}F}$ = 21.8 Hz), 109.4, 107.6, 56.9. The ^{1}H NMR spectrum was in agreement with the literature values.[17]

*A representative procedure for the C-6 nitro reduction in 4-anilinoquinazolines (**43**–**51**)*

A general reaction for the transformation of the C-6 nitroquinazolin-4(3*H*)-ones functionality to the amine is described: To a suitable 6-nitro(4-anilino)quinazoline (50–200 mg), iron powder and ammonium chloride salt ($Fe_{(s)}$/NH_4Cl, 5 molar equivalents each) were added and the reaction mixture was suspended in ethanol (2–5 mL). The suspension was heated to reflux at 70 °C with stirring for 5 h, during which the yellow suspension changed colour to a reddish-brown solution [iron(III)]. At the end of the reaction, the contents were filtered by suction over celite and doubled-filter paper and the residue was further rinsed with ethyl acetate to obtain a light yellow solution. The filtrate was dried over $MgSO_4$, concentrated *in vacuo* and purified by chromatography to obtain the C-6 aminoquinazolin-4(3*H*)-ones as yellow precipitates. These amines often underwent decomposition during melting point determinations.

*N^4-(3-Ethynylphenyl)quinazoline-4,6-diamine (**43**)*

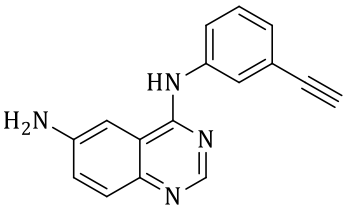

Compound ***43*** was obtained in 42% yield (75.9 mg). ^{1}H NMR (300 MHz, DMSO) δ 9.40 (s, 1H), 8.37 (s, 1H), 8.08 (s, 1H), 7.94–7.88 (m, 1H), 7.54 (d, J = 4.7 Hz, 1H), 7.38 (d, J = 7.9 Hz, 1H), 7.36–7.33 (m, 1H), 7.26 (dd, J = 8.9, 2.3 Hz, 1H), 7.18–7.15 (m, 1H), 5.61 (br s, 2H), 4.17 (s, 1H); ^{13}C NMR (75 MHz, DMSO) δ 156.3, 150.1, 147.8, 143.1, 140.7, 129.3, 129.2, 126.4, 124.7, 124.2, 122.6, 122.1, 117.1, 101.4, 84.2, 80.8; MS 142

(ESI$^+$) *m/z* 261.1135 was calculated for $C_{16}H_{12}N_4$ $[M+H]^+$ and 261.1132 (-0.30 ppm) was determined experimentally; LC chemical purity was 99.0%.

*N^4-(3-Bromophenyl)quinazoline-4,6-diamine (**44**)*

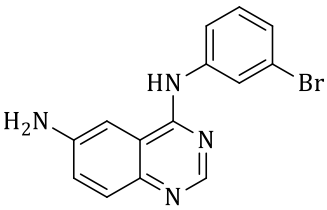

Compound ***44*** was obtained in 69% yield (126 mg). ^{1}H NMR (300 MHz, DMSO) δ 9.45 (s, 1H), 8.39 (s, 1H), 8.24 (d, *J* = 1.9 Hz, 1H), 7.91–7.86 (m, 1H), 7.56 (d, *J* = 8.9 Hz, 1H), 7.35 (d, *J* = 2.5 Hz, 1H), 7.30 (d, *J* = 8.2 Hz, 1H), 7.28–7.20 (m, 2H), 5.63 (br s, 2H); ^{13}C NMR (75 MHz, DMSO) δ 156.1, 150.0, 147.9, 143.2, 142.2, 130.7, 129.2, 125.6, 124.3, 123.9, 121.6, 120.5, 117.2, 101.3; MS (ESI$^+$) *m/z* 315.0240 was calculated for $C_{14}H_{11}BrN_4$ $[M+H]^+$ and 315.0247 (-0.70 ppm) and (317.0227 for ^{81}Br) were determined experimentally; LC chemical purity was 98.7%.

*N^4-(3-Chloro-4-fluorophenyl)quinazoline-4,6-diamine (**45**)*

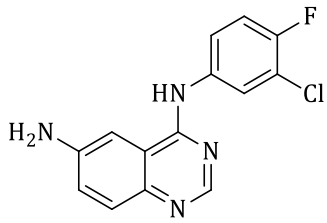

Compound ***45*** was obtained in 63% yield (114 mg). ^{1}H NMR (300 MHz, DMSO) δ 9.47 (s, 1H), 8.37 (s, 1H), 8.21 (dd, *J* = 6.9, 2.6 Hz, 1H), 7.87–7.80 (m, 1H), 7.55 (d, *J* = 8.8 Hz, 1H), 7.41 (dd [appeared as a t], $J_1 = J_2$ = 9.2 Hz, 1H), 7.32 (d, *J* = 2.2 Hz, 1H), 7.26 (dd, *J* = 8.8, 2.3 Hz, 1H), 5.63 (br s, 2H); ^{13}C NMR (75 MHz, DMSO) δ 156.1, 154.9 (d, $J_{C\text{-}F}$ =241.8 Hz), 150.0, 147.9, 143.1, 137.8, 129.2, 124.3, 123.2, 122.2, 122.1, 119.2 (d, $^2J_{C\text{-}F}$ =21.3 Hz), 117.0 (d, $^2J_{C\text{-}F}$ =21.1 Hz), 101.2; MS (ESI$^+$) *m/z* 289.0650 was calculated for $C_{14}H_{10}FClN_4$ $[M+H]^+$ and 289.0665 (-1.50 ppm) was determined experimentally; LC chemical purity was 98.1%.

*7-Chloro-N⁴-(3-ethynylphenyl)quinazoline-4,6-diamine (**46**)*

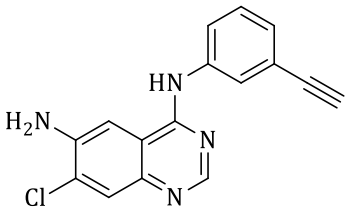

Compound ***46*** was obtained in 48% yield (106 mg). ^{1}H NMR (300 MHz, DMSO) δ 9.60 (s, 1H), 8.40 (s, 1H), 8.04 (s, 1H), 7.88 (d, *J* = 8.2 Hz, 1H), 7.75 (s, 1H), 7.61 (s, 1H), 7.41–7.34 (m, 1H), 7.19 (d, *J* = 7.5 Hz, 1H), 5.81 (br s, 2H), 4.18 (s, 1H);^{13}C NMR (75 MHz, DMSO) δ 156.4, 151.4, 143.9, 143.0, 140.4, 129.3, 128.1, 127.1, 126.7, 124.9, 122.8, 122.2, 116.2, 104.0, 84.1, 81.0; MS (ESI^{+}) *m/z* 295.0745 was calculated for $C_{16}H_{11}ClN_4$ $[M+H]^{+}$ and 295.0747 (-0.20 ppm) was determined experimentally; LC chemical purity was 93.3%.

*N⁴-(3-Bromophenyl)-7-chloroquinazoline-4,6-diamine (**47**)*

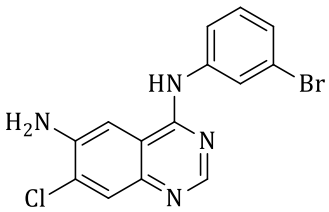

Compound ***47*** was obtained in 63% (116 mg) yield. ^{1}H NMR (300 MHz, DMSO) δ 9.66 (s, 1H), 8.42 (s, 1H), 8.20 (s, 1H), 7.86 (d, *J* = 8.0 Hz, 1H), 7.76 (s, 1H), 7.61 (s, 1H), 7.33 (dd [appeared as a t], $J_1 = J_2$ = 8.1 Hz, 1H), 7.28–7.23 (m, 1H), 5.83 (s, 2H); ^{13}C NMR (75 MHz, DMSO) δ 156.3, 151.2, 144.0, 142.8, 141.9, 130.8, 128.0, 127.2, 126.0, 124.2, 121.6, 120.8, 116.2, 103.9; MS (ESI^{+}) *m/z* 348.9850 was calculated for $C_{14}H_{10}BrClN_4$ $[M+H]^{+}$ and 348.9849 (0.1.0 ppm), and $[^{82}Br]C_{14}H_{10}BrClN_4$ 350.9830 were determined experimentally; LC chemical purity was 92.4%.

*7-Chloro-N⁴-(3-chloro-4-fluorophenyl)quinazoline-4,6-diamine (**48**)*

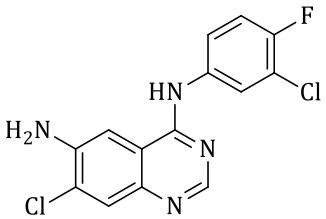

Compound ***48*** was obtained in 80% (138 mg) yield. ^{1}H NMR (300 MHz, DMSO) δ 9.68 (s, 1H), 8.39 (s, 1H), 8.17 (dd, *J* = 6.9, 2.6 Hz, 1H), 7.83–7.77 (m, 1H), 7.76 (s, 1H), 7.58 (s, 1H), 7.42 (dd [appeared as a t], $^{3}J_{H\text{-}F} = {}^{3}J_{H\text{-}H}$ = 9.0 Hz, 1H), 5.83 (s, 2H); ^{13}C NMR (75 MHz, DMSO) δ 156.3, 151.9 (d, $^{1}J_{C\text{-}F}$ = 247.5 Hz), 144.0, 142.9, 137.4, 134.0, 128.1, 127.2, 123.6, 122.5, 119.3 (d, $^{2}J_{C\text{-}F}$ = 19.1 Hz), 116.8 (d, $^{2}J_{C\text{-}F}$ = 21.8 Hz), 116.1, 103.8; MS (ESI^{+}) *m/z* 323.0261 was calculated for $C_{14}H_9Cl_2FN_4$ $[M+H]^{+}$ and 323.0258 (0.30 ppm) was determined experimentally.

*N^4-(3-Ethynylphenyl)-7-methoxyquinazoline-4,6-diamine (**49**)*

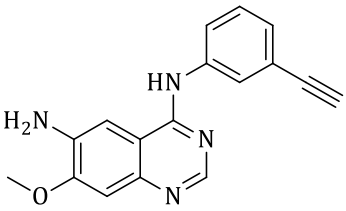

Compound ***49*** was obtained in 66% yield (90.7 mg). ^{1}H NMR (300 MHz, DMSO) δ 9.36 (s, 1H), 8.40 (s, 1H), 8.25–8.20 (m, 1H), 7.88–7.82 (m, 1H), 7.41 (s, 1H), 7.30 (dd [appeared as a t], $J_1 = J_2 = 8.0$ Hz, 1H), 7.23–7.17 (m, 1H), 7.11 (s, 1H), 5.37 (s, 1H), 4.21 (s, 1H), 3.97 (s, 3H); ^{13}C NMR (151 MHz, DMSO) δ 156.4, 154.3, 152.4, 147.1, 146.7, 140.6, 129.2, 126.4, 124.6, 122.5, 122.1, 110.1, 107.6, 105.8, 84.1, 80.8, 56.3; MS (ESI$^+$) *m/z* 291.1240 was calculated for $C_{15}H_{13}BrN_4O$ $[M+H]^+$ and 291.1241 (0.10 ppm) was determined experimentally.

*N^4-(3-Bromophenyl)-7-methoxyquinazoline-4,6-diamine (**50**)*

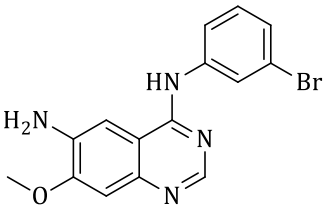

Compound ***50*** was obtained in 74% (68.1 mg) yield; ^{1}H NMR (300 MHz, DMSO) δ 9.36 (s, 1H), 8.40 (s, 1H), 8.23–8.20 (m, 1H), 7.89–7.83 (m, 1H), 7.41 (s, 1H), 7.33–7.27 (m, 1H), 7.22–7.18 (m, 1H), 7.11 (s, 1H), 5.37 (br s, 2H), 3.97 (s, 3H); ^{13}C NMR (75 MHz, DMSO) δ 155.4, 153.2, 150.7, 145.4, 142.5, 139.0, 130.7, 125.2, 123.6, 121.6, 120.2, 111.0, 106.3, 101.3, 56.3; MS (ESI$^+$) *m/z* 345.0340 was calculated for $C_{15}H_{13}BrN_4O$ $[M+H]^+$ and 345.0351 (-3.2 ppm) was determined experimentally; LC chemical purity was 97.9%.

*N^4-(3-Chloro-4-fluorophenyl)-7-methoxyquinazoline-4,6-diamine (**51**)*

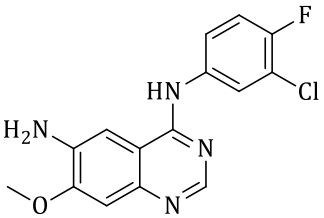

Compound ***51*** was obtained in 76% yield (69.4 mg). ^{1}H NMR (300 MHz, DMSO) δ 9.39 (s, 1H), 8.38 (s, 1H), 8.19 (dd, $^4J_{H\text{-}F}$ = 6.9 Hz, $^4J_{H\text{-}H}$ = 2.6 Hz, 1H), 7.81 (ddd, $^3J_{H\text{-}H}$ = 9.1 Hz, $^4J_{H\text{-}F}$ = 4.3 Hz, $^4J_{H\text{-}H}$ =2.7 Hz, 1H), 7.43–7.35 (m, 2H), 7.10 (s, 1H), 5.38 (br s, 2H), 3.97 (s, 3H); ^{13}C NMR (75 MHz, DMSO) δ 155.5, 153.2, 151.5 (d, $^1J_{C\text{-}F}$ = 255.6 Hz), 150.7, 145.3, 139.0, 138.0, 122.9, 121.8, 118.9 (d, $^2J_{C\text{-}F}$ = 20.3 Hz), 117.0 (d, $^2J_{C\text{-}F}$ = 18.8 Hz), 110.9, 106.4, 101.3, 56.3. The ^{1}H NMR data was in agreement with literature values.[17]

Chapter 6 Experimental methods and .characterisation data

*General amidation and insertion of the C-6 acrylamide linker fragment (**52–58**)*

The appendage of C-6 acrylamide functionality to 4-anilinoquinazoline compounds is described: Under inert conditions, a suitable C-6 amino-substituted 4-anilinoquinazoline compound (50–100 mg scale) was added into DMF (1.5–2.5 mL) solvent and to this was added Hünig's base (3 molar equivalents). The solution was cooled into the ice bath and acryloyl chloride (1.2 molar equivalents) was introduced in a drop wise via syringe. The reaction was then allowed to slowly warm to a room temperature as the ice melted. After 2 h, the reaction was loaded onto the column for chromatographic purification. The following products were obtained as yellow solids;

*N-[4-(3-Ethynylanilino)quinazolin-6-yl]prop-2-enamide (**52**)*

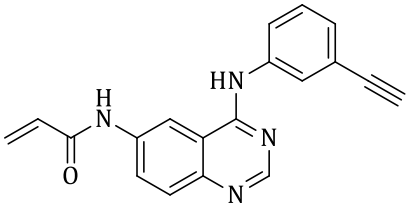

Compound ***52*** was obtained in 58% (35 mg). The melting point was 204–206 °C;^{1}H NMR (300 MHz, DMSO) δ 10.50 (s, 1H), 9.89 (s, 1H), 8.82 (d, *J* = 2.0 Hz, 1H), 8.57 (s, 1H), 8.04–8.00 (m, 1H), 7.93–7.85 (m, 2H), 7.80 (d, *J* = 8.9 Hz, 1H), 7.39 (dd [appeared as a t], $J_1 = J_2$ = 7.1 Hz, 1H), 7.23–7.18 (m, 1H), 6.54 (dd, *J* = 17.0, 10.0 Hz, 1H), 6.35 (dd, *J* = 17.0, 2.1 Hz, 1H), 5.84 (dd, *J* = 10.0, 2.1 Hz, 1H), 4.19 (s, 1H); ^{13}C NMR (75 MHz, DMSO) δ 163.8, 157.9, 153.7, 147.2, 140.2, 137.0, 132.0, 129.3, 128.9, 127.9, 127.7, 127.1, 125.5, 123.3, 122.2, 115.9, 112.8, 84.0, 81.0; MS (ESI^{+}) *m/z* 315.1240 was calculated for $C_{19}H_{14}N_4O$ $[M+H]^{+}$ and 315.1241 (0.10 ppm) was determined experimentally; LC chemical purity was 96.9%.

*N-[4-(3-Bromoanilino)quinazolin-6-yl]prop-2-enamide (**53**)*

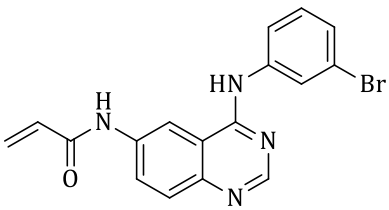

Compound ***53*** was afforded in 63% yield (74 mg). The melting point was 250–252 °C; ^{1}H NMR (400 MHz, DMSO) δ 10.49 (s, 1H), 9.91 (s, 1H), 8.80 (d, *J* = 2.0 Hz, 1H), 8.57 (s, 1H), 8.16 (d, *J* = 1.8 Hz, 1H), 7.89 (dd, *J* = 9.0, 2.1 Hz, 1H), 7.85 (d, *J* = 8.2 Hz, 1H), 7.79 (d, *J* = 8.9 Hz, 1H), 7.33 (dd [appeared as a t], $J_1 = J_2$ = 8.0 Hz, 1H), 7.30–7.24 (m, 1H), 6.51 (dd, *J* = 17.0, 10.1 Hz, 1H), 6.33 (dd, *J* = 17.0, 1.9 Hz, 1H), 5.82 (dd, *J* = 10.1, 1.9 Hz, 1H); ^{13}C NMR (101 MHz, DMSO) δ 164.0, 158.0, 153.8, 147.5, 141.9, 146

137.3, 135.0, 132.2, 131.0, 129.2, 128.2, 127.9, 126.5, 124.9, 121.8, 121.5, 116.1; MS (ESI$^+$) *m/z* 369.03454 was calculated for $C_{17}H_{13}BrN_4O$ $[M+H]^+$ and 369.0352 (0.2 ppm) and 371.0334 for [^{82}Br] were determined experimentally; LC chemical purity was 98.8%.

*N-[4-(3-Chloro-4-fluoroanilino)quinazolin-6-yl]prop-2-enamide [**54 (i)**]*

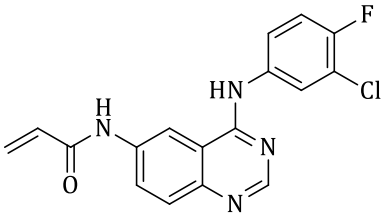

Compound ***54 (i)*** was obtained in 74% (88 mg) yield. The melting point was 230–232 °C [lit.[43] 258–261 °C]; ^{1}H NMR (300 MHz, DMSO) δ 10.52 (s, 1H), 9.95 (s, 1H), 8.81 (d, J = 1.9 Hz, 1H), 8.57 (s, 1H), 8.14 (dd, *J* = 6.9, 2.5 Hz, 1H), 7.89 (dd, $^4J_{H\text{-}F}$ = 9.0, $^4J_{H\text{-}H}$ = 2.1 Hz, 1H), 7.83–7.76 (m, 2H), 7.42 (dd [appeared as a t], $^3J_{H\text{-}F}$ = $^3J_{H\text{-}H}$ = 9.0 Hz, 1H), 6.53 (dd, *J* = 17.0, 10.0 Hz, 1H), 6.35 (dd, *J* = 17.0, 2.0 Hz, 1H), 5.85 (dd, *J* = 10.0, 2.0 Hz, 1H); ^{13}C NMR (75 MHz, DMSO) δ 163.8, 157.8, 155.5 (d, $J_{C\text{-}F}$ = 242.0 Hz), 152.2, 147.1, 137.1, 132.0, 129.0, 128.0, 127.67, 124.2, 123.1, 123.0, 119.3 (d, $^2J_{C\text{-}F}$ = 18.5 Hz), 117.1 (d, $^2J_{C\text{-}F}$ = 21.7 Hz), 115.8, 112.6; MS (ESI$^+$) *m/z* 343.0756 was calculated for $C_{17}H_{12}ClFN_4O$ $[M+H]^+$ and 343.0746 (2 ppm) was experimentally determined; LC chemical purity was 97.4%.

*N-[6-(Acryloylamino)quinazolin-4-yl]-N-(3-chloro-4-fluorophenyl)prop-2-enamide [**54 (ii)**]*

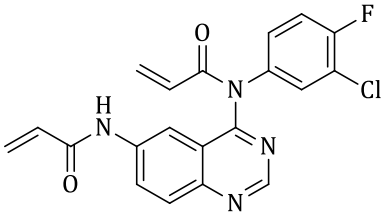

The by-product ***54 (ii)*** was isolated from the reaction above in sacrificial quantities (7 mg) due to a quick addition of acryloyl chloride. The melting point was 110–112 °C; ^{1}H NMR (300 MHz, DMSO) δ 10.69 (s, 1H), 9.15 (s, 1H), 8.56 (d, *J* = 0.5 Hz, 1H), 8.19 (dd, *J* = 9.2, 2.3 Hz, 1H), 8.10 (d, *J*= 8.8 Hz, 1H), 7.67 (dd, $^3J_{H\text{-}F}$ = 6.6, $^4J_{H\text{-}H}$ = 2.6 Hz, 1H), 7.50 (dd [appeared as a t], $^3J_{H\text{-}F}$ = $^3J_{H\text{-}H}$ = 9.0 Hz, 1H), 7.35 (ddd, $^3J_{H\text{-}H}$ = 8.9, $^4J_{H\text{-}F}$ = 4.3, $^4J_{H\text{-}H}$ = 2.6 Hz, 1H), 6.47 (dd, *J* = 17.0, 9.9 Hz, 1H), 6.42–6.49 (m, 2H), 6.23 (dd, *J* = 16.7, 10.0 Hz, 1H), 5.85 (overlapping dd, *J* = 10.0, 2.1 Hz, 1H), 5.83 (overlapping dd, *J* = 10.0, 2.1 Hz, 1H) ; ^{13}C NMR (75 MHz, DMSO) δ 166.0, 164.3 (2C), 160.8, 158.5 (d, $^1J_{C\text{-}F}$ = 241.7 Hz), 153.7, 149.5, 139.5, 137.6, 131.8, 131.0, 130.18, 129.8, 129.3, 129.0, 128.6, 122.1, 120.8 (d, $^2J_{C\text{-}F}$ = 20.3 Hz), 118.3 (d, $^2J_{C\text{-}F}$ = 19.9 Hz), 111.7. MS (ESI$^+$)

m/z 397.0862 was calculated for $C_{20}H_{14}ClFN_4O_2$ $[M+H]^+$ and 397.0858 (4 ppm) was experimentally determined.

*N-[4-(3-Ethynylanilino)-7-methoxyquinazolin-6-yl]prop-2-enamide (**55**)*

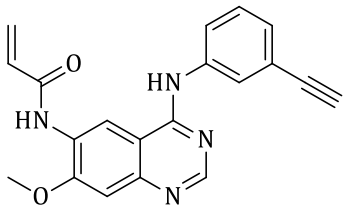

Compound was obtained in 71% yield (41.9 mg). The melting point was 178–180 °C; ^{1}H NMR (300 MHz, DMSO) δ 9.77 (s, 1H), 9.63 (s, 1H), 8.94 (s, 1H), 8.49 (s, 1H), 7.68 (d, *J* = 8.2 Hz, 1H), 7.60 (s, 1H), 7.32–7.22 (m, 2H), 6.95 (d, *J* = 7.6 Hz, 1H), 6.75 (dd, *J* = 17.0, 10.2 Hz, 1H), 6.32 (dd, *J* = 17.0, 2.0 Hz, 1H), 5.81 (dd, *J* = 10.2, 1.9 Hz, 1H), 4.19 (s, 1H) 4.02 (s, 3H); ^{13}C NMR (75 MHz, DMSO) δ 164.0, 157.6, 155.8, 154.7, 149.5, 144.3, 139.9, 132.2, 128.7, 127.6, 127.1, 123.3, 122.1, 120.3, 117.2, 109.5, 107.1, 83.7, 81.3, 56.7. The ^{1}H NMR was in agreement with the the literature.[44]

*N-[4-(3-Bromoanilino)-7-methoxyquinazolin-6-yl]prop-2-enamide (**56**)*

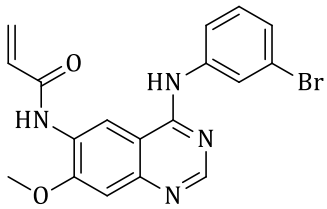

Compound ***56*** was obtained in 67% yield (38.7 mg). The melting point was 222–224 °C; ^{1}H NMR (300 MHz, DMSO) δ 9.79 (s, 2H), 8.96 (s, 1H), 8.56 (s, 1H), 8.18–8.15 (m, 1H), 7.89–7.84 (m, 1H), 7.38–7.22 (m, 3H), 6.76 (dd, *J* = 17.0, 10.2 Hz, 1H), 6.32 (dd, *J* = 17.0, 2.0 Hz, 1H), 5.81 (dd, *J* = 10.2, 2.0 Hz, 1H), 4.03 (s, 3H); ^{13}C NMR (75 MHz, DMSO) δ 164.0, 157.6, 155.8, 154.7, 149.5, 144.3, 139.9, 132.2, 128.7, 127.6, 127.1, 123.3, 122.1, 120.3, 117.1, 109.5, 107.1, 56.7.

*N-[4-(3-Chloro-4-fluoroanilino)-7-methoxyquinazolin-6-yl]prop-2-enamide (**57**)*

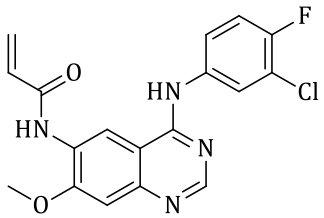

Compound ***57*** was obtained in 80% yield (46.8 mg). The melting point was 218–220 °C; ^{1}H NMR (300 MHz, DMSO) δ 9.82 (overlapping s, 1H), 9.79 (overlapping s, 1H), 8.94 (s, 1H), 8.54 (s, 1H), 8.13 (dd, *J* = 6.9, 2.5 Hz, 1H), 7.85–7.76 (m, 1H), 7.41 (dd, *J* = 16.8, 7.7 Hz, 1H), 7.30 (s, 1H), 6.76 (dd, *J* = 17.0, 10.2 Hz, 1H), 6.32 (dd, *J* = 17.0, 1.9 Hz, 1H), 5.81 (dd, *J* = 10.2, 1.9 Hz, 1H), 4.03 (s, 3H); ^{13}C

NMR (75 MHz, DMSO) δ 164.0, 157.3, 155.8, 154.4, 152.0 (d, $^{1}J_{C\text{-}F}$ = 222.4 Hz), 149.4, 137.2, 132.1, 127.8, 127.5, 124.0, 122.9, 119.2 (d, $^{2}J_{C\text{-}F}$ = 18.1 Hz) 117.0, 116.7 (d, $^{2}J_{C\text{-}F}$ = 20.0 Hz), 109.3, 107.2, 56.7; MS (ESI^{+}) *m/z* 373.0862 was calculated for $C_{18}H_{14}ClFN_4O_2$ $[M+H]^{+}$ and 373.0860 (0.2 ppm) was found experimentally.

*N-[7-Chloro-4-(3-ethynylanilino)quinazolin-6-yl]prop-2-enamide (**58**)*

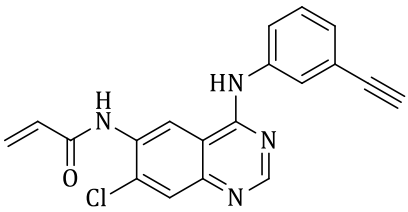

Compound ***58*** was obtained in 33% yield (38.8 mg). ^{1}H NMR (300 MHz, DMSO) δ 10.15 (s, 1H), 9.99 (s, 1H), 8.84 (s, 1H), 8.63 (s, 1H), 8.05–8.02 (m, 1H), 7.99 (s, 1H), 7.92–7.87 (m, 1H), 7.42 (dd [appeared as a t], J_1 = J_2 = 7.9 Hz, 1H), 7.27–7.22 (m, 1H), 6.66 (dd, *J* = 17.0, 10.2 Hz, 1H), 6.36 (dd, *J* = 17.1, 1.9 Hz, 1H), 5.87 (dd, *J* = 10.2, 1.9 Hz, 1H), 4.21 (s, 1H); ^{13}C NMR (75 MHz, DMSO) δ 164.3, 157.7, 155.6, 148.6, 139.7, 134.8, 132.9, 131.4, 129.4, 128.4, 128.3, 127.5, 125.6, 123.4, 122.2, 121.8, 114.5, 83.9, 81.1.

*Synthesis of acetoxy(4-anilino)quinazoline derivatives (**59**–**61**)*

Synthesis of compounds ***59***–***61*** was carried out according to the general procedure that has been described for the synthesis of compounds ***30***–***32***. The appropriate acetoxyquinazoline derivatives at 150–500 mg scale were used to obtain the following compounds;

*4-(3-Ethynylanilino)quinazolin-6-yl acetate (**59**)*

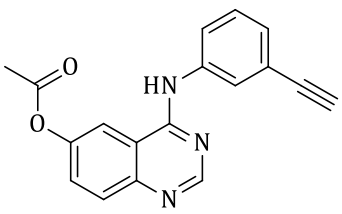

Compound ***59*** was obtained in 56% yield (437 mg). The melting point was 210–212 °C; ^{1}H NMR (300 MHz, DMSO) δ 9.93 (s, 1H), 8.65 (s, 1H), 8.46 (d, *J* = 2.3 Hz, 1H), 8.11 (s, 1H), 7.97–7.92 (m, 1H), 7.85 (d, *J* = 9.0 Hz, 1H), 7.69 (dd, *J* = 9.0, 2.4 Hz, 1H), 7.41 (dd [appeared as a t], J_1 = J_1 = 7.6 Hz, 1H), 7.23 (dd, *J* = 7.6, 1.1 Hz, 1H), 4.21 (s, 1H), 2.37 (s, 3H); ^{13}C NMR (75 MHz, DMSO) δ 169.8, 157.9, 154.7, 148.5, 148.2, 139.9, 129.8, 129.4, 129.0, 127.3, 125.3, 123.1, 122.2, 115.8, 115.4, 84.0, 81.1, 21.2.

*4-(3-Chloro-4-fluoroanilino)quinazolin-6-yl acetate (**60**)*

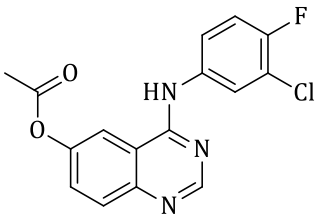

Compound ***60*** was obtained in 64% yield (515 mg). The melting point was 235–237 °C; ^{1}H NMR (300 MHz, DMSO) δ 11.92 (s, 1H), 8.99–8.96 (m, 1H), 8.88 (s, 1H), 8.18–8.03 (m, 2H), 8.00–7.92 (m, 1H), 7.83–7.73 (m, 1H), 7.62–7.50 (m, 1H), 2.39 (s, 3H); ^{13}C NMR (75 MHz, DMSO) δ 169.6, 160.1, 154.1 (d, $^{1}J_{C\text{-}F}$ = 249.2 Hz), 151.4, 150.0, 137.5, 134.4, 131.9, 127.0, 125.8, 125.7, 122.2, 119.6 (d, $^{2}J_{C\text{-}F}$ = 18.2 Hz), 117.6 (d, $^{2}J_{C\text{-}F}$ = 22.5 Hz), 114.9, 21.2.

*4-(3-Ethynylanilino)-7-methoxyquinazolin-6-yl acetate (**61**)*

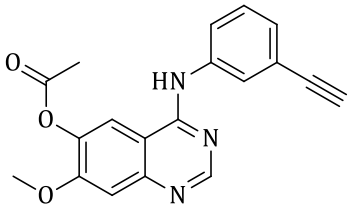

Compound ***61*** was obtained in 54% yield (115 mg). The melting point was 238–340 °C ; ^{1}H NMR (300 MHz, DMSO) δ 11.61 (s, 1H), 8.93 (s, 1H), 8.89 (s, 1H), 7.91 (s, 1H), 7.79 (d, *J* = 8.1 Hz, 1H) 7.59 (s, 1H), 7.54–7.44 (m, 1H), 7.44–7.37 (m, 1H), 4.29 (s, 1H), 4.00 (s, 3H), 2.38 (s, 3H); ^{13}C NMR (75 MHz, DMSO) δ 168.9, 159.3, 157.9, 151.4, 140.7, 140.0, 137.7, 129.9, 129.6, 127.8, 125.5, 122.5, 119.2, 107.7, 101.7, 83.4, 81.8, 57.4, 20.7.

*Hydrolysis of the C-6 acetoxy (4-anilino)quinazoline compounds (**62**–**65**)*

The common hydrolysis procedure for the acetoxy(4-anilino)quinazolines was carried out in alcohol solutions (IPA or EtOH) under basic reaction conditions. The acetoxy protected compounds (100–300 mg scale) in ethanol (5 mL) were treated with ammonium hydroxide (25% NH_4OH, 1.5 mL) solution and the reaction was kept at 40 °C with stirring for 2 h. At the end, excess solvent was removed *in vacuo* and the crude products were diluted with ice-cold water (10 mL), neutralised with 2 N HCl aqueous solutions and extracted into ethyl acetate (3 × 20 mL). The organic extracts were then dried over $MgSO_4$ and purified by chromatographic methods in order to afford the following C-6 hydroxy-substituted 4-anilinoquinazoline compounds;

*4-(3- Ethynylanilino)quinazolin-6-ol (**62**)*

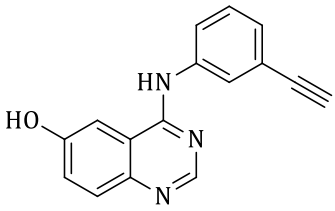

Compound ***62*** was obtained in 57% yield (130 mg). The melting point was 228–230 °C;^{1}H NMR (300 MHz, DMSO) δ 10.11 (s, 1H), 9.55 (s, 1H), 8.49 (s, 1H), 8.10 (br s, 1H), 7.96–7.91 (m, 1H), 7.79 (d, *J* = 2.5 Hz, 1H), 7.69 (d, *J* = 9.0 Hz, 1H), 7.43 (dd, *J* = 9.0, 2.5 Hz, 1H), 7.37 (overlapping dd [appeared as a t], $J_1 = J_2$ = 8.1 Hz, 1H), 7.20 (d, *J* = 7.6 Hz, 1H), 4.19 (s, 1H); ^{13}C NMR (75 MHz, DMSO) δ 157.1, 156.1, 151.8, 144.5, 140.4, 129.8, 129.3, 126.8, 125.0, 124.7, 122.8, 122.2, 116.8, 105.5, 84.1, 80.9; MS (ESI^{+}) *m/z* 262.0975 was calculated $C_{16}H_{11}N_3O$ $[M+H]^{+}$and 262.0975 was determined experimentally.

*4-(3-Bromoanilino)quinazolin-6-ol (**63**)*

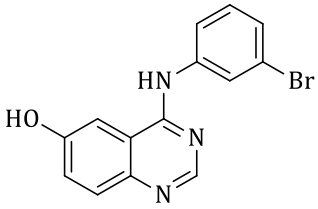

Compound ***63*** was obtained in 85% yield (141 mg). The compound underwent decomposition ^{1}H NMR (300 MHz, DMSO) δ 10.13 (s, 1H), 9.59 (s, 1H), 8.51 (s, 1H), 8.28–8.24 (m, 1H), 7.96–7.89 (m, 1H), 7.80 (d, *J* = 2.5 Hz, 1H), 7.70 (d, *J* = 9.0 Hz, 1H), 7.45 (dd, *J* = 9.0, 2.5 Hz, 1H), 7.34 (dd [appeared as a t], $J_1 = J_2$ = 8.0 Hz, 1H), 7.29–7.21 (m, 1H); ^{13}C NMR (75 MHz, DMSO) δ 156.9, 156.2, 151.7, 144.6, 141.9, 130.8, 129.9, 126.0, 124.8, 124.2, 121.6, 120.8, 116.8, 105.4; MS (ESI^{+}) *m/z* 316.0080 was calculated for $C_{14}H_{10}BrN_3O$ $[M+H]^{+}$and 316.0076 (0.4 ppm) and 318.0056 [^{82}Br] were determined experimentally.

*4-(3-Chloro-4-fluoroanilino)quinazolin-6-ol (**64**)*

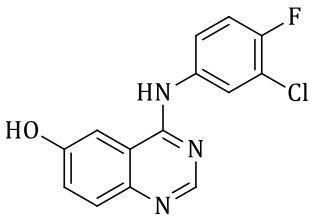

Compound ***64*** was obtained in 64% yield (179 mg). Decomposition occurred during melting point determination; ^{1}H NMR (300 MHz, DMSO) δ 10.13 (s, 1H), 9.62 (s, 1H), 8.49 (s, 1H), 8.24 (dd, *J* = 6.9, 2.5 Hz, 1H), 7.90–7.82 (m, 1H), 7.77 (d, *J* = 2.3 Hz, 1H), 7.70 (d, *J* = 8.9 Hz, 1H), 7.49–7.38 (m, 2H); ^{13}C NMR (75 MHz, DMSO) δ 156.9, 156.18, 151.7 (d, $J_{C\text{-}F}$ = 254.3 Hz), 144.5, 137.4, 137.4, 129.9, 124.8, 123.5, 122.5, 119.2 (d,

$^{2}J_{C\text{-}F}$ = 18.4 Hz), 117.1, 116.7 (d, $J_{C\text{-}F}$ = 21.6 Hz), 105.4; MS (ESI^{+}) *m/z* 290.0491 was calculated for $C_{14}H_9ClFN_3O$ $[M+H]^{+}$ and 290.0491 was determined experimentally.

*4-(3-Ethynylanilino)-7-methoxyquinazolin-6-ol (**65**)*

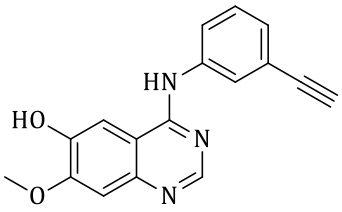

Compound ***65*** was obtained in 71% yield (58 mg). The melting point was 240–242 °C; ^{1}H NMR (300 MHz, DMSO) δ 9.67 (s, 1H), 9.41 (s, 1H), 8.48 (s, 1H), 8.09 (s, 1H), 7.95–7.88 (m, 1H), 7.81 (s, 1H), 7.37 (dd[appeared as a t], $J_1 = J_2$ = 8.1Hz, 1H), 7.21 (s, 1H), 7.17 (d, *J* = 7.6 Hz, 1H), 4.17 (s, 1H), 3.98 (s, 3H); ^{13}C NMR (75 MHz, DMSO) δ 156.5, 154.3, 152.5, 147.2, 146.7, 140.6, 129.3, 126.4, 124.7, 122.5, 122.1, 110.1, 107.6, 105.9, 84.1, 80.8, 56.4; MS (ESI^{+}) *m/z* 292.1080 was calculated for $C_{17}H_{13}N_3O_2$ $[M+H]^{+}$ and 292.1082 (-0.20 ppm) was determined experimentally; LC chemical purity was 97.3%.

*General esterification and insertion of the C-6 acrylate linker (**66**–**69**)*

The acrylate derivatives of 4-anilinoquinazoline compounds were prepared using a procedure similar to synthesis of compounds ***52***–***58*****.** The following compounds were obtained following chromatographic purifications;

*4-(3-Ethynylanilino)quinazolin-6-yl prop-2-enoate (**66**)*

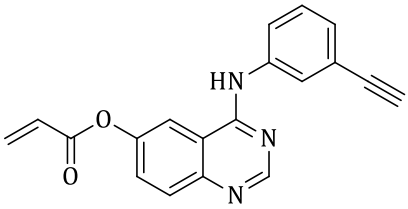

Compound ***66*** was obtained in 81% yield (97.8 mg); The melting point was 174–176 °C; ^{1}H NMR (300 MHz, DMSO) δ 9.79(s, 1H), 8.67 (s, 1H), 8.43 (d, *J* = 2.4 Hz, 1H), 8.09 (m, 1H), 7.96–7.91 (m, 1H), 7.88 (d, *J* = 9.0 Hz, 1H), 7.75 (dd, *J* = 9.0, 2.4 Hz, 1H), 7.42 (dd [appeared as a t], $J_1 = J_2$ = 7.9 Hz, 1H), 7.26–7.21 (m, 1H), 6.64 (dd, *J* = 17.4,1.6 Hz, 1H), 6.58–6.47 (m, 1H), 6.25 (dd, *J* = 10.0, 1.6 Hz, 1H), 4.20 (s, 1H); ^{13}C NMR (75 MHz, DMSO) δ 164.8, 157.9, 154.8, 148.3, 148.2, 139.8, 134.8, 130.0, 129.4, 128.8, 127.8, 127.3, 125.2, 123.0, 122.3, 115.8, 115.3, 83.9, 81.1; MS (ESI^{+}) *m/z*

316.1080 was calculated for $C_{19}H_{13}N_3O_2$ $[M+H]^+$ and 316.1073 (-0.70 ppm) was determined experimentally.

*4-(3-Bromoanilino)quinazolin-6-yl prop-2-enoate (**67**)*

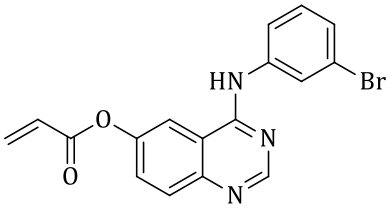

Compound ***67*** was obtained in 79% yield (92.4 mg). The melting point was 184–186 °C ^{1}H NMR (300 MHz, DMSO) δ 9.81 (s, 1H), 8.70 (s, 1H), 8.43 (d, *J* = 2.4 Hz, 1H), 8.26–8.23 (m, *J* = 1.8 Hz, 1H), 7.95–7.86 (m, 2H), 7.76 (dd, *J* = 9.0, 2.3 Hz, 1H), 7.76 (dd [appeared as a t], $J_1 = J_2$ = 7.9 Hz, 1H), 7.33–7.28 (m, 1H), 6.65 (dd, *J* = 17.2, 1.4 Hz, 1H), 6.52 (dd, *J* = 17.3, 10.0 Hz, 1H), 6.25 (dd, *J* = 10.1, 1.4 Hz, 1H); ^{13}C NMR (75 MHz, DMSO) δ 164.7, 157.8, 154.7, 148.3, 148.3, 141.3, 134.9, 130.9, 130.0, 128.9, 127.8, 126.6, 124.5, 121.7, 121.0, 115.8, 115.3; MS (ESI$^+$) *m/z* 370.0186 was calculated for $C_{17}H_{12}BrN_3O_2$ $[M+H]^+$ and 370.0186 and 372.0165 [^{82}Br] were determined experimentally.

*4-(3-Chloro-4-fluoroanilino)quinazolin-6-yl prop-2-enoate (**68**)*

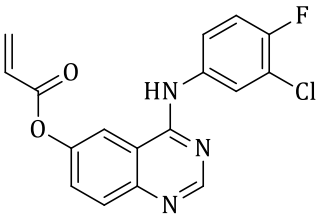

Compound ***68*** was obtained in 72% yield (85.3 mg). The melting point was 158–160 °C; ^{1}H NMR (300 MHz, DMSO) δ 9.84 (s, 1H), 8.67 (s, 1H), 8.39 (d, *J* = 2.4 Hz, 1H), 8.22 (dd, *J* = 6.9, 2.6 Hz, 1H), 7.97–7.88 (d, *J* = 6.9 Hz, 1H), 7.87–7.80 (m, 1H), 7.75 (dd, *J* = 9.0, 2.4 Hz, 1H), 7.45(dd [appeared as a t], $^3J_{C\text{-}F} = {}^3J_{H\text{-}H}$ = 9.0 Hz, 1H), 6.65 (dd, *J* = 17.2, 1.6 Hz, 1H), 6.52 (dd, *J* = 17.2, 10.0 Hz, 1H), 6.25 (dd, *J* = 10.0, 1.6 Hz, 1H);^{13}C NMR (75 MHz, DMSO) δ 164.7, 162.6, 157.7, 154.7, 152.2 (d, $^1J_{C\text{-}F}$ = 242.3 Hz), 148.3, 136.8, 134.9, 130.0, 128.9, 127.8, 123.9, 122.8, 119.2 (d, $^2J_{C\text{-}F}$ = 20.6 Hz), 117.2 (d, $^2J_{C\text{-}F}$ = 21.0 Hz), 115.7, 115.2; MS (ESI$^+$) *m/z* 344.0597 was calculated for $C_{17}H_{11}ClFN_3O_2$ $[M+H]^+$ and 344.0595 (0.20 ppm) was determined experimentally; LC chemical purity was 98.0%.

*4-(3-Ethynylanilino)-7-methoxyquinazolin-6-yl prop-2-enoate (**69**)*

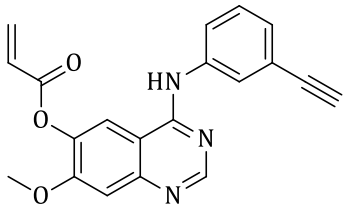

Compound ***69*** was isolated in 84% yield (49.5 mg). The melting point was 158–160 °C; ^{1}H NMR (300 MHz, DMSO) δ 9.62 (s, 1H), 8.63 (s, 1H), 8.41 (s, 1H), 8.08 (s, 1H), 7.91 (d, *J* = 7.5 Hz, 1H), 7.46–7.35 (m, 2H), 7.21 (d, *J* = 7.6 Hz, 1H), 6.67–6.52 (m, 2H), 6.25 (d, *J* = 10.0 Hz, 1H), 4.20 (s, 1H), 3.95 (s, 3H); ^{13}C NMR (75 MHz, DMSO) δ 164.1, 157.4, 155.9, 155.3, 150.7, 140.0, 139.3, 135.1, 129.4, 127.3, 127.0, 124.9, 122.7, 122.2, 116.7, 109.2, 108.9, 84.0, 81.0, 56.9; MS (ESI^{+}) *m/z* 346.1186 was calculated for $C_{20}H_{15}N_3O_3$ $[M+H]^{+}$ and 346.1181 (0.50 ppm) was determined experimentally. LC chemical purity was 94.5%.

*6.3 Preparation of a RAFT agent (**70–74**)*

The RAFT agent used in this study has already been prepared used in our research group and the necessary steps required for synthesis were as described next.[45]

*But-3-yn-2-yl 4-methylbenzene-1-sulfonate (**70**)*

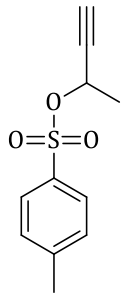

Preparation of compound ***70*** was carried out according to a modified literature procedure.[46] A suspension of KOH (3.20 g, 84.2 mmol) and tosyl chloride (5.25 g, 27.6 mmol) in THF (60 mL) solvent was placed in ice-bath, under inert atmosphere. But-3-yn-2-ol (1.61 g, 22.9 mmol) was added in one portion via syringe to the suspension with stirring. The reaction mixture was then allowed to slowly warm to a room temperature as the ice-melted and it was stopped after 2 h. The resultant white precipitate and excess KOH were filtered off and the solvent was removed from the rotary evaporator. The concentrate was diluted with Diethyl ether (Et_2O, 30 mL), and washed with ice-cold water (3 × 25 mL), dried over $MgSO_4$, filtered and the product was recovered as a colourless oil. The recovered product was purified further by means of a column chromatography using 30% EtOAc/Hex eluent to obtain ***70*** in 84% yield (5.16 g). ^{1}H NMR (300 MHz, $CDCl_3$) δ 7.86–7.80 (m, 2H), 7.38–7.32 (m, 2H), 5.18 (qd, *J* = 6.7, 2.2 Hz, 1H), 2.46 (s, 3H), 2.43 (d, *J* = 2.2 Hz, 1H), 1.59 (d, *J* =

6.7Hz, 3H); ^{13}C NMR (75 MHz, $CDCl_3$) δ 144.9, 133.8, 129.7 (2C), 128.0 (2C), 79.9, 75.5, 67.4, 22.6, 21.7. The ^{1}H NMR data was in agreement with that reported in the literature.[46]

*S-But-3-yn-2-yl O-ethyl carbonodithioate (**71**)*

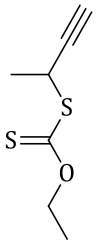

A preparation procedure for compound ***71*** was carried out according to a literature procedure.[47] Tosyl butynyl (2.50 g, 11.1 mmol) and potassium *O*-ethyl carbonodithioate (4.10 g, 25.1 mmol) were dissolved in THF (60 mL) and the reaction was stirred at room temperature for 12 h covered with aluminium foil. The resulting precipitate was filtered off, the filtrate was concentrated and diluted with ice-cold water (60 mL). The product was then extracted into DCM (3 × 60 mL), dried over $MgSO_4$, and filtered. The organic solvent was evaporated *in vacuo* and the crude product was purified by column chromatography to obtain a pale yellow oil in 88% (1.71 g).[47] ^{1}H NMR (300 MHz, $CDCl_3$) δ 4.68 (dq, *J* = 6.9, 2.4 Hz, 2H), 4.48 (q, *J* = 7.2 Hz, 1H), 2.35 (d, *J* = 2.4 Hz, 1H), 1.63 (d, *J* = 6.9 Hz, 3H), 1.44 (m, t, *J* = 6.9 Hz 3H); ^{13}C NMR (75 MHz, $CDCl_3$) δ 212.1, 82.9, 71.5, 70.1, 35.0, 21.2, 13.8. The ^{1}H NMR data matched that reported in the literature.[47]

*1 H-Imidazole-1-sulfonyl azide hydrochloride (**72**)*

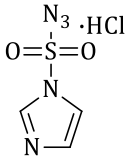

The azide transfer agent was a necessary precursor for the next azide compound that was synthesized immediately hereafter. Thus, preparation of this azide transferring agent was carried out in a step-by-step procedure as described by Goddard-Borger.[48] The resultant product was obtained as a white powder in 41% yield (8.59 g). ^{1}H NMR (300 MHz, D_2O) δ 9.21–9.19 (m, 1H), 7.91–7.87 (m, 1H), 7.49–7.46 (m, 1H). The ^{1}H NMR spectra resembled the one reported in the literature.[48]

*3-Azido-1,1-diethoxypropane (**73**)*

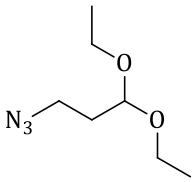

Preparation of the azido compound ***73*** was performed according to the literature procedure using 1*H*-imidazole-1-sulfonyl azide hydrogen chloride at 1.2 molar equivalents excess to the amine at 1.01 g scale (4.04 mmol).[48] Following a chromatographic purification of the product using hexane as an eluent, pale-yellow oil was obtained in 98% yield (565 mg). ^{1}H NMR (300 MHz, $CDCl_3$) δ 4.62 (br t, *J* = 5.6 Hz, 1H), 3.75–3.61 (m, 2H), 3.59–3.46 (m, 2H), 3.39 (br t, *J* = 6.8 Hz, 2H), 1.95–1.85 (m, 2H), 1.23 (t, *J* = 7.0 Hz, 6H); ^{13}C NMR (75 MHz, $CDCl_3$) δ 100.5, 61.9 (2C), 47.5, 33.2, 15.3 (2C). The ^{1}H NMR was in agreement with that reported in the literature.[48]

*S-{1-[1-(3,3-Diethoxypropyl)-1H-1,2,3-triazol-4-yl]ethyl} O-ethyl carbonodithioate (**74**)*

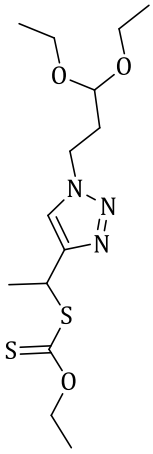

A triazole-based RAFT agent was synthesised according to a published procedure by the Klumperman's research group with minor modifications.[47] 3-Azido-1,1-diethoxypropane (2.00 g, 11.6 mmol) was added to $CuSO_4 \cdot 5H_2O$ (292 mg, 1.17 mmol), sodium ascorbate (620 mg, 3.13 mmol) in DMF (2 mL). The reaction mixture was placed in the ice-bath and *S*-but-3-yn-2-yl *O*-ethyl carbonodithioate (2.23 g, 12.8 mmol) was added in a drop-wise manner via a syringe. The reaction was allowed to warm to a room temperature and stirring was continued for 1.5 h. The ambient colour transition from the hydrated copper blue to the yellow and finally the permanent light brown colour were observed as the reaction progressed. The reaction mixture was filtered and purified over a silica gel column to afford colourless oil in 91% yield (3.85 g). ^{1}H NMR (300 MHz, $CDCl_3$) δ 7.44 (s, 1H), 5.01 (q, *J* = 7.2 Hz, 1H), 4.57 (q, *J* = 7.1 Hz, 2H), 4.39 (t, *J* = 5.5 Hz, 1H), 4.37 (t, *J* = 7.1 Hz, 2H), 3.65–3.50 (m, 2H), 3.46–3.35 (m, 2H), 2.14 (dt, *J* = 7.1, 5.5 Hz, 2H), 1.74 (d, *J* = 7.2 Hz, 3H), 1.34 (t, *J* = 7.1 Hz, 3H), 1.13 (t, *J* = 7.0 Hz, 7H); ^{13}C NMR (75 MHz, $CDCl_3$) δ 213.2, 148.1, 121.5, 100.3, 69.9, 62.2 (2C), 46.2, 40.9, 34.4, 20.2, 15.3 (2C), 13.8. The ^{1}H NMR was in agreement with that reported in the literature.[45]

*6.4 Polymerisation of N-vinylpyrrolidone (NVP, **75**)*

Polymerisation procedure for PVP was also carried out by selecting optimal conditions reported by Reader *et al*.[45] in which polymerisation exhibited the most controlled system with low polydispersity. Thus, NVP (5.00 g, 45.0 mmol), AIBN (44 mg, 0.27 mmol) and RAFT agent (373 mg, 1.07 mmol) were dissolved in 1,4-dioxane (5 mL) solvent. The reaction mixture was subjected to three freeze-pump-thaw cycles and polymerisation reaction was conditioned at 60 °C for 24 h. At the end, the reaction was stopped by precipitating the polymer into Et_2O and the solvent was decanted. The precipitate was then dissolved into DCM under stirring and precipitated back into Et_2O. The procedure was repeated three times before the polymer was dried under high vacuum at a room temperature to obtain a white powder. The ^{1}H NMR data corresponded to that reported in the literature.[45]

*6.5 Modification of PVP polymer xanthate endgroup via amynolysis (**76**)*

Under inert conditions, a PVP polymer (2.50 g, 1.59 mmol) was dissolved into acetone (10 mL) and cyclohexylamine (730 µL, 6.37 mmol) was added to the solution and the reaction was stirred at a room temperature for 5 h. At the end of the reaction, Et_2O was once again used to precipitate the thiol-terminated polymer and the solvent was decanted. The precipitated polymer was dissolved back into dichloromethane, stirred and precipitated again into Et_2O solvent. The procedure was repeated three times before a thiol-terminated PVP polymer was dried under high vacuum at a room temperature. The product was obtained as a white powder in 96% yield (2.27 g).

*6.6 Conjugation of PVP to 4-anilinoquinazolines via Michael addition reaction (**77**–**84**)*

In a screw top V-vial was added a PVP polymer (50mg, 0.03 mmol), TCEP·HCl (10.0 mg, 0.03 mmol), and a suitable 4-aniliquinazoline compound (~12.5 mg, 1.1 molar equivalents) were dissolved to 1 mL with DMF solvent. To this solution was added 20% NH_4OH (10 µL) and the reaction mixture was stirred at a room temperature for 16 h. At

the end, the resultant solution was purified by dialysis using 10% ethanol in deionised water over 24 h and then 100% deionised water for another 24 h. The aqueous samples were freeze-dried from a lyophilizer to afford conjugates in 84–98% quantitative yield as precipitates.

6.7 References

1. Steck, E., A; Fletcher, L., T, *Journal of the American Chemical Society* **1947,** *70*, 439-440.

2. Ebrahimi, S.; Saiadi, S.; Dakhilpour, S.; Mirsattari, S. N.; Massah, A. R., *Zeitschrift für Naturforschung B* **2015,** *71*, 95-104.

3. Kita, Y.; Nishii, Y.; Onoue, A.; Mashima, K., *Advanced Synthesis and Catalysis* **2013,** *355*, 3391-3395.

4. Yu, J.; Zhang-Negrerie, D.; Du, Y., *European Journal of Organic Chemistry* **2016,** *2016*, 562-568.

5. Wu, Y.; Jiang, C.; Wu, D.; Gu, Q.; Luo, Z.-Y.; Luo, H.-B., *Chemical Communications* **2016,** *52*, 1286-1289.

6. Karthikeyan, P.; Jagadeesh, R. V.; Sree Sandhya, Y.; Puttaswamy; Nithya, P.; Senthil Kumar, S.; Bhagat, P. R., *Applied Organometallic Chemistry* **2011,** *25*, 34-46.

7. Zhao, H.; Fu, H.; Qiao, R., *Journal of Organic Chemistry* **2010,** *75*, 3311-3316.

8. Wang, D.; Gao, F., *Chemistry Central Journal* **2013,** *7*, 1-15.

9. Liu, G.; Qiu, M.; Sun, L.; Wen, Q.; Xu, S.; Wang, X. G.; Wang, P., *Letters in Organic Chemistry* **2016,** *13*, 44-48.

10. Morley, J. S.; Simpson, J. C. E., *Journal of Chemical Society* **1947**, 360-366.

11. Wang, B.; Li, Z.; Wang, X. N.; Tan, J. H.; Gu, L. Q.; Huang, Z. S., *Chinese Chemical Letters* **2011,** *22*, 951-953.

12. Kulkarni, S. S.; Singh, S.; Shah, J. R.; Low, W.-K.; Talele, T. T., *European Journal of Medicinal Chemistry* **2012,** *50*, 264-273.

13. Bellamy, F. D.; Ou, K., *Tetrahedron Letters* **1984,** *25*, 839-842.

14. Tordeux, M.; Wakselman, C., *Journal of Fluorine Chemistry* **1995,** *74*, 251-254.

15. Rajšner, M.; Metyšová, J.; Svátek, E.; Mikšík, F.; Protiva, M., *Collection of Czechoslovak Chemical Communications* **1975,** *40*, 719-737.

16. Moussy, A.; Benjahad, A.; Schalon, C.; Pez, D.; Chevenier, E.; Sandrinelli, F.; Martin, J.; Picoul, W. WO2014/202763 A1. 2014.

17. Tu, Y.; OuYang, Y.; Xu, S.; Zhu, Y.; Li, G.; Sun, C.; Zheng, P.; Zhu, W., *Bioorganic and Medicinal Chemistry* **2016,** *24*, 1495-1503.

18. Chao, Q.; Deng, L.; Shih, H.; Leoni, L. M.; Genini, D.; Carson, D. A.; Cottam, H. B., *Journal of Medicinal Chemistry* **1999,** *42*, 3860-3873.

19. Buha, V. M.; Rana, D. N.; Chhabria, M. T.; Chikhalia, K. H.; Mahajan, B. M.; Brahmkshatriya, P. S.; Shah, N. K., *Medicinal Chemistry Research* **2013,** *22*, 4096-4109.

20. Xiong, C.; Changgeng, Q.; Haixiao, Z.; Rudi, B. US2009111772 (A1). 2009.

21. Bridges, A. J.; Zhou, H.; Cody, D. R.; Rewcastle, G. W.; McMichael, A.; Showalter, H. D. H.; Fry, D. W.; Kraker, A. J.; Denny, W. A., *Journal of Medicinal Chemistry* **1996,** *39*, 267-276.

22. Pedersen, E. B., *Tetrahedron* **1977,** *33*, 217-220.

23. Wang, S.; Yang, Z.; Liu, J.; Xie, K.; Wang, A.; Chen, X.; Tan, Z., *Chemical Communications* **2012,** *48*, 9924-9926.

24. Kalbandhe, A. H.; Kavale, A. S.; Thorat, P. B.; Karade, N. N., *Synthetic Letters* **2016,** *27*, 763-768.

25. Böttcher, S.; Thiem, J., *European Journal of Organic Chemistry* **2014,** *2014*, 564-574.

26. Alexandre, F.-R.; Berecibar, A.; Wrigglesworth, R.; Besson, T., *Tetrahedron* **2003,** *59*, 1413-1419.

27. Ban, H. S.; Usui, T.; Nabeyama, W.; Morita, H.; Fukuzawa, K.; Nakamura, H., *Organic and Biomolecular Chemistry* **2009,** *7*, 4415-4427.

28. Beyer, J.; Susanna, L.-F.; Andrea, M.; Wolfgang, S., *Synthesis* **1998,** *7*, 1047-1051.

29. Dey, S.; Gadakh, S. K.; Sudalai, A., *Organic and Biomolecular Chemistry* **2015,** *13*, 10631-10640.

30. Tomita, M.; Kugo, T., *Pharmaceutical Bulletin* **1954,** *2*, 115-118.

31. Klemenc, *Monatshefte fuer Chemie* **1912,** *33*, 389.

32. Wang, M.; Gao, M.; Zheng, Q.-H., *Bioorganic and Medicinal Chemistry Letters* **2014,** *24*, 4455-4459.

33. Wang, M.; Gao, M.; Zheng, Q.-H., *Bioorganic and Medicinal Chemistry Letters* **2014,** *24*, 4455-4459.

34. Knesl, P.; Röseling, D.; Jordis, U., *Molecules* **2006,** *11*, 286-297.

35. Arnott, E. A.; Chan, L. C.; Cox, B. G.; Meyrick, B.; Phillips, A., *Journal of Organic Chemistry* **2011,** *76*, 1653-1661.

36. Pawar, V. G.; Sos, M. L.; Rode, H. B.; Rabiller, M.; Heynck, S.; van Otterlo, W. A. L.; Thomas, R. K.; Rauh, D., *Journal of Medicinal Chemistry* **2010,** *53*, 2892-2901.

37. Johnström, P.; Fredriksson, A.; Thorell, J.-O.; Stone-Elander, S., *Journal of Labelled Compounds and Radiopharmaceuticals* **1998,** *41*, 623-629.

38. Waiker, D. K.; Karthikeyan, C.; Poongavanam, V.; Kongsted, J.; Lozach, O.; Meijer, L.; Trivedi, P., *Bioorganic and Medicinal Chemistry* **2014,** *22*, 1909-1915.

39. Hou, X.; Zhang, J.; Zhao, X.; Chang, L.; Hu, P.; Liu, H., *Chinese Journal of Chemistry* **2014,** *32*, 538-544.

40. Marvania, B.; Lee, P.-C.; Chaniyara, R.; Dong, H.; Suman, S.; Kakadiya, R.; Chou, T.-C.; Lee, T.-C.; Shah, A.; Su, T.-L., *Bioorganic and Medicinal Chemistry* **2011,** *19*, 1987-1998.

41. Schnuur, R. C.; Arnold, L. D. EP2163546 (A1). 2016.

42. Dengming, X.; Yan, Z.; Yuandong, H.; Huting, Y.; Jijung, L.; Yong, P.; Hui, Z.; Hong, L.; Fansheng, K.; Yongxin, H. US2016214964 (A1). 2014.

43. Michalczyk, A.; Klüter, S.; Rode, H. B.; Simard, J. R.; Grütter, C.; Rabiller, M.; Rauh, D., *Bioorganic and Medicinal Chemistry* **2008,** *16*, 3482-3488.

44. Zhang, Q.; Zhu, H. WO2011/084796 (A3), 2011.

45. Reader, P. W.; Pfukwa, R.; Jokonya, S.; Arnott, G. E.; Klumperman, B., *Polymer Chemistry* **2016,** *7*, 6450-6456.

46. Hastings, C. J.; Fiedler, D.; Bergman, R. G.; Raymond, K. N., *Journal of the American Chemical Society* **2008,** *130*, 10977-10983.

47. Akeroyd, N.; Pfukwa, R.; Klumperman, B., *Macromolecules* **2009,** *42*, 3014-3018.

48. Goddard-Borger, E. D.; Stick, R. V., *Organic Letters* **2007,** *9*, 3797-3800.

Chapter 7: Conclusion and recommendations for future work

Chapter 7: Conclusion and recommendations for future work

Abstract
This chapter contains the concluding remarks based on the research outcomes of the objectives of the study. Recommendations for further improving the anti-tumour efficacy of PVP-(4-phenyl amine)quinazoline conjugates based on the findings of this study are briefly communicated.

7.1 Conclusion

In this research study, polymer-drug conjugates of 4-anilinoquinazoline small-molecule EGFR tyrosine kinase inhibitors and PVP, covalently bound by an acid-labile linker group, were developed. A small library of 4-anilinoquinazoline compounds with a α,β-unsaturated carbonyl moiety (acrylamides and acrylates) at the C-6 position were synthesised. These quinazoline-based anti-tumour agents, commonly used for clinical application in adenocarcinoma lung cancer, were then conjugated to a pre-defined thiol-terminated PVP polymer using the Michael addition reaction, thus affording PVP-(4-phenyl amine)quinazoline conjugates.

The resultant amphiphilic polymer-drug conjugates were assembled into a spherical micellar drug delivery system. The drug release profiles for these formulations were realised under physiological and acidic conditions, and the hydrolytic stability of the covalent linker groups was established. A high degree of drug release selectivity in an acidic environment was obtained, to favour the tumouritropic drug delivery aspect of pH-sensitive micelle formulations. Based on the results of our studies, the mode of the EGFR kinase inhibition mechanism in the present formulation of polymer-bound 4-anilinoquinazoline was determined to be reversible and ATP-competitive in nature. Preliminary *in vitro* biological assays strongly demonstrated the influence of the inhibition mechanisms to be a determinant factor for the anti-tumour efficacy of 4-anilinoquinazolines. Hence, the polymer-drug conjugates exhibited anti-tumour activities that were comparable to the corresponding small molecules (reversible inhibitors). The conjugates also shared reduced anti-tumour efficacy profiles with the respective small molecules against drug-resistance-inducing secondary mutation EGFR T790M.

Chapter 7: Conclusion and recommendations for future work

In general, compounds carrying the acrylamide Michael acceptor showed excellent anti-tumour activity and the β-thiopropionamide polymer conjugate showed good anti-tumour activity in comparison with Gefitinib. Due to the sustained EGFR kinase inhibition by the irreversible inhibitors, their anti-tumour potency proved superior to reversible inhibitors, irrespective of the present formulation of the micelles. Based on the overall outcome of this work, further developments in the chemistry of the present conjugates are planned, as described in the next section.

7.2 Recommendations for future research

In consideration of the potential advantages offered by the polymer-drug conjugates, a number of modifications to the present formulation are proposed for further investigation. First, the potency of the conjugates must be enhanced to the level or beyond that of the irreversible EGFR kinase inhibitors. In doing so, the criteria of this modification should take into account the mutation status of the EGFR target. At present, double mutant EGFR L858R/T790M tumour cells can be overcome by irreversible kinase inhibitors,[1] but the newly acquired mutant EGFR T790M/C797S is very likely to be circumvented by the allosteric inhibitors.[2] Given this scenario, the first attempt would involve upgrading the PVP-(4-phenyl amino)quinazoline conjugates to irreversible EGFR kinase inhibitors. Thus, generating the α,β-unsaturated Michael acceptor under physiologically relevant acidic conditions would generally be the universal reaction of interest.

Among the three broadly categorised elimination mechanisms (E1, E1cb, E2) that can generate an olefin adjacent to a carbonyl group, the E1cb has recently been used by the research group of Tautonas as an alternative and very attractive for reversible-covalent inhibition.[3] Unfortunately, generating the Michael acceptor under the reported E1cb elimination conditions requires an α,β-unsaturated olefin that is substituted with an electron-withdrawing group in the α-position of the carbonyl. Moreover, the authors have reported this system to undergo reversible cleavage under physiological conditions,[3a] which is unfavourable for our present conjugation design. Thus, in the near future, we intend to explore a modified Reich olefin formation reaction using the

sulfoxides. This is a largely under-exploited reaction, relative to making use of the well-known seleneoxides.[4] To apply this reaction to our design, the current set up can potentially be modified as shown in **Figure 7.2 (a)**.

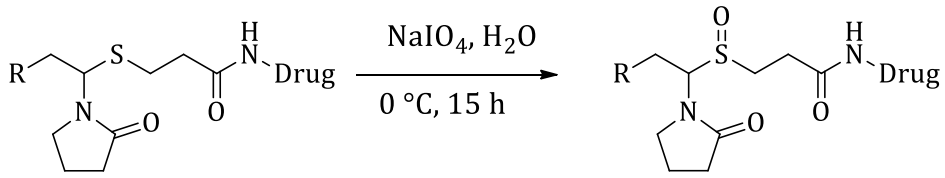

Current polymer-drug conjugate

Proposed polymer-drug conjugate

Figure 7.2 (a) Modification of β-thiopropionamide conjugate linker group by oxidation of the thioether. For a simplified presentation, only the last NVP monomer and the amide linker are shown in full.

The selective mono-oxidation of polymer-drug conjugate [**Fig. 7.2 (a)**] presents a versatile chemistry that can be exploited in many forms, including a change in drug release mechanism.[5] The proposed *retro*-Michael addition reaction [see **Fig. 7.2 (b)]** is perceived to proceed via simultaneous elimination of the vicinal substituents on the alkane skeleton, being S=O and H, via a cyclic transition state that involves abstraction of a β-proton in a *syn* fashion to form the α,β-unsaturated olefin.[4] The same β-elimination mechanisms leading to the formation of olefins using sulfoxides are well distinguished in other reactions, such as the Morin rearrangement.[6] This reaction is an ideal case of intramolecular E2 elimination for which (i) acrylamide (covalent-irreversible) and/or (ii) sulfenic acid (covalent-reversible) functionalities could be formed. In the former case of (i), β-elimination via abstraction of the more acidic proton in the α-position to the carbonyl (electron-withdrawing group) is a more favourable kinetic product under physiological conditions.[5]

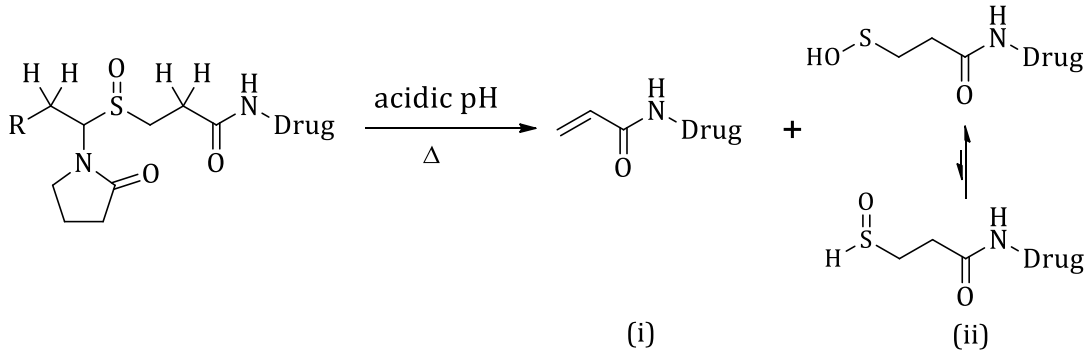

Figure 7.2 (b) Proposed β-eliminative cleavage products of modified PVP-(4 phenyl amine)quinazoline conjugates under acidic tumour microenvironment.

The latter case (ii) represents a thermally promoted E2 reaction in which NVP loses its β-proton to form a sulfenic acid terminated product.[4b, 7] Thermally promoted E2 reactions have been observed for seleneoxides at room temperature in acidic media,[7] but they are generally substituent sensitive. Nevertheless, sulfenic acid exhibits electrophilic character and can undergo condensation with cysteine to form disulfide bonds.[8] It is often regarded as a transient oxidation state to the formation of disulfides under physiologic conditions. The biggest challenge will however be the hydrolytic cleavage of the amide bond of the linker group. Hence, careful execution of these experiments is very critical, and this would perhaps lead to a different choice of the linker group. The reactions similar to the *retro*-Michael eliminations have been applied in time-delayed fragrance delivery systems of the enone functionality in different skeletons such as damascone.[9] In a biological setting, the formation of the more bioactive Brefeldin A, an α,β-unsaturated antibiotic lactone, has been speculated to form via *syn* elimination of the sulfoxide analogues.[10]

Presented with the most recent EGFR C797S,[11] it must be appreciated that this mutation is resistant to irreversible EGFR kinase inhibitor drugs with electrophilic Michael acceptors. This has opened a new opportunity for the discovery of more electrophilic agents that can form a covalent bond with the serine (–OH) in tumour cells. The aliphatic serine (–OH, pK_a >13) has almost the same nucleophilicity as water and is relatively inert to the Michael acceptors under acidic conditions.[12] We thus also intend to explore the E1 reaction using 2-thioethanol derivatives as solubilising groups for quinazoline-based kinase EGFR kinase inhibitors. The thioethanol functionality has a potential to form

highly reactive thiiranium ion intermediate [refer to **Fig. 7.12 (c)]** in a stepwise fashion in an acidic environment,[13]and it can be used to target a number of cellular nucleophiles such as cysteine thiols (SH) and serine (OH). It can also be viewed as poly(alcohol) chain mimicry for enhancing the aqueous solubility.[14] This new functionality can potentially expand the use of 4-anilininoquinazoline compounds against lung adenocarcinoma patients that accrue both EGFR L858R/T790M and EGFR C797S mutations. It is expected that further anti-tumour efficacy of the modified PVP-(4-phenyl amine)quinazoline conjugates will also be achieved.

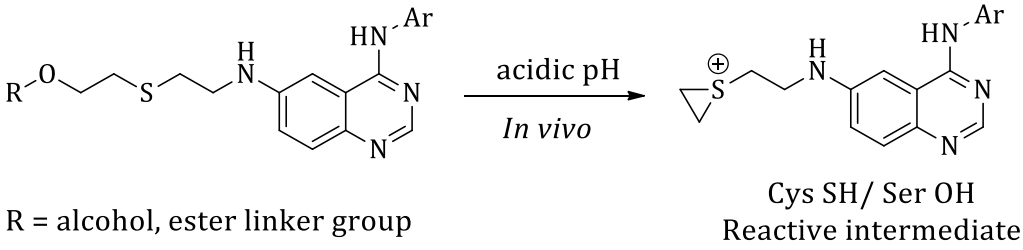

Figure 7.2 (c) Proposed new linker group for reversible-covalent (EGFR C797S) or irreversible-covalent inhibition (EGFR T790M), depending on targeted nucleophile.

This is the end of the current work on the synthesis of polymer-bound SMKIs. An outline of future prospects will be communicated in the near future.

7.3 References

1. (a) Sullivan, I.; Planchard, D., *Therapeutic Advances in Respiratory Disease* **2016,** *10*, 549-565; (b) Thress, K. S.; Paweletz, C. P.; Felip, E.; Cho, B. C.; Stetson, D.; Dougherty, B.; Lai, Z.; Markovets, A.; Vivancos, A.; Kuang, Y.; Ercan, D.; Matthews, S. E.; Cantarini, M.; Barrett, J. C.; Janne, P. A.; Oxnard, G. R., *Nature Medicine* **2015,** *21*, 560-562.

2. Jia, Y.; Yun, C.-H.; Park, E.; Ercan, D.; Manuia, M.; Juarez, J.; Xu, C.; Rhee, K.; Chen, T.; Zhang, H.; Palakurthi, S.; Jang, J.; Lelais, G.; DiDonato, M.; Bursulaya, B.; Michellys, P.-Y.; Epple, R.; Marsilje, T. H.; McNeill, M.; Lu, W.; Harris, J.; Bender, S.; Wong, K.-K.; Jänne, P. A.; Eck, M. J., *Nature* **2016,** *534*, 129-132.

3. (a) Serafimova, I. M.; Pufall, M. A.; Krishnan, S.; Duda, K.; Michael, S. C.; Maglathlin, R. L.; McFarland, J. M.; Miller, R. M.; Frödin, M.; Taunton, J., *Nature Chemical Biology* **2012,** *8*, 471-476; (b) Lee, C.-U.; Grossmann, T. N., *Angewandte Chemie International Edition* **2012,** *51*, 8699-8700.

4. (a) Reich, H. J.; Renga, J. M.; Reich, I. L., *Journal of the American Chemical Society* **1975,** *97*, 5434-5447; (b) Janssen, J. W. A. M.; Kwart, H., *The Journal of Organic Chemistry* **1977,** *42*, 1530-1533.

5. Gupta, V.; Carroll, K. S., *Biochimica et Biophysica Acta* **2013,** *1840*, 847-875.

6. Morin, R. B.; Jackson, B. G.; Mueller, R. A.; Lavagnino, E. R.; Scanlon, W. B.; Andrews, S. L., *Journal of the American Chemical Society* **1969,** *91*, 1401-1407.

7. Crimmins, M. T.; Pace, J. M.; Nantermet, P. G.; Kim-Maede, A. S.; Thomas, J. B.; Watterson, S. H.; Wagman, A. S., *Journal of American Chemical Society* **2000,** *122*, 8453-8463.

8. (a) Sanchez, R.; Riddle, M.; Woo, J.; Momand, J., *Protein Science : A Publication of the Protein Society* **2008,** *17*, 473-481; (b) Rehder, D. S.; Borges, C. R., *Biochemistry* **2010,** *49*, 7748-7755.

9. Ferh, C.; Galindo, J., *Helvetica Chimica Acta* **2005,** *88*, 3128-3136.

10. Fox, B., M.; Vroman, J. A.; FanWick, P. E.; Cushman, M., *Journal of Medicinal Chemistry* **2001,** *44*, 3915-3924.

11. Wang, S.; Tsui, S. T.; Liu, C.; Song, Y.; Liu, D., *Journal of Hematology and Oncology* **2016,** *9*, 59.

12. Stark, G. R., *Biochemistry* **1965,** *4*, 2363-2367.

13. Fuhrhop, J. H.; Liman, U.; Koesling, V., *Journal of American Chemical Society* **1988,** *110*, 6840.

14. Rewcastle, G. W.; Murray, D. K.; Elliott, W. L.; Fry, D. W.; Howard, C. T.; Nelson, J. M.; Roberts, B. J.; Vincent, P. W.; Hollis Showalter, H. D.; Winters, R. T.; Denny, W. A., *Journal of Medicinal Chemistry* **1998,** *41*, 742-751.